NASA CONTRACTOR REPORT 177335

WIND TUNNEL ACOUSTIC STUDY OF A PROPELLER INSTALLED BEHIND AN AIRPLANE EMPENNAGE: DATA REPORT

J. F. Wilby
E. G. Wilby

(NASA-CR-177335) WIND TUNNEL ACOUSTIC STUDY OF A PROPELLER INSTALLED BEHIND AN AIRPLANE EMPENNAGE: DATA REPORT (Bolt, Beranek, and Newman, Inc.) 267 p HC A12/MF A01 CSCL 20A

N85-23377

G3/71 Unclas 20172

CONTRACT NAS2–11085
January 1985

NASA

NASA CONTRACTOR REPORT 177335

WIND TUNNEL ACOUSTIC STUDY OF A PROPELLER INSTALLED BEHIND AN AIRPLANE EMPENNAGE: DATA REPORT

J.F. Wilby
E.G. Wilby
BBN Laboratories Incorporated
A Subsidiary of Bolt Beranek and Newman Inc.
Canoga Park, CA 91303

Prepared for
Ames Research Center
Contract NAS2-11085
January 1985

National Aeronautics and
Space Administration

Ames Research Center
Moffett Field, California 94035

TABLE OF CONTENTS

TABLE OF CONTENTS
(continued)

LIST OF FIGURES

LIST OF FIGURES
(Continued)

LIST OF FIGURES
(Continued)

LIST OF FIGURES
(Continued)

LIST OF FIGURES
(Continued)

LIST OF FIGURES

LIST OF FIGURES

Figure | Page

LIST OF FIGURES

LIST OF TABLES

ACKNOWLEDGEMENT

This report presents acoustic data acquired during NASA Test 706 in the NASA Ames #1 7x10-foot Wind Tunnel. Although the authors of the report participated in the planning and performance of the test, and in the subsequent data reduction, credit for the overall planning, performance and, finally, for the success of the program should go solely to Mr. Paul T. Soderman, the NASA Ames Technical Monitor. In addition, the authors wish to acknowledge the great help provided by Ms. Lisa Lee in the extensive data reduction effort which followed the completion of the tests.

1. INTRODUCTION

1.1 Scope of Report

An acoustic test of a propeller mounted behind an airplane empennage was performed by NASA Ames on a model in the Ames Research Center No.1 7x10-foot wind tunnel during March-April 1984. Technical assistance in the planning and performance of the test, and in the subsequent data reduction was provided by Bolt Beranek and Newman Inc. (BBN). This report presents the results of the work performed by BBN. It describes the model configurations and conditions investigated during the tests, discusses the data acquisition, reduction and analysis procedures, presents acoustic data acquired and provides data interpretation. The total test program included measurements of the wake behind the empennage. Results from these wake tests were analyzed separately by NASA and are not included in this report.

1.2 Propeller Noise

In recent years there has been a resurgence of interest in the generation and control of noise from airplane propellers. This renewed interest has included both interior and exterior noise of propeller-driven aircraft and has covered the range of propellers from conventional general aviation (GA) designs to advanced turboprops (ATP) for high-subsonic cruise. At the same time new aircraft designs have included configurations with propellers mounted on the rear of the airplane, acting in the pusher rather than the tractor role. Aircraft with aft-mounted propellers include the Lear Fan 2100 [1], Beech Starship 1 [2], Gates-Piaggio GP-180 [2] and certain configurations for the ATP airplane [3]. The propellers may be mounted on the centerline of the airplane [1], on the trailing edge of wings on aircraft with canards [2] or on the trailing edge of aft pylons or horizontal stabilizers [3]. However, in all cases the propellers operate in the wake of the upstream control surfaces. It is this phenomenon of noise generation from propellers operating in the wakes of upstream surfaces that is the main impetus for the present study.

Removal of the propeller plane to a location well aft of the passenger cabin has the advantage of reducing the propeller-induced sound levels in the cabin and hence the weight requirements for soundproofing treatments. However, operation of the propeller in a non-uniform flow field, such as exists downstream of control surfaces has the potential for increasing the far field radiated sound levels during take-off and approach. There is also the possibility that forward-radiated sound will enter the passenger cabin.

The influence of a non-uniform flow field on acoustic radiation from a rotating propeller has been observed in comparisons between static and forward flight data. A comparison of this type for a conventional twin-engined propeller-driven airplane [4] shows a marked reduction in the radiated sound pressure levels of higher order harmonics of the blade passage frequency (Figure 1). In this particular example the propeller tip rotational Mach number was 0.85 and the corresponding helical Mach number in flight was 0.87. The physical interpretation of the results is that, under static conditions, the turbulence eddies in the inflow are elongated and subjected to chopping by the propeller, as shown diagrammatically in Figure 2.

The wake from an upstream surface can be considered, to some extent, to be similar to the static conditions for a propeller operating in free space. There is a repetitious interaction between a propeller blade and an inhomogeneous flow field. There have been several investigations of the effect as it pertains to acoustic radiation from fans and compressor rotors operating downstream of inlet guide vanes in turbofan and turbojet engines [5-12] but the corresponding literature for propellers is sparse [13,14].

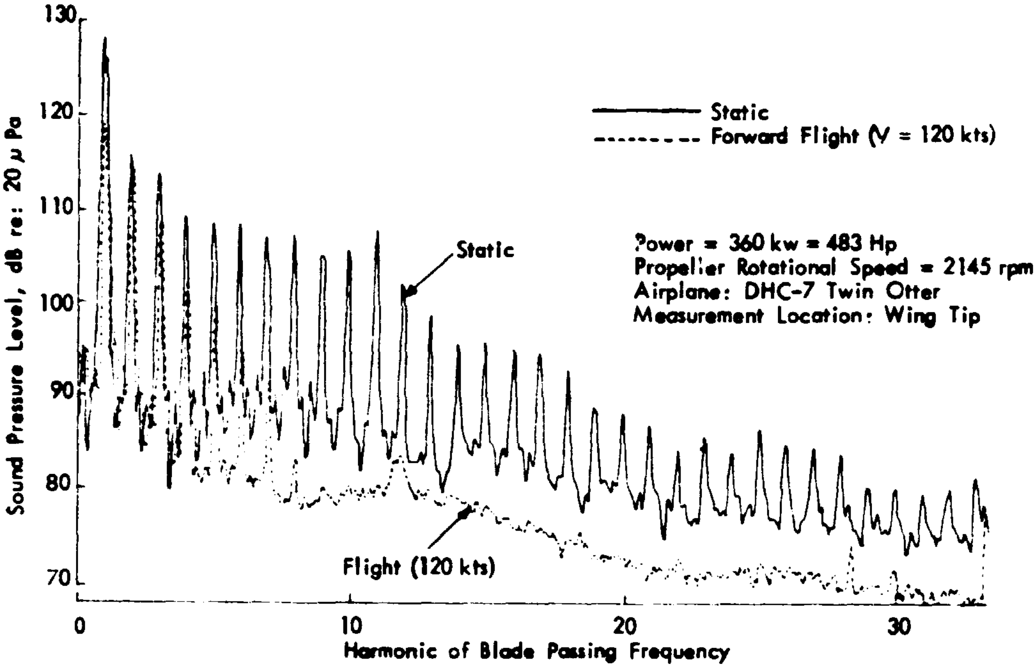

FIGURE 1. COMPARISON OF PROPELLER NOISE SPECTRA FOR STATIC AND FORWARD FLIGHT CONDITIONS [4]

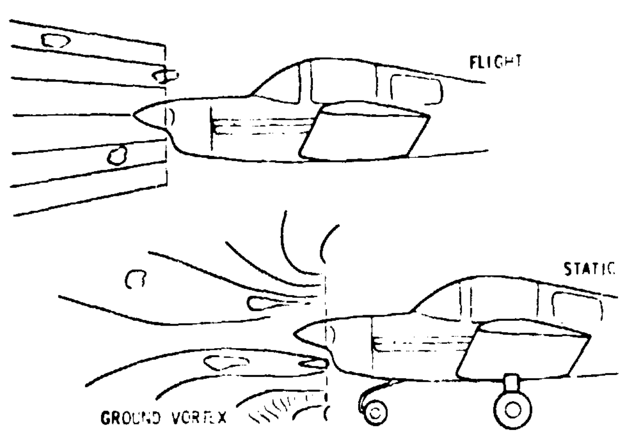

FIGURE 2. DIAGRAMMATIC REPRESENTATION OF PROPELLER INFLOW TURBULENCE

The fan noise studies resulted in several prediction curves for sound level as a function of stator/rotor separation distance. These curves are plotted in Figure 3 where the separation distance is non-dimensionalized with respect to stator chord. It is seen that there is a wide variation in slope for the curves in Figure 3, ranging from -6dB per doubling of separation distance, as given by Smith and House [8], to approximately -2dB per doubling of separation. The empirical curve of Lowson differs from the others in that it shows two different relationships, one associated with separation distances which are less than one chord length and the other with separation distances greater than one chord. It is possible that the two regimes might be associated with potential field interaction and wake interaction respectively. Certainly the -4 dB/separation doubling, as predicted by Lowson for small separations, is similar to the range of -3 dB to -5 dB shown in the data of Sharland [5] and Fincher [6]. However, other studies [12] imply that the potential field and viscous interference (wake) effects are equal at a stator/rotor separation of approximately about one-tenth of the chord length.

Published data for tractor and pusher propellers on the Cessna 02-T or Model 337 [13,14] are concerned mainly with static test conditions, although the authors state that similar effects were noted during flight tests. The Cessna Model 337, as shown in Figure 4, is a twin-boom airplane with two engines and propellers; the rear propeller is mounted on the aft of the passenger cabin and the forward propeller is at the front of the cabin. The two propellers are of similar design, and both have three blades and a diameter of 2.13 m (84 inches).

Figure 4 also contains narrowband acoustic spectra associated with static operation of the front and rear propellers separately. The spectrum for the forward propeller shows components at the first two harmonics of the blade passage frequency ($mB = 3,6$ where m is the harmonic order, $m = 1$ being the fundamental, and B the number

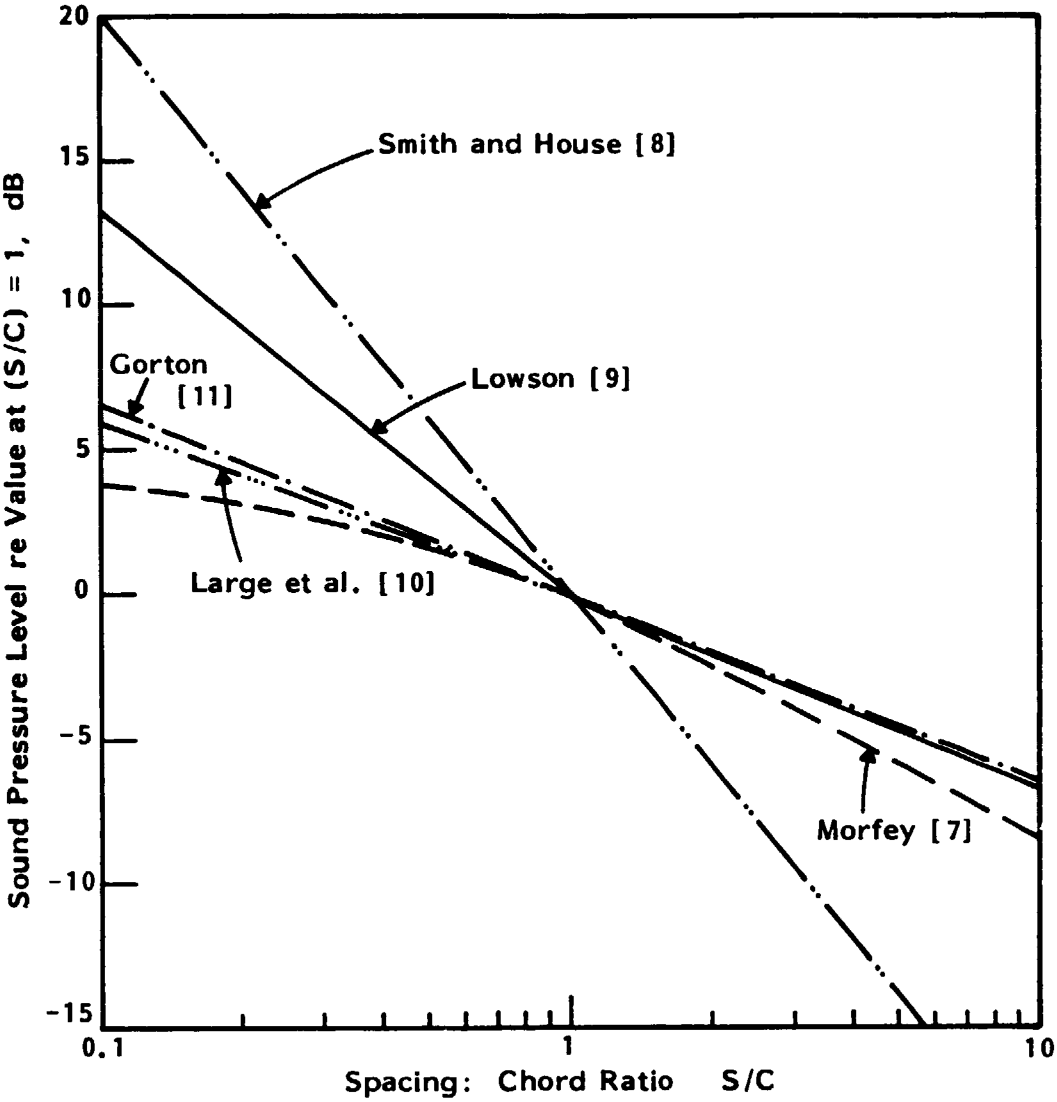

FIGURE 3. EFFECT OF ROTOR SPACING ON NOISE RADIATION FROM AN AXIAL-FLOW FAN

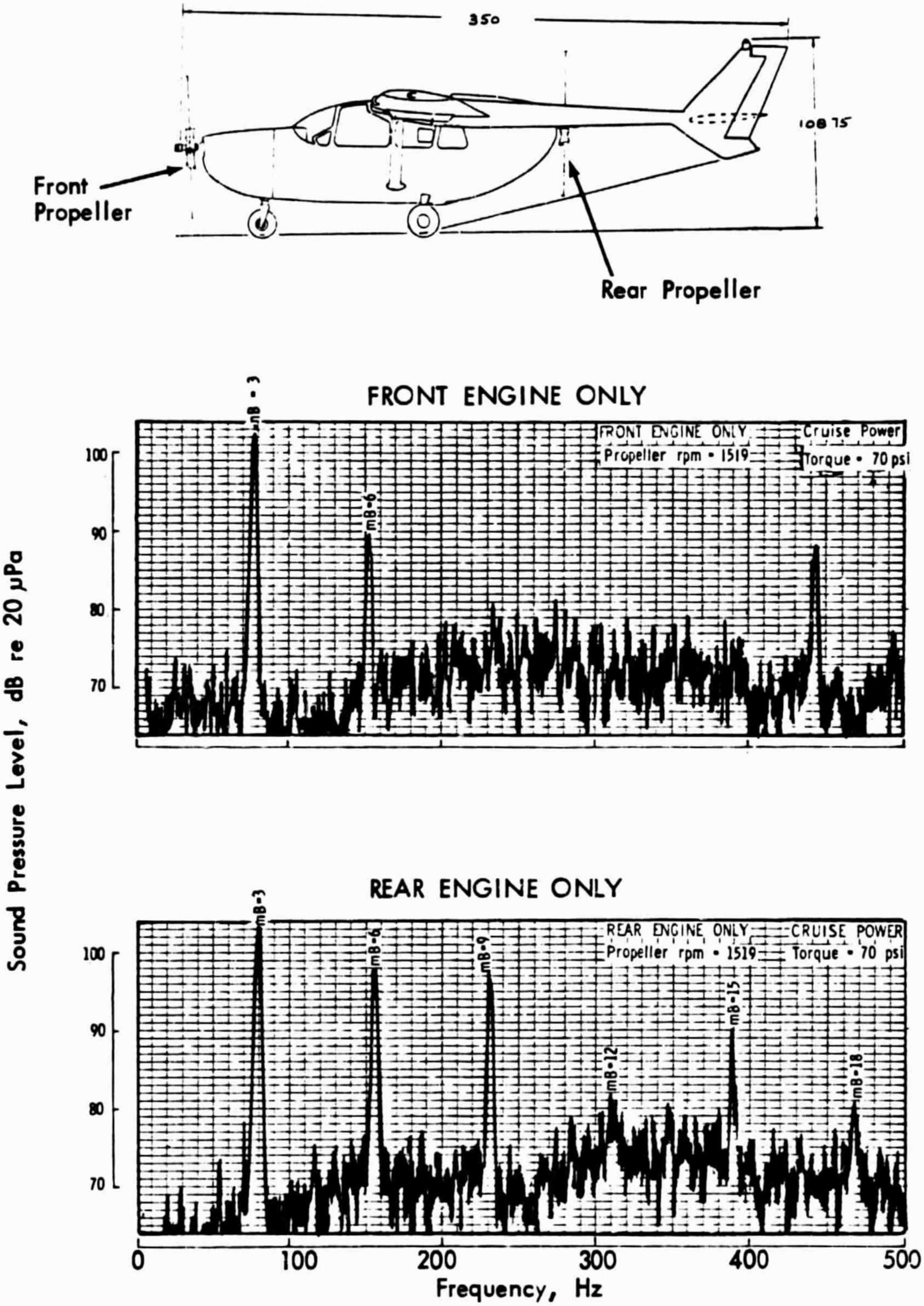

FIGURE 4. COMPARISON OF PROPELLER NOISE LEVELS FOR FRONT AND REAR ENGINES OF CESSNA MODEL 337 [13] (STATIC TEST, 50 FEET RADIUS, PLANE OF ROTATION)

of blades), whereas the spectrum for the rear propeller contains contributions from the first six harmonics (mB = 3 through 18). In the case of the Cessna 337, propeller in-flow conditions are influenced by the fuselage, the downwash from the wing and the exhaust from the turboprop engine.

The conclusion to be drawn from inlet guide vane studies and the measurements on propeller-driven aircraft is that propellers operating in the wake of upstream surfaces will probably generate higher sound levels than propellers operating in relatively undisturbed airflow such as is encountered by tractor propellers. The objective of the present experimental study is to extend the understanding of the phenomenon as it relates to both discrete frequency and broadband noise.

1.3 Overview of Test Program

The test program discussed in this report involved the operation of a model scale propeller in the open test section of the NASA Ames Research Center #1 7x10-foot wind tunnel. The propeller was located immediately downstream of a model airplane fuselage on which were mounted empennages of different configurations. Sound pressure levels were measured at ten locations outside the flow in the test section and at three locations in the flow. The acoustic data were reduced in terms of narrowband and one-third octave band spectra so that the different contributions to the acoustic field could be identified and analyzed.

The majority of the acoustic measurements were made at two flow speeds (45.7 and 62.5 m/s or M = 0.13 and 0.18) and three propeller rotational speeds (4000, 6000 and 8200 rpm). Three empennage configurations (Y-, V-, and I-tails) were tested and the airplane fuselage was oriented in two configurations (ψ = 0°, 90°) to simulate sideline and overhead conditions. Consideration was given to the influence of the flow shear layer on the sound pressure levels measured outside the tunnel flow, and appropriate adjustments made to the data. Finally, the effect of the empennage on the radiated sound field was analyzed for the various test conditions.

1.4 Outline of Report

A description of the acoustic test performed on the propeller and empennage is given in Section 2. The description includes the wind tunnel test chamber and model configuration, data acquisition and reduction procedures, and the test conditions investigated. Data analysis procedures, including adjustments made to the measured sound levels to account for shear layer effects, distance normalization and broadband effects on discrete frequency sound levels, are given in Section 3. Then Section 4 presents an evaluation of the data, including the roles played by various hardware items in the tunnel test section. Section 5 provides an analysis of the harmonic components of the propeller noise field; a general discussion of the results is given in Section 6.

2. TEST DESCRIPTION

2.1 Wind Tunnel Test Section

The acoustic tests were performed in the open test section of the NASA Ames Research Center #1 7x10-foot wind tunnel. In the open configuration the test section sidewalls and ceiling are removed but the floor is retained. Thus, the section is open on three sides. The floor of the test section is continuous with the surrounding wooden floor of the platform which contains the tunnel operator's stations and a work bench area.

The nozzle for the open test section is formed by the contraction downstream of the tunnel settling chamber, and a collector is installed at the entry to the first stage diffuser. A new collector with a convex contour was installed for the present tests, the collector being covered with sound-absorbing foam to minimize acoustic reflections. A plan of the tunnel is shown in Figure 5 and a photograph of the collector is given in Figure 6. The open test section is 2.1 m (7 feet) high and 3.0 m (10 feet) wide at the nozzle and has a length of about 4.3 m (14 feet) from nozzle lip to collector entry.

The test section is surrounded by a test chamber which has dimensions of approximately 13.7 x 16.8 x 9.1 m (45 x 55 x 30 ft). The chamber is of steel construction and has some acoustic treatment in the form of acoustic tiles bonded to the ceiling and wall panels. The average absorption coefficients for the chamber lie in the range from 0.47 to 0.66 in the frequency range from 250 to 8000 Hz [15]. However, these values of the absorption coefficient were not adequate for the propeller noise tests. Thus, additional sound-absorbing materials in the form of foam panels were placed on the platform, on either side of the test section, and inclined relative to the vertical so that any residual acoustic energy would be reflected upwards. In addition, sheets of foam 7.6 cm

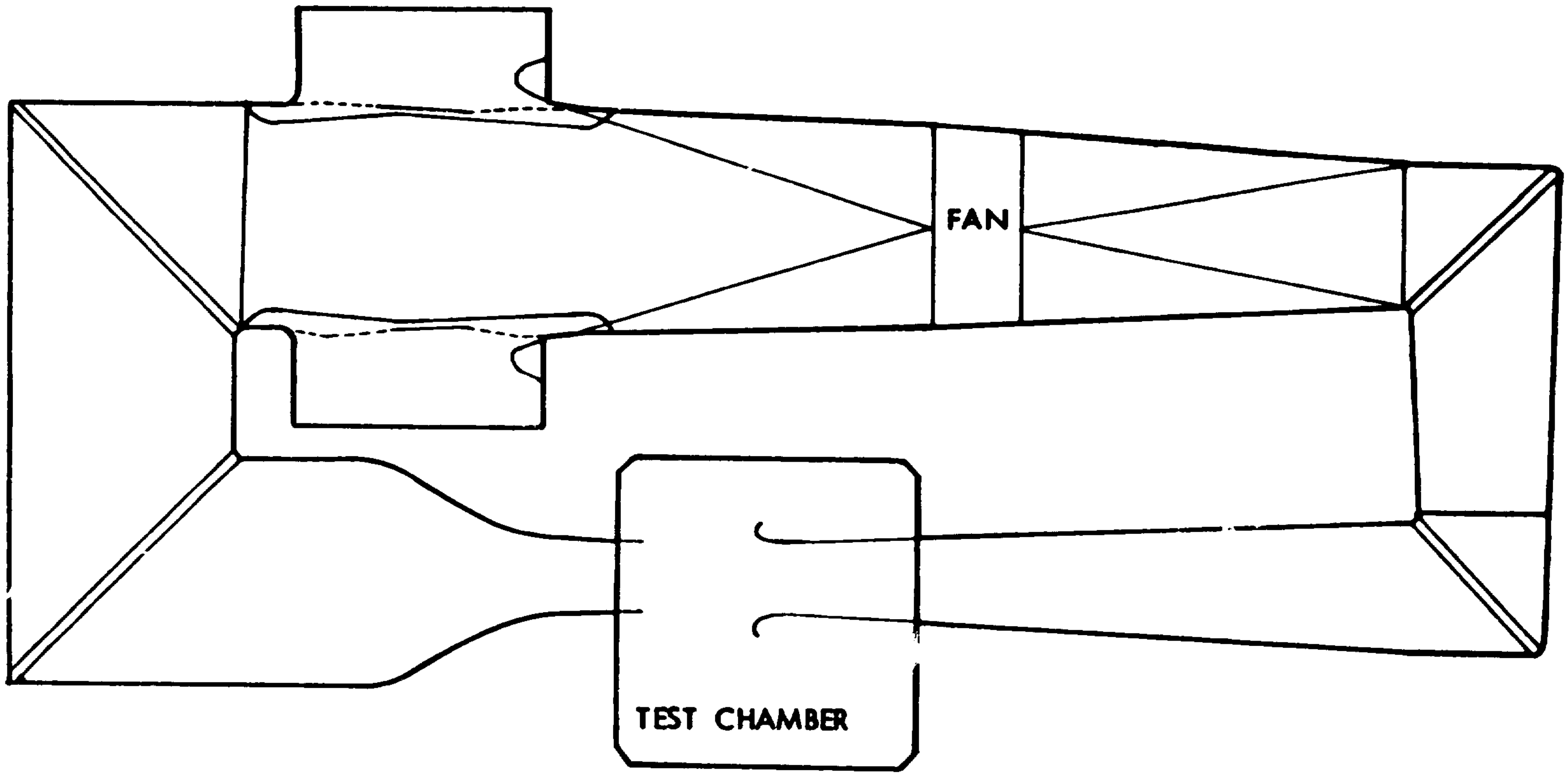

FIGURE 5. PLAN OF 7' x 10' WIND TUNNEL

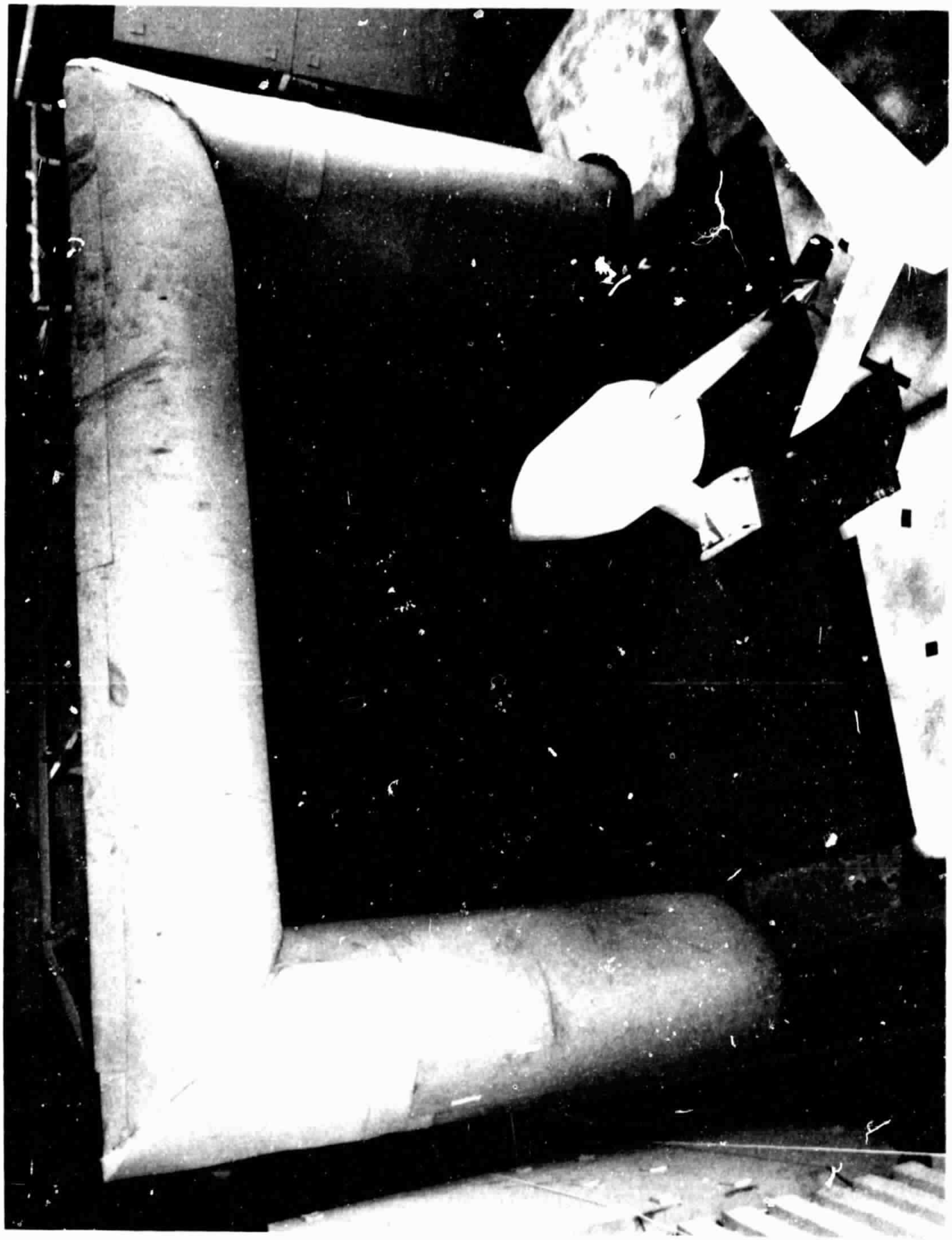

FIGURE 6. FLOW COLLECTOR IN OPEN TEST SECTION

(3 inches) thick were placed on the test section and platform floors, between the model propeller and the microphones used to measure the acoustic field. The foam panels and the floor treatment can be seen in Figures 7 and 8. The photograph in Figure 8 also shows the permanent acoustic treatment on the chamber walls and ceiling.

Optimum positioning of the sound-absorbing panels was achieved by reviewing data associated with an impulsive noise source (pistol shots) at the location of the model propeller. However, the geometry of the test section, tunnel, and test chamber still influences conditions at some measurement locations.

2.2 Model Configuration

2.2.1 General Configuration

The general configuration of the test model can be seen in Figure 8. It consisted essentially of two items; a model fuselage with empennage attached and a propeller drive system consisting of a motor and shaft contained in an aerodynamic housing. Essentially the propeller was a tractor propeller mounted separately from the airframe structure. Approximate dimensions for the set-up are given in Figure 9.

The model fuselage was mounted on two swept airfoil struts which could be moved parallel to the tunnel centerline in order to vary the separation distance between the empennage and the propeller. The propeller drive system was fixed in the longitudinal direction but could be moved vertically to vary the height above and below the fuselage centerline. The axial position of the propeller in the test section was chosen to optimize the angular range available for acoustic measurements.

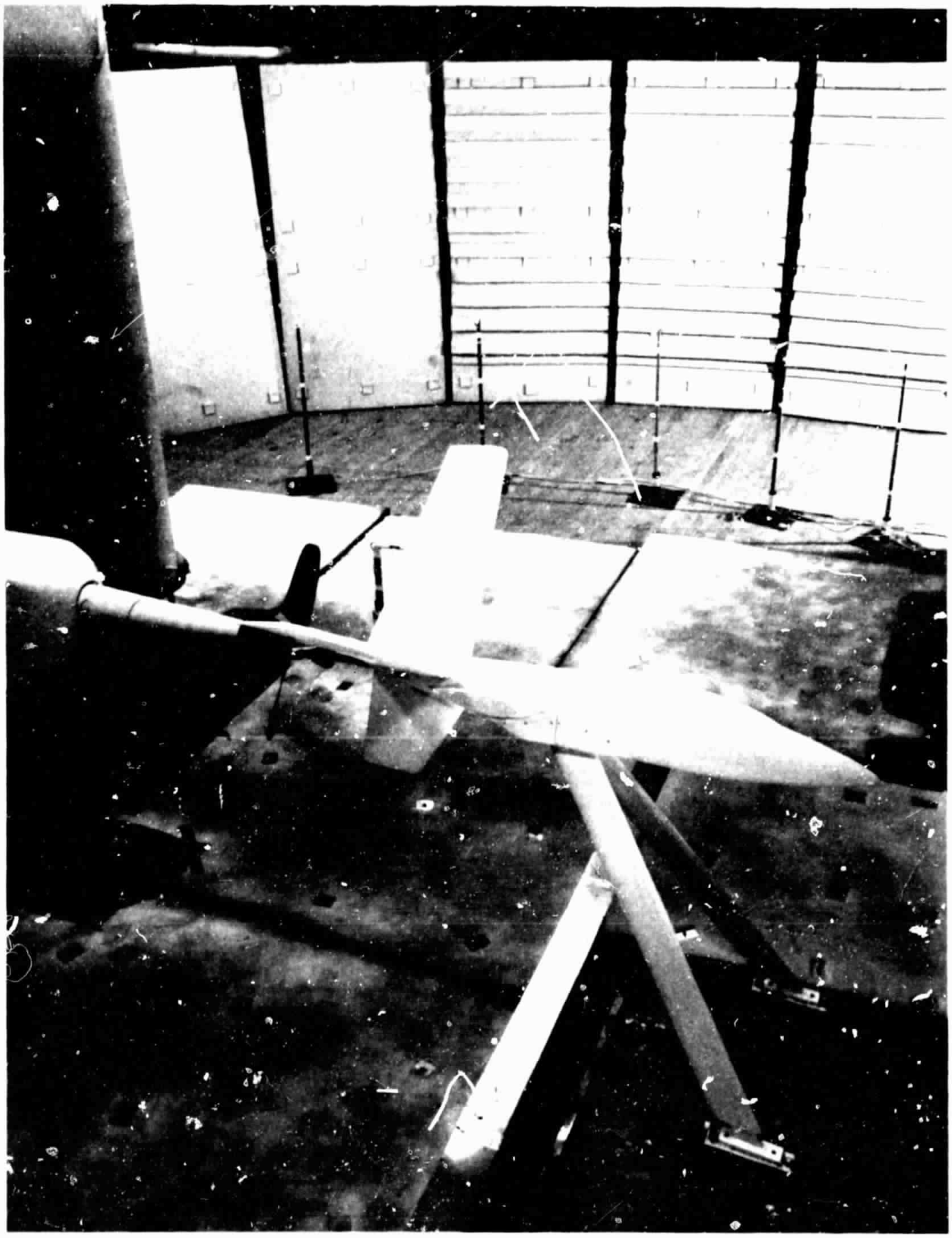

FIGURE 7. OPEN TEST SECTION WITH SOUND-ABSORBING PANELS ON SOUTH SIDE (FUSELAGE ORIENTATION $\psi = 0°$)

ORIGINAL PAGE IS
OF POOR QUALITY

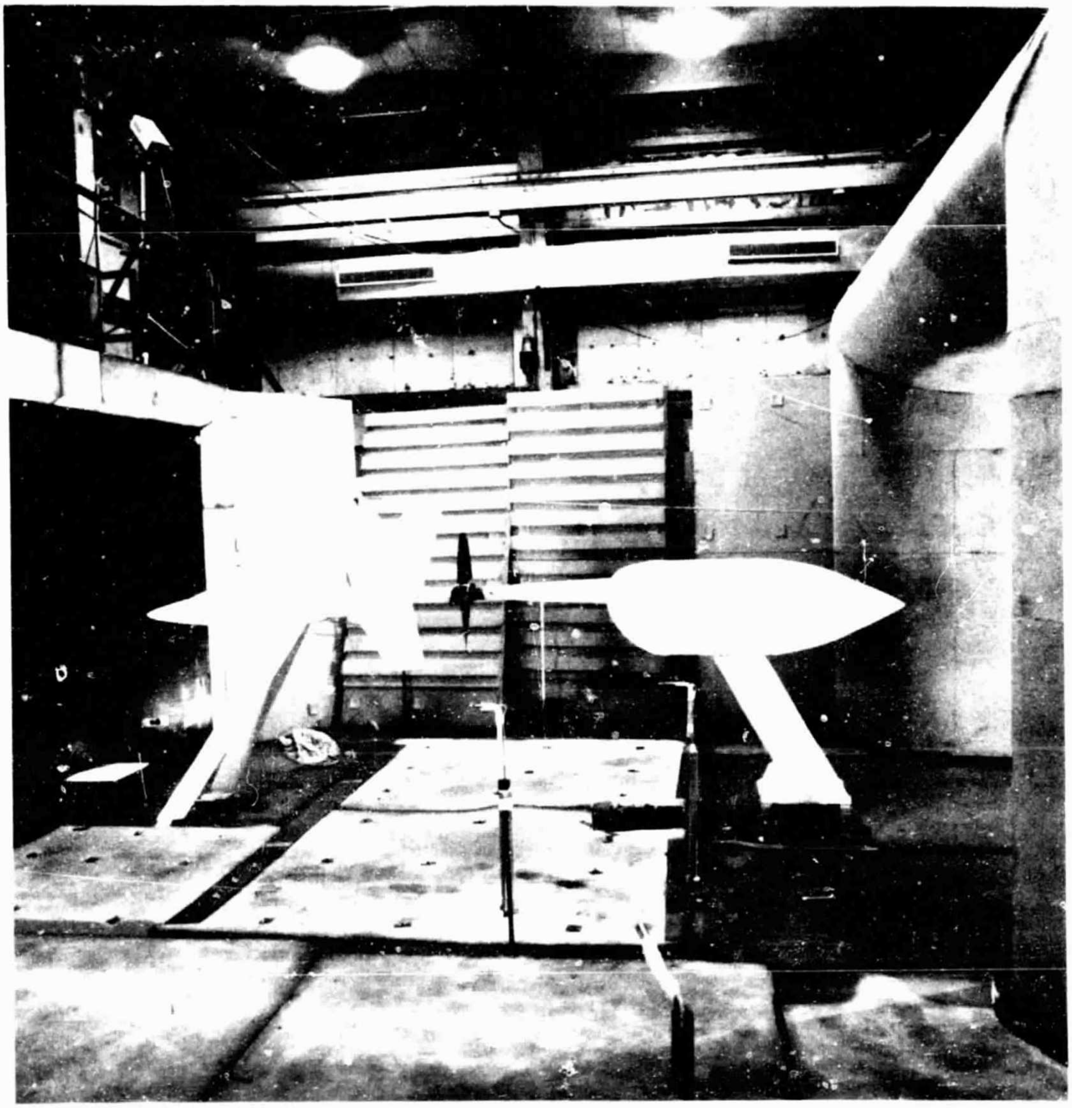

FIGURE 8. OPEN TEST SECTION WITH SOUND-ABSORBING PANELS ON NORTH SIDE

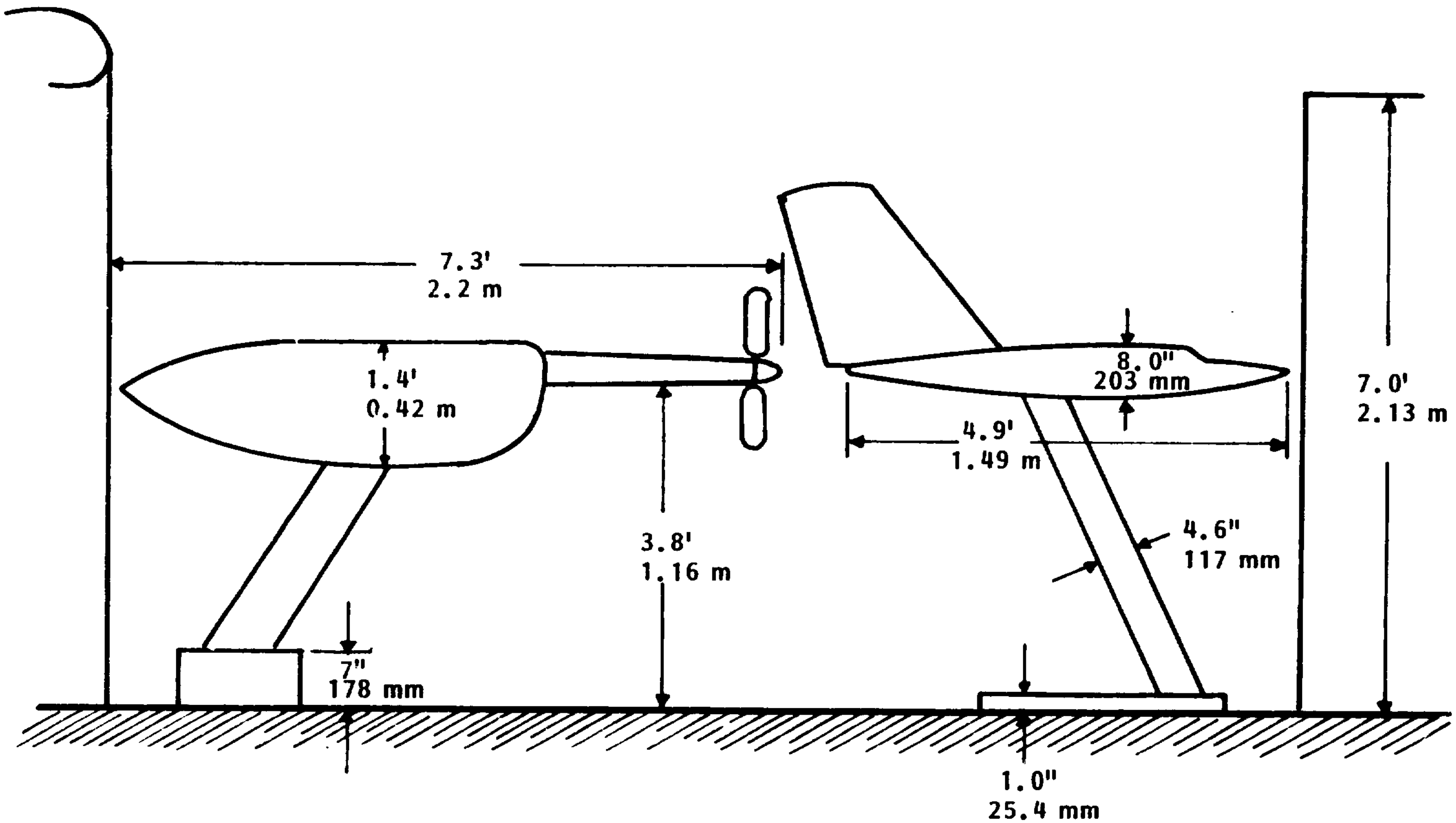

FIGURE 9. DIAGRAM OF TEST MODEL AND PROPELLER DRIVE MECHANISM IN TEST SECTION

Inspection of Figure 8 will show that the dimensions of the model fuselage and empennage are not in correct proportions. This is because the fuselage was used simply as an aerodynamic fairing on which the empennage could be mounted. The dimensions of the empennage were determined on the basis of the model scale for the propeller rather than the fuselage. The model fuselage was installed without a wing.

2.2.2 Model Empennage

Three empennage configurations were selected for test. These configurations consisted essentially of a V-tail with and without a dorsal fin, and a vertical fin. For convenience the V-tail with dorsal fin is referred to in this report as the Y-tail and the vertical fin as the I-tail. The fuselage model with the Y-tail installed is shown in Figure 8. A view from beneath the Y-tail is shown in Figure 10 and a head-on view in Figure 11. The fuselage with I-tail installed is shown in Figure 12.

Tests were performed with the fuselage model oriented as shown in Figure 8 so that sound levels could be measured to the side. Then the fuselage was rotated through 90° and sound levels measured beneath the airplane. These configurations are identified by $\psi = 0°$ and $\psi = 90°$. In the $\psi = 90°$ arrangement the fuselage model was mounted on one side of the support struts, as shown in Figures 11 and 13. The mounting was faired over to minimize the generation of aerodynamic noise.

Representative dimensions for the test empennages are shown in Figure 14.

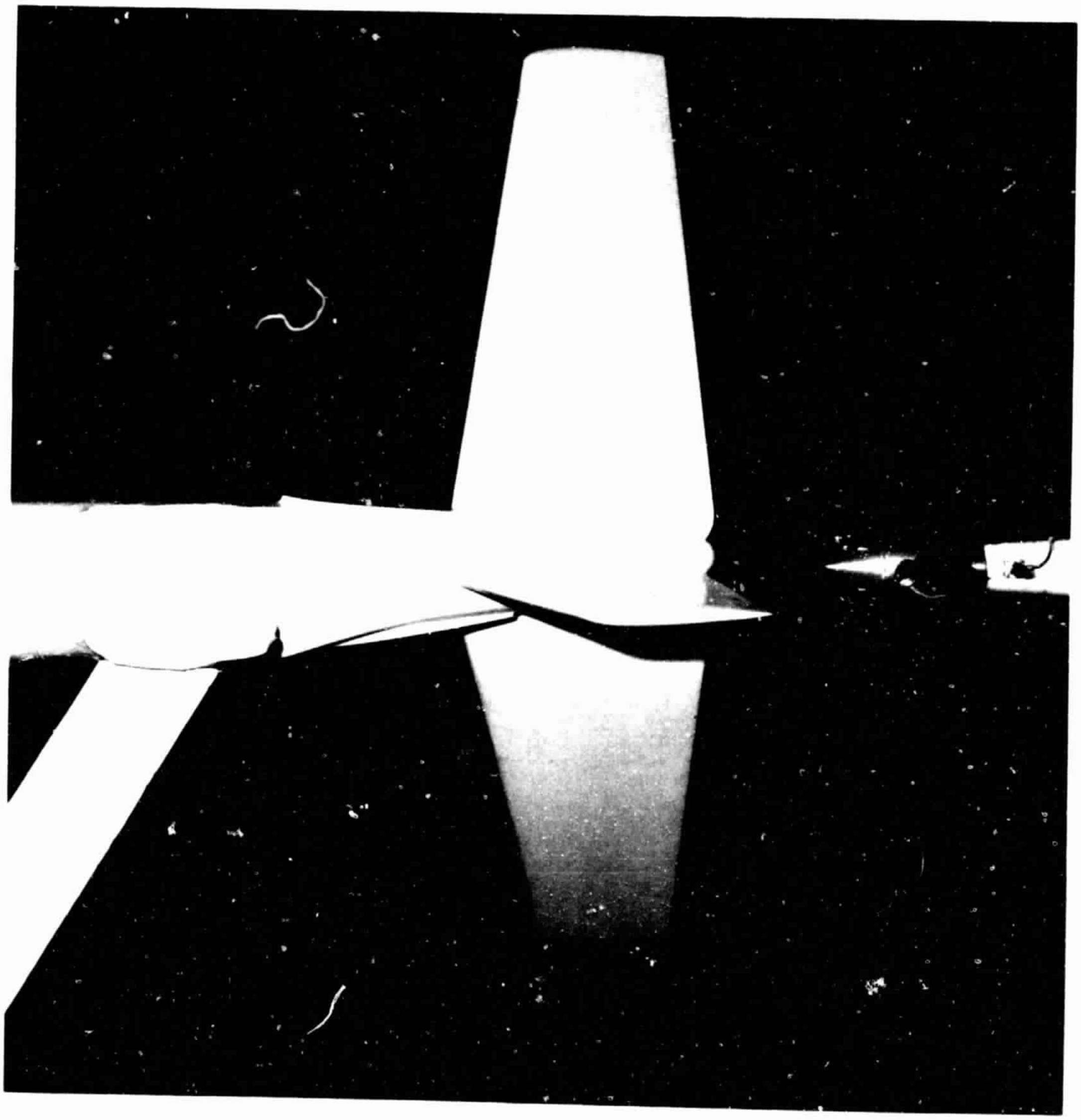

FIGURE 10. Y-TAIL EMPENNAGE FROM BELOW

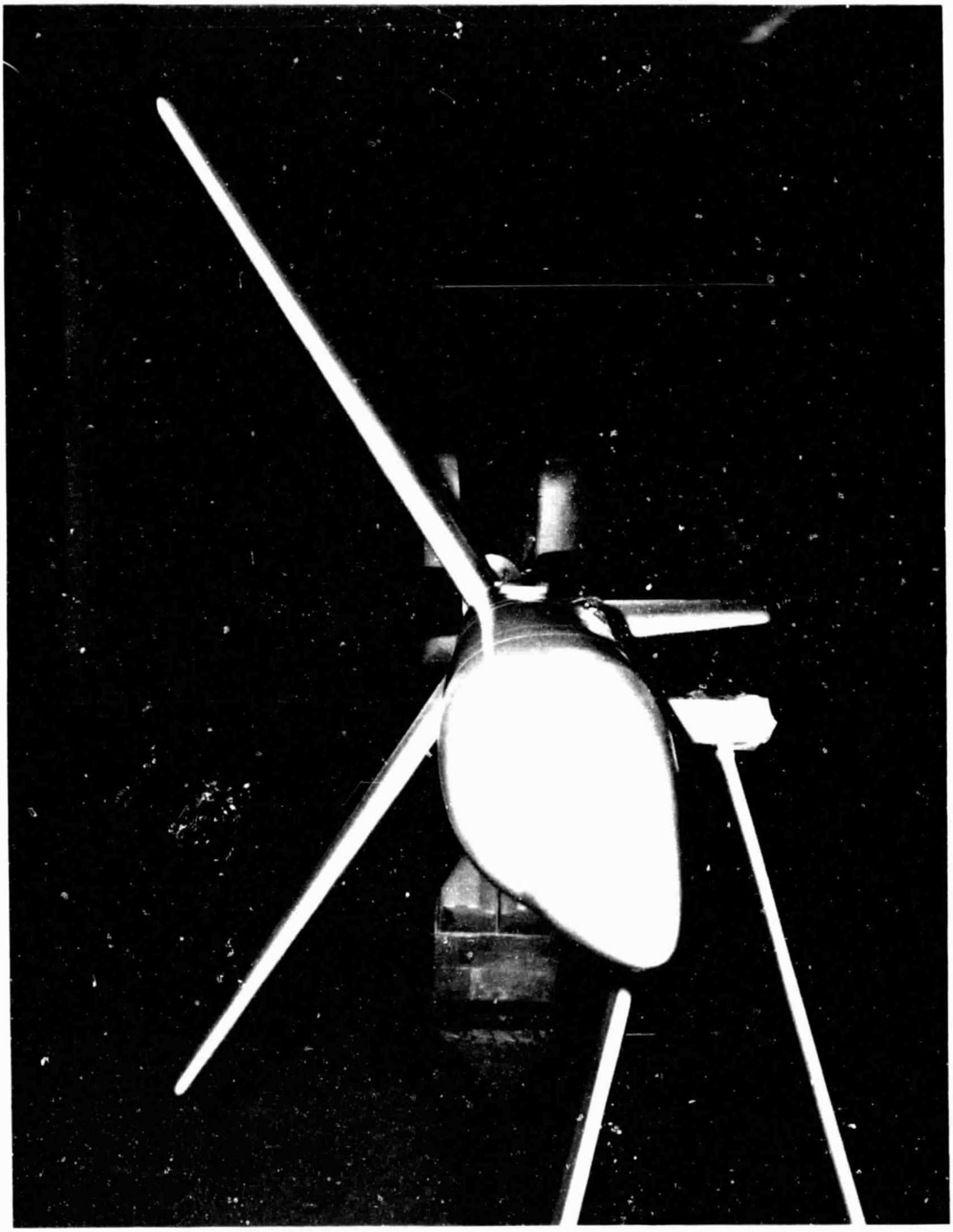

FIGURE 11. HEAD-ON VIEW OF MODEL WITH Y-TAIL IN FUSELAGE ORIENTATION $\psi = 90°$

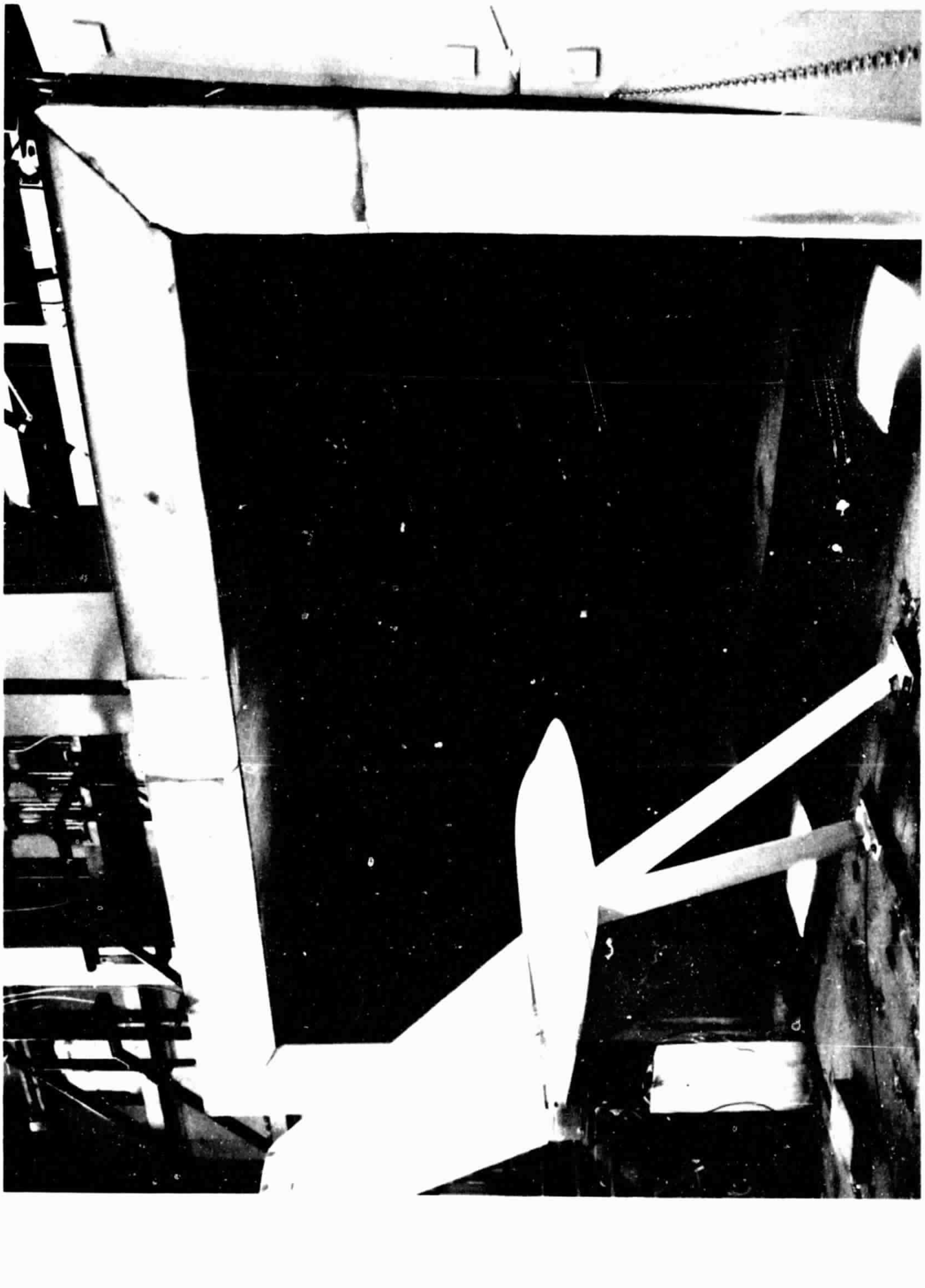

FIGURE 12. FUSELAGE WITH I-TAIL EMPENNAGE (ψ = 0°)

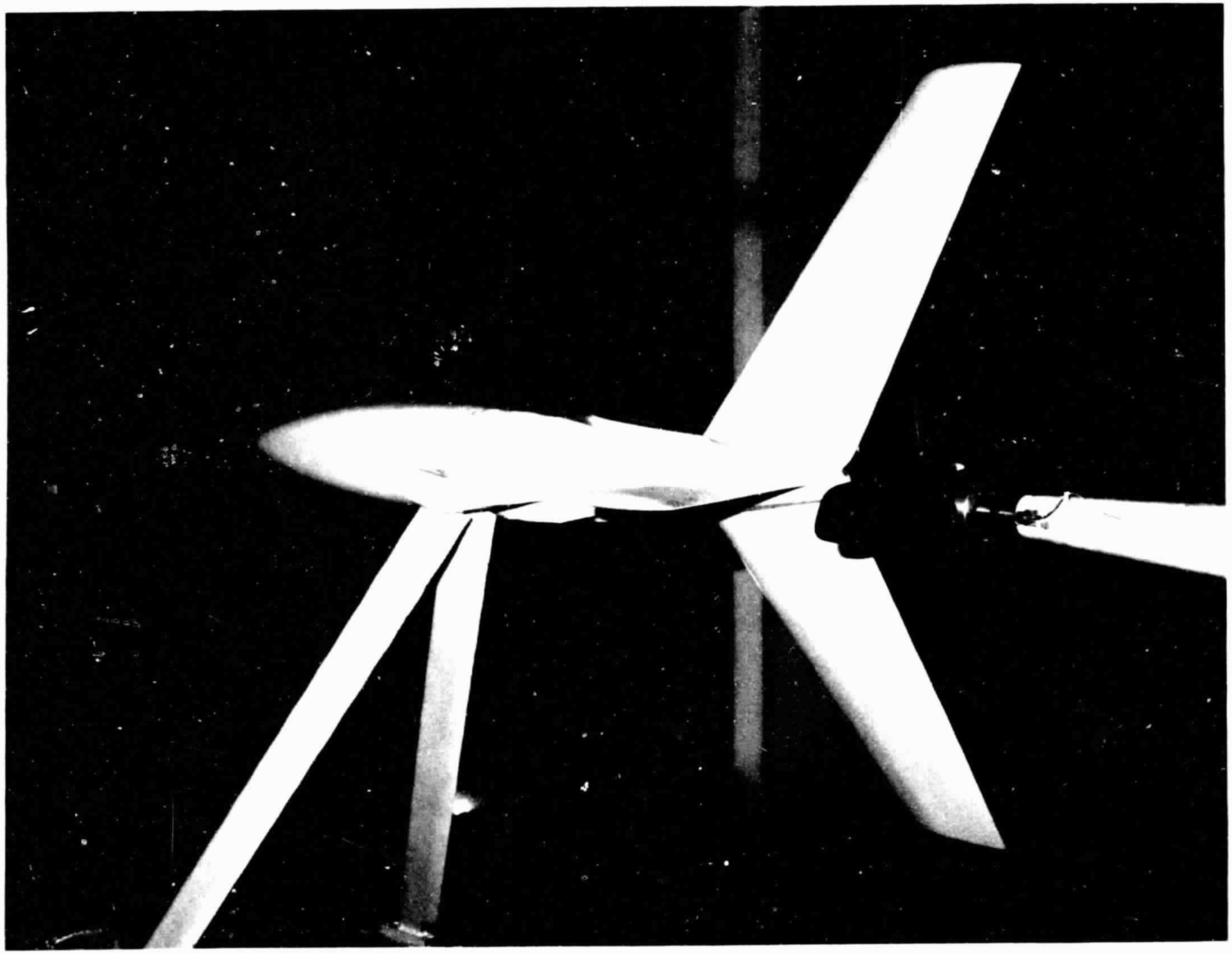

FIGURE 13. TEST MODEL SHOWING MOUNTING FOR ψ = 90° ORIENTATION

(a) Y-Tail, Side View

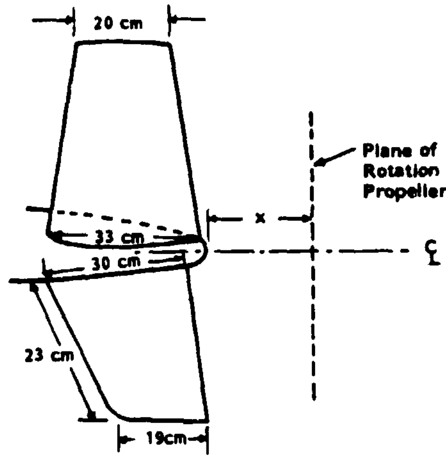

(b) Y-Tail, Rear View

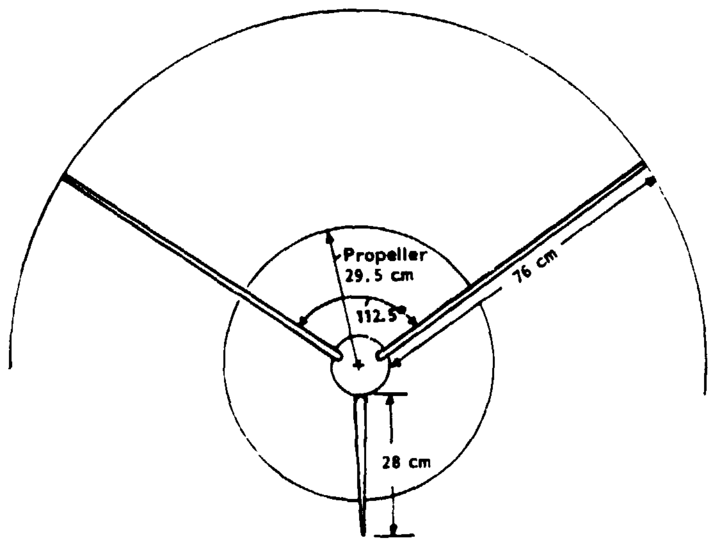

(c) I-Tail, Side View

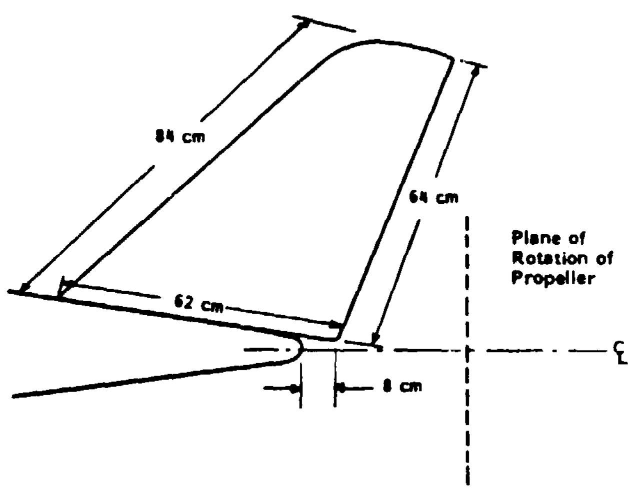

FIGURE 14. DIAGRAMS OF TEST EMPENNAGES

2.2.3 Model Propeller

The model propeller used in the test had four blades having the designation SR-2. These blades have zero sweep, as is the case for the majority of general aviation (GA) propellers but, compared to conventional GA designs, the SR-2 blade has a long chord and a relatively low thickness-to-chord ratio of 2% at the tip. Typical dimensions for the test propeller are given in Table 1, which also contains a plan of the blade shape.

A photograph of the model propeller mounted on the spinner and drive shaft is shown in Figure 15. The blade pitch angle was adjusted manually. Appropriate values of the angle were determined for the different airflow speeds and propeller rotational speeds, and the angle was adjusted prior to each test run.

The SR-2 propeller was selected initially by NASA as a baseline for comparison with swept blade designs under evaluation for the advanced turboprop (ATP) airplane. In the case of the ATP design the flight condition of primary interest is cruise at $M = 0.80$ and a blade-tip rotational Mach number of about 0.80, rather than take-off and approach, the conditions explored in the present tests. Wind tunnel acoustic measurements for the model SR-2 propeller (with 8 blades) under cruise conditions can be found in References 16 through 18. The propeller was used in the present tests because of its ready availability.

2.3 Instrumentation

2.3.1 Data Acquisition

Acoustic data from the tests were acquired using thirteen Bruel and Kjaer Type 4133, 1.3 cm (0.5 inch) diameter microphones. Signals from the microphones were passed through Bruel and Kjaer Type 222-2 conditioners to a 14-channel Ampex FR1300 tape recorder. The data

Table 1

Test Propeller Characteristics

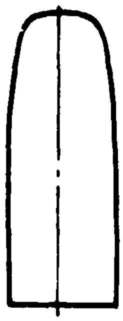

SR-2

Propeller diameter	59.1 cm	(23.3 inches)
Hub diameter	9.8 cm	(3.9 inches)
Chord	9.2 cm	(3.6 inches)
Thickness	0.16 cm	(0.06 inch)
Tip Sweep Angle	0°	

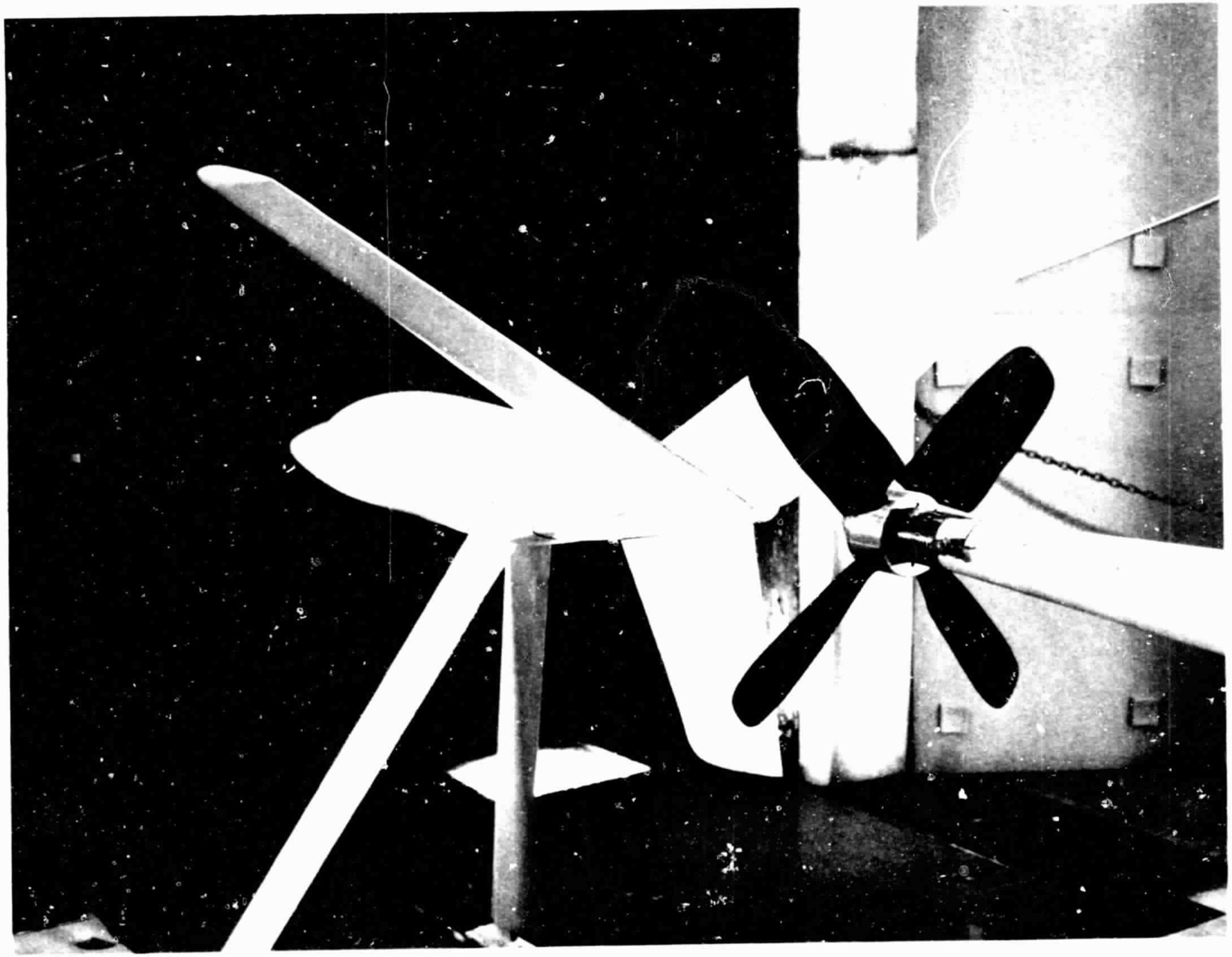

FIGURE 15. VIEW OF MODEL PROPELLER INSTALLED IN TEST RIG BEHIND Y-TAIL EMPENNAGE

were recorded on magnetic tape for a minimum of 30 seconds per run. During data recording the microphone signals were monitored on a Tektronix Model 475 oscilloscope. In addition sample on-line narrowband analysis was performed using a Hewlett Packard Type 5420B Digital Signal Analyzer. A block diagram of the data acquisition system is given in Figure 16.

Locations of the B&K microphones are shown in Figure 17 and listed in Table 2. Microphones 1 through 6 were arranged in an arc of radius 4.27 m (14 ft) outside the tunnel flow with the microphones pointing towards the model propeller. Five of these microphones, mounted on 1.1 m (3.5 ft) high stands can be seen in Figure 7. Two other microphones (#10 and #13) were located in the same horizontal plane but on the opposite side of the test section. One of the microphone stands can be seen in Figure 8. These two microphones were out of the main flow of the tunnel but may have encountered some buffet from the edge of the free shear layer. The microphones could not be moved further from the flow because of constraints imposed by access to the tunnel control area. Microphones #11 and 12 were placed in the vertical plane above the test section, also in an arc of radius 4.27 m (14 ft) centered at the propeller axis. These microphones were not influenced by the tunnel flow.

Three microphones were located within the tunnel flow. In these cases the microphones were fitted with Bruel and Kjaer Type UA0386 nose cones and were oriented so that they pointed in the upstream direction. Two of the microphone installations (#7 and #8) can be seen in Figure 8. The third in-flow microphone was located ahead of the model fuselage and close to the tunnel centerline.

The microphone array remained fixed throughout the acoustic test program. When the test model was oriented ($\psi = 0°$) as shown in Figure 8 microphones 1 through 6 and microphones 10 and 13 represented measurements to the side of an airplane in flight;

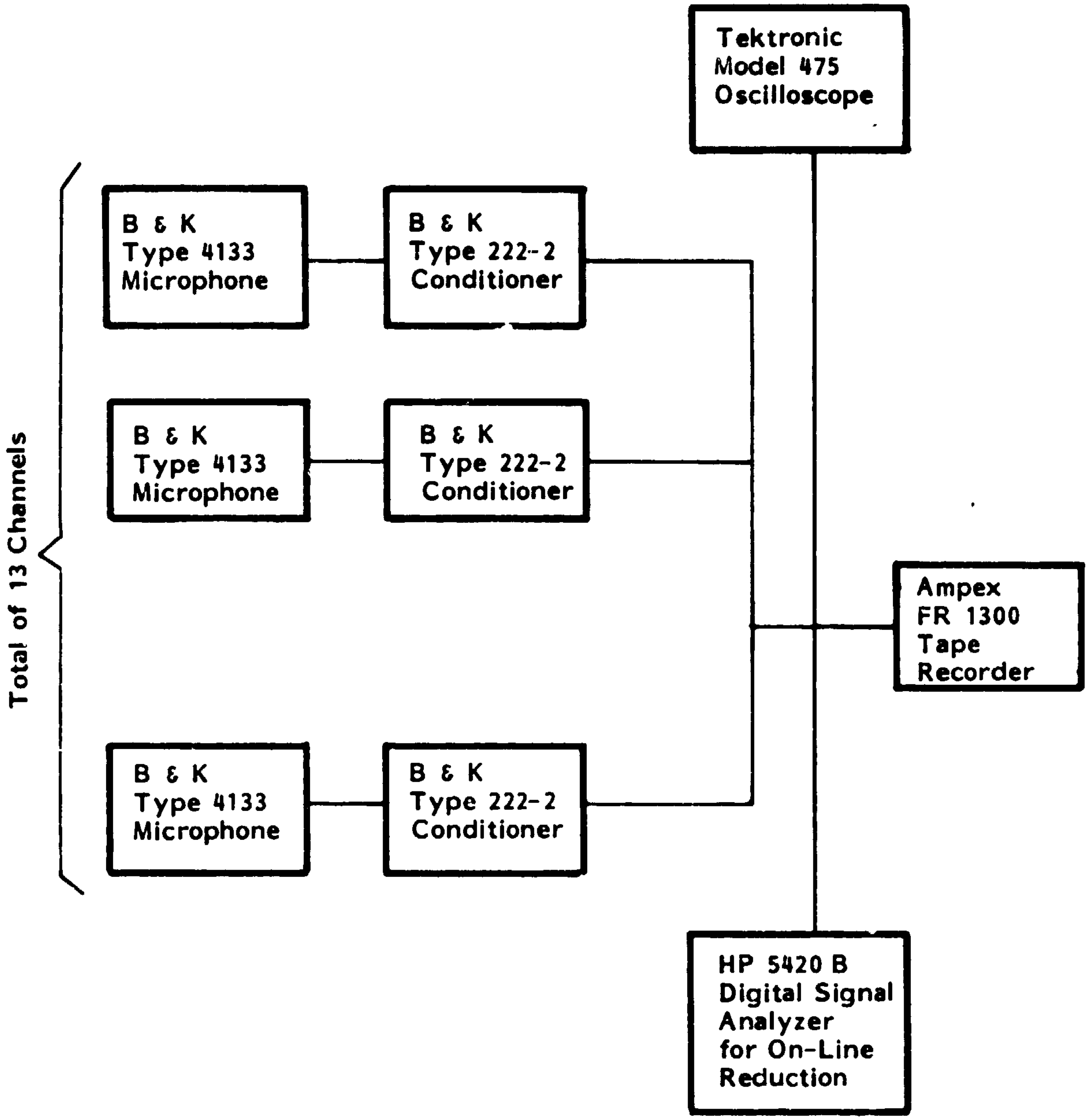

FIGURE 16. BLOCK DIAGRAM FOR DATA ACQUISITION SYSTEM

(a) Plan View

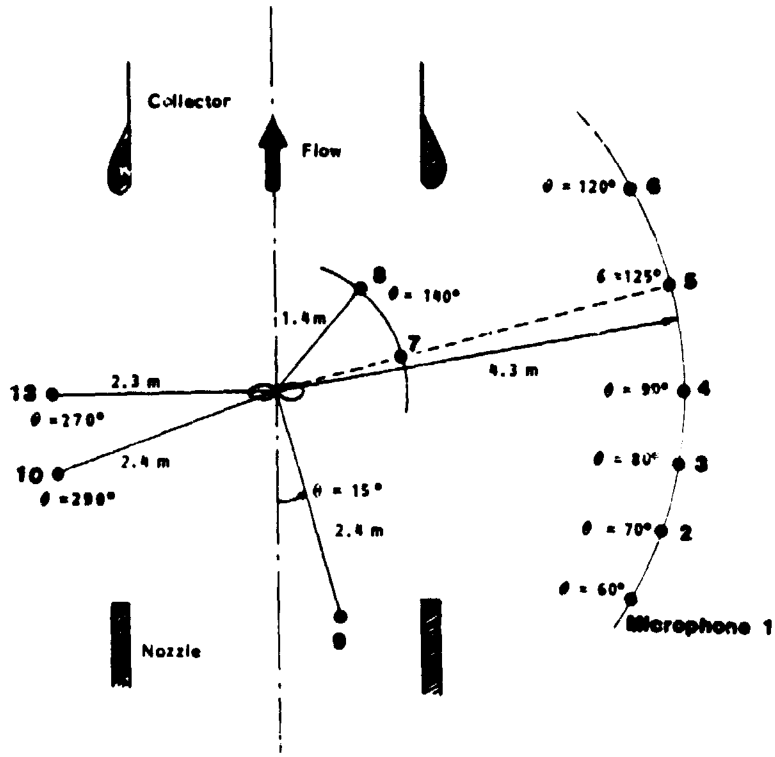

(b) View Looking Downstream (θ = 90/270°)

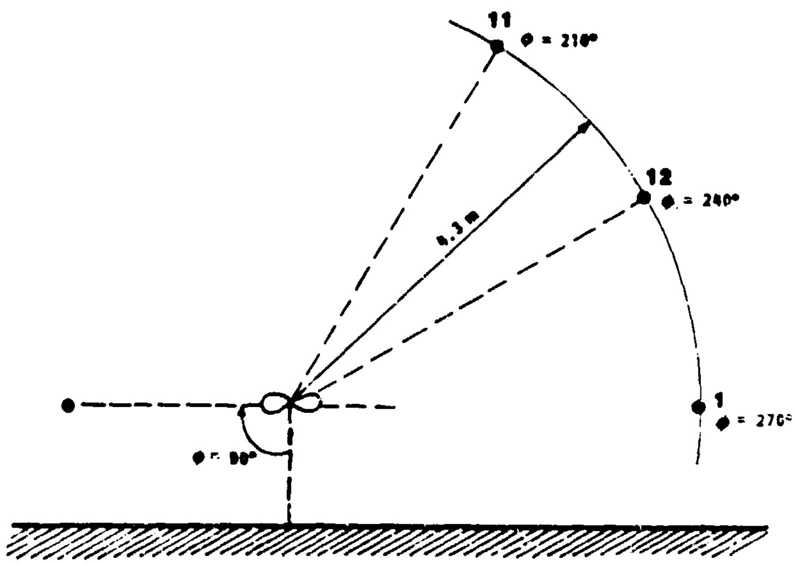

FIGURE 17. DIAGRAM OF MICROPHONE LOCATIONS

TABLE 2. MICROPHONE LOCATIONS

Mic. #	Radius M	Radius Ft	θ^* deg.	ϕ^* Deg. $\psi = 0$	ϕ^* Deg. $\psi = 90°$	Nose Cone Fitted	Mic. In. Flow	Remarks
1	4.3	14.0	60	270	0	No	No	
2	4.3	14.0	70	270	0	No	No	
3	4.3	14.0	80	270	0	No	No	
4	4.3	14.0	90	270	0	No	No	
5	4.3	14.0	105	270	0	No	No	
6	4.3	14.0	120	270	0	No	No	Possibly some buffet from flow
7	1.4	4.5	105	270	0	Yes	Yes	
8	1.4	4.5	140	270	0	Yes	Yes	
9	2.4	8.0	15	270	0	Yes	Yes	
10	2.4	7.9	290	90	180	No	No	Possibly some buffet from flow
11	4.3	14.0	90	210	300	No	No	
12	4.3	14.0	90	240	330	No	No	
13	2.3	7.6	270	90	180	No	No	Possibly some buffet from flow

θ = 0° along tunnel centerline in upstream direction; positive θ in counterclockwise direction viewed from above

ϕ = 0° directly below airplane; positive θ in counterclockwise direction viewed in upstream direction microphones 11 and 12 were above the airplane. Then, when the model was rotated through 90° (ψ= 90°) the array of microphones 1 through 6 was located beneath the airplane and microphones 10 and 13 above the airplane.

2.3.2 Data Reduction

The data reduction instrumentation is shown in the block diagram in Figure 18. Signals from the Ampex FR1300 tape recorder were reduced into narrowband or one-third octave band sound pressure level spectra. The narrowband data reduction was performed using a Hewlett-Packard system and the one-third octave band data reduction using a GenRad Model 1995 Integrating Real Time Analyzer. The data reduction process was controlled by means of a Hewlett-Packard 87XM Personal Computer.

One-third octave band spectra were reduced using the GenRad 1995 Real Time Analyzer with a flat response from 25 Hz to 20,000 Hz and a linear weighting function. The spectra were obtained by integrating over a 15-second sample length. The computer program GENRAD3 (see Appendix A) was used on the HP87 computer as controller, taking the integrated spectrum from the GenRad 1995, adjusting for microphone gains, adding shear layer corrections to the spectrum, normalizing the data to a distance of 4.3 m (14 ft), calculating the A-weighted level and plotting and listing the corrected or uncorrected spectrum levels. The spectrum levels could be stored on disc, using the HP-9121D Flexible Disc Memory, identified by run number, data point and microphone number for future reference.

Narrowband spectra were obtained using the HP5420 FFT Narrowband Analyzer. The set-up state used for the data reduction is shown in Figure 19 together with an example of the spectrum for a calibration signal. The data were reduced in the frequency range 0 to 6400 Hz, with 512 spectral lines (high resolution auto-spectrum),

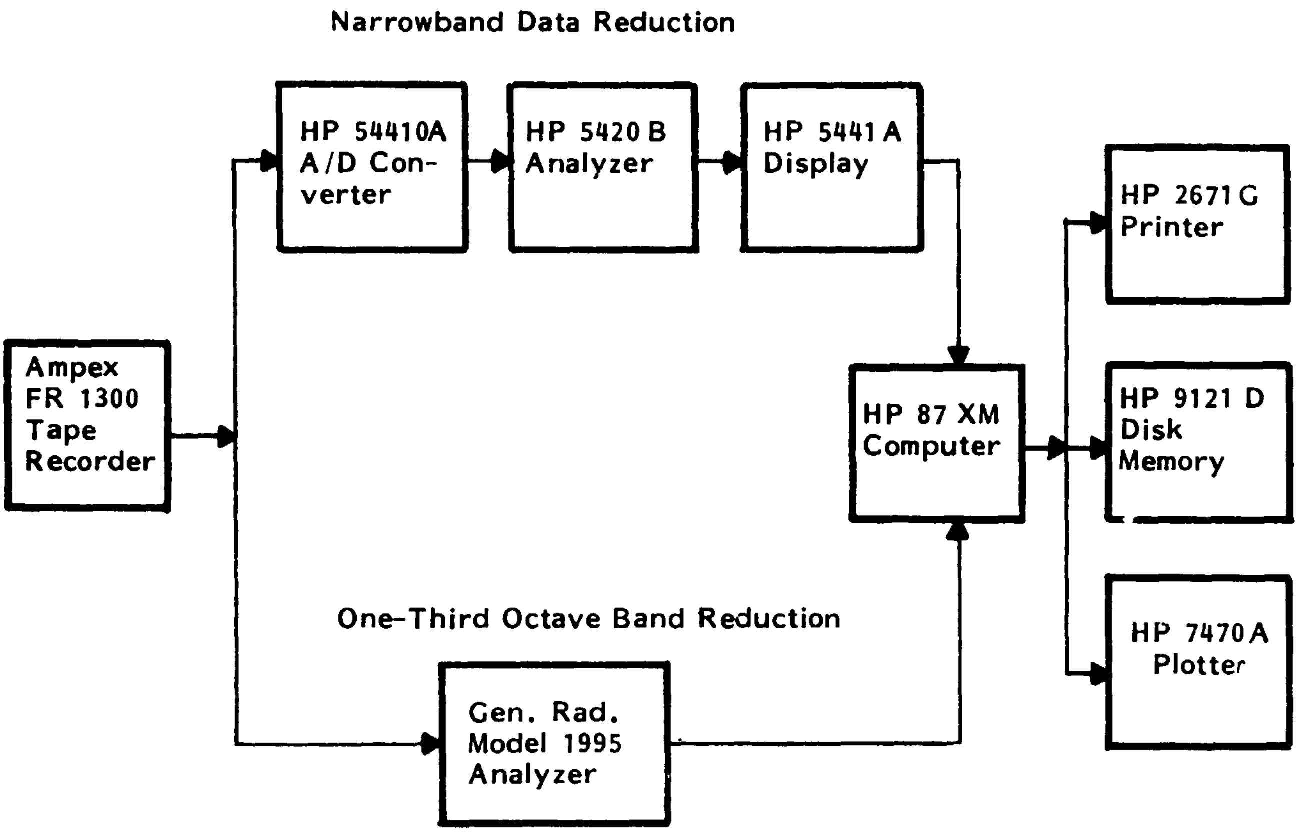

FIGURE 18. BLOCK DIAGRAM FOR DATA REDUCTION SYSTEM

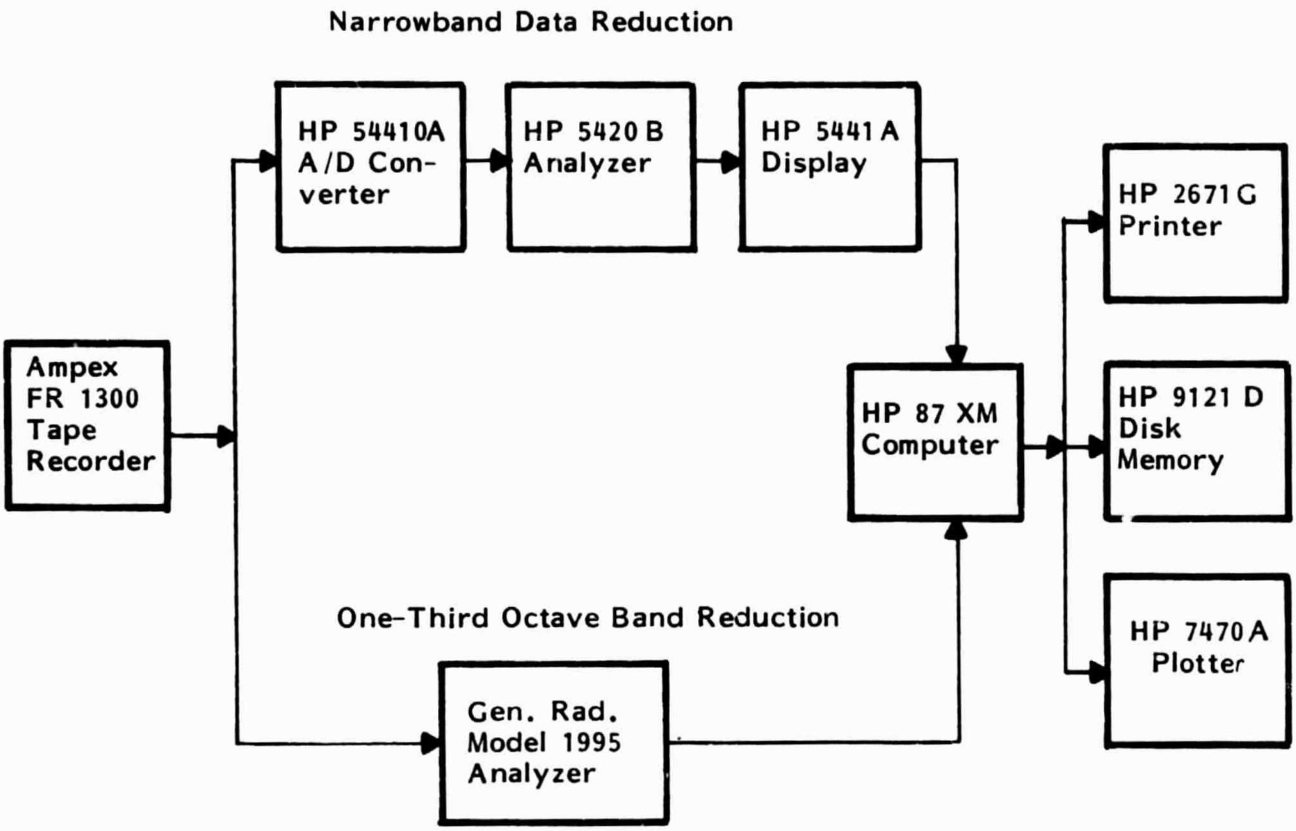

FIGURE 18. BLOCK DIAGRAM FOR DATA REDUCTION SYSTEM

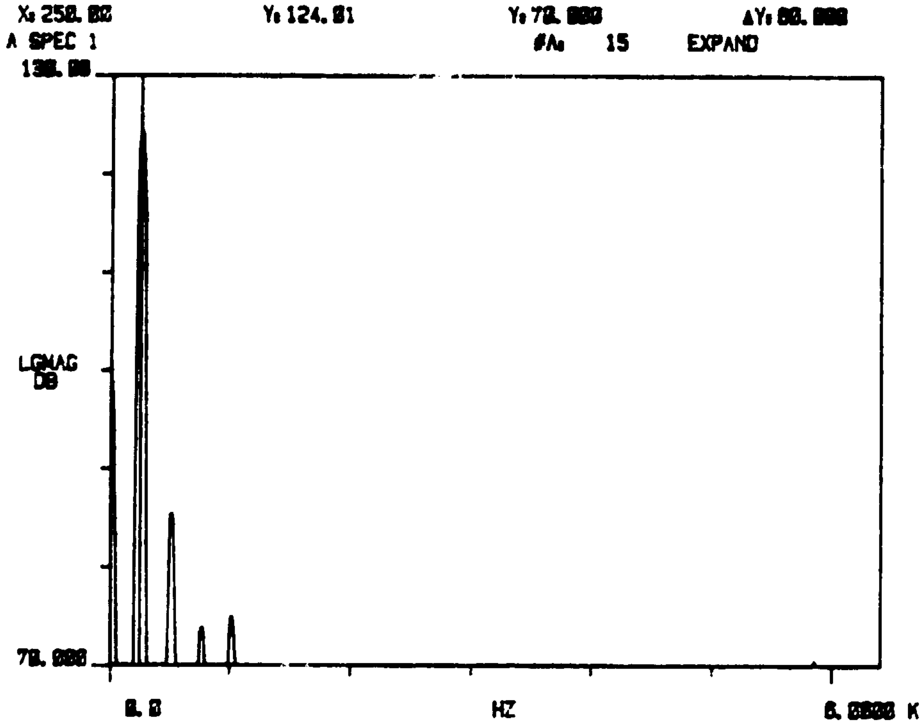

SETUP STATE

MEASUREMENT : HI-RES AUTO SPECTRUM

AVERAGE : 1000 , STABLE

SIGNAL : SINUSOIDAL

TRIGGER : FREE RUN , CHNL 1

CENT FREQ : 0.0 HZ

BANDWIDTH : 6.40000 KHZ

TIME LENGTH : 80.0000 mS

ΔF : 12.5000 HZ   ΔT : 39.0625 μS

ADC CHNL	RANGE	AC/DC	DELAY	CAL (C1/C2)
• 1	2.5 V	AC	0.0 S	3.25000 E+0
2	10 V	AC	0.0 S	1.00000

FIGURE 19. TYPICAL SETUP STATE FOR HP 5420 ANALYZER DURING DATA REDUCTION

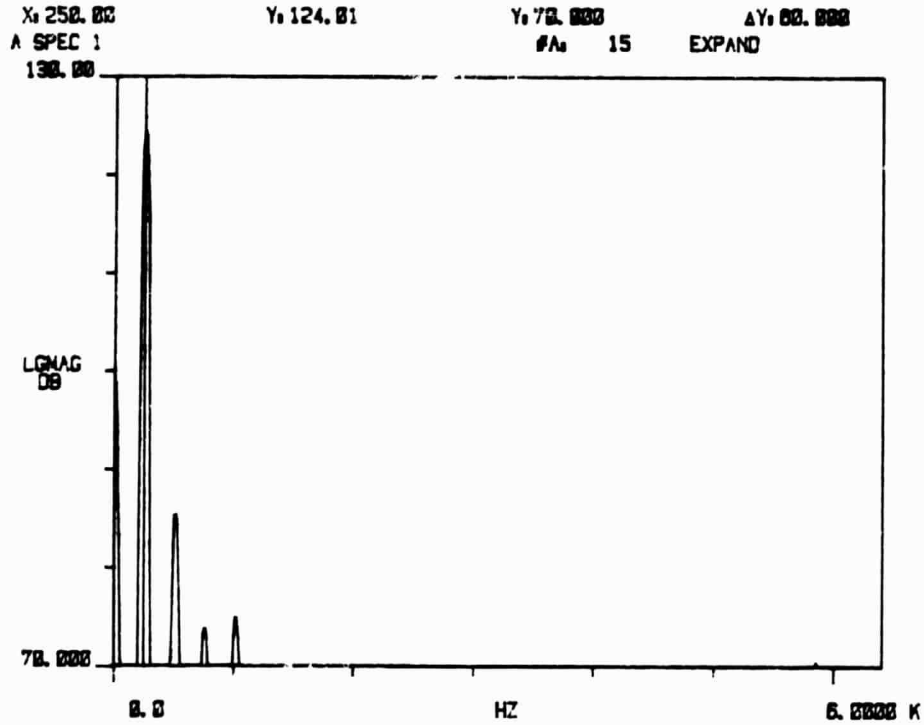

SETUP STATE

MEASUREMENT : HI-RES AUTO SPECTRUM

AVERAGE : 1000 , STABLE

SIGNAL : SINUSOIDAL

TRIGGER : FREE RUN , CHNL 1

CENT FREQ : 0.0 HZ

BANDWIDTH : 6.40000 KHZ

TIME LENGTH : 80.0000 mS

ΔF : 12.5000 HZ   ΔT : 39.0625 µS

ADC CHNL	RANGE	AC/DC	DELAY	CAL (C1/C2)
* 1	2.5 V	AC	0.0 S	3.25000 E+0
2	10 V	AC	0.0 S	1.00000

FIGURE 19. TYPICAL SETUP STATE FOR HP 5420 ANALYZER DURING DATA REDUCTION

giving a frequency resolution of 12.5 Hz. At least 30 averages were performed to produce the final spectrum.

The analysis mode selected for the HP5420 was that for sinusoidal-type signals. This mode has the property of giving the correct maximum spectrum level for narrowband peaks of bandwidth less than the filter bandwidth. However it results in a relatively wide filter bandwidth; for the conditions given earlier the effective filter bandwidth was approximately 42 Hz (12.5 x 3.4). Since the output of the analyzer in the sinusoidal mode is "power in the band", the broadband levels must be adjusted by the filter bandwidth (-16 dB) to give the power spectral density level.

Having obtained the average spectrum levels, the harmonics could be indicated on the HP 5420 by setting the cursor on the first harmonic (or fundamental) of the blade passage frequency and selecting the harmonic indicator for a maximum of 21 harmonics. This process stored the harmonic frequencies and associated sound levels in memory for later retrieval by the HP 87 controller.

The narrowband spectrum levels (512 lines maximum), bandwidth, harmonic frequencies and harmonic sound pressure levels could be transferred from the HP 5420 to the HP 87 by use of computer program CEDAR2 (see Appendix A). Adjustments were made for gain, shear layer corrections and normalization to a standard radial distance of 4.3 m (14 feet). The adjusted or unadjusted spectra could be plotted and stored on disc; the harmonic frequencies and levels could be listed and stored on disc. As for one-third octave band analysis, run number, data point and microphone number were used as identifiers for future retrieval of the data.

giving a frequency resolution of 12.5 Hz. At least 30 averages were performed to produce the final spectrum.

The analysis mode selected for the HP5420 was that for sinusoidal-type signals. This mode has the property of giving the correct maximum spectrum level for narrowband peaks of bandwidth less than the filter bandwidth. However it results in a relatively wide filter bandwidth; for the conditions given earlier the effective filter bandwidth was approximately 42 Hz (12.5 x 3.4). Since the output of the analyzer in the sinusoidal mode is "power in the band", the broadband levels must be adjusted by the filter bandwidth (-16 dB) to give the power spectral density level.

Having obtained the average spectrum levels, the harmonics could be indicated on the HP 5420 by setting the cursor on the first harmonic (or fundamental) of the blade passage frequency and selecting the harmonic indicator for a maximum of 21 harmonics. This process stored the harmonic frequencies and associated sound levels in memory for later retrieval by the HP 87 controller.

The narrowband spectrum levels (512 lines maximum), bandwidth, harmonic frequencies and harmonic sound pressure levels could be transferred from the HP 5420 to the HP 87 by use of computer program CEDAR2 (see Appendix A). Adjustments were made for gain, shear layer corrections and normalization to a standard radial distance of 4.3 m (14 feet). The adjusted or unadjusted spectra could be plotted and stored on disc; the harmonic frequencies and levels could be listed and stored on disc. As for one-third octave band analysis, run number, data point and microphone number were used as identifiers for future retrieval of the data.

2.4 Test Conditions

The test configurations and conditions are listed in Table 3. The first five test runs were performed with the test section empty and then with only the propeller system in the tunnel flow. Test runs 6 through 8 were then conducted with the model fuselage present without an empennage and at the $\psi = 0°$ orientation. Similar tests were performed later for $\psi = 90°$ (runs 60 through 64). These two values of ψ were selected so that the main microphone array represented sideline ($\psi = 0°$) or flyover ($\psi = 90°$) positions. Measurements for the Y-tail configuration were performed in runs 9 through 25 and runs 30 through 40 for $\psi = 0°$, and runs 65 through 73 for $\psi = 90°$. Four runs (26 through 29) were conducted with the dorsal fin off (V-tail) and $\psi = 0°$. Then the vertical fin configuration (I-tail) was tested in runs 41 - 49 for $\psi = 0°$ and runs 50 - 59 for $\psi = 90°$.

The tests involved a number of limited parametric variations. Two flow speeds of 45.7 m/s (150 ft/sec) and 62.5 m/s (205 ft/sec) and three propeller rotational speeds (4000, 6000 and 8200 rpm) were used for most of the runs. Appropriate values were selected for blade angle for each combination of flow speed and rpm.

The distance between the model fuselage and propeller was varied in both longitudinal (x-coordinate) and vertical (y-coordinate) directions with the main interest being directed to the Y-tail configuration. The origin for the (x,y) coordinates given in Table 3 was on the fuselage centerline at the rear-most point on the tail cone. For most tests the empennage angle of incidence was zero but this was adjusted to 5° for four runs (30 - 33) while the longitudinal separation distance was varied for the Y-tail.

2.4 Test Conditions

The test configurations and conditions are listed in Table 3. The first five test runs were performed with the test section empty and then with only the propeller system in the tunnel flow. Test runs 6 through 8 were then conducted with the model fuselage present without an empennage and at the $\psi = 0°$ orientation. Similar tests were performed later for $\psi = 90°$ (runs 60 through 64). These two values of ψ were selected so that the main microphone array represented sideline ($\psi = 0°$) or flyover ($\psi = 90°$) positions. Measurements for the Y-tail configuration were performed in runs 9 through 25 and runs 30 through 40 for $\psi = 0°$, and runs 65 through 73 for $\psi = 90°$. Four runs (26 through 29) were conducted with the dorsal fin off (V-tail) and $\psi = 0°$. Then the vertical fin configuration (I-tail) was tested in runs 41 - 49 for $\psi = 0°$ and runs 50 - 59 for $\psi = 90°$.

The tests involved a number of limited parametric variations. Two flow speeds of 45.7 m/s (150 ft/sec) and 62.5 m/s (205 ft/sec) and three propeller rotational speeds (4000, 6000 and 8200 rpm) were used for most of the runs. Appropriate values were selected for blade angle for each combination of flow speed and rpm.

The distance between the model fuselage and propeller was varied in both longitudinal (x-coordinate) and vertical (y-coordinate) directions with the main interest being directed to the Y-tail configuration. The origin for the (x,y) coordinates given in Table 3 was on the fuselage centerline at the rear-most point on the tail cone. For most tests the empennage angle of incidence was zero but this was adjusted to 5° for four runs (30 - 33) while the longitudinal separation distance was varied for the Y-tail.

TABLE 3. ACOUSTIC TEST CONFIGURATIONS

RUN	DATA POINT	V		q		ψ	TAIL	i_r	N	β	X		Y		REMARKS
		m/s	ft/s	N/m^2	lb/ft^2	Deg.		Deg.	rpm	Deg.	mm	inch	mm	inch	
1	1	28-34	90-110	480-720	10-15	-	-	-	-	-	-	-	-	-	Test Section Empty
2	1	28-68	90-260	480-2870	10-60	-	-	-	-	-	-	-	-	-	Test Section Empty
3	1	0	0	0	0	-	-	-	0-8200	-	-	-	-	-	RPM Sweep, Blades off
4	1	0	0	0	0	-	-	-	1500	6	-	-	-	-	Only propeller system in tunnel
4	2	0	0	0	0	-	-	-	2000	6	-	-	-	-	Only propeller system in tunnel
4	3	0	0	0	0	-	-	-	3000	6	-	-	-	-	Only propeller system in tunnel
4	4	0	0	0	0	-	-	-	4000	6	-	-	-	-	Only propeller system in tunnel
4	5	0	0	0	0	-	-	-	6000	6	-	-	-	-	Only propeller system in tunnel
4	6	0	0	0	0	-	-	-	7000	6	-	-	-	-	Only propeller system in tunnel
4	7	0	0	0	0	-	-	-	8200	6	-	-	-	-	Only propeller system in tunnel
5	1	45.7	150	1290	27	-	-	-	4000	38	-	-	-	-	Only propeller system in tunnel
5	2	45.7	150	1290	27	-	-	-	6000	25	-	-	-	-	Only propeller system in tunnel
5	3	45.7	150	1290	27	-	-	-	8200	16	-	-	-	-	Only propeller system in tunnel
5	4	62.5	205	2390	50	-	-	-	4000	45	-	-	-	-	Only propeller system in tunnel
5	5	62.5	205	2390	50	-	-	-	6000	30	-	-	-	-	Only propeller system in tunnel
5	6	62.5	205	2390	50	-	-	-	8200	21	-	-	-	-	Only propeller system in tunnel
6	1	45.7	150	1290	27	0	OFF	-	—	-	-	-	-	-	Fuselage only
6	2	62.5	205	2390	50	0	OFF	-	—	-	-	-	-	-	Fuselage only
7	1	62.5	205	2390	50	0	OFF	-	8200	21	-	-	-	-	Fuselage only
8	1	62.5	205	2390	50	0	OFF	-	4000	45	-	-	-	-	Fuselage only

TABLE 3. ACOUSTIC TEST CONFIGURATIONS

RUN	DATA POINT	V		q		ψ	TAIL	i_r	N	β	X		Y		REMARKS
		m/s	ft/s	N/m²	lb/ft²	Deg.		Deg.	rpm	Deg.	mm	inch	mm	inch	
1	1	28-34	90-110	480-720	10-15	-	-	-	-	-	-	-	-	-	Test Section Empty
2	1	28-68	90-260	480-2870	10-60	-	-	-	-	-	-	-	-	-	Test Section Empty
3	1	0	0	0	0	-	-	-	0-8200	-	-	-	-	-	RPM Sweep, Blades off
4	1	0	0	0	0	-	-	-	1500	6	-	-	-	-	Only propeller system in tunnel
4	2	0	0	0	0	-	-	-	2000	6	-	-	-	-	Only propeller system in tunnel
4	3	0	0	0	0	-	-	-	3000	6	-	-	-	-	Only propeller system in tunnel
4	4	0	0	0	0	-	-	-	4000	6	-	-	-	-	Only propeller system in tunnel
4	5	0	0	0	0	-	-	-	6000	6	-	-	-	-	Only propeller system in tunnel
4	6	0	0	0	0	-	-	-	7000	6	-	-	-	-	Only propeller system in tunnel
4	7	0	0	0	0	-	-	-	8200	6	-	-	-	-	Only propeller system in tunnel
5	1	45.7	150	1290	27	-	-	-	4000	38	-	-	-	-	Only propeller system in tunnel
5	2	45.7	150	1290	27	-	-	-	6000	25	-	-	-	-	Only propeller system in tunnel
5	3	45.7	150	1290	27	-	·	-	8200	16	-	-	-	-	Only propeller system in tunnel
5	4	62.5	205	2390	50	-	-	-	4000	45	-	-	-	-	Only propeller system in tunnel
5	5	62.5	205	2390	50	-	-	-	6000	30	-	-	-	-	Only propeller system in tunnel
5	6	62.5	205	2390	50	-	-	-	8200	21	-	-	-	-	Only propeller system in tunnel
6	1	45.7	150	1290	27	0	OFF	-	—	-	-	-	-	-	Fuselage only
6	2	62.5	205	2390	50	0	OFF	-	—	-	-	-	-	-	Fuselage only
7	1	62.5	205	2390	50	0	OFF	-	8200	21	-	-	-	-	Fuselage only
8	1	62.5	205	2390	50	0	OFF	-	4000	45	-	-	-	-	Fuselage only

TABLE 3. ACOUSTIC TEST CONFIGURATIONS
(Continued)

RUN	DATA POINT	V		q		ψ	TAIL	i_r	N	β	X		Y		REMARKS
		m/s	ft/s	N/m²	lb/ft²	Deg.		Deg.	rpm	Deg.	mm	inch	mm	inch	
9	1	45.7	150	1290	27	0	Y	0	-	-	-	-	-	-	Propeller off
9	2	62.5	205	2390	50	0	Y	0	-	-	-	-	-	-	Propeller off
10	1	62.5	205	2390	50	0	Y	0	8200	21	146	5.8	0	0	
11	1	62.5	205	2390	50	0	Y	0	8200	21	229	9.0	0	0	
12	1	62.5	205	2390	50	0	Y	0	8200	21	305	12.0	0	0	
13	1	62.5	205	2390	50	0	Y	0	8200	21	403	15.9	0	0	
14	1	62.5	205	2390	50	0	Y	0	8200	21	575	22.6	0	0	
15	1	62.5	205	2390	50	0	Y	0	8200	21	108	4.3	0	0	
16	1	62.5	205	2390	50	0	Y	0	8200	21	238	9.4	0	0	
17	1	62.5	205	2390	50	0	Y	0	6000	30	238	9.4	0	0	
18	1	62.5	205	2390	50	0	Y	0	3800	45	238	9.4	0	0	
19	1	45.7	150	1290	27	0	Y	0	4000	38	238	9.4	0	0	
20	1	45.7	150	1290	27	0	Y	0	6000	25	238	9.4	0	0	
21	1	45.7	150	1290	27	0	Y	0	8200	16	238	9.4	0	0	
22	1	62.5	205	2390	50	0	Y	0	7300	21	238	9.4	0	0	
22	2	62.5	205	2390	50	0	Y	0	7400	21	238	9.4	0	0	
22	3	62.5	205	2390	50	0	Y	0	7600	21	238	9.4	0	0	
22	4	62.5	205	2390	50	0	Y	0	7800	21	238	9.4	0	0	
22	5	62.5	205	2390	50	0	Y	0	8000	21	238	9.4	0	0	
22	6	62.5	205	2390	50	0	Y	0	8200	21	238	9.4	0	0	

TABLE 3. ACOUSTIC TEST CONFIGURATIONS
(Continued)

RUN	DATA POINT	V		q		ψ	TAIL	i_r	N	β	X		Y		REMARKS
		m/s	ft/s	N/m^2	lb/ft^2	Deg.		Deg.	rpm	Deg.	mm	inch	mm	inch	
9	1	45.7	150	1290	27	0	Y	0	-	-	-	-	-	-	Propeller off
9	2	62.5	205	2390	50	0	Y	0	-	-	-	-	-	-	Propeller off
10	1	62.5	205	2390	50	0	Y	0	8200	21	146	5.8	0	0	
11	1	62.5	205	2390	50	0	Y	0	8200	21	229	9.0	0	0	
12	1	62.5	205	2390	50	0	Y	0	8200	21	305	12.0	0	0	
13	1	62.5	205	2390	50	0	Y	0	8200	21	403	15.9	0	0	
14	1	62.5	205	2390	50	0	Y	0	8200	21	575	22.6	0	0	
15	1	62.5	205	2390	50	0	Y	0	8200	21	108	4.3	0	0	
16	1	62.5	205	2390	50	0	Y	0	8200	21	238	9.4	0	0	
17	1	62.5	205	2390	50	0	Y	0	6000	30	238	9.4	0	0	
18	1	62.5	205	2390	50	0	Y	0	3800	45	238	9.4	0	0	
19	1	45.7	150	1290	27	0	Y	0	4000	38	238	9.4	0	0	
20	1	45.7	150	1290	27	0	Y	0	6000	25	238	9.4	0	0	
21	1	45.7	150	1290	27	0	Y	0	8200	16	238	9.4	0	0	
22	1	62.5	205	2390	50	0	Y	0	7300	21	238	9.4	0	0	
22	2	62.5	205	2390	50	0	Y	0	7400	21	238	9.4	0	0	
22	3	62.5	205	2390	50	0	Y	0	7600	21	238	9.4	0	0	
22	4	62.5	205	2390	50	0	Y	0	7800	21	238	9.4	0	0	
22	5	62.5	205	2390	50	0	Y	0	8000	21	238	9.4	0	0	
22	6	62.5	205	2390	50	0	Y	0	8200	21	238	9.4	0	0	

TABLE 3. ACOUSTIC TEST CONFIGURATIONS (Continued)

RUN	DATA POINT	V		q		ψ	TAIL	i_r	N	β	X		Y		REMARKS
		m/s	ft/s	N/m²	lb/ft²	Deg.		Deg.	rpm	Deg.	mm	inch	mm	inch	
23	1	62.5	205	1390	50	0	Y	0	8200	23	238	9.4	0	0	
24	1	62.5	205	2390	50	0	Y	0	8200	24	238	9.4	0	0	
25	1	62.5	205	2390	50	0	Y	0	8200	19	238	9.4	0	0	
26	1	62.5	205	2390	50	0	V	0	8200	21	238	9.4	0	0	Dorsal fin off
27	1	62.5	205	2390	50	0	V	0	8200	21	308	12.1	0	0	Dorsal fin off
28	1	62.5	205	2390	50	0	V	0	8200	21	111	4.4	0	0	Dorsal fin off
29	1	62.5	205	2390	50	0	V	0	8200	21	568	22.4	0	0	Dorsal fin off
30	1	62.5	205	2390	50	0	Y	5	8200	21	229	9.0	0	0	
31	1	62.5	205	2390	50	0	Y	5	8200	21	111	4.4	0	0	
32	1	62.5	205	2390	50	0	Y	5	8200	21	302	11.9	0	0	
33	1	62.5	205	2390	50	0	Y	5	8200	21*	568	22.4	0	0	*Blade changed during tests
34	1	62.5	205	2390	50	0	Y	0	8200	21*	241	9.5	-76	-3	*Blade changed during tests
35	1	62.5	205	2390	50	0	Y	0	8200	21*	111	4.4	-76	-3	*Blade changed during tests
36	1	62.5	205	2390	50	0	Y	0	8200	21*	568	22.4	-76	-3	*Blade changed during tests
37	1	62.5	205	2390	50	0	Y	0	8200	21	568	22.4	-76	-3	
38	1	62.5	205	2390	50	0	Y	0	8200	21	241	9.5	-76	-3	
39	1	62.5	205	2390	50	0	Y	0	8200	21	235	9.3	76	+3	
40	1	62.5	205	2390	50	0	Y	0	8200	21	572	22.5	76	+3	
41	1	62.5	205	2390	50	0	I	0	8200	21	562	22.1	0	0	
42	1	62.5	205	2390	50	0	I	0	8200	21	384	15.1	0	0	

TABLE 3. ACOUSTIC TEST CONFIGURATIONS
(Continued)

RUN	DATA POINT	V		q		ψ	TAIL	i_r	N	β	X		Y		REMARKS
		m/s	ft/s	N/m²	lb/ft²	Deg.		Deg.	rpm	Deg.	mm	inch	mm	inch	
43	1	62.5	205	2390	50	0	I	0	8200	21	222	8.8	0	0	
44	1	62.5	205	2390	50	0	I	0	8200	21	308	12.1	0	0	
45	1	62.5	205	2390	50	0	I	0	6000	30	308	12.1	0	0	
46	1	62.5	205	2390	50	0	I	0	3980	45	308	12.1	0	0	
47	1	45.7	150	1290	27	0	I	0	4000	38	308	12.1	0	0	
48	1	45.7	150	1290	27	0	I	0	6000	25	308	12.1	0	0	
49	1	45.7	150	1290	27	0	I	0	8200	16	308	12.1	0	0	
50	1	45.7	150	1290	27	90	I	0	8200	16	305	12.0	0	0	
51	1	62.5	205	2390	50	90	I	0	8200	21	305	12.0	0	0	
52	1	62.5	205	2390	50	90	I	0	8200	21	368	14.5	0	0	
53	1	62.5	205	2390	50	90	I	0	8200	21	572	22.5	0	0	
54	1	62.5	205	2390	50	90	I	0	8200	21	219	8.6	0	0	
55	1	62.5	205	2390	50	90	I	0	6000	30	305	12.0	0	0	
56	1	62.5	205	2390	50	90	I	0	4000	45	305	12.0	0	0	
57	1	45.7	150	1290	27	90	I	0	8200	16	305	12.0	0	0	Repeat of Run 50-1
58	1	45.7	150	1290	27	90	I	0	——	—	305	12.0	0	0	
59	1	62.5	205	2390	50	90	I	0	——	—	305	12.0	0	0	
60	1	45.7	150	1290	27	90	OFF	-	——	—	305	12.0	0	0	
61	1	62.5	205	2390	50	90	OFF	-	——	—	305	12.0	0	0	
62	1	62.5	205	2390	50	90	OFF	-	8200	21	305	12.0	0	0	

TABLE 3. ACOUSTIC TEST CONFIGURATIONS
(Continued)

RUN	DATA POINT	V		q		ψ	TAIL	i_r	N	β	X		Y		REMARKS
		m/s	ft/s	N/m²	lb/ft²	Deg.		Deg.	rpm	Deg.	mm	inch	mm	inch	
63	1	62.5	205	2390	50	90	OFF	-	6000	30	305	12.0	0	0	
64	1	62.5	205	2390	50	90	OFF	-	4000	45	305	12.0	0	0	
65	1	62.5	205	2390	50	90	Y	0	4000	45	229	9.0	0	0	
66	1	62.5	205	2390	50	90	Y	0	6000	30	229	9.0	0	0	
67	1	62.5	205	2390	50	90	Y	0	8200	21	229	9.0	0	0	
68	1	62.5	205	2390	50	90	Y	0	8200	21	308	12.1	0	0	
69	1	62.5	205	2390	50	90	Y	0	8200	21	403	15.9	0	0	
70	1	62.5	205	2390	50	90	Y	0	8200	21	572	22.5	0	0	
71	1	62.5	205	2390	50	90	Y	0	8200	21	124	4.9	0	0	
72	1	45.7	150	1290	27	90	Y	0	8200	16	229	9.0	0	0	
73	1	45.7	150	1290	27	90	Y	0	—	—	-	-	-	-	
73	2	62.5	205	2390	50	90	Y	0	—	—	-	-	-	-	

The origin of the x-coordinate was selected as the rear-most point on the fuselage as a matter of convenience. However, the separation distance with most relevance to the test data is probably that between the trailing edge of the empennage and the plane of rotation of the propeller. This distance can be determined from the x-coordinate if two other parameters are known -- the distance of the trailing edge of the root of the empennage from the x-origin and the sweep of the trailing edge of the empennage. Estimates of these parameters can be obtained from Figure 14. In the case of the Y-tail, the root of the trailing edge of the V-structure is 0.5 cm (0.25 in.) forward of the tail cone, and the trailing edge is swept forward so that at the tip of the propeller the trailing edge of the empennage is 5 cm (2 inches) forward of the tail cone. Thus if the separation between tail cone and propeller plane is 23 cm (9 inches) the propeller will be 23.5 to 28 cm aft of the V-trailing edge. Corresponding distances for the dorsal fin are 27 to 23 cm, the trailing edge being swept back. The trailing edge of the I-tail is swept backwards at an angle of about 22° and the root tip of the trailing edge is 8 cm aft of the fuselage tail cone. Thus if x is 23 cm (9 inches) the separation between empennage trailing edge and propeller plane will vary from 15 cm at the empennage root to about 4 cm at the propeller tip.

The operating conditions for the propeller are given in Table 4. Propeller tip rotational Mach numbers were in the range 0.36 to 0.74, and helical Mach numbers in the range 0.39 to 0.77. The values can be compared with typical values for general aviation aircraft [19] where both Mach numbers lie in the range 0.65 to 0.90. In the case of the propeller advance ratio the test values were 0.59 to 1.59 which corresponds fairly closely to the flight range of 0.8 to 1.5. Looking at specific test rpm conditions it is found that the Mach numbers and advance ratio at 8200 rpm are similar to flight values but the test Mach numbers are lower than flight values at 6000 and 4000 rpm. Blade passage frequencies associated with 4000, 6000 and 8200 rpm are 266.7, 400.0 and 546.7 Hz respectively.

TABLE 4. PROPELLER OPERATING CONDITIONS

FLOW SPEED, V_f m/s (ft/s)	45.7 (150)			62.5 (205)		
FLOW MACH NUMBER, M_f	0.13			0.18		
Propeller RPM	4000	6000	8200	4000	6000	8200
Blade Angle (Degrees)	38	25	16	45	30	21
Tip Rotational Speed, V_r m/s (ft/s)	124 (406)	186 (609)	254 (832)	124 (406)	186 (609)	254 (832)
Tip Rotational Mach No. M_r	0.36	0.54	0.74	0.36	0.54	0.74
Tip Helical Speed, V_h m/s (ft/s)	136 (433)	191 (627)	258 (845)	139 (455)	196 (624)	261 (857)
Tip Helical Mach No. M_h	0.39	0.56	0.76	0.41	0.57	0.77
Advance Ratio $J = V_f/ND$	1.16	0.77	0.59	1.59	1.06	0.77
Blade Passage Frequency f_B (Hz)	266.7	400.0	546.7	266.7	400.0	546.7

The test conditions can also be compared with design operating conditions for the SR-2 propeller. In this case the prop design conditions are associated with cruise at M = 0.80, and a propeller tip rotational Mach number of 0.80. However the wind tunnel test conditions refer to take-off flight rather than cruise, in which case the 8200 rpm conditions are similar to the SR-2 flight conditions.

3. DATA ANALYSIS PROCEDURES

3.1 General Approach

The main emphasis of the data presentation in this report is directed towards the narrowband acoustic spectra. There are several reasons for this emphasis but the main reason is that discrete frequency components associated with harmonics of the blade passage frequency can be readily identified and separated from broadband contributions. While this is possible for low order harmonics using one-third octave band analysis it is not possible at higher frequencies because there may be more than one harmonic in a given frequency band or the integrated broadband level may mask the discrete frequency component.

The use of narrowband spectra also makes the task of identifying "facility" noise components possible. These components may be discrete or narrowband contributions from support struts and other items immersed in the tunnel flow or may be general broadband noise from the flow itself. One objective of the analysis process is to identify such interference sources so that they can be separated from the propeller noise data.

3.2 Adjustment to Harmonic Sound Pressure Levels

Visual inspection of narrowband acoustic spectra such as the example shown in Figure 20 readily identifies several harmonic components associated with the blade passage frequency when these components stand well above the general background level. However other harmonic components have associated sound pressure levels which are fairly close to the adjacent broadband values. Although these harmonics can be identified using the harmonic pattern identification capability of the narrowband analyzer, the measured sound pressure levels will contain significant contributions from the broadband components. Thus an adjustment was made to the

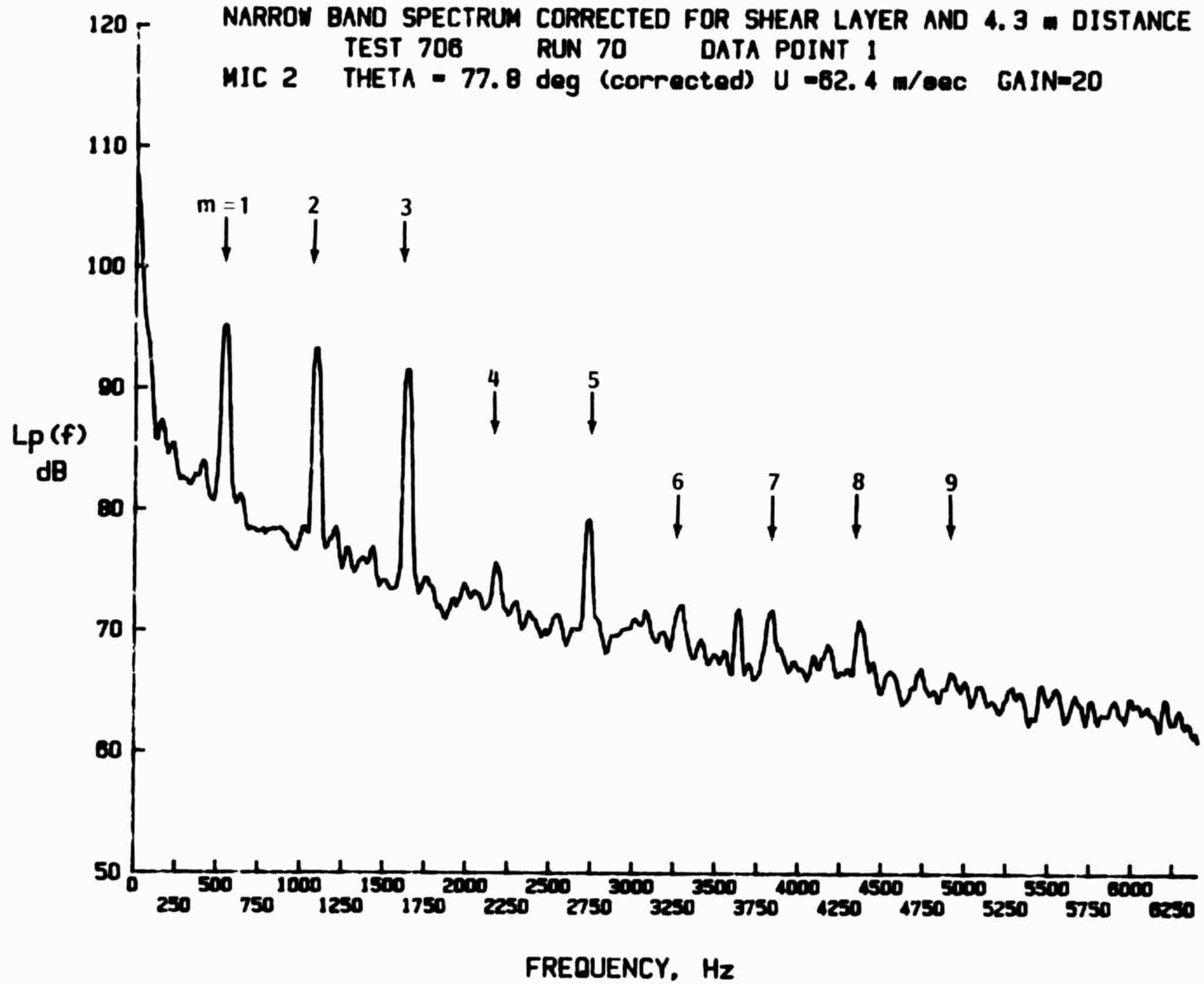

FIGURE 20. SAMPLE NARROWBAND SOUND PRESSURE LEVEL SPECTRUM OF PROPELLER NOISE MEASURED DURING TEST PROGRAM

measured values in order to obtain estimates of the discrete frequency contribution at the harmonics of the propeller blade passage frequency.

The adjustment was performed under the assumption that the discrete frequency and broadband components were uncorrelated so that calculations could be made on an energy basis. Furthermore, it was assumed that the broadband contribution at the frequency of the harmonic of interest could be estimated by interpolation of the measured sound pressure levels on either side of the spectral peak at the harmonic frequency. The discrete frequency sound pressure level could then be estimated from the energy difference between the measured data and the interpolated broadband contribution. As an example, if the measured peak at harmonic m = 6 in Figure 20 is 71.8 dB and the interpolated broadband component is 67.8 dB, then the estimated sound pressure level from the propeller harmonic component is 69.6 dB.

3.3 Distance Normalization

Since most of the microphones were located at a distance of 4.3 m (14 feet) from the propeller hub, the data were normalized to this reference distance. The normalization was performed according to the inverse square law. The resulting adjustments are given in Table 5.

3.4 Shear Layer Effect

The use of an open test section for the measurement of propeller noise has the advantage that the microphones can be placed outside the flow. Thus there is no problem of aerodynamic self-noise on the microphones. However there is a disadvantage in that the acoustic waves have to pass through the shear layer of the free jet from the tunnel nozzle. The effect of the shear layer on the far field sound pressure levels has been investigated by several

Table 5. Distance Normalization

Microphone	Adjustment to Sound Pressure Level (dB)
1	0
2	0
3	0
4	0
5	0
6	0
7	-9.9
8	-9.9
9	-4.9
10	-5.0
11	0
12	0
13	-5.3

authors [20-28]. Two phenomena have been considered -- refraction when crossing the shear layer and scattering by the turbulence in the shear layer. The influence of scattering on the present test data will be discussed in Section 3.5; refraction effects are considered here.

The scope of the present wind tunnel test did not permit any investigation of the shear layer effects. Thus, recourse is had to published results. Tests in the full-scale DNW tunnel [27] have shown that the analytical results of Amiet [20] are adequate up to a frequency of about 10,000 Hz for a tunnel flow speed of 40 m/s and up to 5,000 Hz for a flow speed of 80 m/s. Deviations from the theoretical results were found at higher frequencies and flow speeds. Empirical relationships are given by Ross et al [27] but these are not required for the present test data where interest is centered on frequencies up to 6000 Hz and flow speeds to 62.5 m/s.

The analytical model of Amiet [20] represents the shear layer as a plane of zero thickness and assumes that the observer is in the geometric and acoustic far-fields of the source. However, there is no restriction on the distance from the source to the shear layer. The geometry of the model is shown in Figure 21, where the source and observer are assumed to be in a plane normal to the shear layer and parallel to the flow. The line from the source to the observer makes an angle θ with the shear layer. The actual path of a sound ray is represented by the line SCO, and location O' is the position at which the sound would be heard in the absence of a shear layer. Thus, in order to get the true directivity of the propeller noise in the absence of a shear layer, adjustments must be estimated for the observed directivity and sound pressure level. Using the notation of Figure 21, the appropriate equations for the directivity adjustment at constant

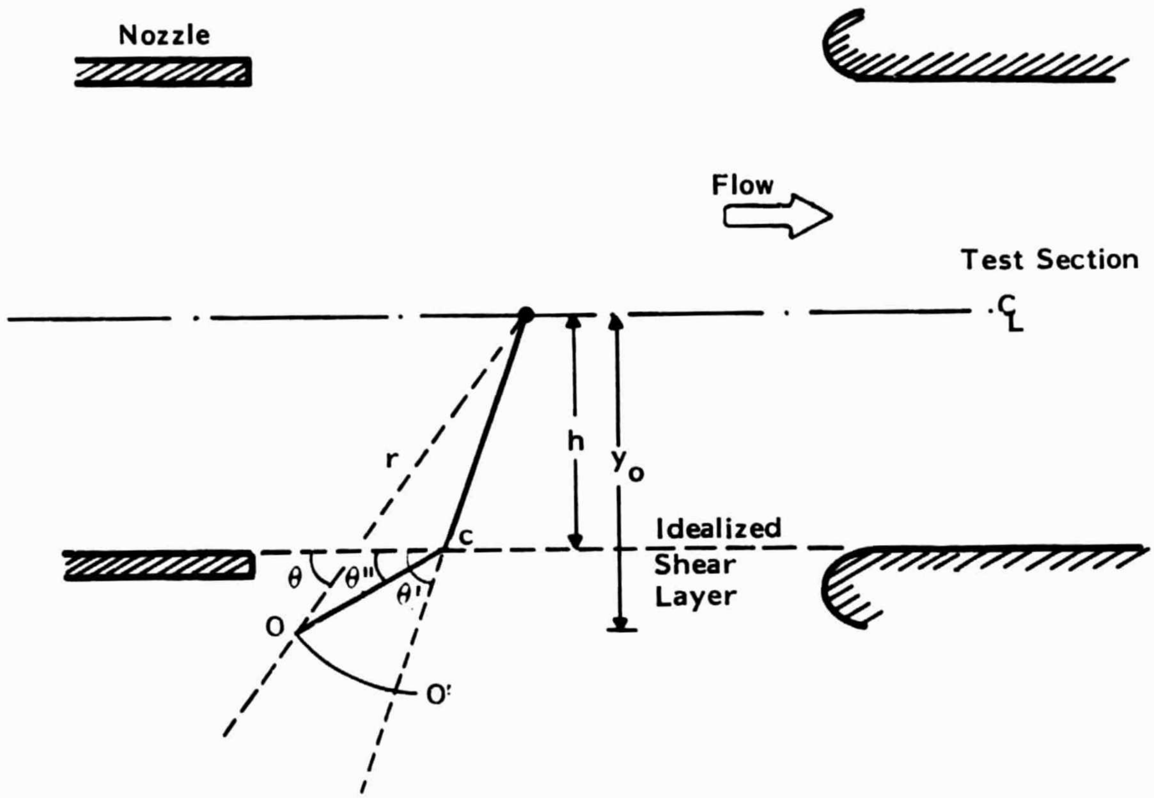

FIGURE 21. DIAGRAM OF SOUND TRANSMISSION THROUGH SHEAR LAYER OF ZERO THICKNESS

radius [20] are:-

$$\tan\theta' = \zeta/(\beta^2\cos\theta'' - M) \tag{1}$$

$$y_o\cot\theta = h\cot\theta' + (y_o - h)\cot\theta'' \tag{2}$$

where

$$\zeta = \left[(1 + M\cos\theta'')^2 - \cos^2\theta''\right]^{\frac{1}{2}}$$

and

$$\beta = (1 - M^2)^{\frac{1}{2}}$$

The adjustment to the measured sound pressure level is

$$\Delta SPL = 20\log\left(\frac{p_o'}{p_o}\right) \quad dB \tag{3}$$

where

$$\frac{p_o'}{p_o} = \left\{\frac{h\cos\theta''}{r\zeta^2}\left[\sin\theta'' + \left(\frac{y_o}{h} - 1\right)\zeta\right]^{\frac{1}{2}}\left[\sin^3\theta'' + \left(\frac{y_o}{h} - 1\right)\zeta^3\right]^{\frac{1}{2}}\right\}$$
$$\cdot \frac{1}{2\sin\theta''}\left[M^2(1+M\cos\theta'')^2 + (1-M^2\cos^2\theta'')\right]^{\frac{1}{2}}\left[\zeta + \sin\theta''(1+M\cos\theta'')\right] \tag{4}$$

Adjustments to the angle and sound pressure level, calculated according to Eqs.(1) - (4) are listed in Table 6. It is seen that the adjustments to the sound level are small, being generally less than 1 dB; adjustments to the directivity angle are less than 10°. Similar adjustments were estimated by Trebble et al [29] for tests on model scale propellers at flow speeds of 30 m/s. When computing the adjustments listed in Table 6 it was assumed that the distance h from the source to the shear layer was 1.5 m (5 ft) for all microphone locations except 11 and 12 (Microphones 7 through 9 were excluded, of course, since they were located within the flow). Microphones 11 and 12 were above the horizontal plane containing the source and the other microphones. Strictly speaking Microphones 11 and 12 do not satisfy the condition of Amiet's analytical model that the source and observer lie in a plane normal

Table 6. Adjustments Due to Refraction at Shear Layer

Micro-phone #	θ degrees	V = 62.5 m/s		V = 45.7 m/s	
		θ' degrees	ΔSPL dB	θ' degrees	ΔSPL dB
1	60	68.5	1.2	65.9	0.8
2	70	77.8	0.9	75.5	0.6
3	80	87.2	0.6	85.2	0.4
4	90	96.8	0.2	95.0	0.1
5	105	111.2	-0.2	109.7	-0.2
6	120	126.1	-0.6	124.6	-0.5
10	290	285.6	0.7	286.9	0.5
11	90	97.5	0.2	95.5	0.1
12	90	96.3	0.2	94.6	0.1
13	270	266.3	0.2	267.3	0.1

to the shear layer. However, this violation is neglected for present purposes and values of h are computed as though the source/observer plane was normal to the shear layer. Estimated values of h are 1.2 m (4.0 ft) for microphone 11 and 1.8 m (5.8 ft) for microphone 12.

3.5 Turbulence Scattering

It has been observed [22,26-28] that when a discrete frequency acoustic signal passes through the turbulence in a shear layer there is a broadening of the frequency peak. The broadening is associated with a reduction in the peak value of the sound level of the discrete frequency, the total energy in the spectral peak remaining roughly constant. This spectral broadening is of consequence in the present test only if there is an observable change in the sound pressure levels of the propeller harmonics. If the filter bandwidth used in the data reduction is sufficiently larger that the energy of the harmonic stays within the bandwidth, then there will be no observable variation in harmonic level. On the other hand if the filter bandwidth is less than the spectral peak the observed level of the harmonic will be lower than it should be, and an adjustment will be required.

First, it is appropriate to review the published experimental findings [26-28]. The data indicate that spectral broadening becomes increasingly important as frequency, shear layer thickness, and flow speed or Mach number increases. Ross [26] used measurements in the scale model of the DNW wind tunnel to develop an empirical relationship between the spectral broadening and reduction of peak level on one hand and the flow parameters on the other. The relationship between the peak bandwidth Δf_{10} (at the 10 dB down points) and the flow parameters was given as

$$\Delta f_{10} = 380 \ (M\delta/\lambda)^{0.67} \tag{5}$$

where M is the flow Mach number, δ the shear layer thickness and λ the acoustic wavelength. Significant effects on the peak sound pressure level were observed when $(M\delta/\lambda)$ exceeded 0.5.

In later work Ross et al [27] determined somewhat different relationships based on measurements in the fullscale DNW tunnel. Although they do not give a specific equation for the spectral bandwidth they note that it increases almost linearly with tone frequency, approximately as the third power of airflow speed, and somewhat weakly with shear layer thickness. From the small amount of information given [27] an empirical relationship can be developed for the bandwidth Δf_3 of the 3 dB down points.

$$\frac{\Delta f_3}{f} = 2.46 \times 10^{-6} \, V^{2.1424} \qquad (6)$$

where flowspeed V is measured in m/s.

Suppose now that it is assumed that the dependence of Δf_3 on δ is the same as that given in the earlier work [26].

$$\text{i.e., } \Delta f_3 \propto \delta^{0.67}$$

Then the empirical relationship of Eq.(6) becomes

$$\frac{\Delta f_3}{f} = 3.14 \times 10^{-6} \, V^{2.1424} \, \delta^{0.67} \qquad (7)$$

In deriving Eq.(7) it was assumed, as in [26], that the shear layer thickness can be estimated from

$$\delta = 0.16 \, x \qquad (8)$$

where x is the distance downstream from the nozzle lip.

Eqs.(7) and (8) can now be applied to the current propeller/empennage test configuration. With V = 62.5 m/s and δ estimated to be 0.26 m at the propeller plane, then

$$\frac{\Delta f_3}{f} = 0.89\%$$

Thus, at $f = 500$ Hz, $\Delta f_3 = 4.4$ Hz and at $f = 6000$ Hz $f_3 = 53$ Hz. Here it is assumed that $\theta = 90°$. For propagation in the forward direction ($\theta < 90°$) the shear layer will be thinner but the path through the shear layer will be increased because of the angle of incidence. The net change, relative to $\theta = 90°$, is probably small. In the aft direction ($\theta > 90°$), the path through the shear layer will be longer than at $\theta = 90°$, with a consequential increase in the scattering effect. To estimate this effect consider microphone location 6 at $\theta = 120°$. Using Eq.(8) the predicted thickness of the shear layer is 0.40 m but the path traveled by the acoustic ray will be about 0.46 m because the ray will not be incident normally to the layer. The empirical prediction method now gives

$$\Delta f_3 = 6.6 \text{ Hz at } 500 \text{ Hz}$$

and $$\Delta f_3 = 79 \text{ Hz at } 6000 \text{ Hz}.$$

It is now possible to review the measured narrowband spectra. This can be done in several ways.

(a) by comparing the bandwidths of the spectral peaks at different frequencies to see if the bandwidth increases with frequency,

(b) by comparing the bandwidths of the spectral peaks at a given location outside the shear layer with and without tunnel flow, or,

(c) by comparing spectra at locations in (#7) and outside (#5) the flow.

Figure 22 compares narrowband sound pressure level spectra measured at microphone location 2 without (Figure 22(a)) and with (Figure 22(b)) flow in the test section. Qualitatively, the bandwidths of the harmonic peaks appear to be independent of both frequency and flow speed. In all cases the bandwidth of the peaks is that of the effective narrowband filter used in the data reduction process, i.e., 42 Hz (see Section 2.3.2).

In Figure 23* spectra are compared for microphone locations 5 and 7 at the same test condition. The spectrum measured in the flow exhibits a peak bandwidth which is independent of frequency, whereas there is an indication that the bandwidth of the harmonic peaks increases slightly with frequency outside the flow.

Finally, spectra measured at microphone locations 2 and 6 are compared in Figure 24*. It is apparent that the bandwidth of the peaks increases with frequency at location 6 but not at location 2. This result is consistent with the spectral broadening predicted earlier. If the broadened peak has a bandwidth less than the data reduction filter bandwidth of 42 Hz then there will be no observable change in the apparent bandwidth of the harmonic peaks. However when the broadened peak bandwidth exceeds 42 Hz, there will be an apparent increase in the bandwidth in the measured spectra. Using the simple empirical analysis presented earlier, the broadening of the harmonic peaks would start to become evident at location 6 at frequencies above about 3200 Hz. At location 2 the corresponding bounding frequency would be approximately 6000 Hz. Thus spectral broadening would be expected at location 6 but not at location 2 -- in agreement with observations.

Determination of the effect of this spectral broadening on the measured harmonic sound pressure levels is a more difficult proposition. None of the references [22, 26-28] develops an empirical relationship which specifically addresses the problem, and the shapes of the broadened peaks show different characteristics from

---

* See Appendix B for further discussion.

(a) Flow Speed = 0 m/s

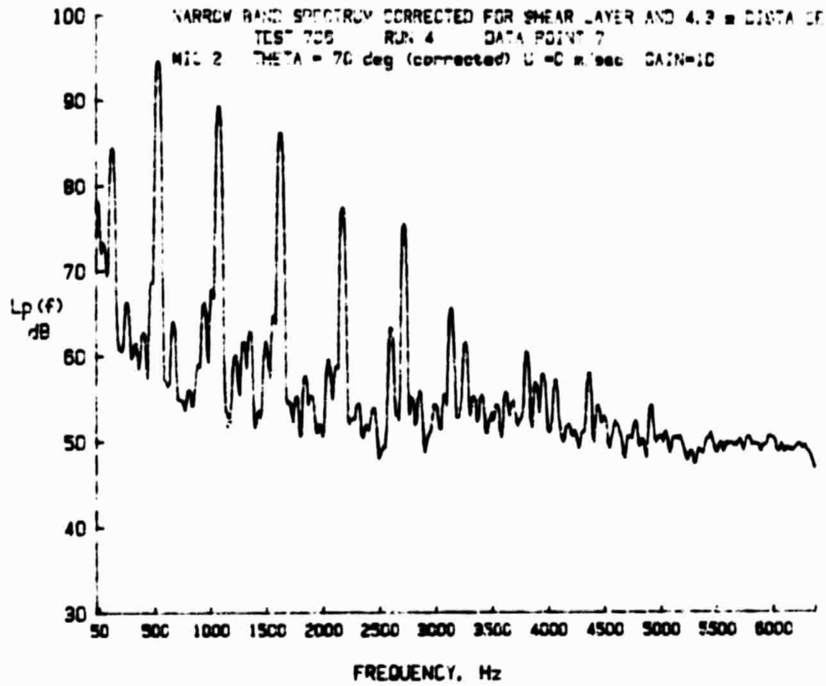

(b) Flow Speed = 62.4 m/s

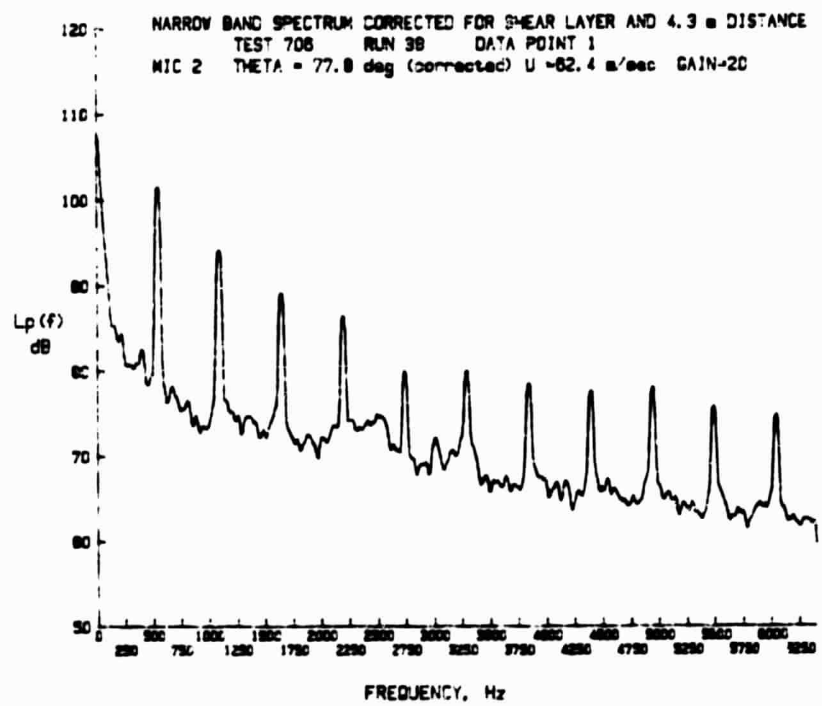

FIGURE 22. NARROWBAND PROPELLER NOISE SPECTRA MEASURED WITH AND WITHOUT AIRFLOW (MICROPHONE 2)

(a) Microphone 7 (In Flow)

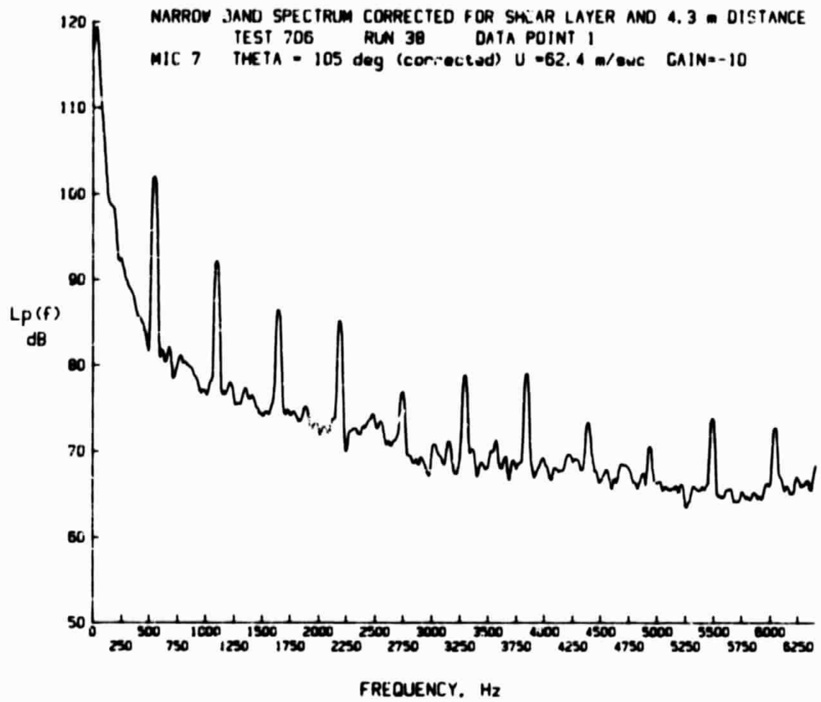

(b) Microphone 5 (Out of Flow)

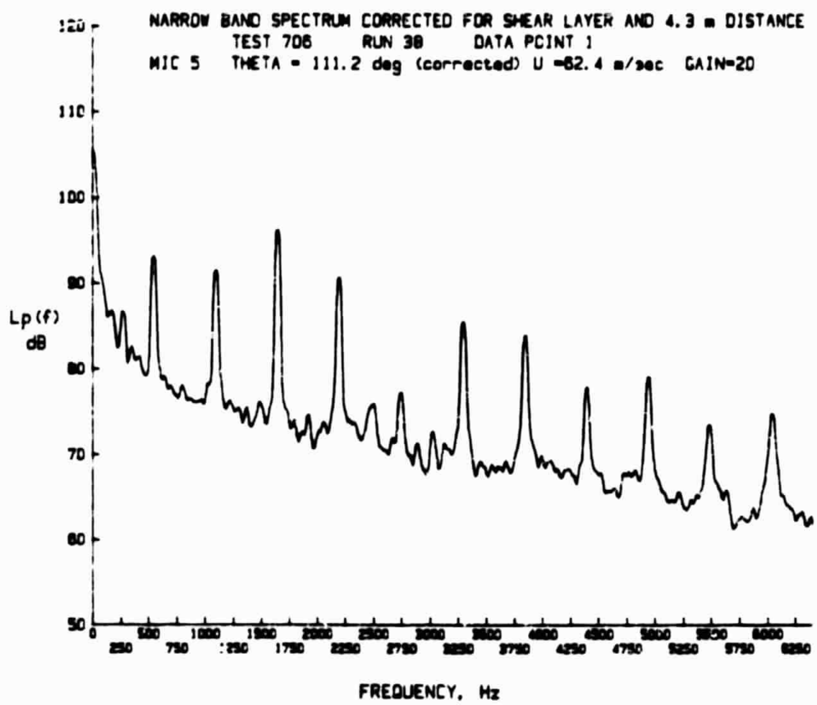

FIGURE 23. COMPARISON OF NARROWBAND PROPELLER NOISE SPECTRA MEASURED IN AND OUT OF FLOW

(a) Microphone 2 (Forward of Plane of Rotation)

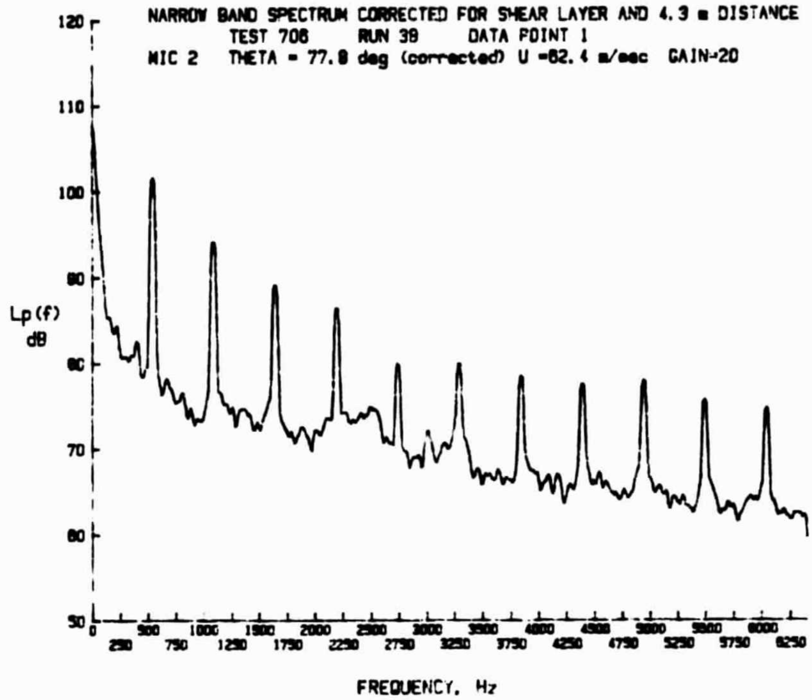

(b) Microphone 6 (Aft of Plane of Rotation)

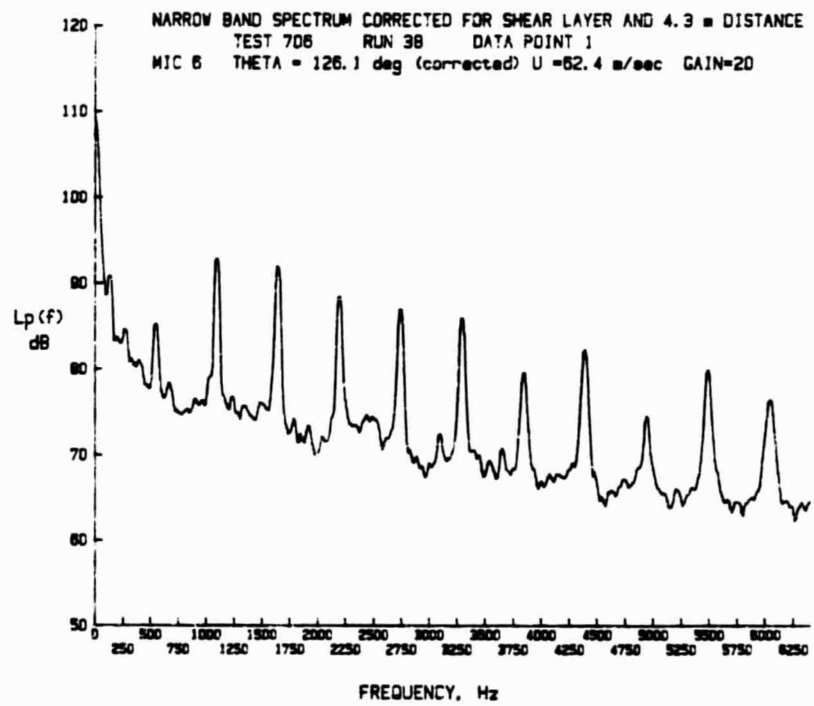

FIGURE 24. COMPARISON OF NARROWBAND PROPELLER NOISE SPECTRA MEASURED FORWARD AND AFT OF PLANE OF ROTATION

test to test. Ross et al [27] develop an empirical equation to modify Amiet's analytical model at high frequencies and emission angles of 40° to 120°. They speculate that the modification includes the influence of shear layer turbulence because the corrections are greatest at the most forward and rearward angles. However the correction is positive in one case and negative in the other; it seems more reasonable to expect that spectral broadening due to turbulence would always cause corrections of the same sign (positive) for discrete frequency components.

In the absence of any well-defined approach, no corrections to sound pressure level have been made in this report to account for spectral broadening of the harmonic peaks. Corrections can be introduced at some future date when the evidence is more clear. At this time only a warning is made that measured sound levels of the high frequency harmonics may be low due to spectral broadening induced by shear layer turbulence. It is probable, however, that the general results of the study will be unaffected by the omission of this correction.

4. EVALUATION OF TEST DATA

4.1 Introduction

The main objective of the test program is to determine the noise generated by interaction between the propeller and the wake from the empennage. First, however, it is necessary to determine the background or baseline sound pressure levels associated with the presence of the test hardware in the test section. The hardware includes microphone stands, model fuselage with support struts and propeller drive system. Also it is necessary to determine the sound pressure levels generated by the propeller (with and without the fuselage present) before the empennage is introduced.

A review of the background sound pressure levels is presented in this section, before the propeller sound pressure levels are discussed in detail in subsequent sections of this report. It is not necessary in the review to present data for all the microphone locations since it is found that, at least for the broadband noise, the acoustic field is not highly directional. Thus conclusions drawn, for example, for microphone 2 locations are generally applicable to other microphones, except for the three microphones in the flow. Consequently the data presented in this section are usually associated with one microphone location, namely #2.

4.2 Noise due to Test Hardware

Broadband sound pressure levels were measured in the test chamber when the propeller drive system (without propeller) and the fuselage (without empennage) were present in the test section. Figure 25 compares narrowband spectra measured at microphone location 2 for the two test flow speeds. Similar comparisons can be obtained for the other microphones located outside the flow. It is seen that, in general, there is an increase of 9 to 10 dB

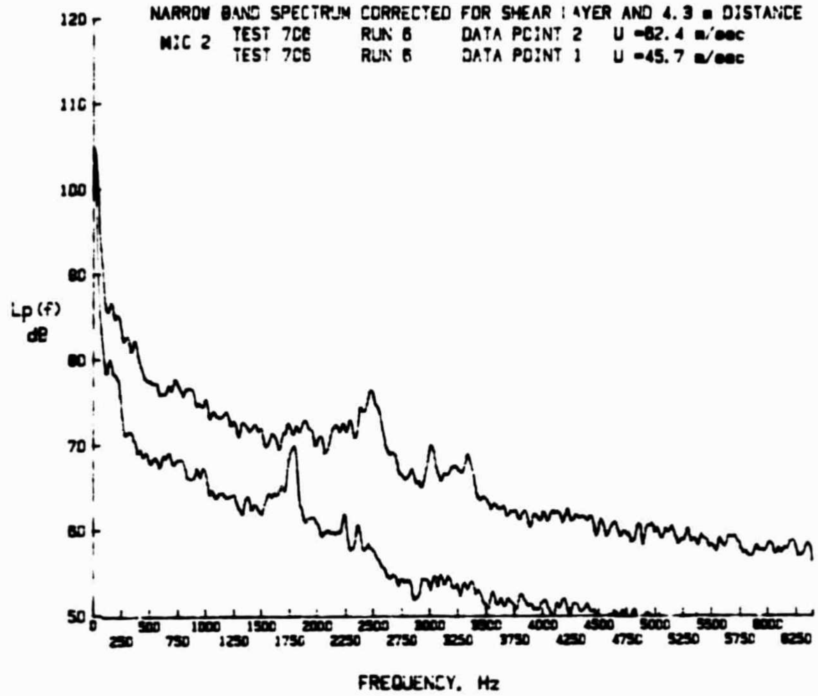

FIGURE 25. SOUND PRESSURE LEVEL SPECTRA MEASURED OUT OF FLOW (MICROPHONE 2) WHEN PROPELLER NOT OPERATING (FUSELAGE WITHOUT EMPENNAGE)

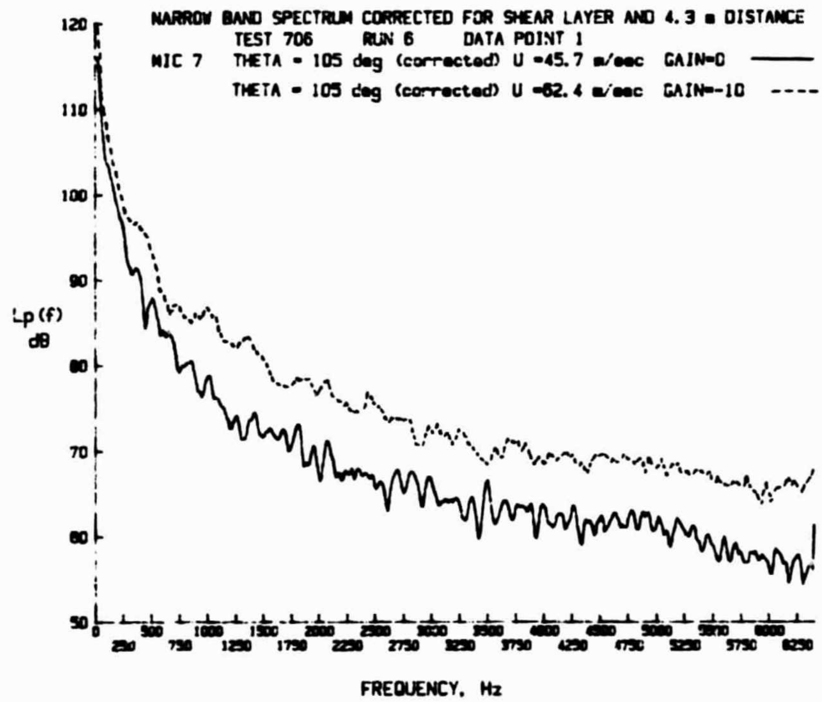

FIGURE 26. SOUND PRESSURE LEVEL SPECTRA MEASURED IN FLOW (MICROPHONE 7) WHEN PROPELLER NOT OPERATING (FUSELAGE WITHOUT EMPENNAGE)

in sound pressure level when the flow speed is increased from 45.7 m/s to 62.4 m/s. This increase corresponds to a velocity law of

$$\bar{p}^2 \propto V^{6.6} \text{ to } V^{7.4}$$

where $\bar{p}^2$ is the mean square acoustic pressure. This relationship is similar to the V^6 power law generally associated with acoustic radiation from a dipole-type source.

Exceptions to the general velocity law occur at peaks in the spectra which exhibit a trend of frequency increasing linearly with flow speed. At 45.7 m/s the frequency of the prominent peak is 1780 Hz and at 62.4 m/s the corresponding frequency is 2470 Hz. During the course of the test program it was determined that these components were generated by flow interaction with the support struts for microphones 7, 8 and 9 which were located in the tunnel flow. Following Run 46 boundary layer flow trips were placed on the leading edges of the support struts and the associated noise components were eliminated from the acoustic spectra for subsequent runs.

A comparison of narrowband spectra measured at microphone 7 in the flow is shown in Figure 26. In this case, however, the sound pressure level increases more slowly with flow speed than was the case for the data in Figure 25. The law relating mean square pressure and flow speed is now

$$\bar{p}^2 \propto V^{4.0} \text{ to } V^{5.5}$$

This law is similar to that predicted for aerodynamic self-noise on the microphone rather than radiated acoustic noise. This is physically reasonable, particularly when it is observed that the pressure levels recorded by microphone 7 are higher than those measured in the acoustic radiation field (see Figure 27). The difference in pressure levels is such that the peaks associated

(a) V = 45.7 m/s

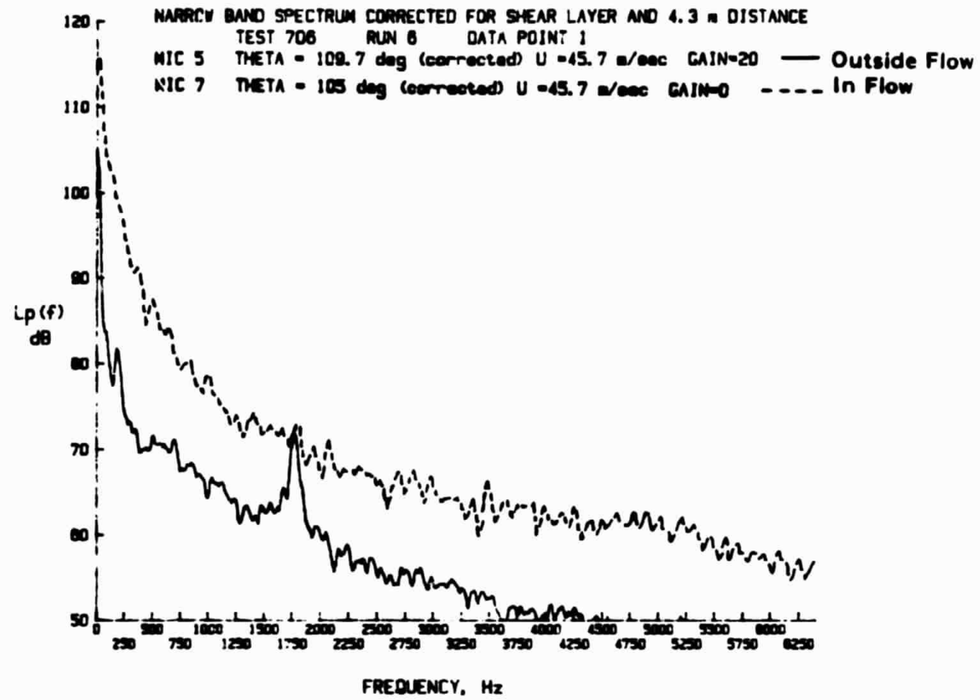

(b) V = 62.4 m/s

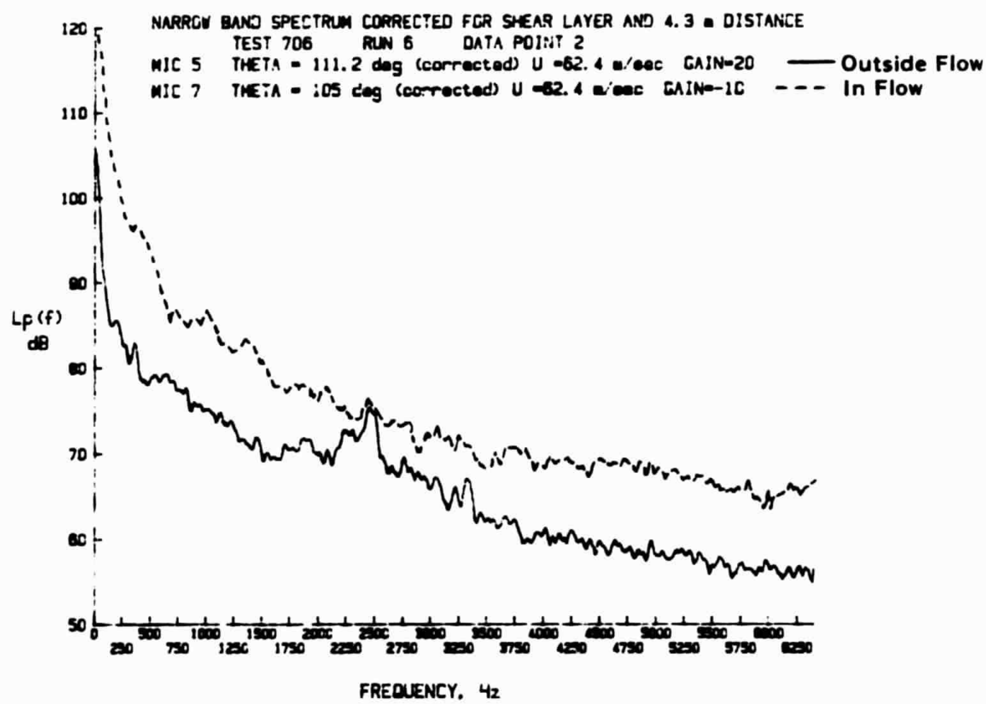

FIGURE 27. COMPARISON OF SOUND PRESSURE LEVEL SPECTRA MEASURED IN AND OUT OF FLOW WHEN PROPELLER NOT OPERATING (FUSELAGE WITHOUT EMPENNAGE)

with radiation from the microphone support struts are masked by the aerodynamic self-noise of microphone 7.

The effect of the empennage on sound pressure levels in the test chamber was found to be negligible. This can be seen in Figure 28 which compares sound pressure levels measured at microphone location 2 when the fuselage was installed first without an empennage and then with the Y-tail. The data are associated with a flow speed of 62.4 m/s and fuselage orientations of $\psi = 0°$ and $90°$.

A direct comparison of sound pressure level spectra measured for the two orientations of the fuselage is provided by Figure 29. In this case the data were measured at microphones 2 and 13, located on different sides of the test section. The spectra show no significant effect of angle of orientation except for the elimination of broadband peaks associated with noise generated by flow over the microphone support struts. As stated earlier this acoustic component was eliminated following Run 46 by the attachment of flow trips to the strut leading edges. The strut noise is present for Run 9 but not for Run 73.

4.3 Propeller Noise

The propeller noise field generated by the test model can be considered from a number of viewpoints. However, since the purpose of the present test is to investigate the effect of the empennage the evaluation of the data will place emphasis on this aspect.

Narrowband sound pressure levels measured with and without the propeller operating are shown in Figures 30 through 35. The data in Figures 30 and 31 refer to propeller rotational speeds of 4000 rpm and Figures 32 through 35 are associated with 8200 rpm. In all cases the fuselage has an empennage attached at the rear. Results for the lower propeller rpm show that the broadband sound pressure levels are not much higher than the background levels,

(a) $\psi = 0°$

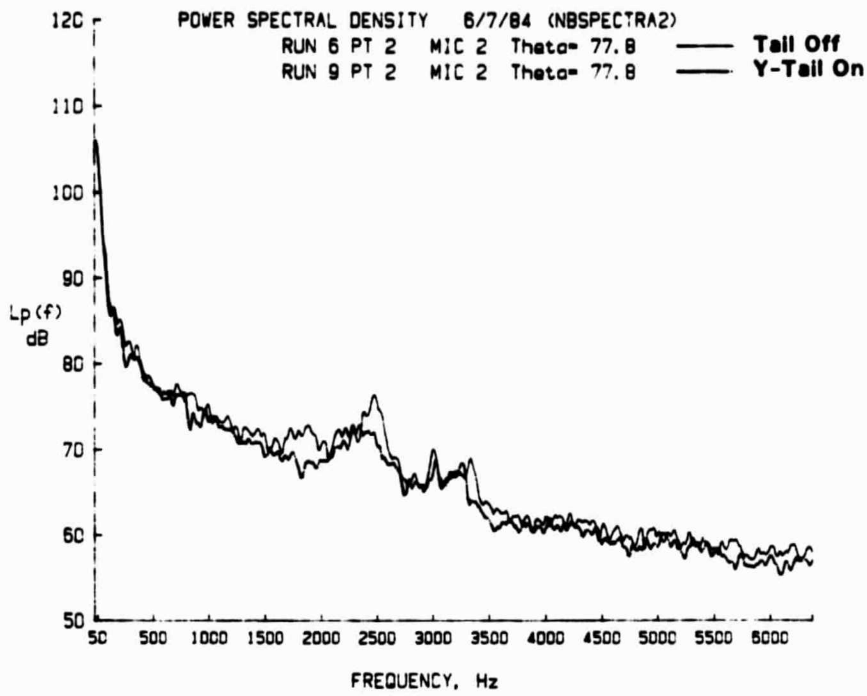

(b) $\psi = 90°$

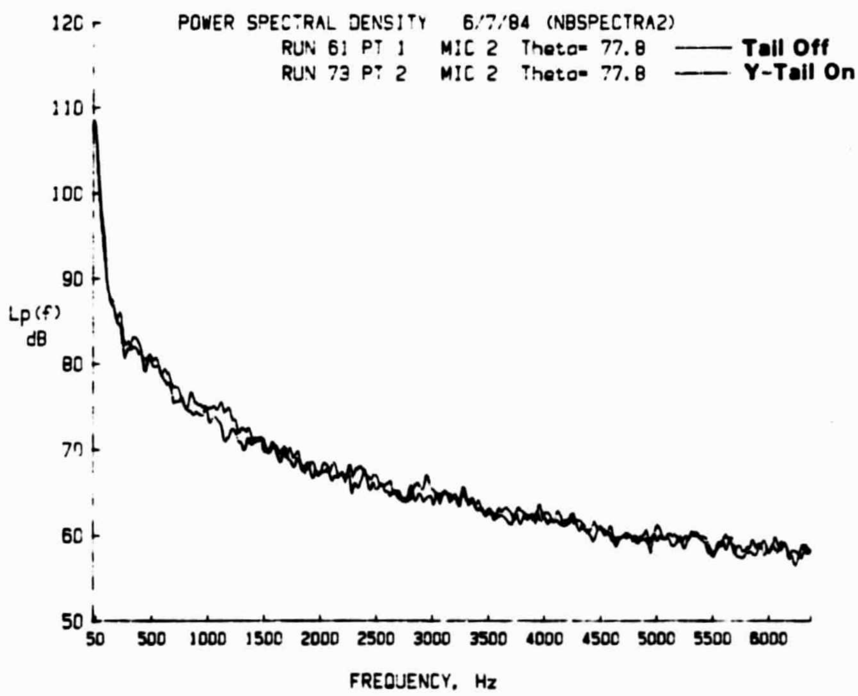

FIGURE 28. INFLUENCE OF EMPENNAGE ON BROADBAND SOUND PRESSURE LEVELS WHEN PROPELLER NOT OPERATING (Y-TAIL)

(a) Microphone Location 2

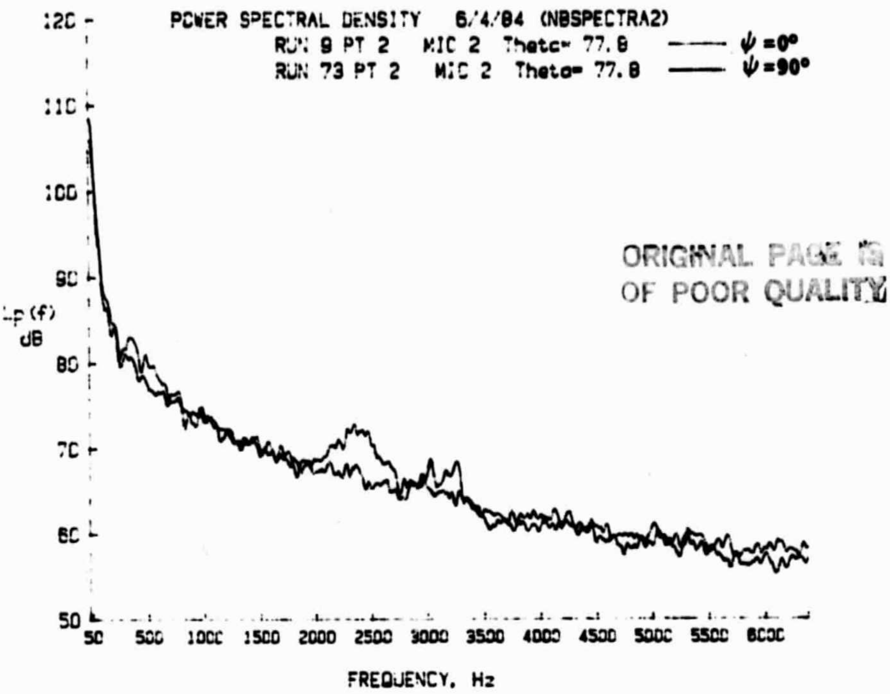

(b) Microphone Location 13

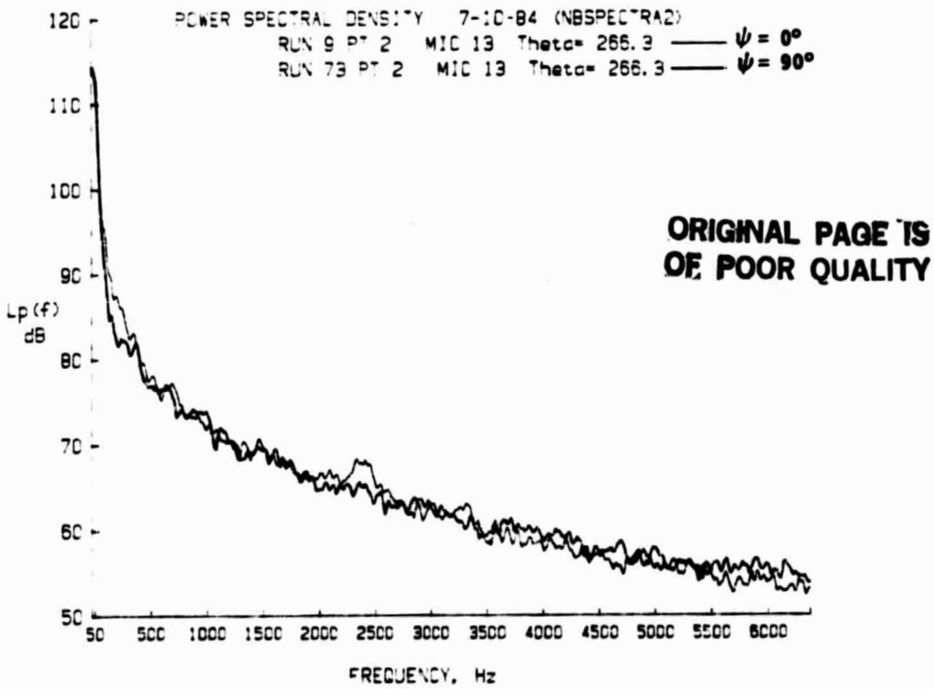

FIGURE 29. INFLUENCE OF FUSELAGE ORIENTATION ON BROADBAND SOUND PRESSURE LEVELS WHEN PROPELLER NOT OPERATING (Y-TAIL)

(a) V = 45.7 m/s

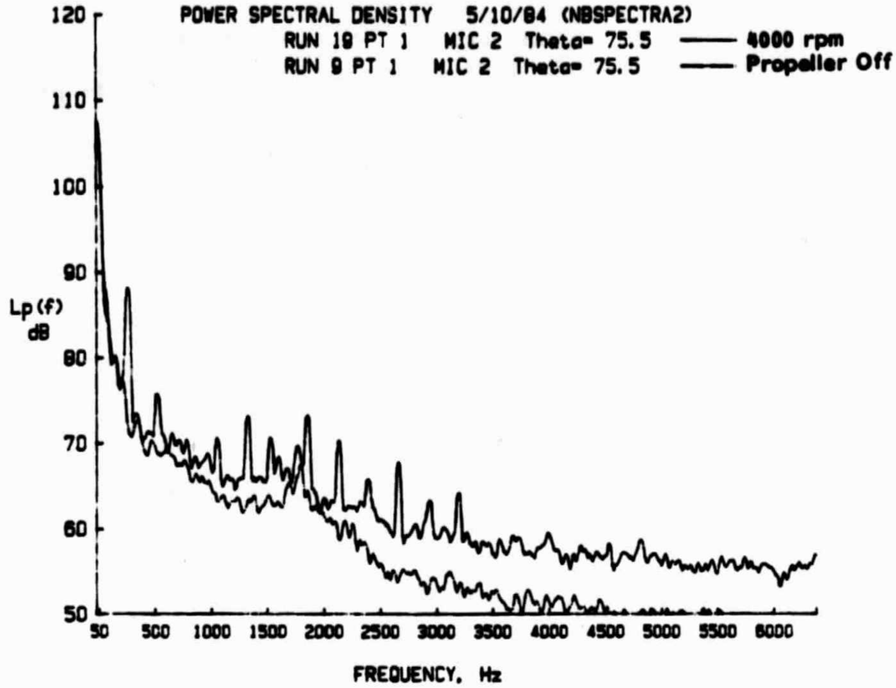

(b) V = 62.4 m/s

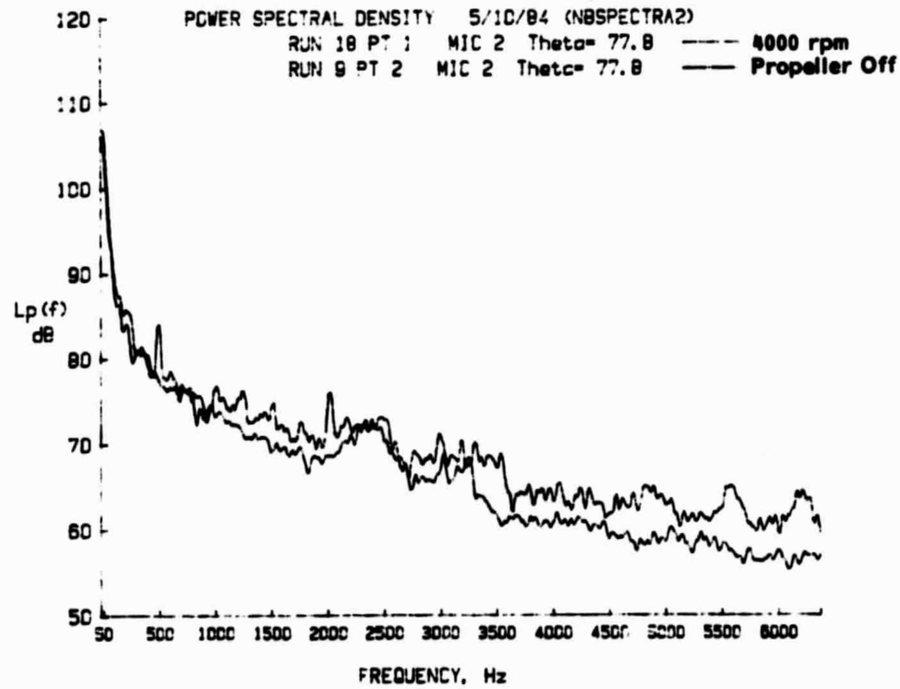

FIGURE 30. COMPARISON OF SOUND PRESSURE LEVELS AT MICROPHONE 2 WITH AND WITHOUT PROPELLER OPERATING (Y-TAIL, ψ=0°, 4000 RPM)

(a) V = 45.7 m/s

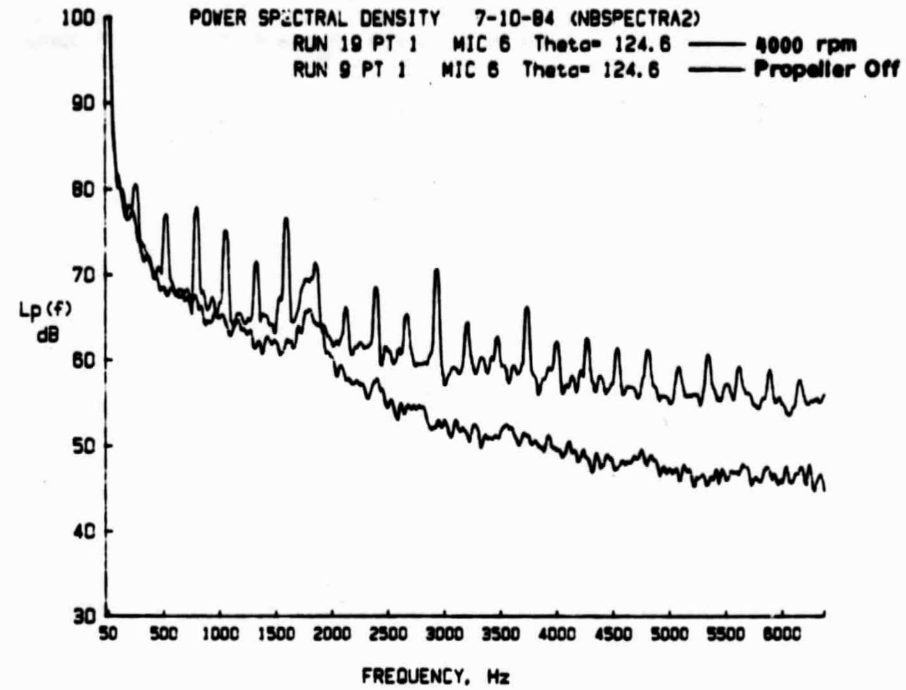

(b) V = 62.4 m/s

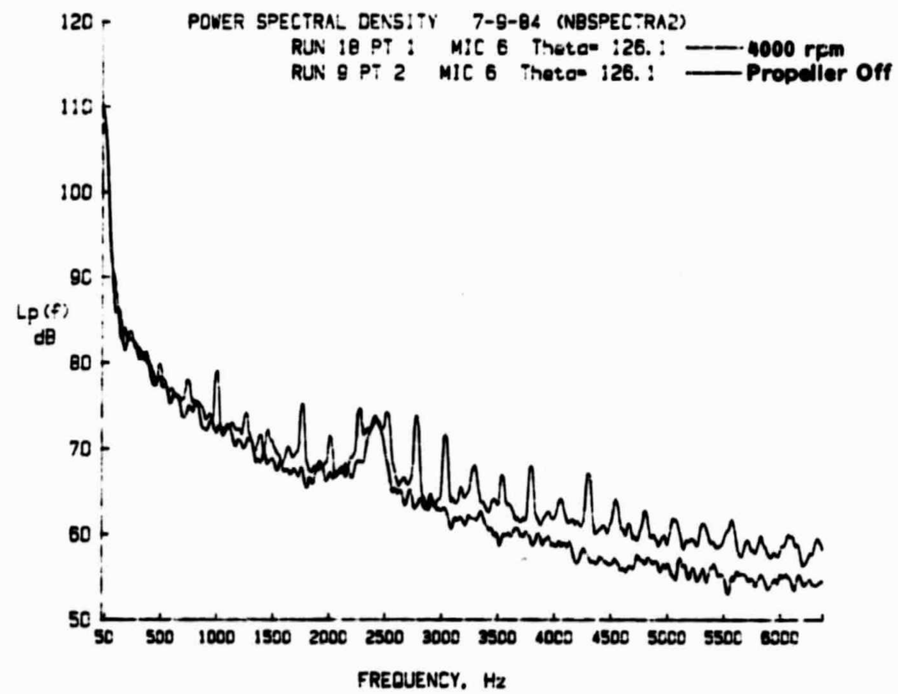

FIGURE 31. COMPARISON OF SOUND PRESSURE LEVELS AT MICROPHONE 6 WITH AND WITHOUT PROPELLER OPERATING (Y-TAIL, ψ =0°, 4000 RPM)

(a) V = 45.7 m/s

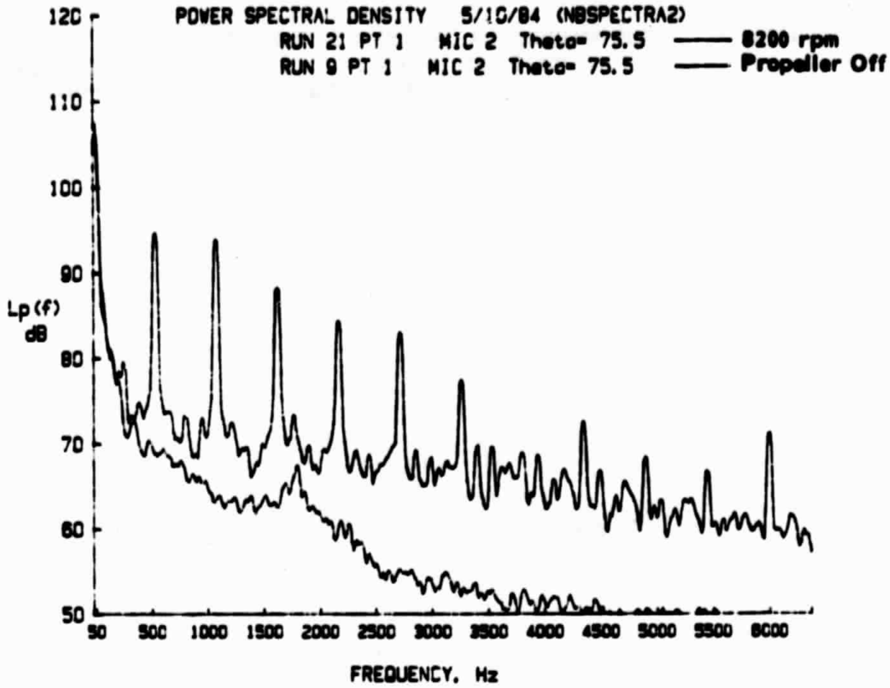

(b) V = 62.4 m/s

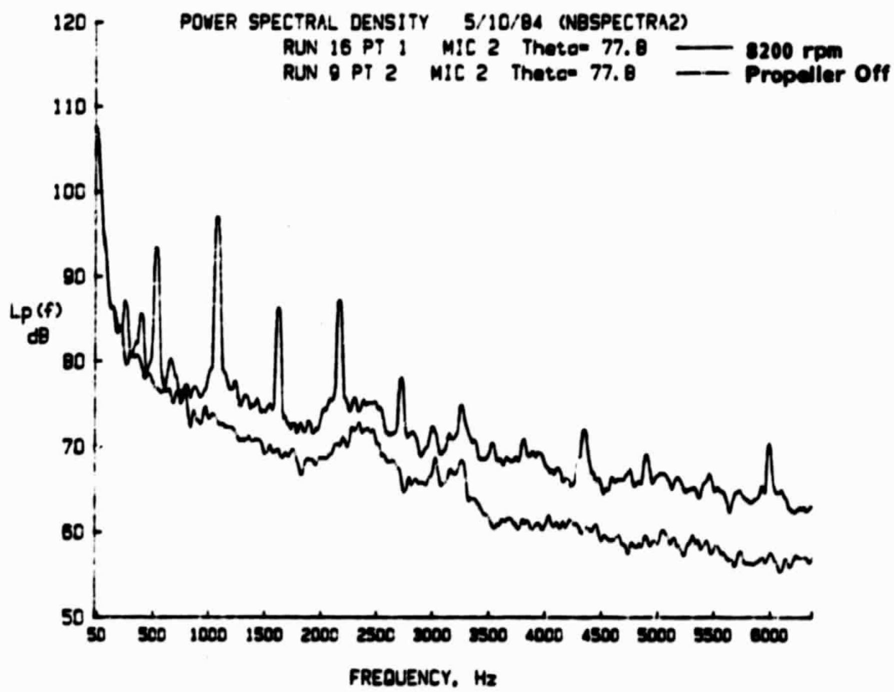

FIGURE 32. COMPARISON OF SOUND PRESSURE LEVELS AT MICROPHONE 2 WITH AND WITHOUT PROPELLER OPERATING (Y-TAIL, ψ=0°, 8200 RPM)

(a) V = 45.7 m/s

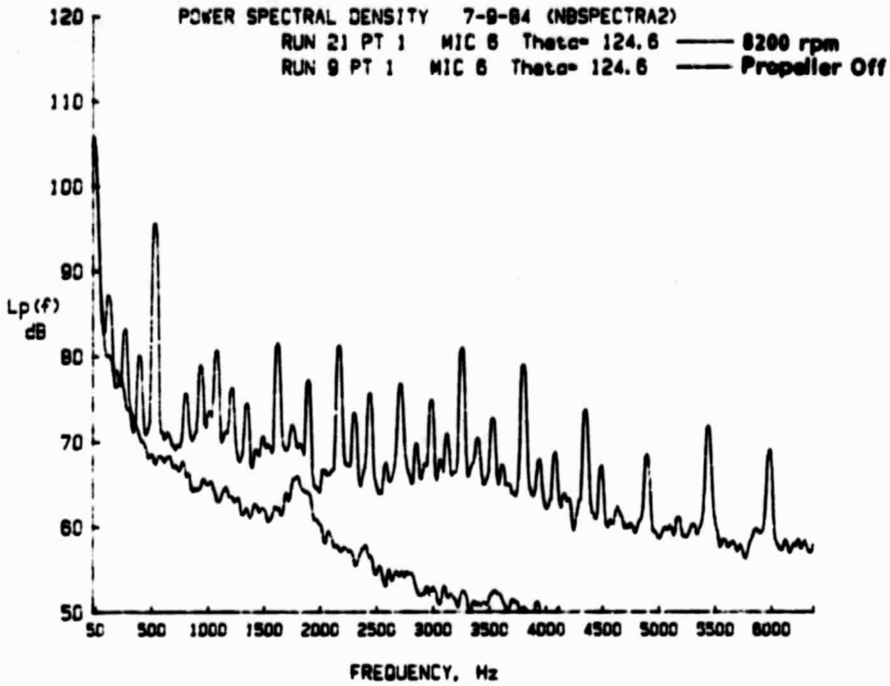

(b) V = 62.4 m/s

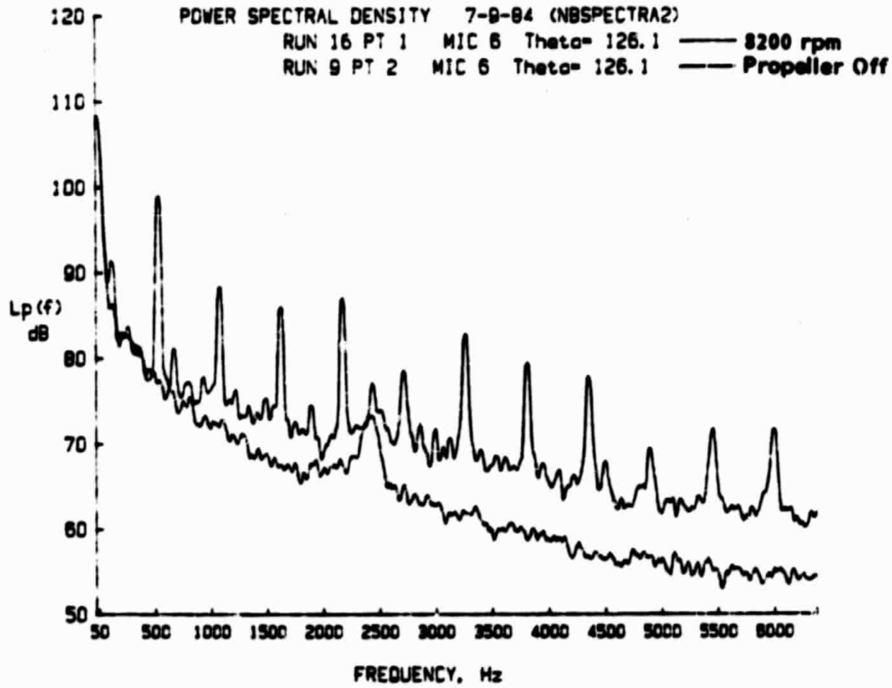

FIGURE 33. COMPARISON OF SOUND PRESSURE LEVELS AT MICROPHONE 6 WITH AND WITHOUT PROPELLER OPERATING (Y-TAIL, ψ=0°, 8200 RPM)

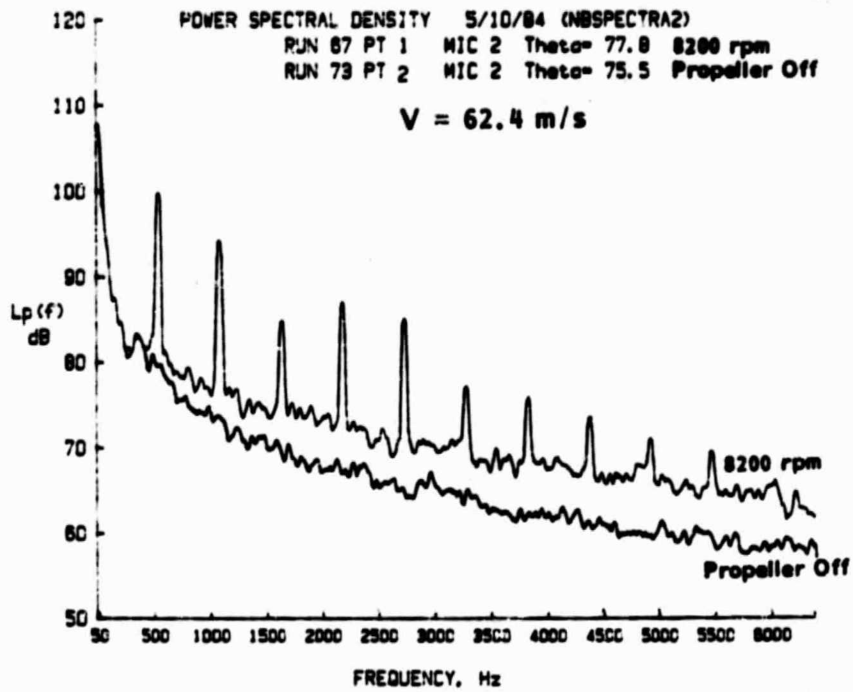

FIGURE 34. COMPARISON OF SOUND PRESSURE LEVELS AT MICROPHONE 2 WITH AND WITHOUT PROPELLER OPERATING (Y-TAIL, ψ =90°, 8200 RPM)

(a) V = 45.7 m/s

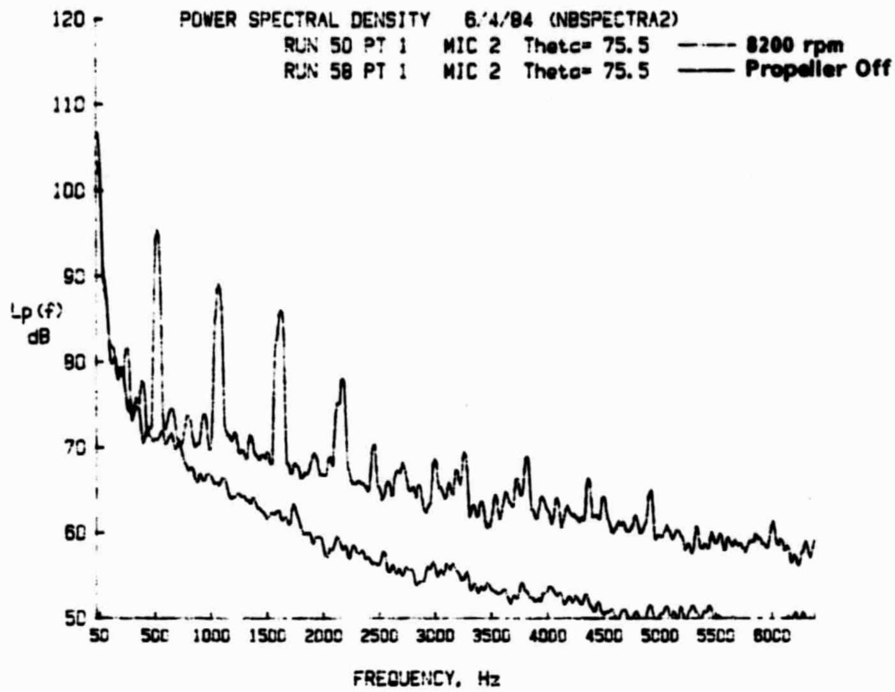

(b) V = 62.4 m/s

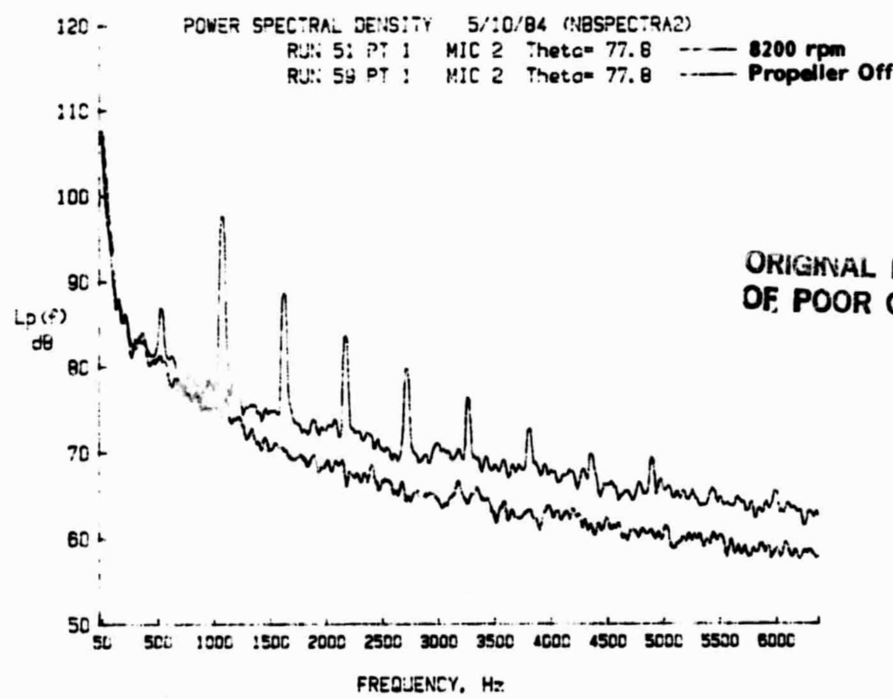

FIGURE 35. COMPARISON OF SOUND PRESSURE LEVELS AT MICROPHONE 2 WITH AND WITHOUT PROPELLER OPERATING (I-TAIL, ψ=90°, 8200 RPM)

particularly at the higher flow speed and frequencies below about 2500 Hz.

As propeller rpm increases the broadband and discrete frequency components generated by the propeller increase relative to the background, as can be seen by comparing Figures 30 and 32 or Figures 31 and 33. Even so the difference between propeller and background sound levels is smaller at the higher flow speed than it is at the lower flow speed. For example, Figures 31 and 32 show that the propeller broadband noise at high frequencies is about 13 dB above the background at a flow speed of 45.7 m/s and only 7 dB at a flow speed of 62.4 m/s.

Figures 34 and 35 show that the general relationships between propeller noise and background noise for a fuselage with empennage are also observed for a fuselage orientation of $\psi = 90°$ and for other empennage configurations (I-tail).

An alternative approach to evaluating the propeller noise is to compare sound levels generated by a propeller with and without a fuselage structure upstream. Such a comparison is shown in Figure 36 for two fuselage orientations (0° and 90°) and a flow speed of 62.4 m/s. In this case it is seen that the presence of the fuselage (without empennage) causes an increase in the propeller broadband sound pressure levels but it is usually small. For the test conditions shown in Figure 36 the increase is about 1 dB for $\psi = 0°$ and about 3 dB for $\psi = 90°$.

The discrete frequency components in Figure 36 show no identifiable trend, some harmonics increase in sound pressure level when the fuselage is introduced, others decrease in level and yet others remain unchanged. However, harmonic sound pressure levels will be discussed in greater detail in Section 5 of this report.

(a) $\psi = 0°$

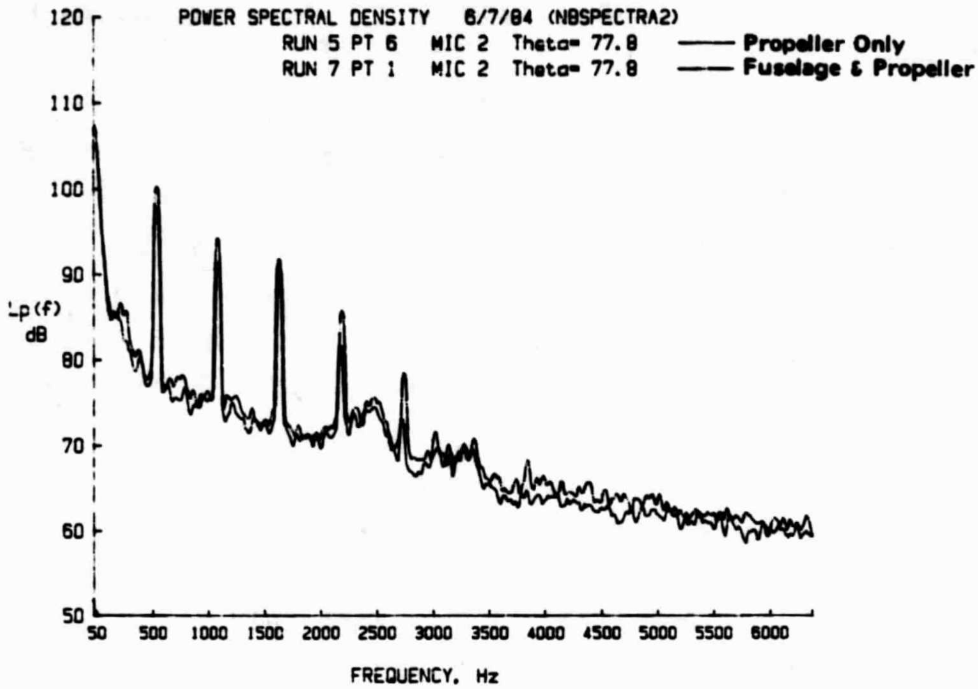

(b) $\psi = 90°$

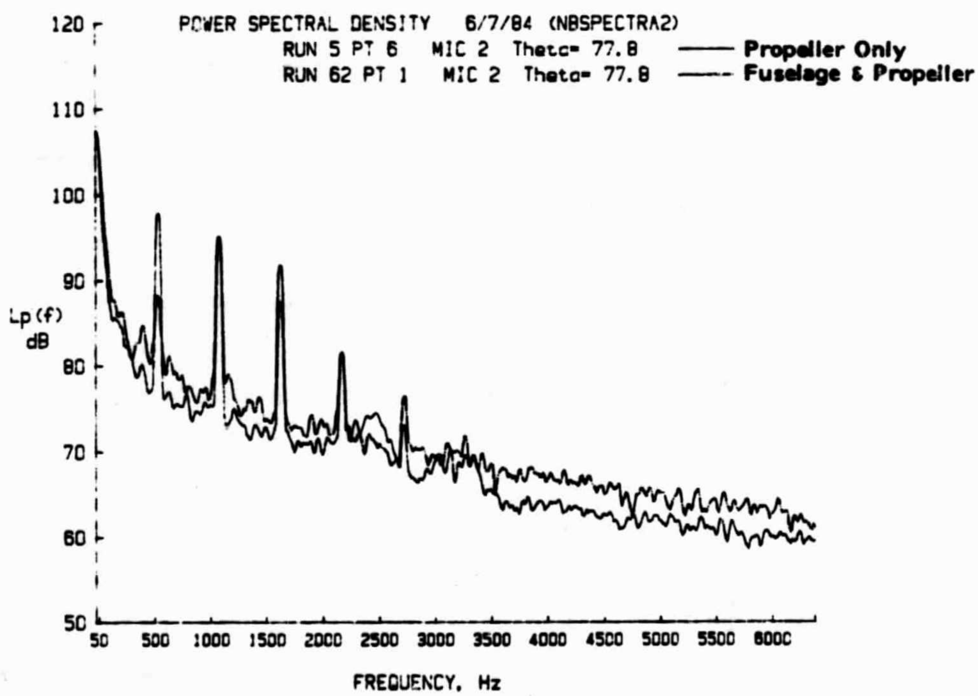

FIGURE 36. COMPARISON OF PROPELLER SOUND PRESSURE LEVELS WITH AND WITHOUT FUSELAGE UPSTREAM (NO EMPENNAGE, 62.4 M/S, 8200 RPM)

Perhaps a more important approach, from the standpoint of the present study, is to compare sound levels generated by the propeller when the fuselage is without, and then with, an empennage. Comparisons of this type are shown in Figures 37 through 39 where it is seen that there is only a very small (sometimes negligible) increase in broadband sound pressure level when the empennage is introduced. Separation distance between empennage and propeller also appears to have only a small influence (Figure 40) on the broadband sound pressure levels.

In summary, broadband sound pressure levels generated by the propeller downstream of an empennage are higher than those for the propeller alone, but it is difficult to determine the precise role played by the empennage because the changes in sound level are small relative to the case of a fuselage without empennage. The situation for discrete frequency components at harmonics of the blade passage frequency is different in that the empennage can cause a significant increase in the level of the higher order harmonics. This will be discussed further in Section 5.

4.4 Repeatability of Data

One question that often arises in propeller noise tests, particularly those which involve flight test studies, involves data repeatability. Time constraints did not allow much scope for repeat runs at identical conditions but it was possible to perform one condition on three different occasions (with small changes in the value of the separation distance x). The three runs are 11-1, 16-1, and 22-6, and they are associated with the Y-tail, flow speed of 62.4 m/s and 8200 rpm. For run 11-1, X = 229 mm and for runs 16-1 and 22-6, X = 238 mm, a difference of less than 4%.

Figure 41 presents comparisons of the narrowband spectra for the three runs measured at three microphone locations. Several observations can be made:-

(a) Microphone 2

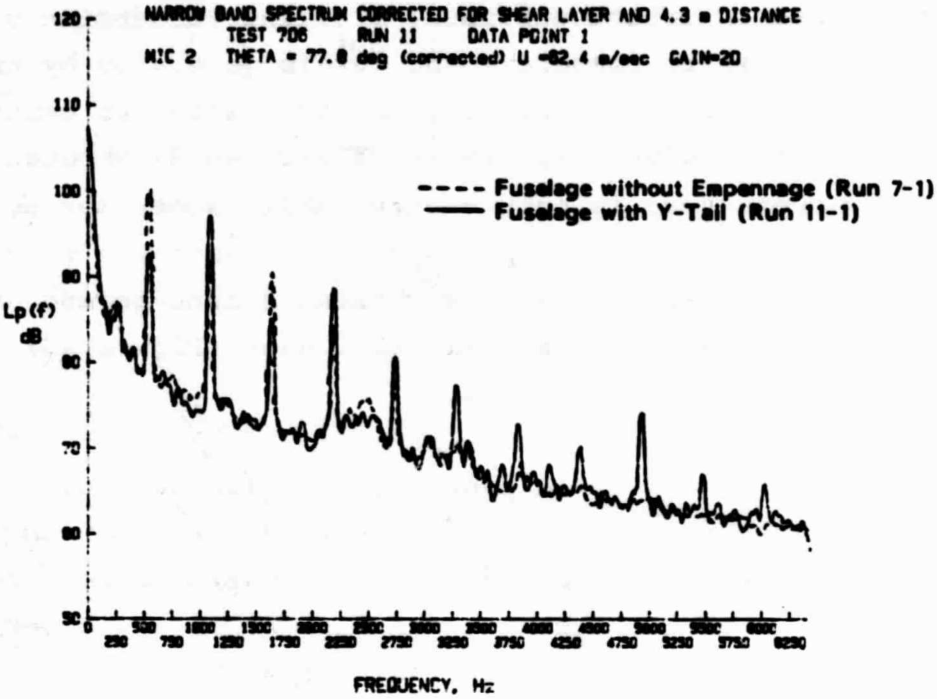

(b) Microphone 6

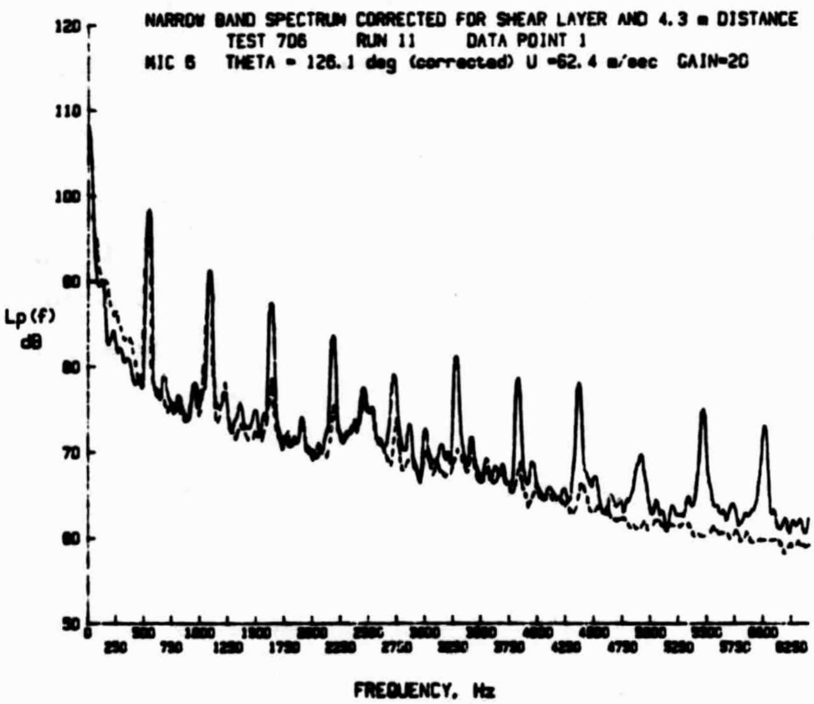

FIGURE 37. INFLUENCE OF EMPENNAGE ON NARROWBAND SOUND PRESSURE LEVELS WITH PROPELLER OPERATING (ψ =0°)

(a) Microphone 2

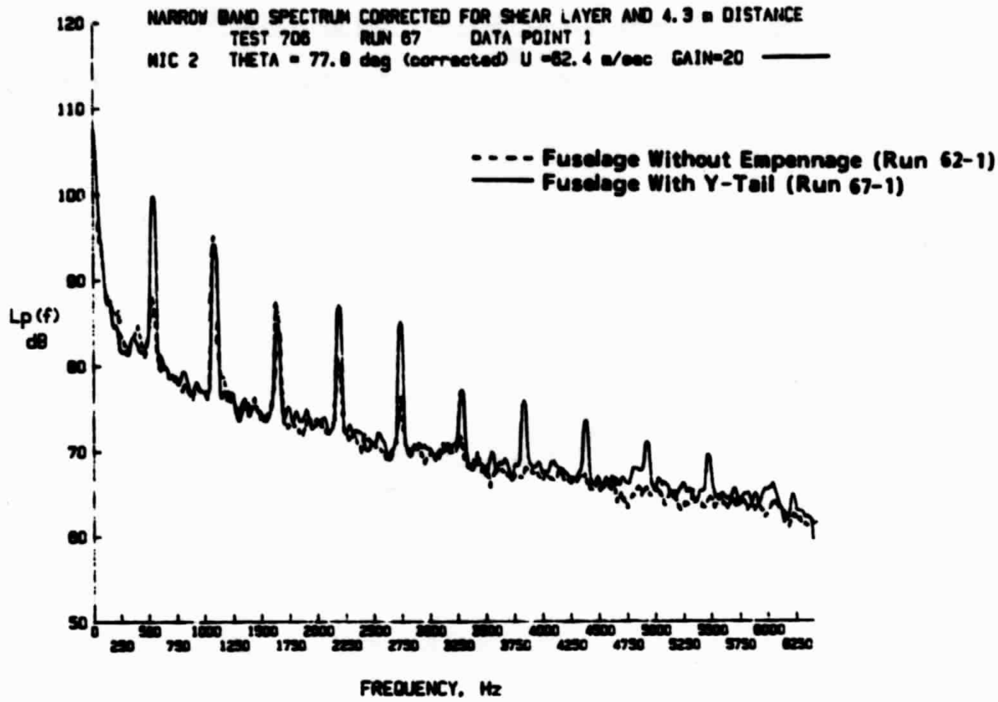

(b) Microphone 6

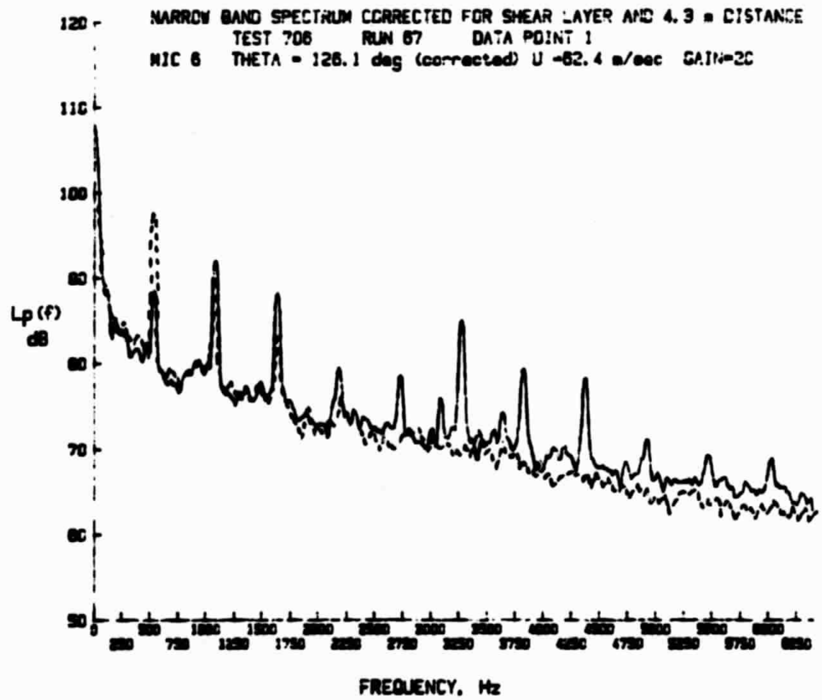

FIGURE 38. INFLUENCE OF EMPENNAGE ON NARROWBAND SOUND PRESSURE LEVELS WITH PROPELLER OPERATING (ψ=90°, 8200 RPM)

(a) Microphone 2

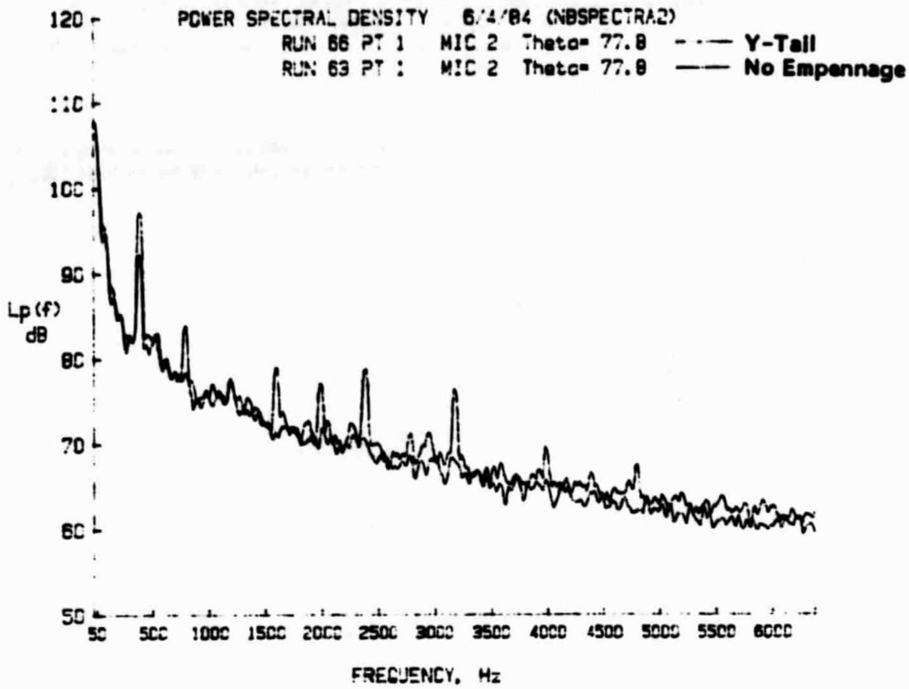

(b) Microphone 6

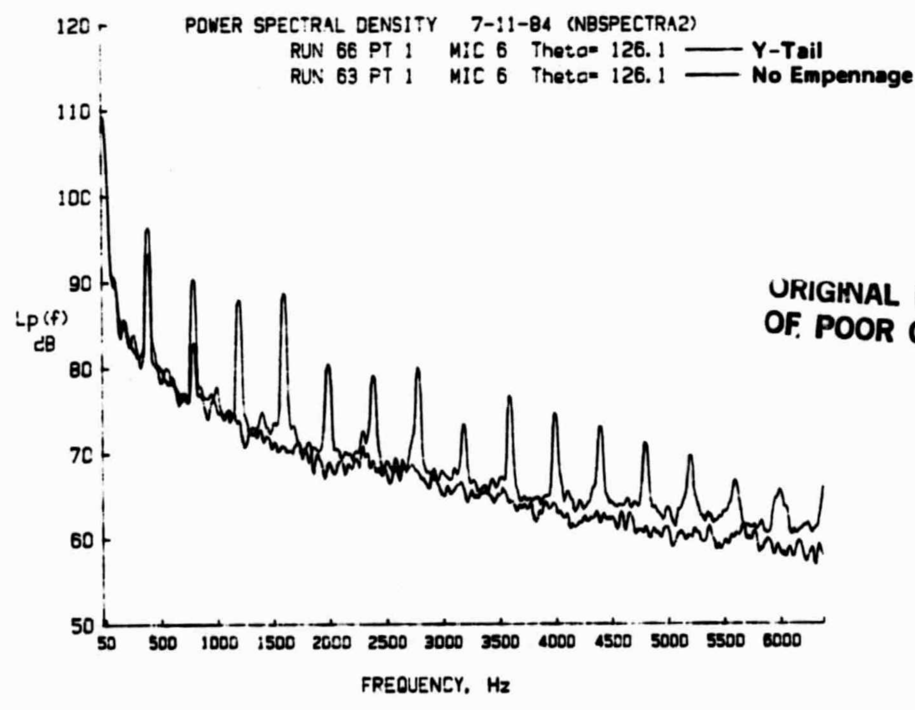

ORIGINAL PAGE IS OF POOR QUALITY

FIGURE 39. INFLUENCE OF EMPENNAGE ON NARROWBAND SOUND PRESSURE LEVELS WITH PROPELLER OPERATING (ψ =90°, 6000 RPM)

(a) Microphone 2

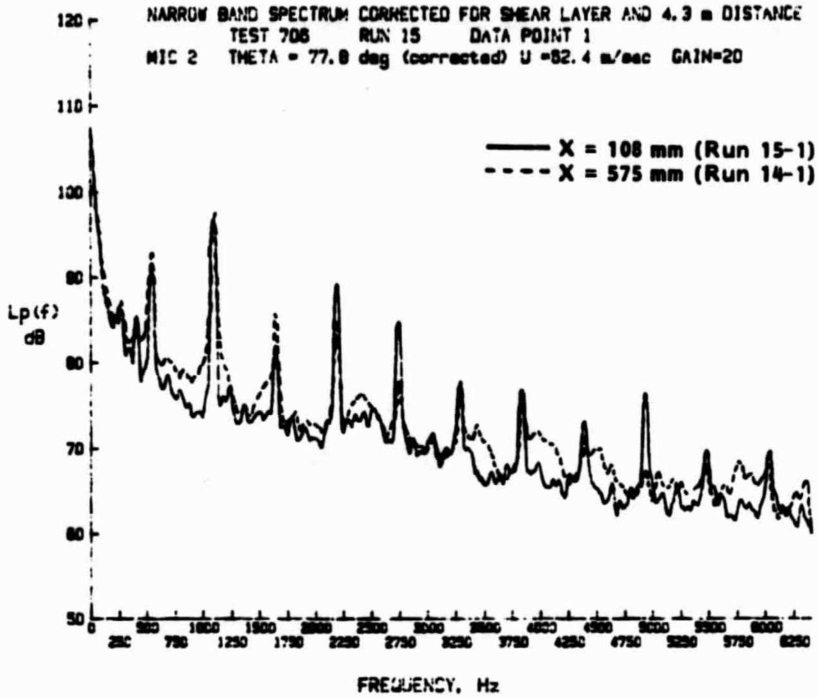

(b) Microphone 6

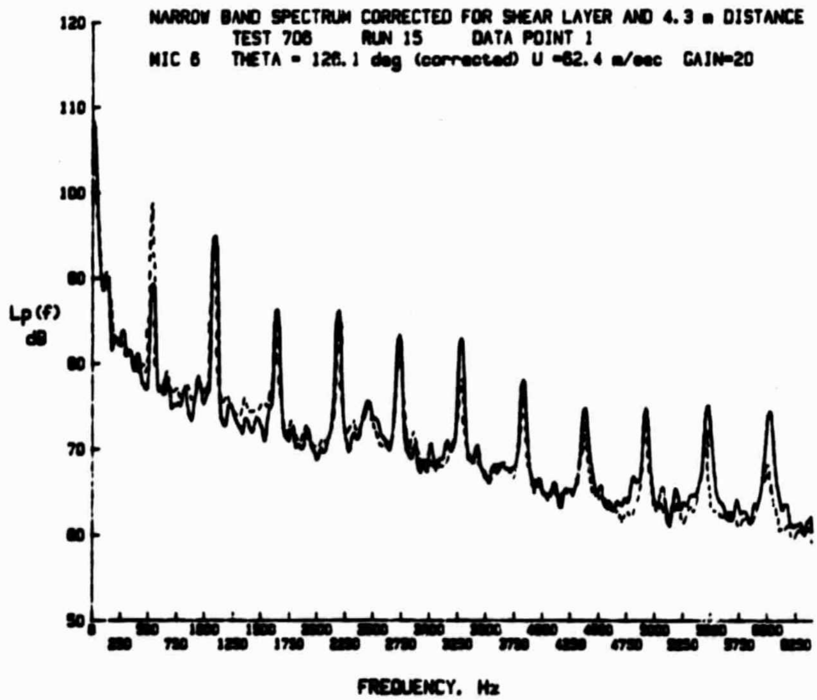

FIGURE 40. INFLUENCE OF SEPARATION BETWEEN EMPENNAGE AND PROPELLER ON NARROWBAND SOUND PRESSURE LEVELS (Y-TAIL)

(a) Microphone

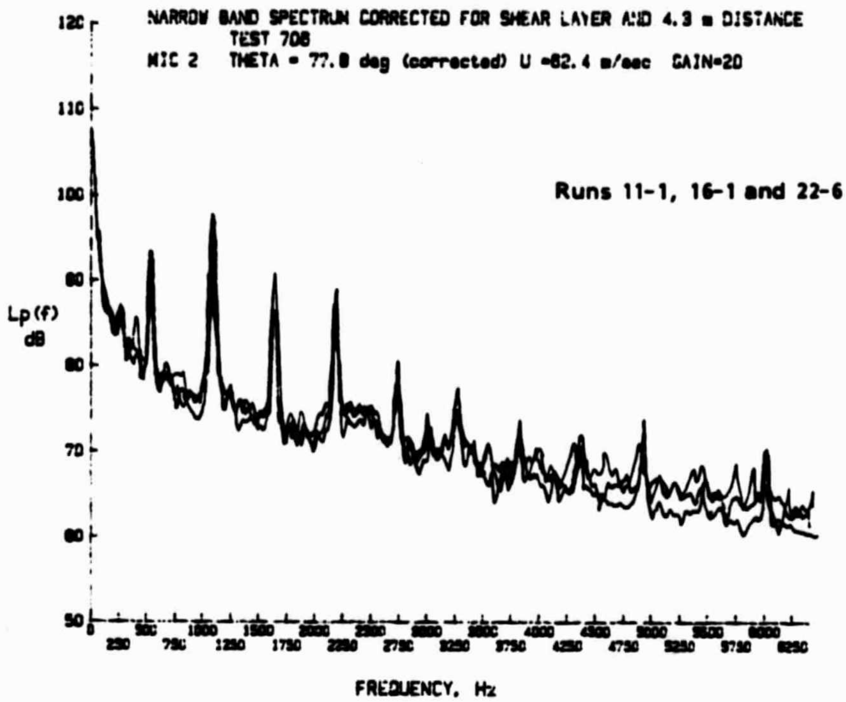

(b) Microphone 5

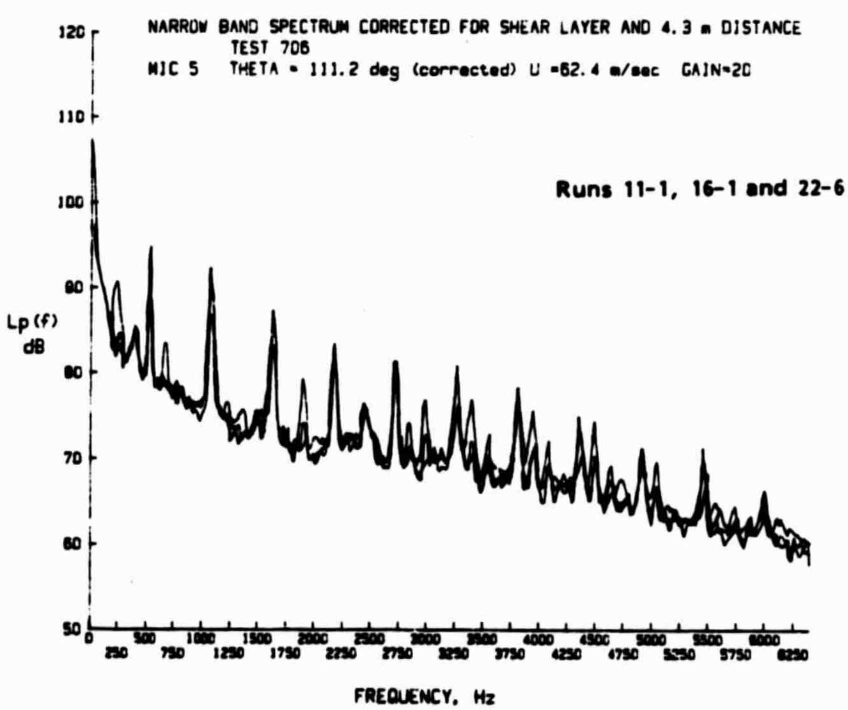

FIGURE 41. COMPARISON OF NARROWBAND SOUND PRESSURE LEVELS FOR REPEATED RUNS (Y-TAIL, 62.4 M/S, 8200 RPM)

(c) Microphone 6

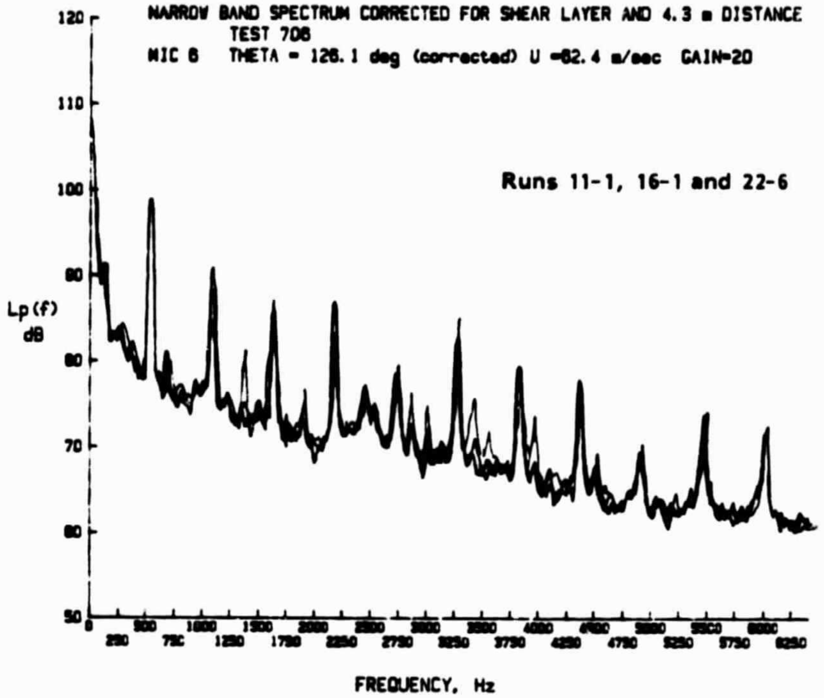

FIGURE 41. CONTINUED

(a) Multiples of the propeller shaft rotational frequency are in more evidence in some spectra than in others

(b) Broadband noise levels show good repeatability at some locations but not at others, and

(c) There appears to be a fairly wide variation in harmonic sound pressure levels.

The appearance and disappearance of harmonic components at multiples of the propeller shaft rotational frequency were observed several times during the test program. While it was not possible to obtain definite evidence, it is believed that the phenomenon was associated with the changes in blade angle from run to run. These adjustments were made manually and it is possible that small misalignments could occur on one blade with a resulting generation of acoustic components at the shaft rotational frequency.

Omitting the shaft rotation components, the broadband spectral components generally show good repeatability from run to run at microphone locations 5 and 6 but rather poor repeatability at high frequencies at location 2. In this latter case the data band is 3 to 4 dB wide.

Evaluation of the repeatability of sound pressure levels at harmonics of the blade passage frequency is not practical from spectral plots such as those in Figure 41. A more informative presentation is in terms of harmonic level as shown in Figure 42. In some cases, such as microphone location 12, the data show very little variation from run to run whereas in other cases (e.g. microphone 3) the sound pressure levels for a given harmonic show a range of 10 dB or more.

(a) Microphone 1

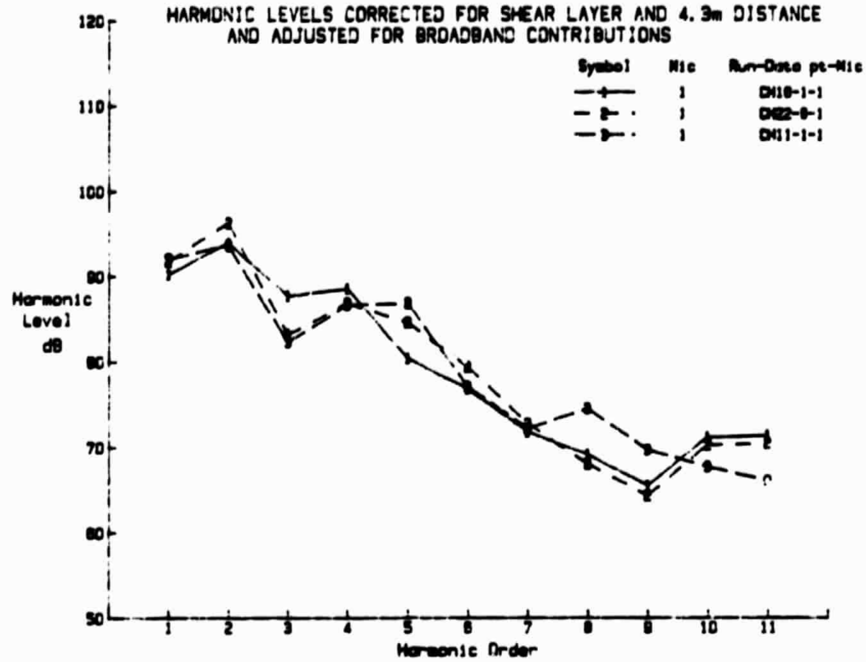

(b) Microphone 2

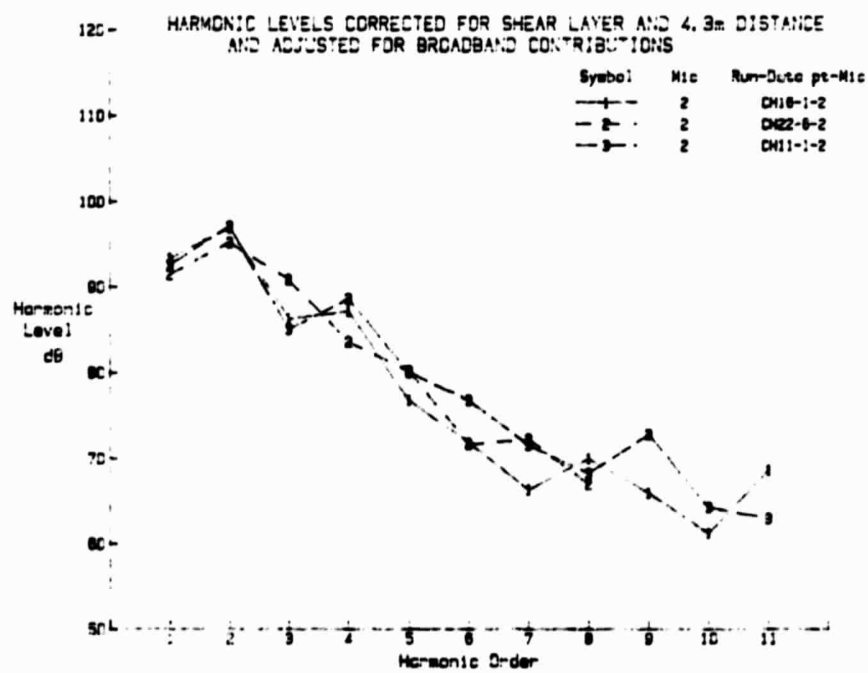

FIGURE 42. COMPARISON OF BLADE PASSAGE FREQUENCY HARMONIC LEVELS FOR REPEAT RUNS (Y-TAIL, 62.4 M/S, 8200 RPM)

(c) Microphone 3

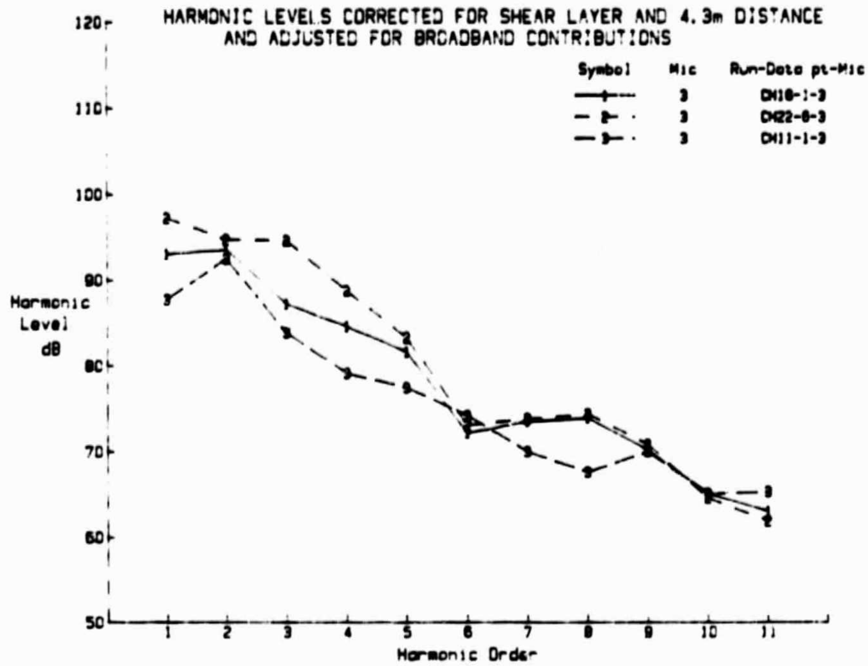

(d) Microphone 4

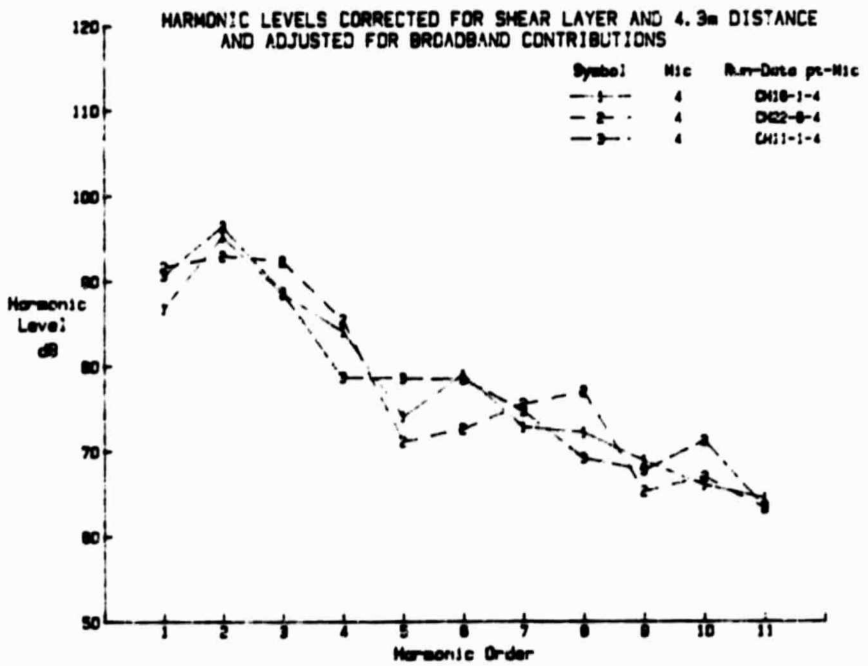

FIGURE 42. CONTINUED

(e) Microphone 5

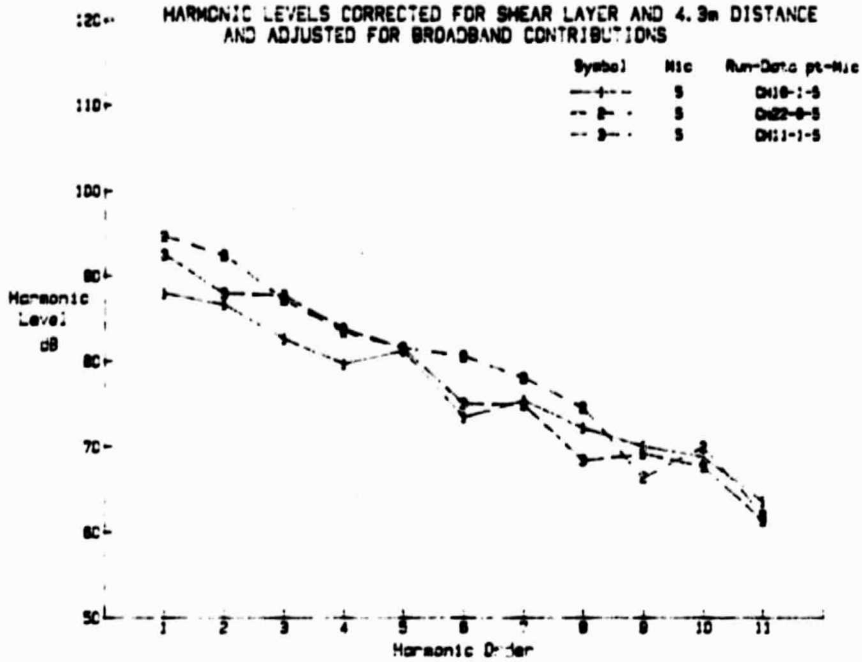

(f) Microphone 6

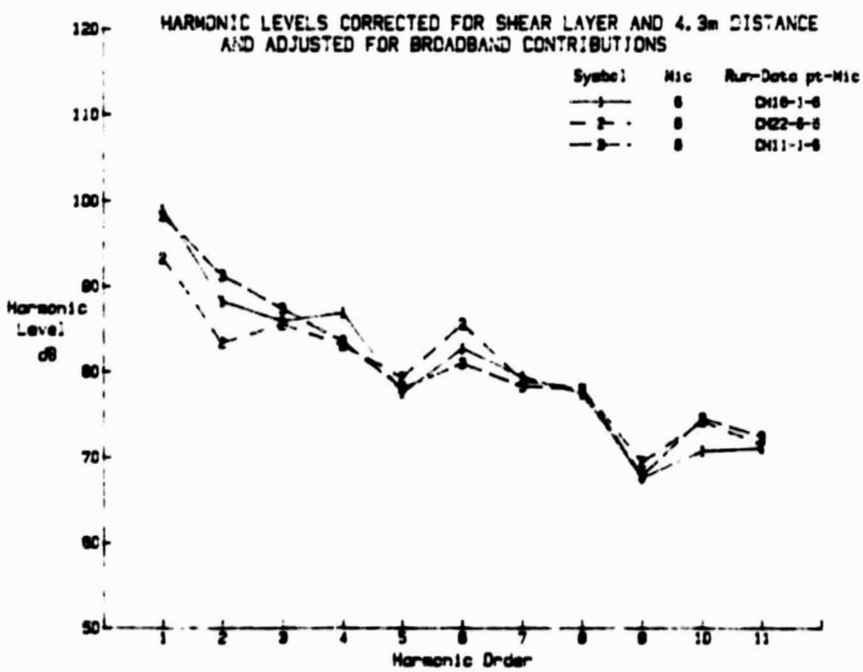

FIGURE 42. CONTINUED

(g) Microphone 11

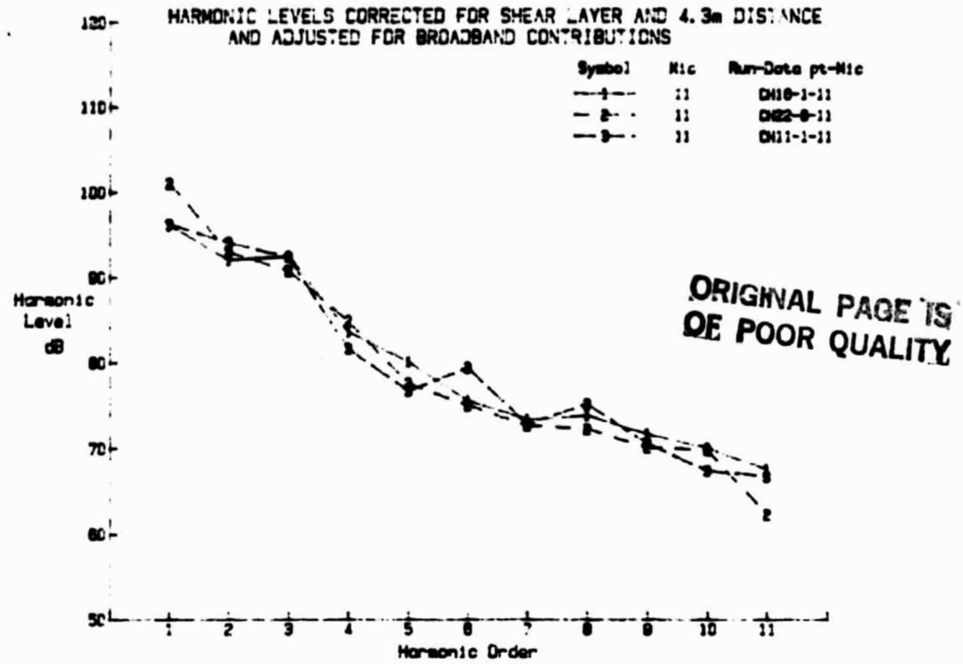

(h) Microphone 12

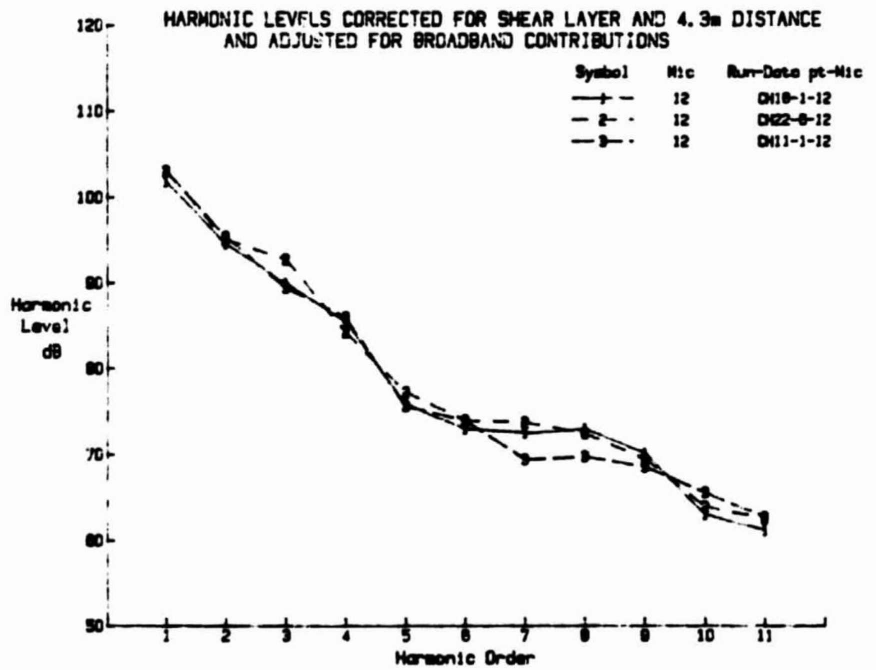

FIGURE 42. CONTINUED

C-2

Visual inspection of Figure 42 does not indicate any particular trend with harmonic order or microphone location. Thus, the range of sound pressure levels at each harmonic order was averaged over all eight locations and linear regression performed on the averages. The results indicated that the repeatability of harmonic sound pressure level was slightly better at higher harmonic order than at lower order. The linear regression equation for the average range of sound pressure level, $\overline{\Delta SPL}$ for a given harmonic order m was

$$\overline{\Delta SPL} = -0.14m + 4.63 \text{ dB}$$

with a regression coefficient of -0.59. The equation indicates that the average range of data at a given microphone location will be 4.5 dB for harmonic m = 1 and 3.1 dB for harmonic of order 11 .

In an alternative analysis the range of sound pressure levels for each harmonic can be averaged for each microphone location. The averages can then be plotted as a function of radiation angle θ' (defined as in Figure 17). The resulting relationship is shown in Figure 43, which suggests that data repeatability is worst near the plane of rotation of the propeller.

The large variability in the data for nominally identical test conditions is of concern because it can mask trends associated with parametric variations. A similar problem occurs during flight test. A better understanding of the phenomena involved would be a useful addition to propeller noise technology.

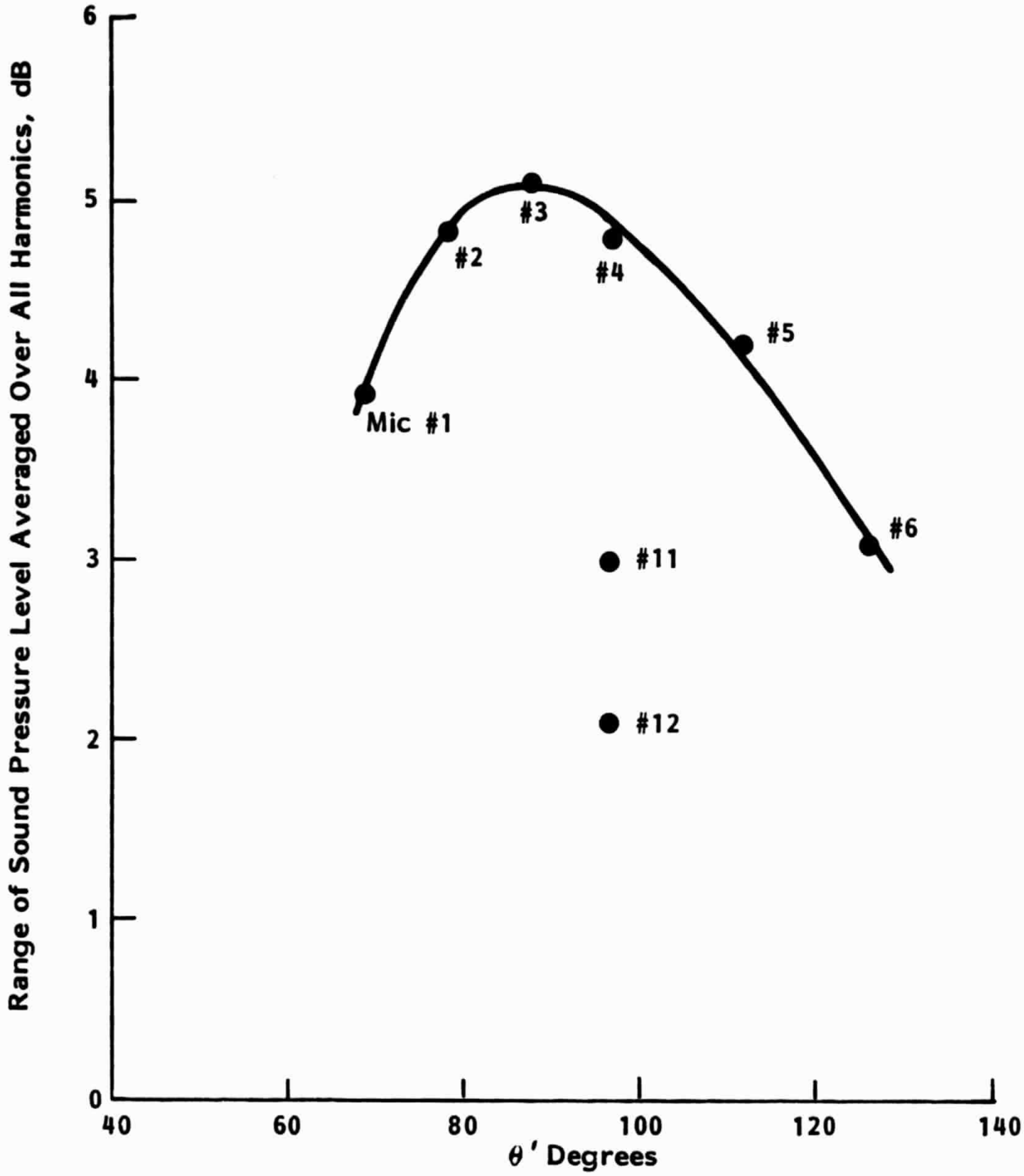

FIGURE 43. AVERAGE RANGE OF HARMONIC SOUND PRESSURE LEVELS FOR REPEAT RUNS AS A FUNCTION OF ANGLE OF RADIATION

4.5 Summary

This evaluation of the narrowband acoustic spectra has shown that the background noise generated by the test hardware without the propeller is usually lower than that generated by the propeller. The exception to this rule occurs for broadband noise at low frequencies. However, the presence of the empennage causes only a small change in broadband sound pressure level. Consequently a detailed analysis of broadband propeller noise does not appear to be worthwhile.

Visual inspection of the narrowband spectra indicates that the presence of the empennage has a significant effect on the sound pressure levels of the higher order harmonics. Thus further discussion of the harmonic levels is contained in Section 5. The data evaluation did show, however, that the repeatability of the harmonic sound pressure levels is not particularly good; this will impact the accuracy of parametric studies.

5. HARMONIC SOUND PRESSURE LEVELS

5.1 General

The wind tunnel test program described in this report generated an extensive data bank and it is possible to present here only a limited discussion of the measured sound pressure levels. The discussion in this section is restricted to the sound pressure levels at harmonics of the blade passage frequency and the intent is to point out some of the main features of the data.

Much of the data is associated with a propeller rotational speed of 8200 rpm and it is convenient to use harmonic order rather than actual frequency as a means of identifying the harmonics of interest. The same approach is followed when data are presented for lower rotational speeds, and data for different rpm are compared on the basis of harmonic order rather than actual frequency. This means, for example, that sound pressure levels at harmonic order 10 are compared directly for propeller speeds of 4000 and 8200 rpm even though the sound pressure levels occur at 2667 and 5467 Hz respectively.

Data are presented for harmonic orders 1 through 11. This range was selected as it contained most of the harmonic information for the test conditions investigated and, at a propeller speed of 8200 rpm, corresponded to the data reduction frequency range 0 - 6400 Hz.

5.2 Propeller Operating Alone

Measurements made when the propeller was operating in the absence of the model fuselage and empennage give some indication of the basic acoustic characteristics of the propeller. Harmonic sound pressure levels were measured when there was no flow in the tunnel and when the tunnel flow was 45.7 and 62.5 m/s. Sample harmonic levels measured at microphone 2 are shown in Figure 44 for flow speeds of 0 and 45.7 m/s and propeller rotational speeds of 4000, 6000 and 8200 rpm. The data indicate that the harmonic levels decrease rapidly as harmonic order increases for the lower rotational speeds. The rate of decrease is less at 8200 rpm with the 5th harmonic being about 20 dB below the first harmonic level.

When flow is introduced there is an increase in the broadband sound pressure levels which tends to mask the higher order harmonic components (see Figure 45). Thus it is not possible to determine whether or not the higher order harmonic levels are lower than for the zero flow case, as they are for the flight case shown in Figure 1. At low orders, the harmonic components can be identified (Figure 44(b)) and the sound pressure levels are similar to those for zero flow speed. This is consistent with airplane test data such as that shown in Figure 1.

5.3 Influence of Empennage

The main interest is in the influence of the fuselage and empennage on the propeller sound field. This influence can be seen in the spectral comparisons presented in Figures 46 and 47. The data were measured at microphone 2 for two flow speeds and two fuselage orientations, and for comparable separations between empennage and propeller plane.

The first observation is that, at low orders such as m = 1 to 4, the harmonic sound pressure levels appear to be independent of empennage configuration. In fact the sound levels do not change significantly when the fuselage and empennage are introduced. The situation is different at higher mode orders. In this frequency regime the harmonic levels are too low to be identified when there is no fuselage present. When the fuselage is introduced there is a small increase in sound pressure level so that additional harmonic components can be identified in the mid-frequency range

(a) V = 0 m/s

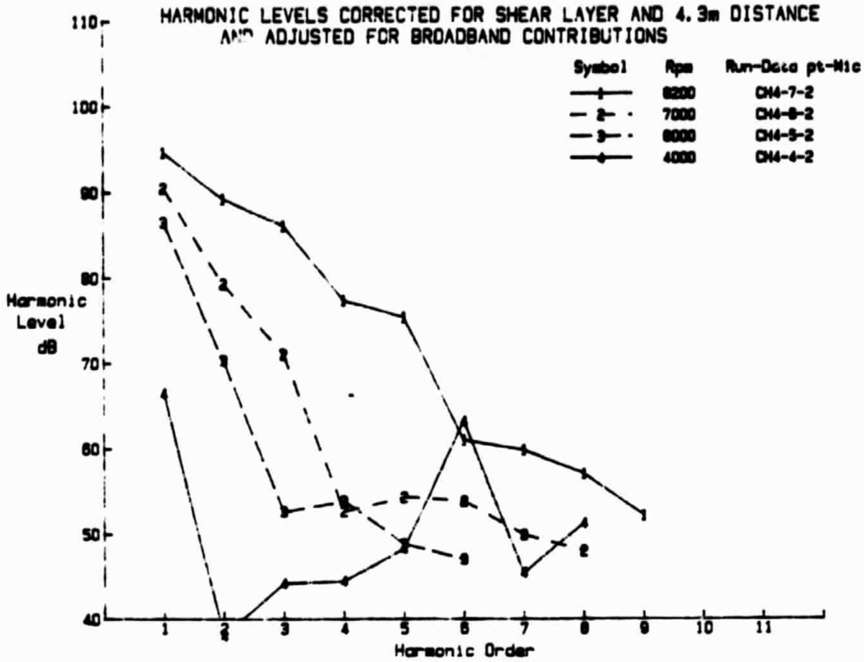

(b) V = 45.7 m/s

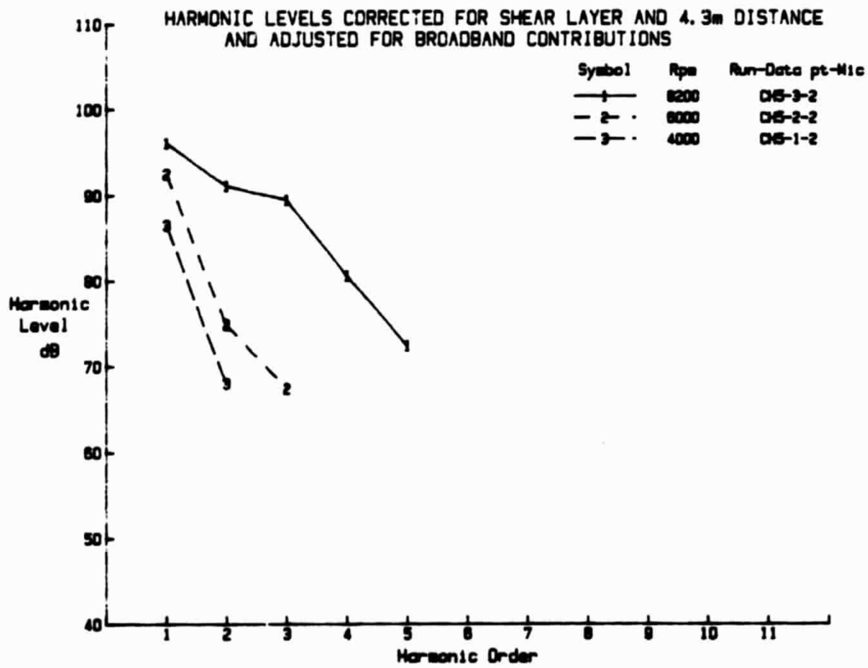

FIGURE 44. HARMONIC LEVELS FOR PROPELLER OPERATING ALONE AT DIFFERENT RPM (MICROPHONE 2)

ORIGINAL PAGE IS
OF POOR QUALITY

(a) V = 0 m/s

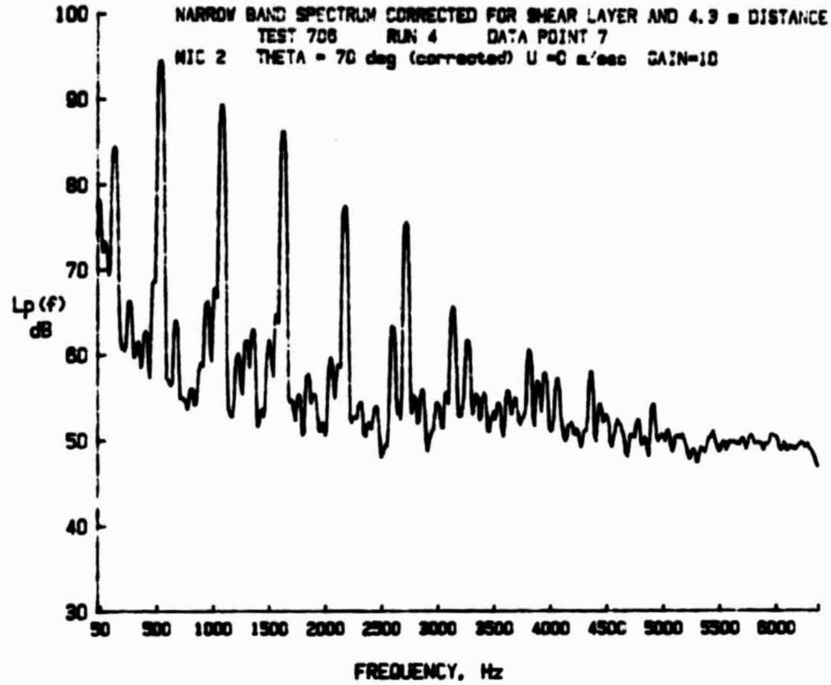

(b) V = 45.7 m/s

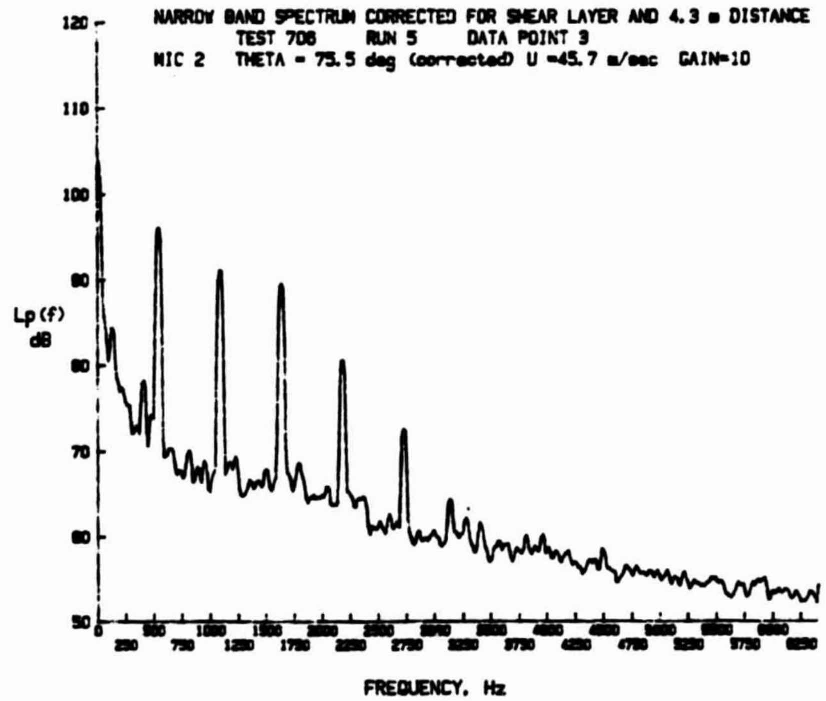

FIGURE 45. NARROWBAND SOUND PRESSURE LEVELS FOR PROPELLER OPERATING ALONE (8200 RPM; MICROPHONE 2)

(a) V = 45.7 m/s

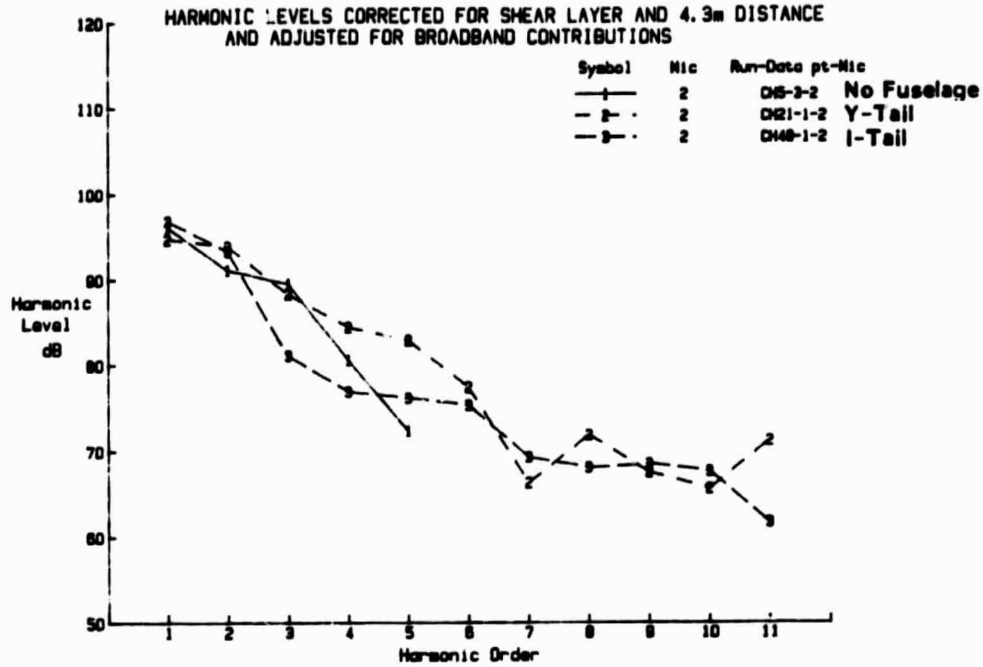

(b) V = 62.4 m/s

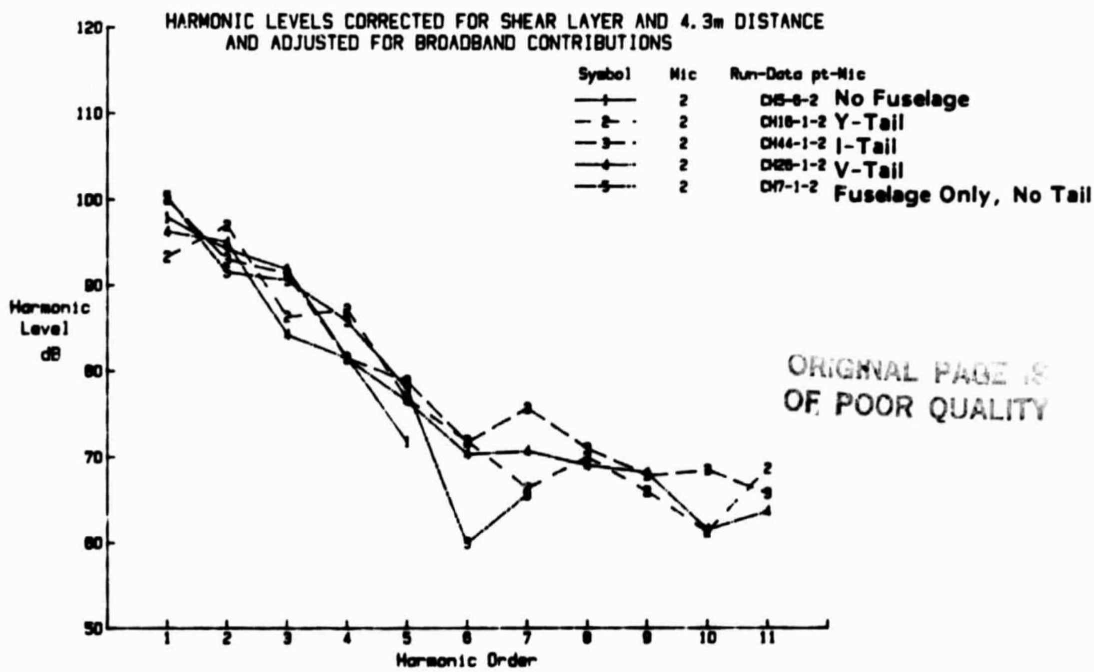

FIGURE 46. COMPARISON OF HARMONIC SOUND PRESSURE LEVELS MEASURED AT MICROPHONE 2 FOR DIFFERENT EMPENNAGE CONFIGURATIONS (ψ = 0°, 8200 RPM)

(a) V = 45.7 m/s

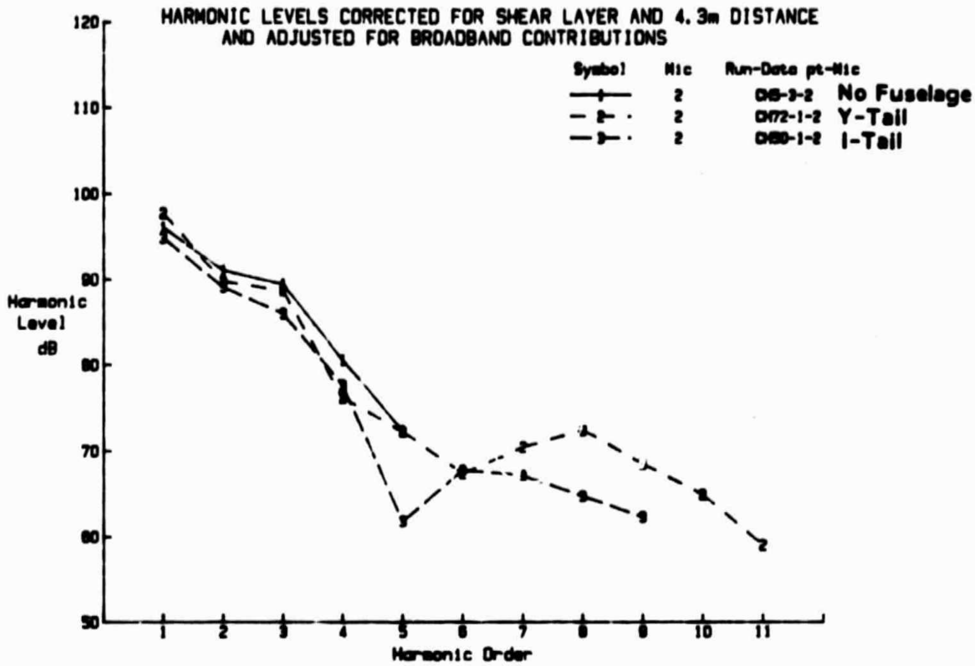

(b) V = 62.4 m/s

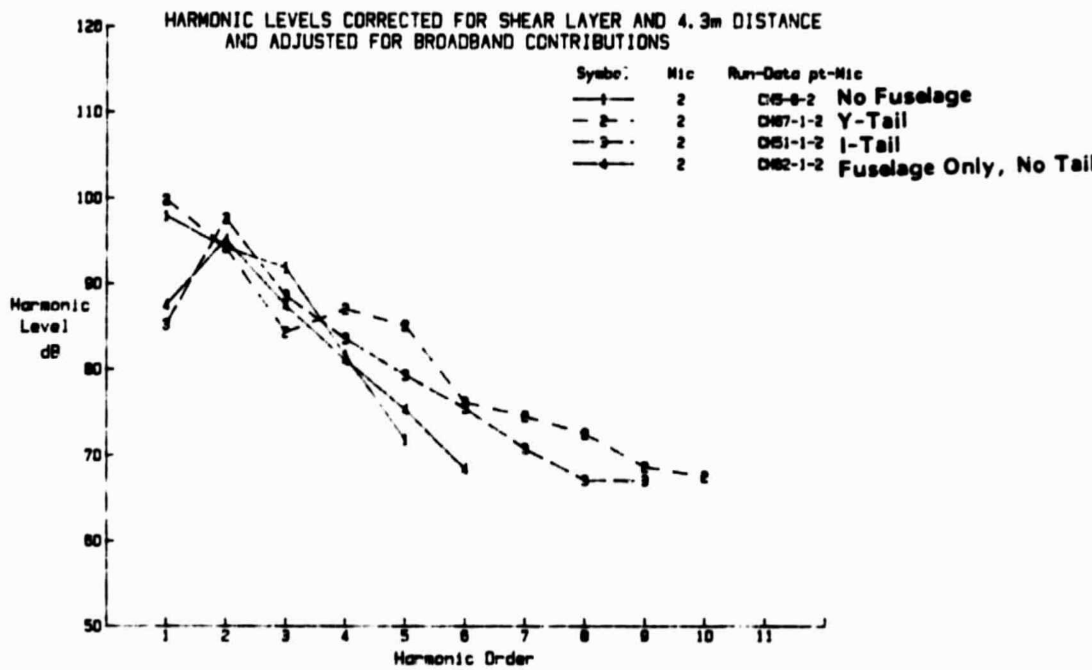

FIGURE 47. COMPARISON OF HARMONIC SOUND PRESSURE LEVELS MEASURED AT MICROPHONE 2 FOR DIFFERENT EMPENNAGE CONFIGURATIONS (ψ = 90°, 8200 RPM)

(m = 5 to 7). Finally, when the empennage is added there is a significant increase in harmonic levels for harmonic orders greater than 4 or 5. The precise magnitude of the increase cannot be determined in the absence of data where the empennage is not installed, but in some cases it is about 5 to 10 dB.

The general review given in Figures 46 and 47 for data measured at microphone location 2 can be considered in somewhat greater detail by considering each empennage separately. Figures 48 and 49 present representative harmonic spectra measured at several locations and two fuselage orientations for the Y-tail empennage. The spectra compare sound levels with and without the Y-tail installed. In Figure 46 data are included for microphone 9 which is in the flow, upstream of the propeller and fuselage. This spectrum is different from those at other locations in that the sound levels vary very slowly with harmonic order rather than decreasing rapidly. Even so, it is more difficult to determine the change in harmonic level induced by the empennage because the high self-noise level due to flow over the microphone masks most of the harmonic components when there is no empennage installed.

The spectra presented in Figures 48 and 49 are consistent with the conclusions drawn from Figures 46 and 47. At mode order 1 to 4 the empennage has no significant effect on the sound levels but at higher mode orders the sound levels increase when the empennage is installed. The term "no significant" is used here in the sense that any changes in sound pressure level that do occur at low values of harmonic order m are within the data variability range observed in Figure 42 for the repeated runs.

A comparison of harmonic sound pressure levels associated with the Y-tail and V-tail configurations indicates that there is no significant difference between the two empennage with respect to radiated noise. The representative data given in Figure 50 show sound pressure levels which are similar for the two configurations.

(a) Microphone 9

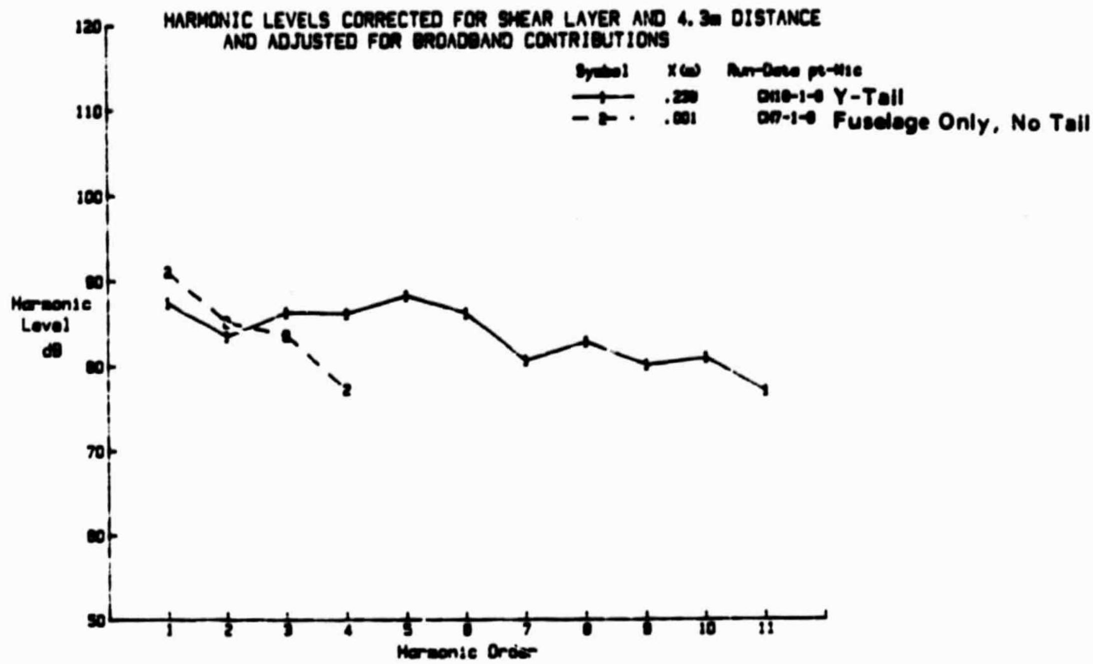

(b) Microphone 2

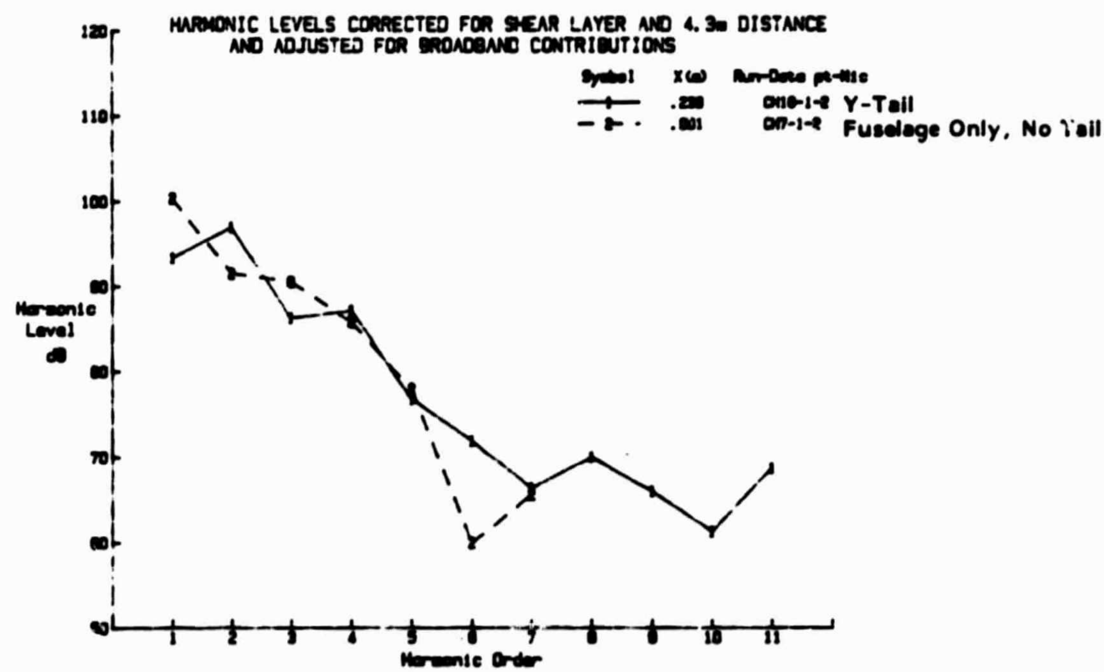

FIGURE 48. INFLUENCE OF Y-TAIL ON HARMONIC LEVELS (8200 RPM, 62.4 M/S, X = 23.8 CM, $\psi = 0°$)

(c) Microphone 4

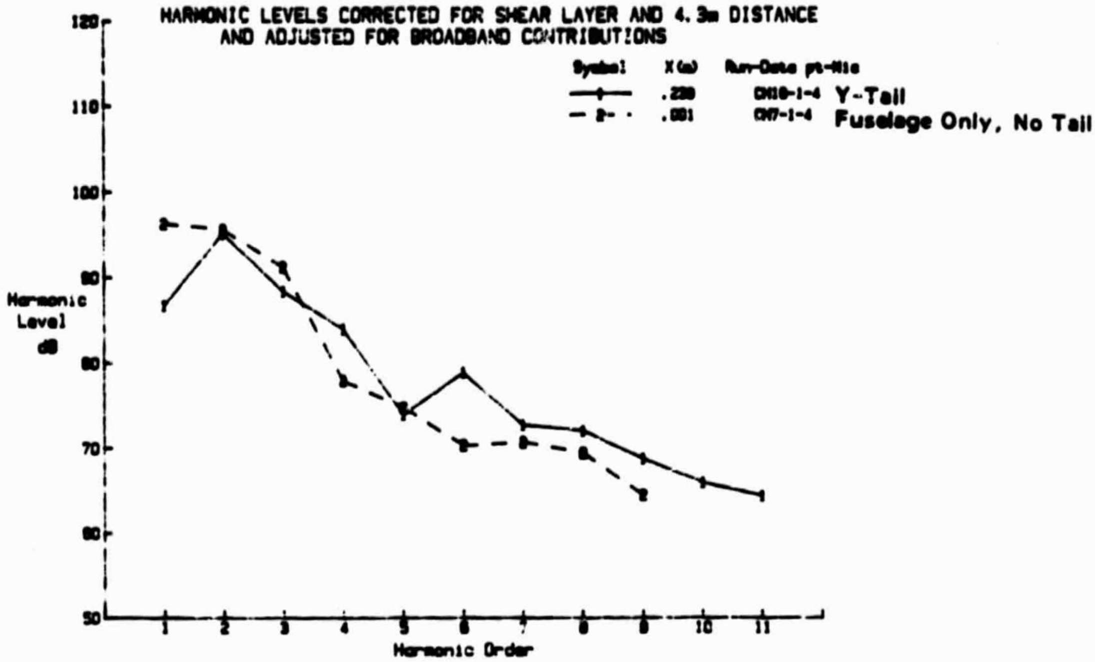

(d) Microphone 6

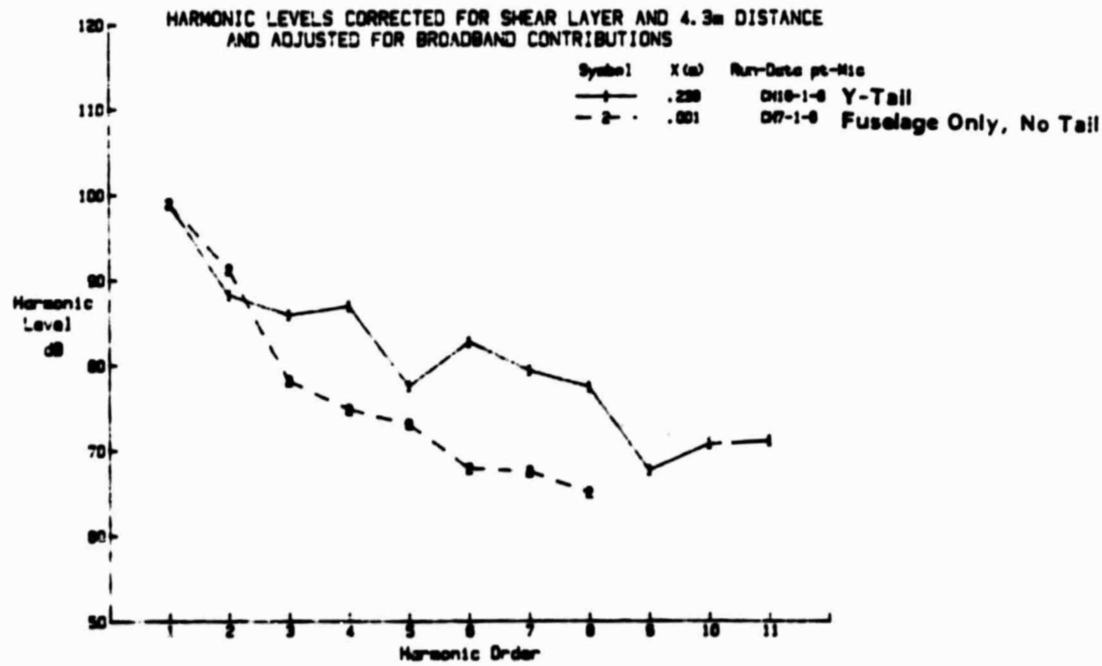

FIGURE 48. CONTINUED

(a) Microphone 2

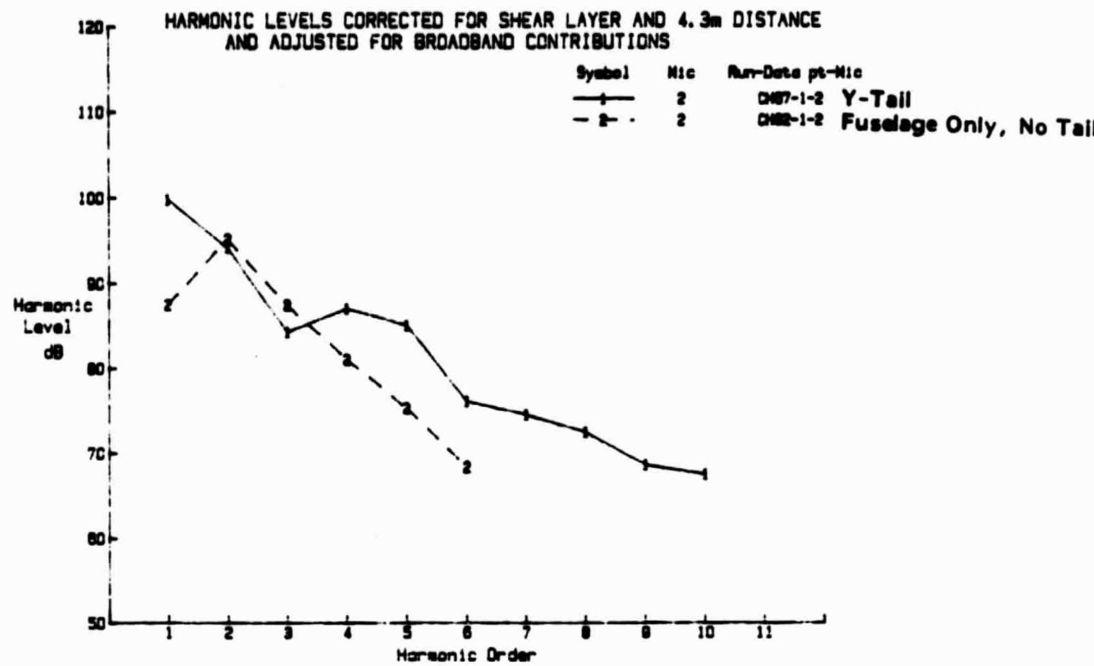

(b) Microphone 4

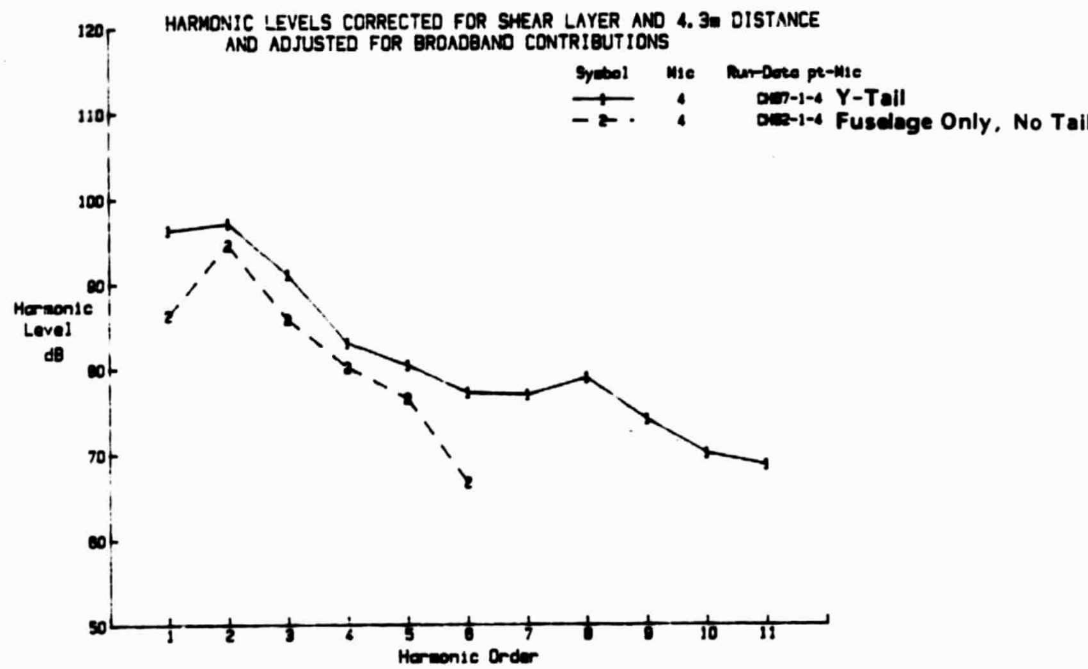

FIGURE 49. INFLUENCE OF Y-TAIL ON HARMONIC LEVELS (8200 RPM, 62.4 M/S, X = 23.8 CM, ψ = 90°)

(c) Microphone 6

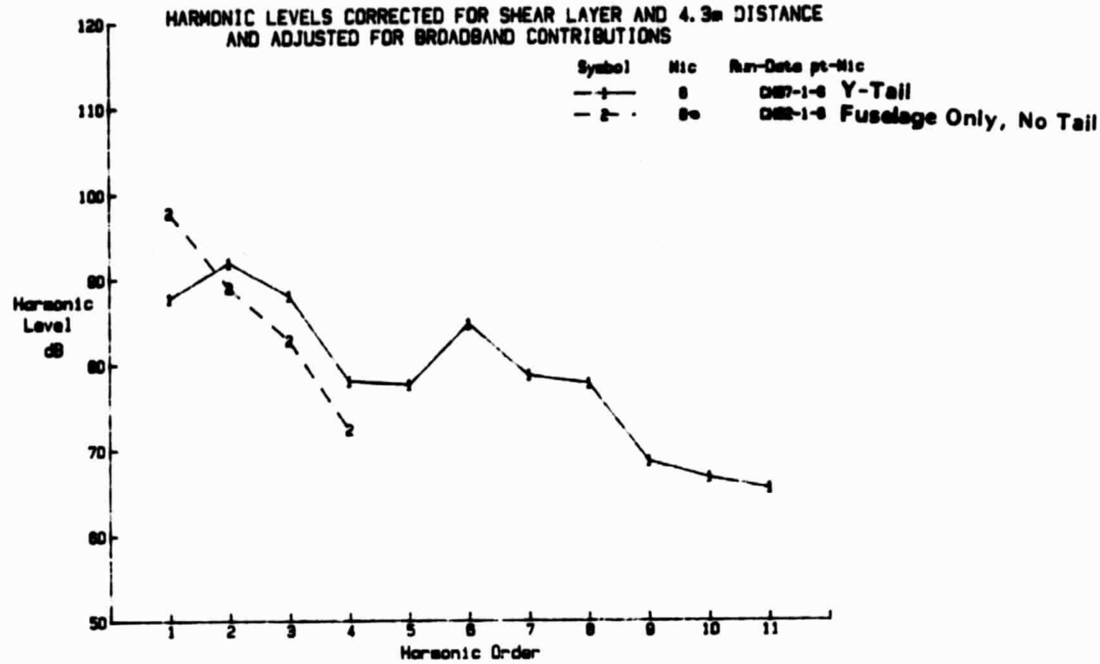

(d) Microphone 11

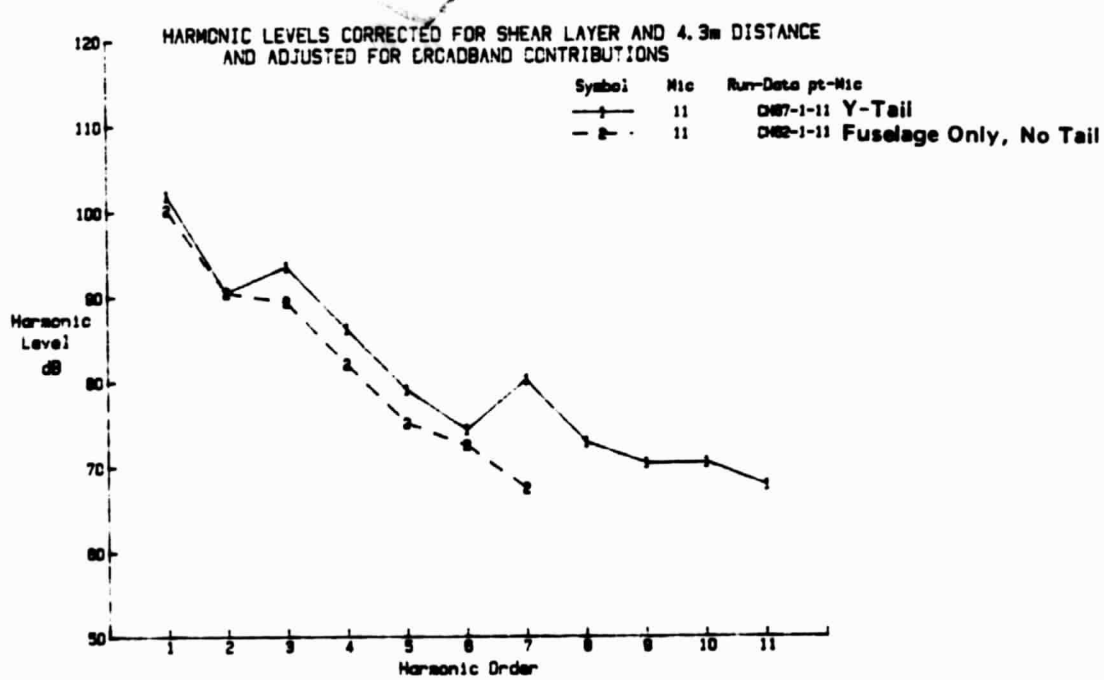

FIGURE 49. CONTINUED

(a) Microphone 9

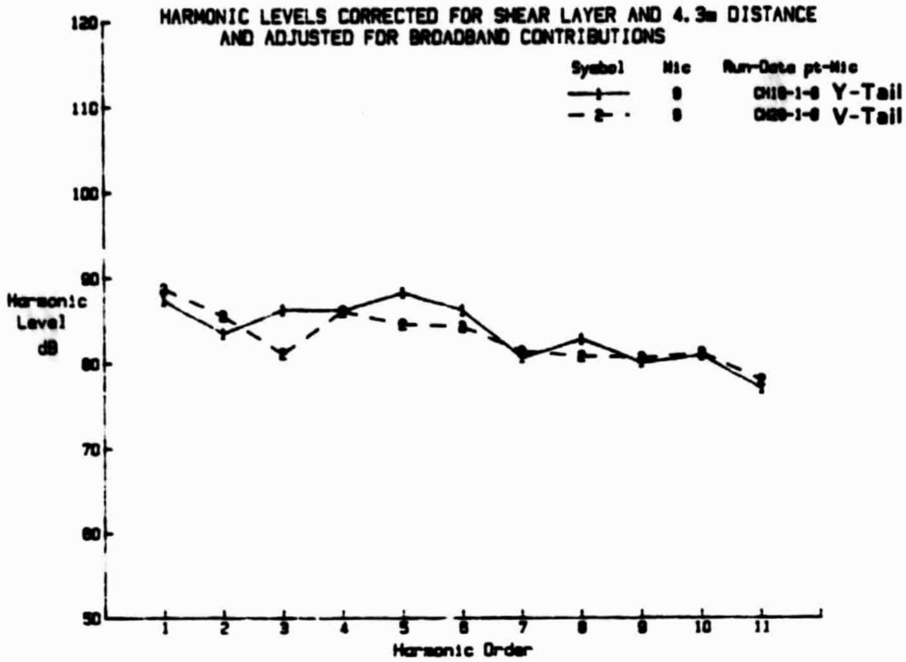

(b) Microphone 2

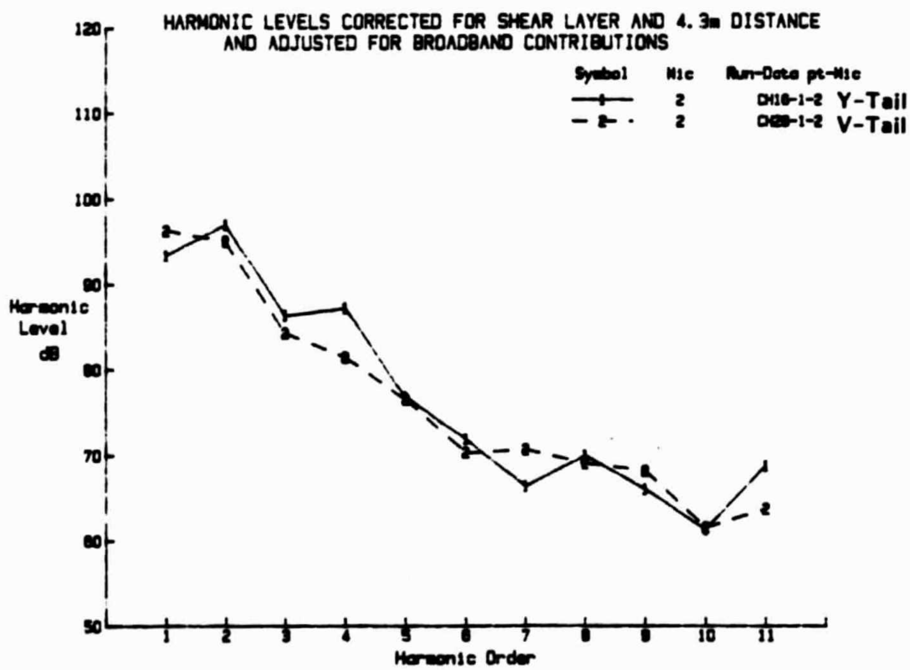

FIGURE 50. COMPARISON OF HARMONIC LEVELS FOR Y-TAIL AND V-TAIL EMPENNAGES (8200 RPM, 62.4 M/S, X = 23.8 CM, ψ = 0°)

(c) Microphone 4

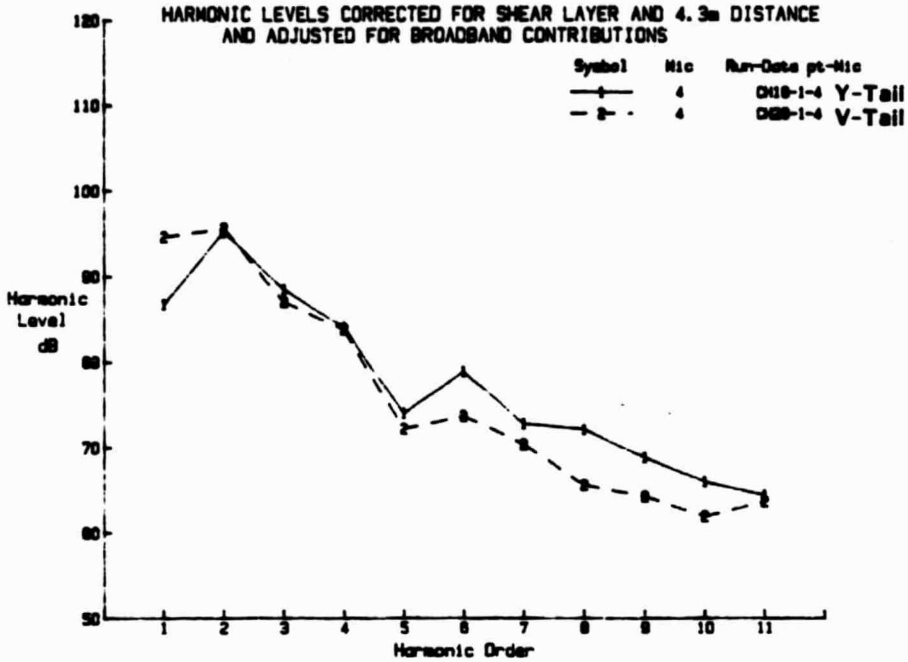

(d) Microphone 6

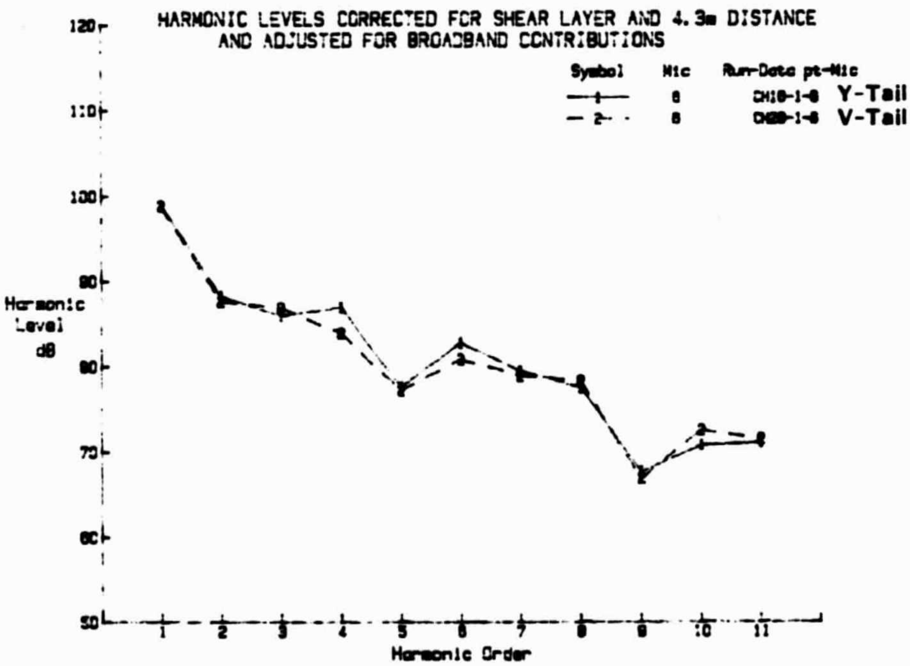

FIGURE 50. CONTINUED

Harmonic spectra for the I-tail empennage are presented in Figures 51 and 52. The data are quite similar to those in Figures 48 and 49 for the Y-tail. Thus the general conclusions remain the same. However, one additional comment can be made. The increase in harmonic level for large values of m appears to be most pronounced as the angular coordinate θ of the measurement location tends toward 0° or 180°. The smallest changes in sound pressure level occur at measurement locations closest to the plane of rotation of the propeller.

5.4 Blade Angle

For most of the tests the blade angle β was adjusted to the design value for the appropriate rotational and flow speeds. However, one test was performed during which β was given several off-design values when the propeller rotational speed was 8200 rpm and the flow speed was 62.4 m/s (Runs 22 through 25). The design angle for this test condition was 21°; measurements were also performed for blade angles of 19°, 23° and 24°. A comparison of the resulting harmonic sound pressure levels is given in Figure 53.

Inspection of the data indicates that the design angle of 21° is not always associated with the lowest sound pressure level at a given harmonic order and measurement location. There are some instances where the design angle is associated with the highest measured sound pressure levels. It is interesting to note, however, that the spectra contained in Figure 53 are quite similar to those in Figure 42 for corresponding measurement locations. The similarity occurs in both spectral shape and the range of measured sound pressure levels for a given harmonic order and microphone location. The data in Figure 42 are associated with nominally identical test conditions so that the variation in sound pressure level is an indication of data repeatability. It was speculated in Section 4.4 that errors in blade angle setting could be one cause of the data scatter. The data in Figure 53 indicate that

(a) Microphone 9

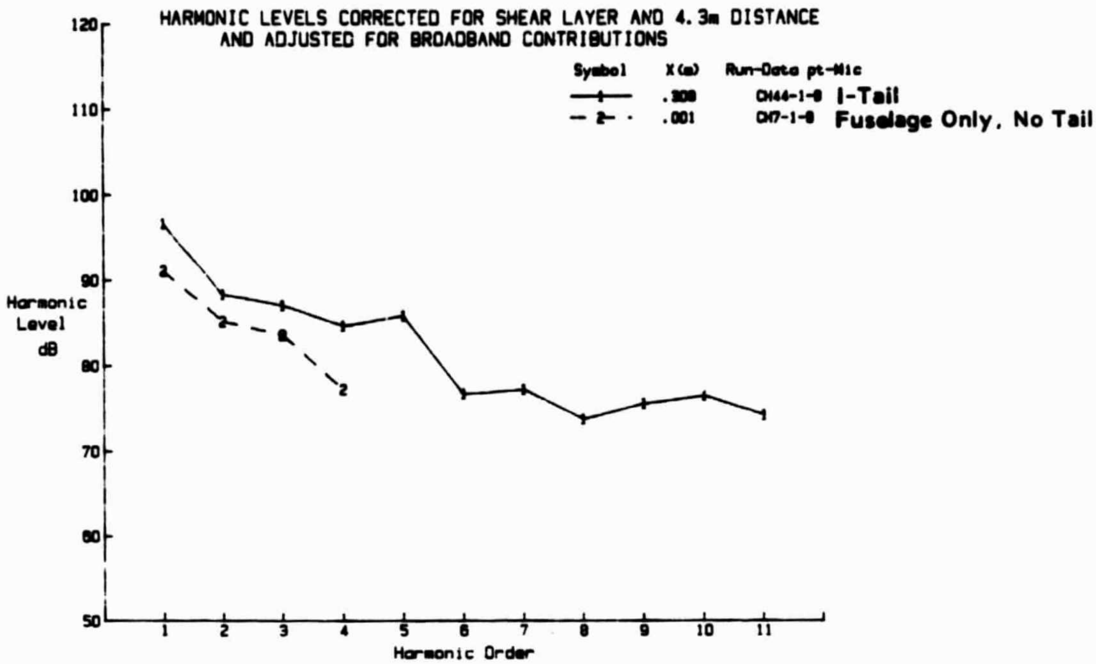

(b) Microphone 2

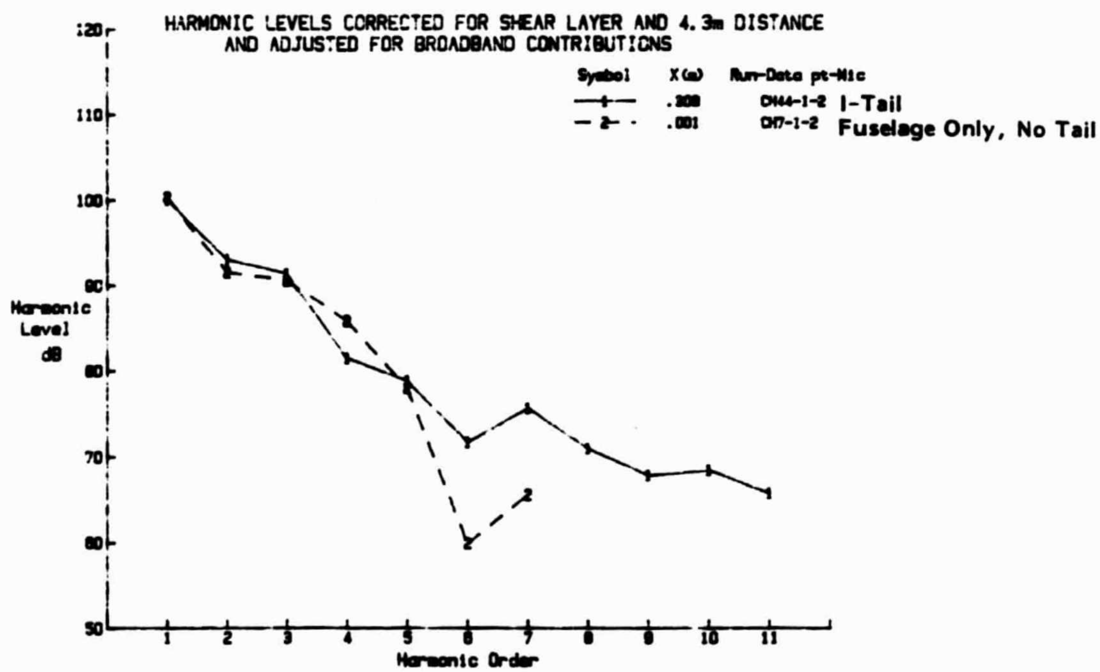

FIGURE 51. INFLUENCE OF I-TAIL ON HARMONIC LEVELS (8200 RPM, 62.4 M/S, X = 30.8 CM, $\psi = 0°$)

(c) Microphone 4

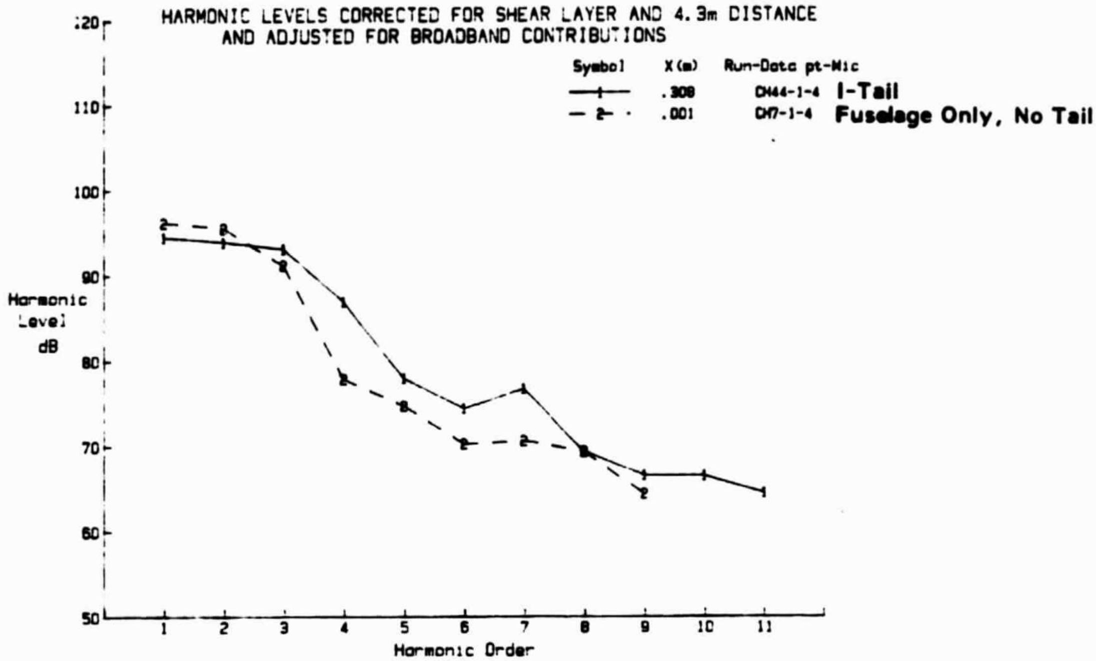

(d) Microphone 6

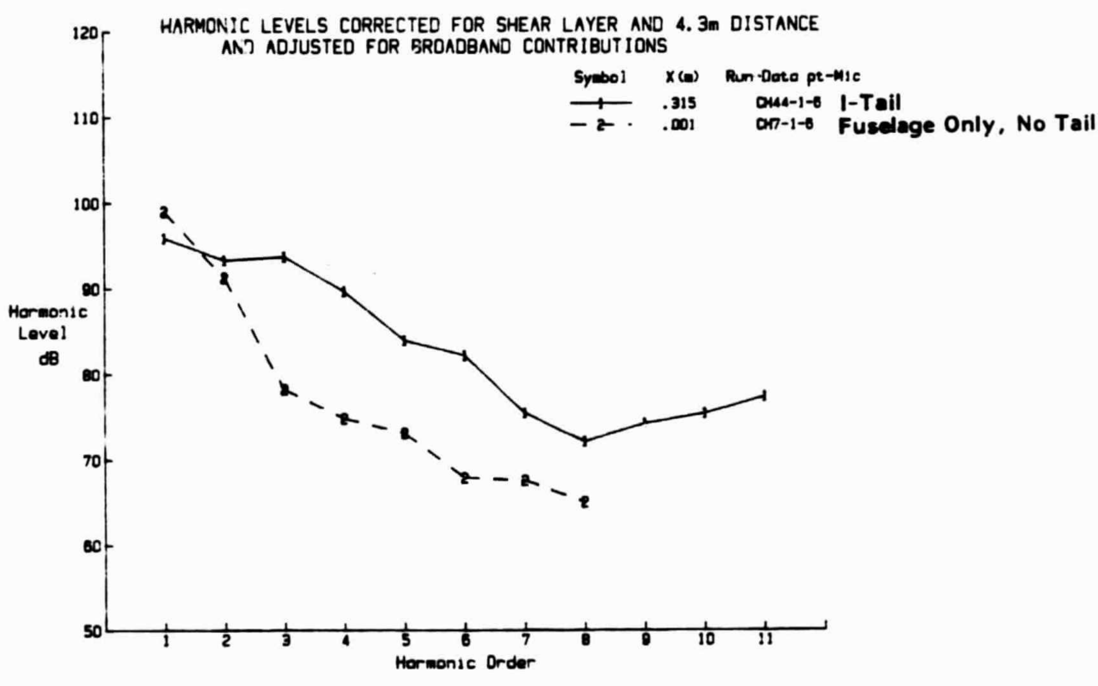

FIGURE 51. CONTINUED

(a) Microphone 2

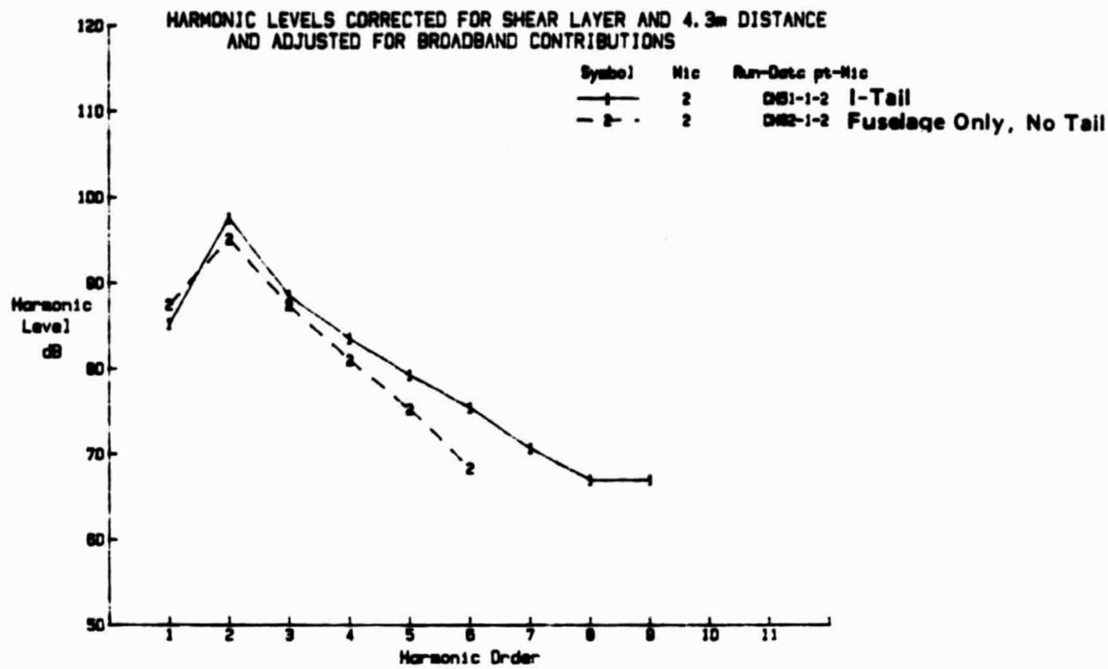

(b) Microphone 4

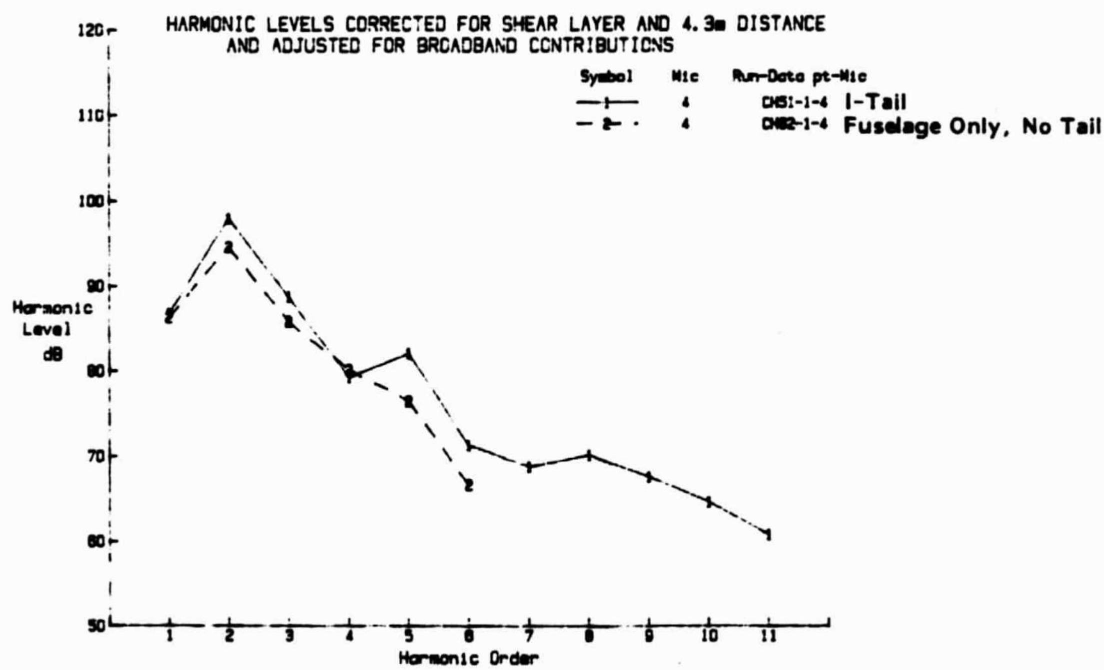

FIGURE 52. INFLUENCE OF I-TAIL ON HARMONIC LEVELS (8200 RPM, 62.4 M/S, X = 30.5 CM, ψ = 90°)

(c) Microphone 6

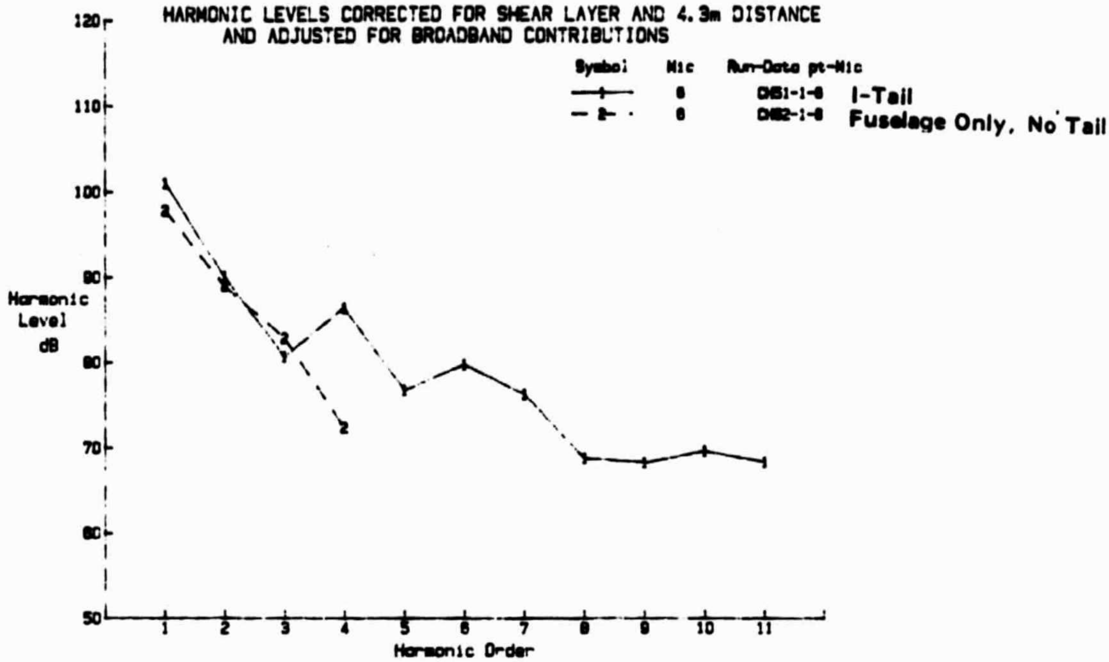

(d) Microphone 11

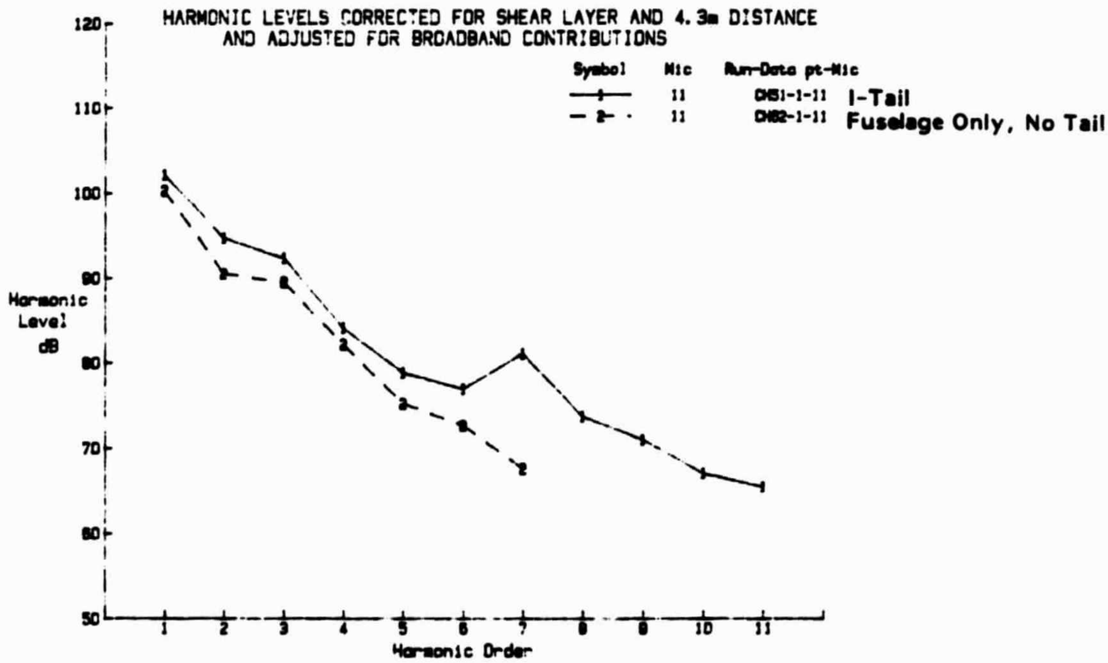

FIGURE 52. CONTINUED

(a) Microphone 2

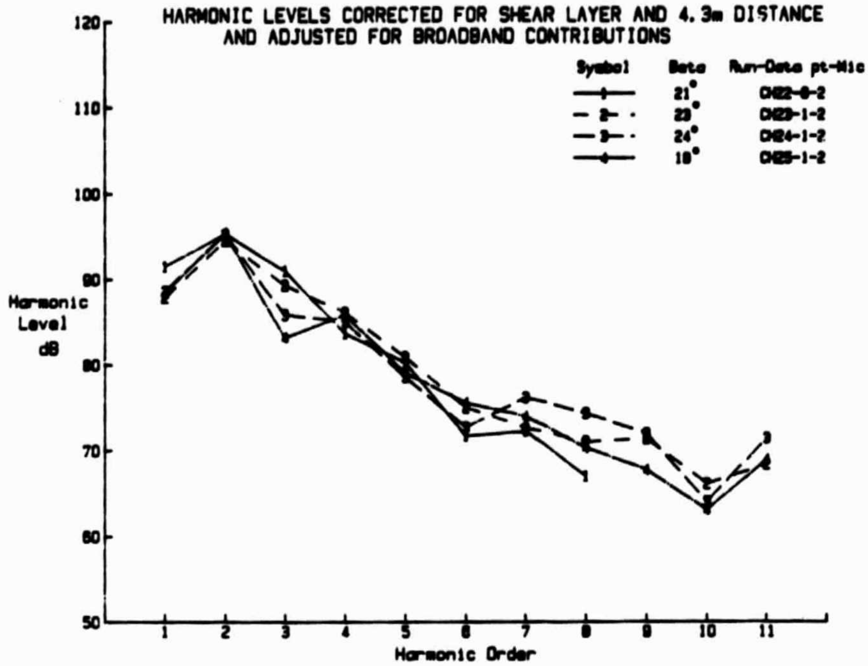

(b) Microphone 3

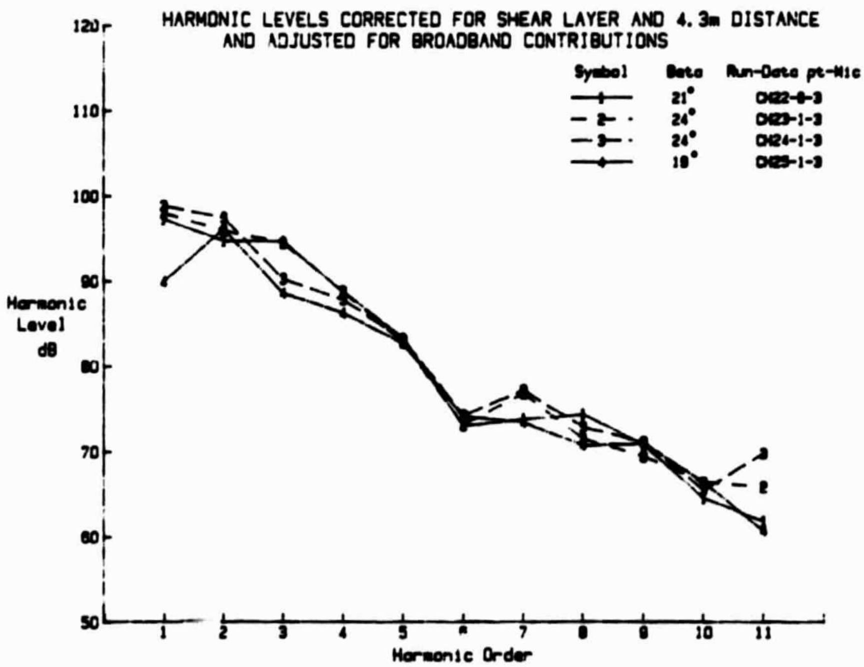

FIGURE 53. EFFECT OF BLADE ANGLE ON HARMONIC SOUND PRESSURE LEVELS (Y-TAIL, 8200 RPM, 62.4 M/S, X = 23.8 CM)

(c) Microphone 4

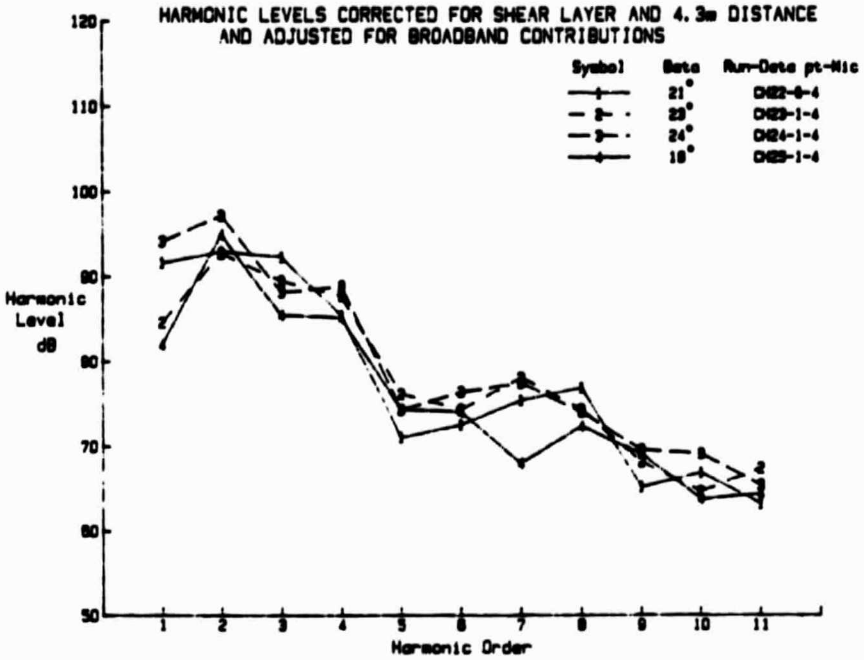

(d) Microphone 6

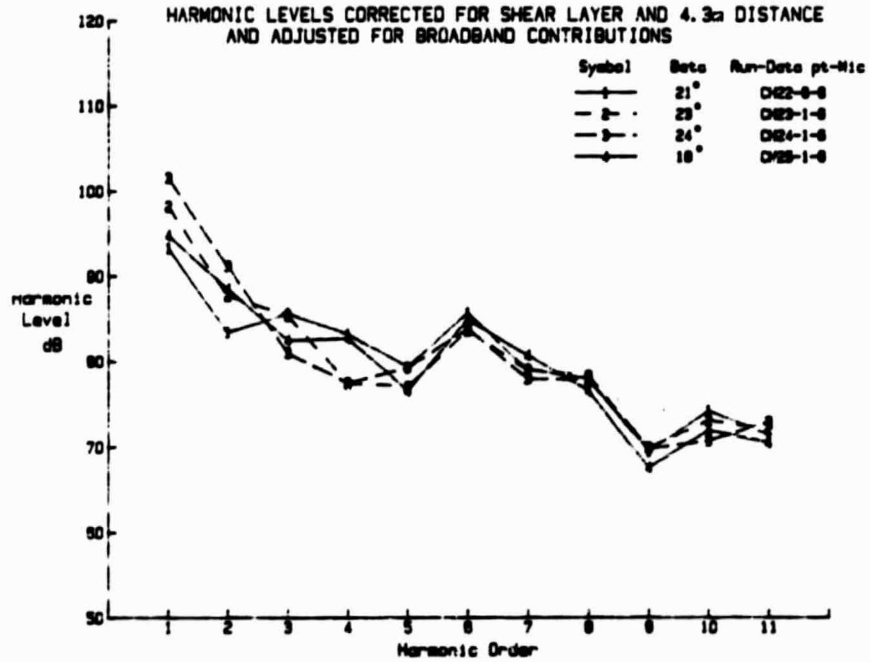

FIGURE 53. CONTINUED

(e) Microphone 11

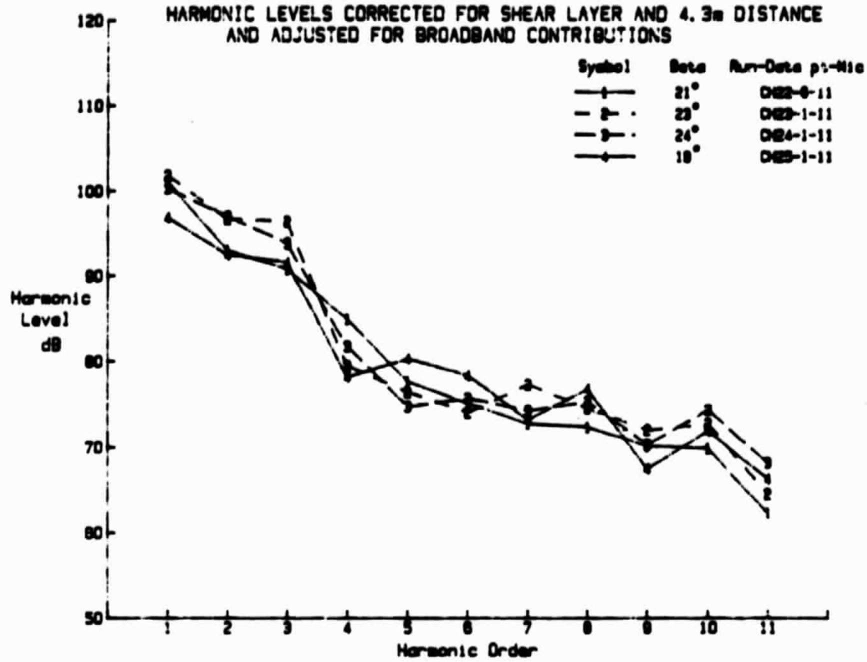

(f) Microphone 12

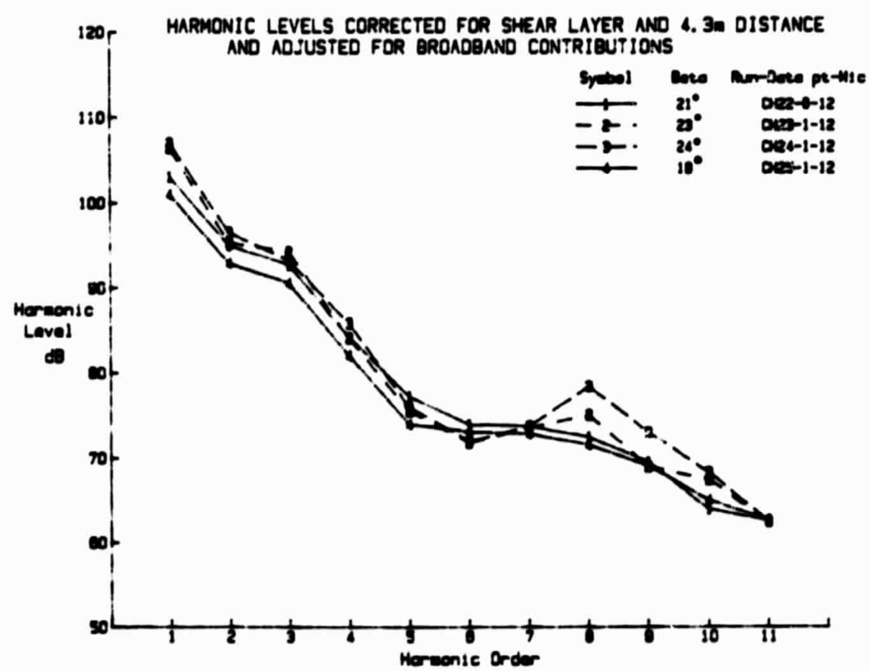

FIGURE 53. CONTINUED

the explanation could be true if the blade angle error was as high as ±2°. It seems unlikely that the error would be so large. Furthermore, since the data variability is much larger at some measurement locations thatn at others, it is possible that the explanation lies in the propagation path rather than the source.

5.5 Propeller rpm

Harmonic sound pressure levels measured at different propeller rotational speeds are shown in Figures 54 through 58. It should be remembered in reviewing these data that a given harmonic occurs at different frequencies for different values of rpm.

Figures 54 through 57 present harmonic sound pressure levels measured at the three main test propeller speeds of 4000, 6000, and 8200 rpm. In general, the data show the highest sound pressure levels occurring at the highest rotational speed and the lowest levels at the lowest rpm. However, as harmonic order increases the sound pressure levels associated with different rotational speeds tend to merge to a common curve. This is particularly evident in Figures 54(a), 56(b), and 57(b).

The high rpm range is presented in more detail in Figure 58 where the rpm is increased up to 8200 in steps of 200 rpm. Although the data still show a general trend of harmonic sound level increasing with propeller rotational speed, the pattern is confused by the variability of the results. At one harmonic, such as m = 4 in Figure 58(b), the highest sound pressure level is associated with the highest propeller speed; but for the next harmonic, m = 5, the highest propeller speed is associated with the lowest sound pressure level. In the same figure harmonic m = 3 shows an orderly progression of increasing sound pressure level with increasing rotational speed. The reasons for this apparent data variability require further investigation.

5.6 Flow Speed

Two non-zero flow speeds were used in the propeller noise tests, and representative data for these two speeds are compared in Figures 59 through 61. The harmonic levels in Figures 59 and 60 refer to two microphone locations outside the tunnel airflow, and Figure 61 presents data for two locations in the flow.

The general trend given by the data is that the harmonic sound pressure levels are slightly higher at the higher flow speeds. Exceptions to this trend are observed at some microphone locations for the $\psi = 0°$ orientation of the fuselage, when sound levels show little difference between the two flow speeds.

The changes in flow speed result in changes in flow Mach number, blade tip helical Mach number, and advance ratio J. In addition, blade angle β is changed for each combination of flow speed and propeller rpm. The change in helical Mach number is relatively small, being only 1.2%, but flow Mach number and propeller advance ratio are directly proportional to flow speed and change by about 37%. For propellers operating out of the influence of wakes, the important parameters for harmonic sound level are propeller rotational and helical Mach numbers. Other factors appear to be influencing the present results; presumably the strength of the wakes entering the propeller disc increases with flow speed and has an influence on the radiated sound pressure levels.

5.7 Fuselage Orientation

The fuselage/empennage combination was tested at two orientations, identified as $\psi = 0°$ and $90°$. For configuration $\psi = 0°$ the main microphone array was located to the side of the model airplane and for $\psi = 90°$ the array was essentially beneath the airplane. Since the model empennages are not symmetric about the axis of the fuselage it is anticipated that there will be some spatial variation

(a) Microphone 2

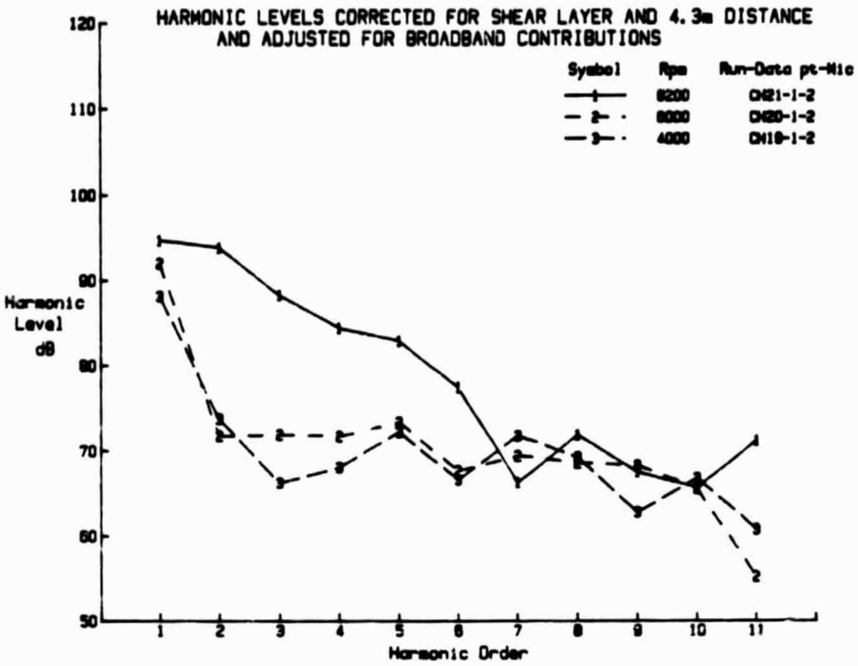

(b) Microphone 6

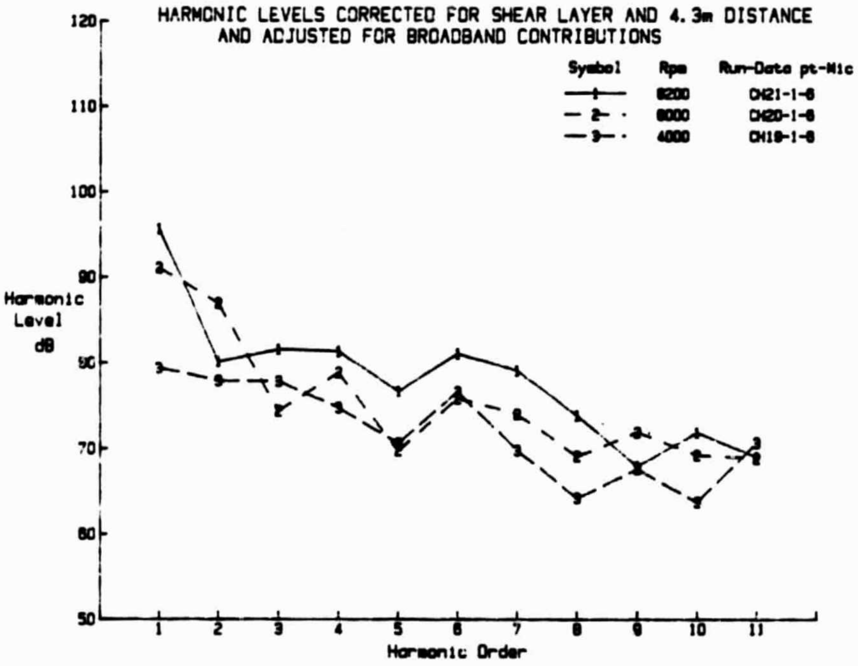

FIGURE 54. HARMONIC SOUND PRESSURE LEVELS AT DIFFERENT PROPELLER RPM (Y-TAIL, V = 45.7 M/S, ψ = 0°)

(a) Microphone 2

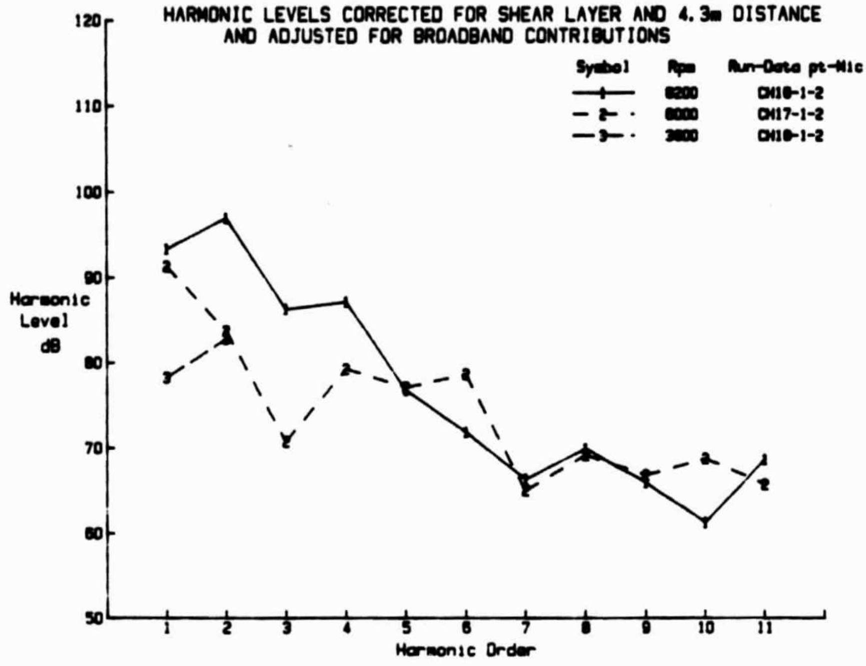

(b) Microphone 6

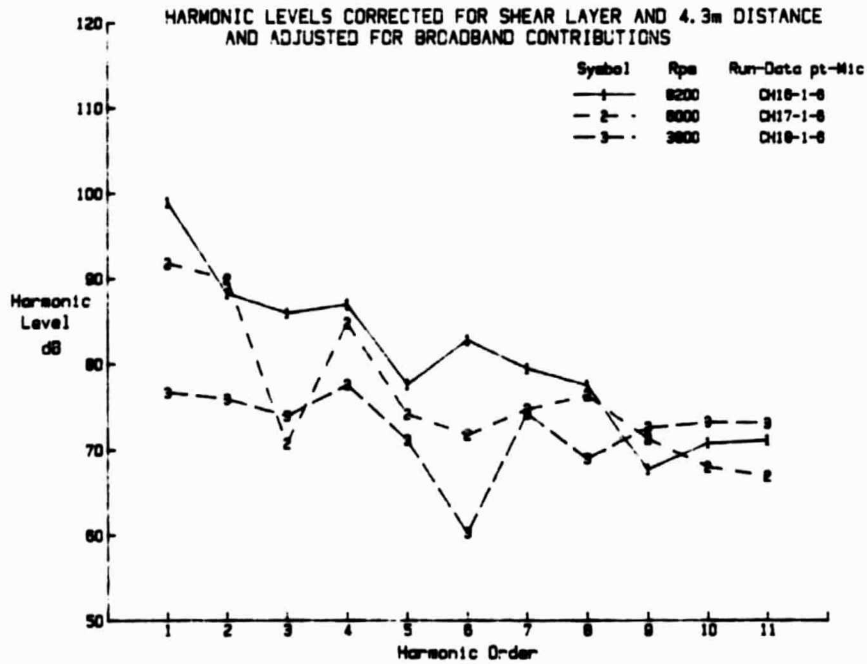

FIGURE 55. HARMONIC SOUND PRESSURE LEVELS AT DIFFERENT PROPELLER RPM (Y-TAIL, V = 62.4 M/S, ψ = 0°)

(a) Microphone 1

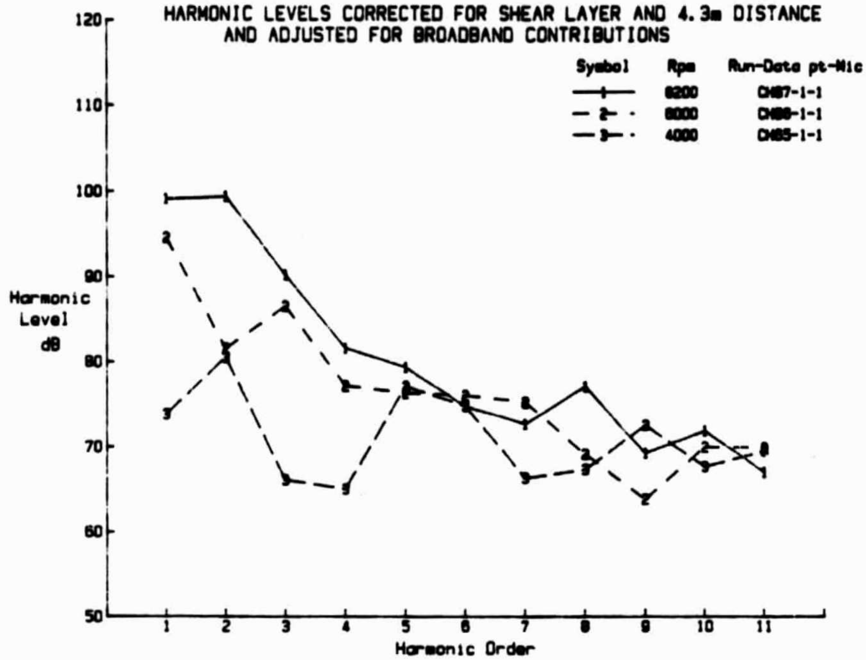

(b) Microphone 2

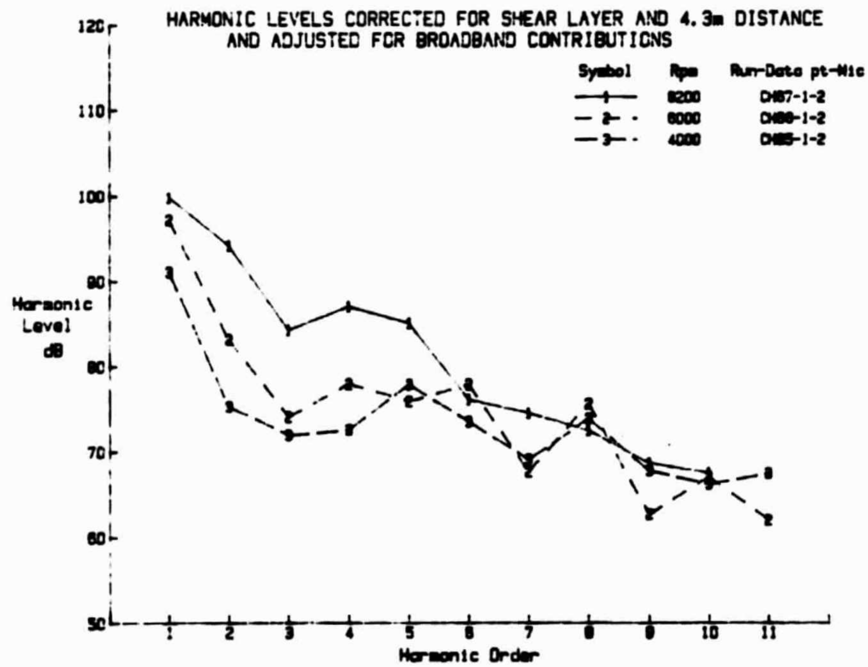

FIGURE 56. HARMONIC SOUND PRESSURE LEVELS AT DIFFERENT PROPELLER RPM (Y-TAIL, V = 62.4 M/S, ψ = 90°)

(c) Microphone 4

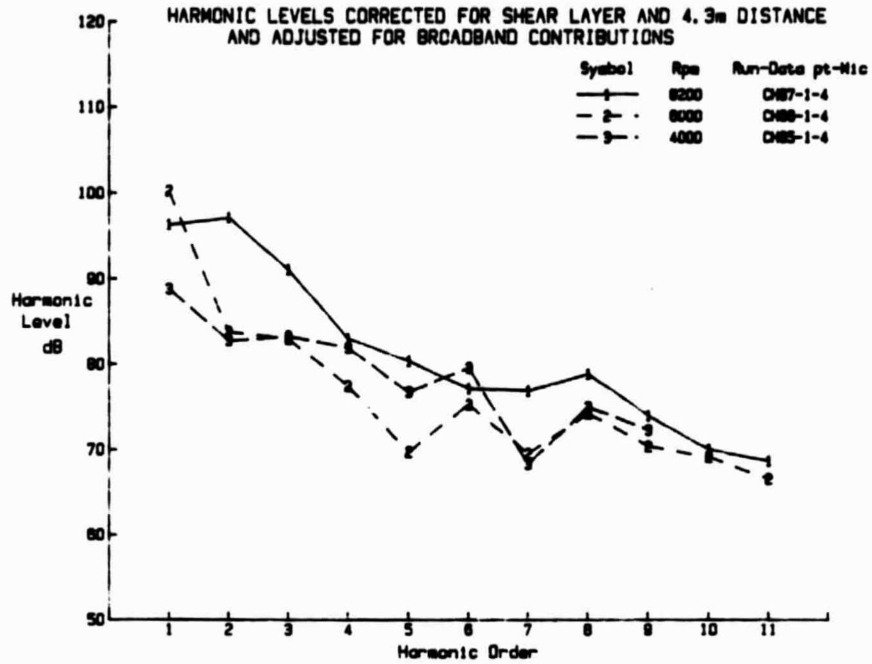

(d) Microphone 6

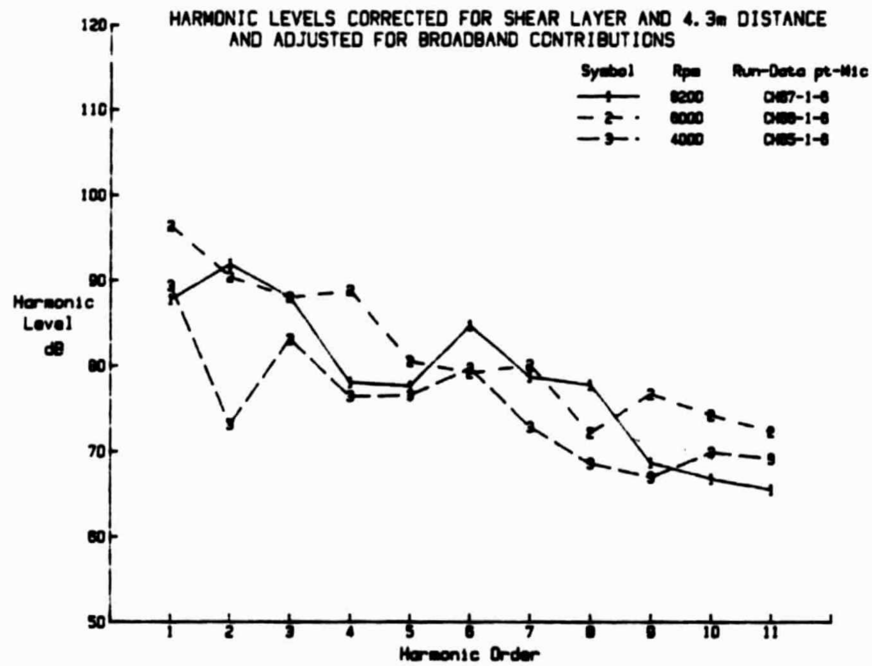

FIGURE 56. CONTINUED

(a) $\psi = 0°$

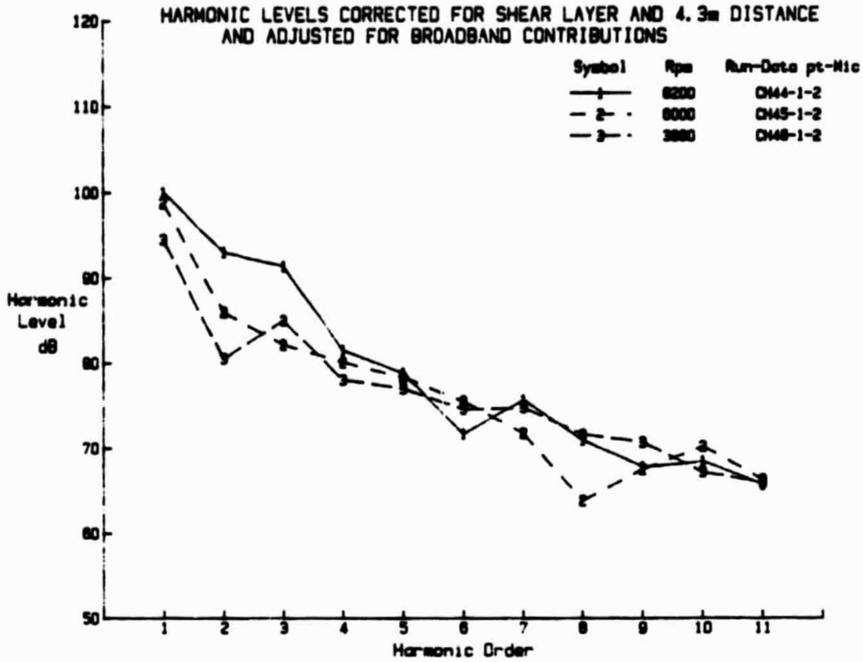

(b) $\psi = 90°$

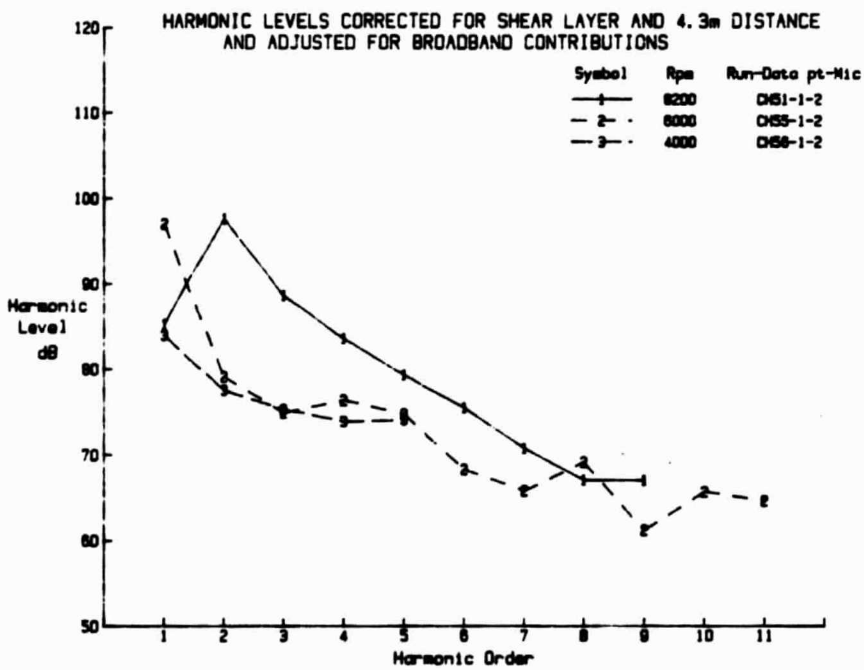

FIGURE 57. HARMONIC SOUND PRESSURE LEVELS AT DIFFERENT PROPELLER RPM (I-TAIL, V = 62.4 M/S, MICROPHONE 2)

(a) Microphone 2

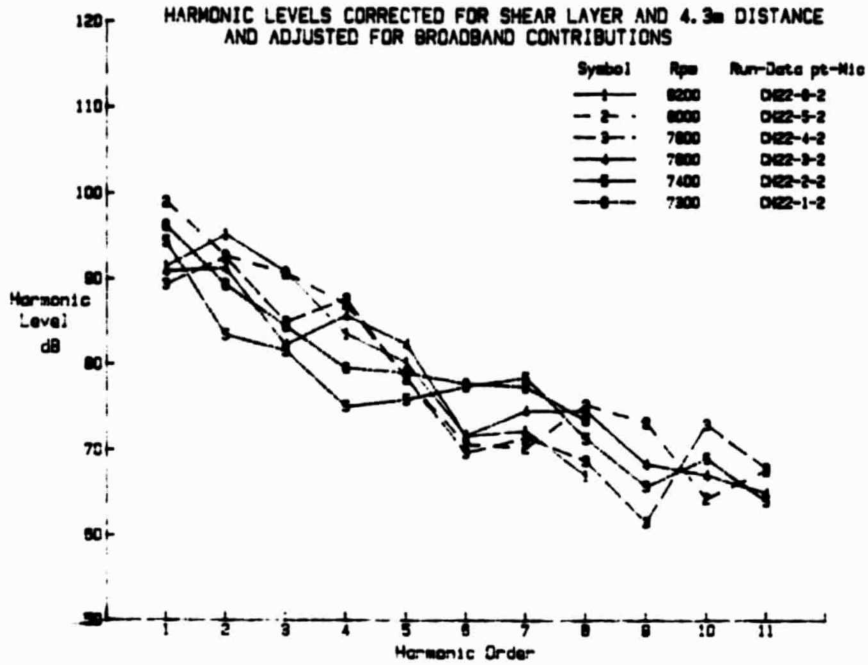

(b) Microphone 4

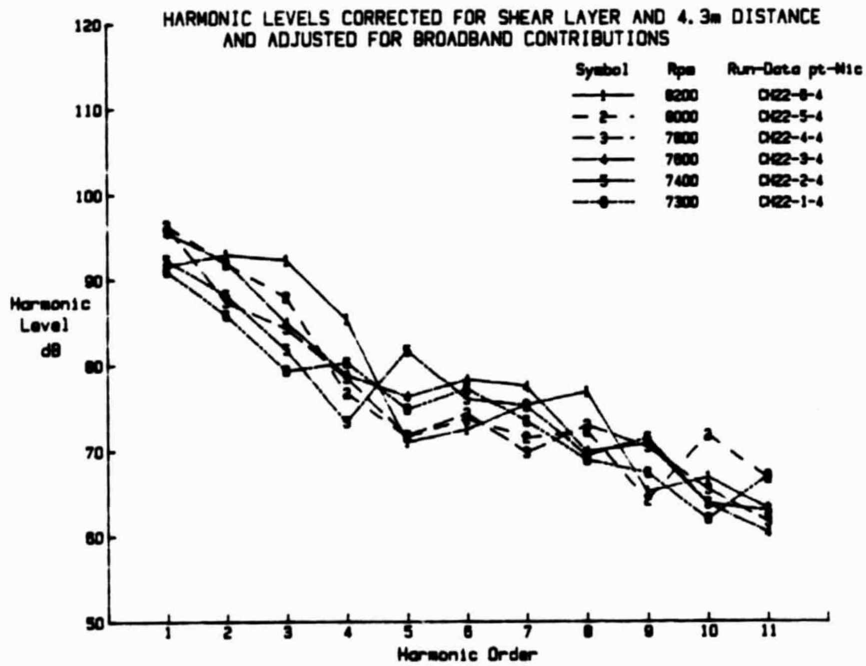

FIGURE 58. HARMONIC SOUND PRESSURE LEVELS AT DIFFERENT PROPELLER RPM FROM 7300 TO 8200 (Y-TAIL, V = 62.4 M/S, ψ = 0°)

(c) Microphone 6

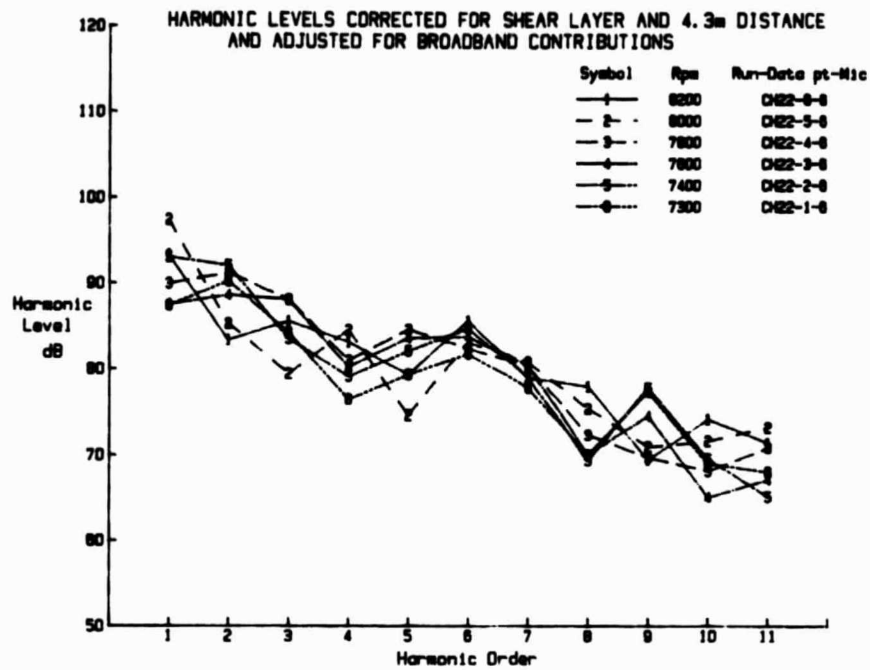

(d) Microphone 11

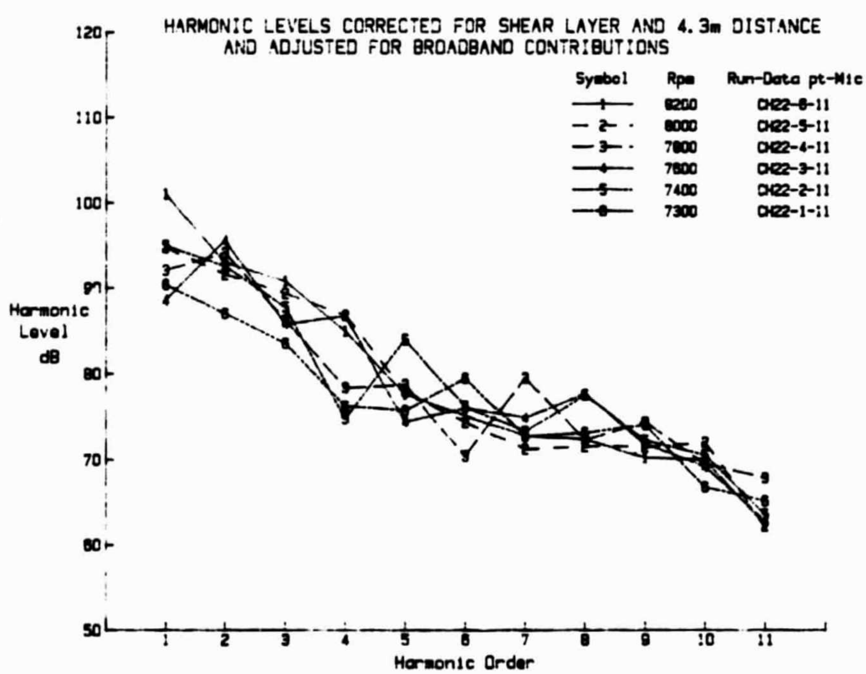

FIGURE 58. CONTINUED

(a) $\psi = 0°$

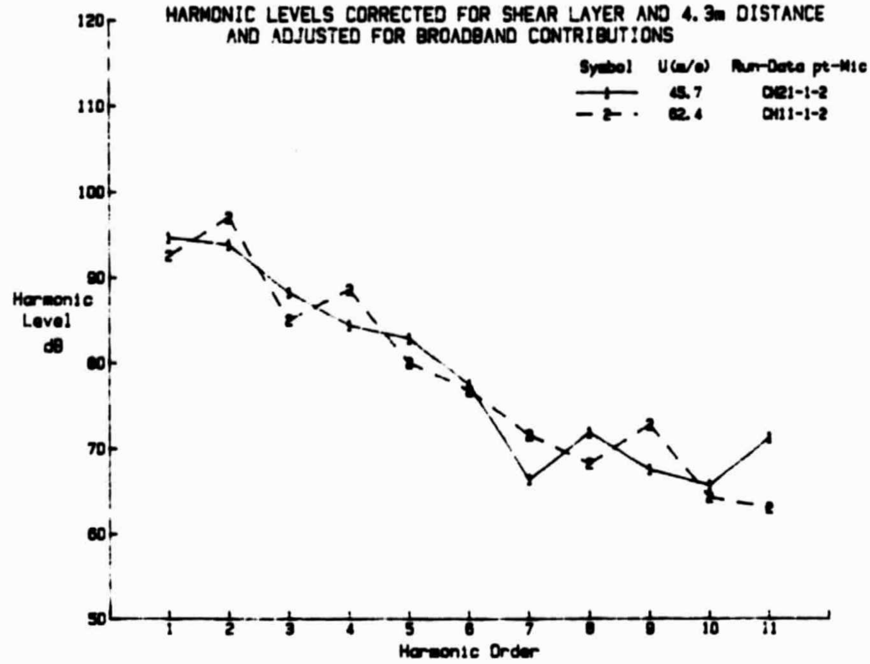

(b) $\psi = 90°$

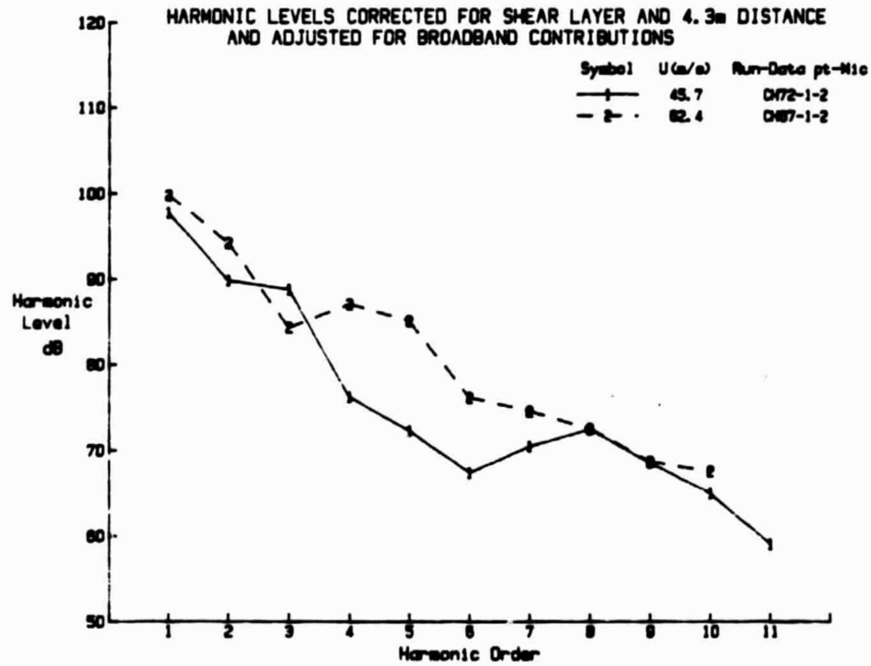

FIGURE 59. COMPARISON OF HARMONIC SOUND PRESSURE LEVELS AT DIFFERENT FLOW SPEEDS (MICROPHONE 2, 8200 RPM)

(a) $\psi = 0°$

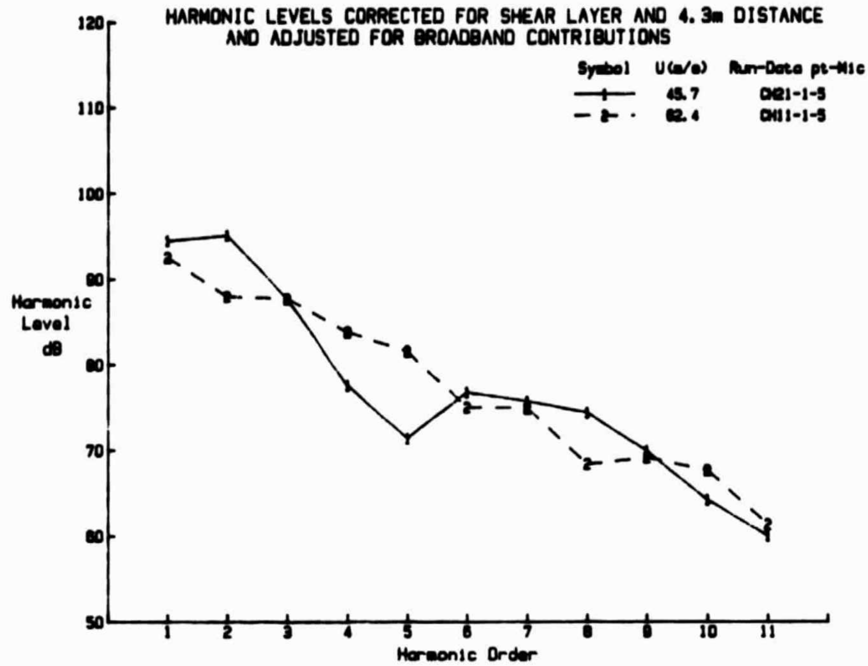

(b) $\psi = 90°$

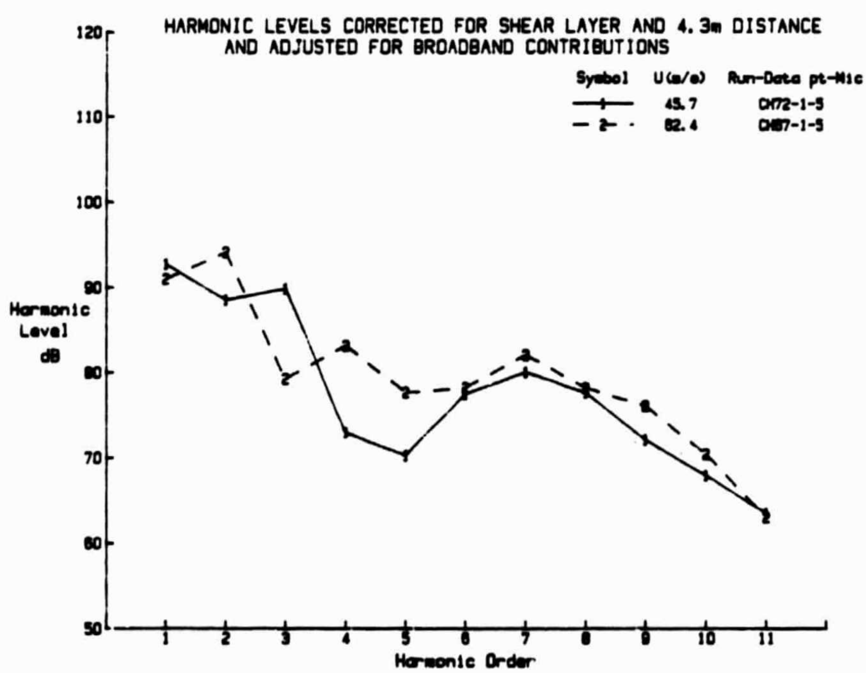

FIGURE 60. COMPARISON OF HARMONIC SOUND PRESSURE LEVELS AT DIFFERENT FLOW SPEEDS (MICROPHONE 5, 8200 RPM)

(a) Microphone 8

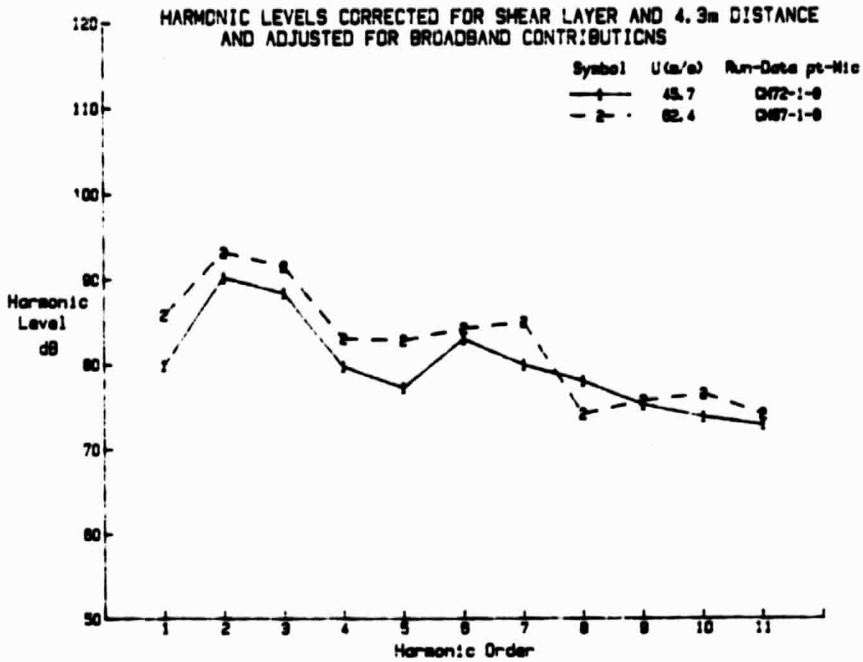

(b) Microphone 9

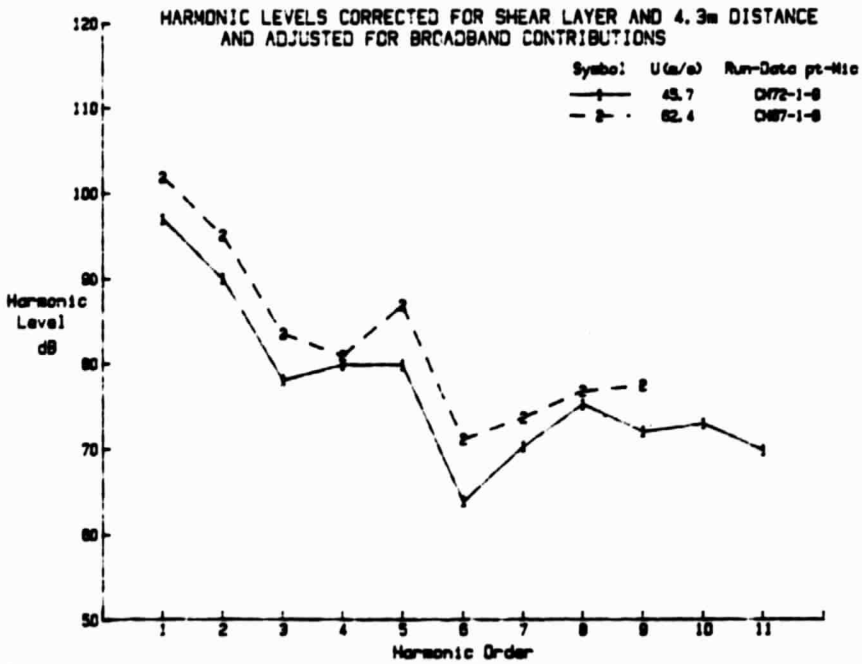

FIGURE 61. COMPARISON OF HARMONIC SOUND PRESSURE LEVELS AT DIFFERENT FLOW SPEEDS (MICROPHONES 8 AND 9)

in harmonic sound pressure level in the vertical plane. If this is true then the sound pressure levels at a given microphone location could depend on the fuselage orientation.

Figure 62 compares harmonic sound pressure levels measured at six microphone locations when the fuselage, with Y-tail, was oriented at $\psi = 0°$ and 90°. The propeller speed was 8200 rpm and the flow speed 62.4 m/s. The comparisons indicate that the sound pressure levels are generally higher for $\psi = 90°$ than for $\psi = 0°$. This means that the sound levels are higher beneath the airplane than they are to the side. The difference seems to be greatest at microphones in the neighborhood of the plane of rotation of the propeller (i.e., at locations 3 and 4). The same trend is observed also at location 12, which is not directly beneath or to the side of the airplane but is 30° away from those locations. In the case of microphone 11, the location is either 30° from directly above the airplane (when $\psi = 0°$) or 30° below the sideline ($\psi = 90°$). The data for this location do not show the trend of higher levels at $\psi = 90°$ than at 0°, presumably because the location does not fit the pattern of being beneath or to the side of the airplane.

5.8 Axial Separation

The effect of axial separation between the empennage and the plane of rotation of the propeller was of particular interest to the investigation, as can be seen from the test configurations listed in Table 3. This interest arose because of the previous work on fan noise in turbofan engines (see the discussion in Section 1.2) and because the strength of the wake from the empennage should decay as distance downstream of the empennage increases.

Before proceding to review the test data, attention should be drawn to the manner in which the separation between the empennage and propeller is expressed. In Table 3 the separation distance is

(a) Microphone 2

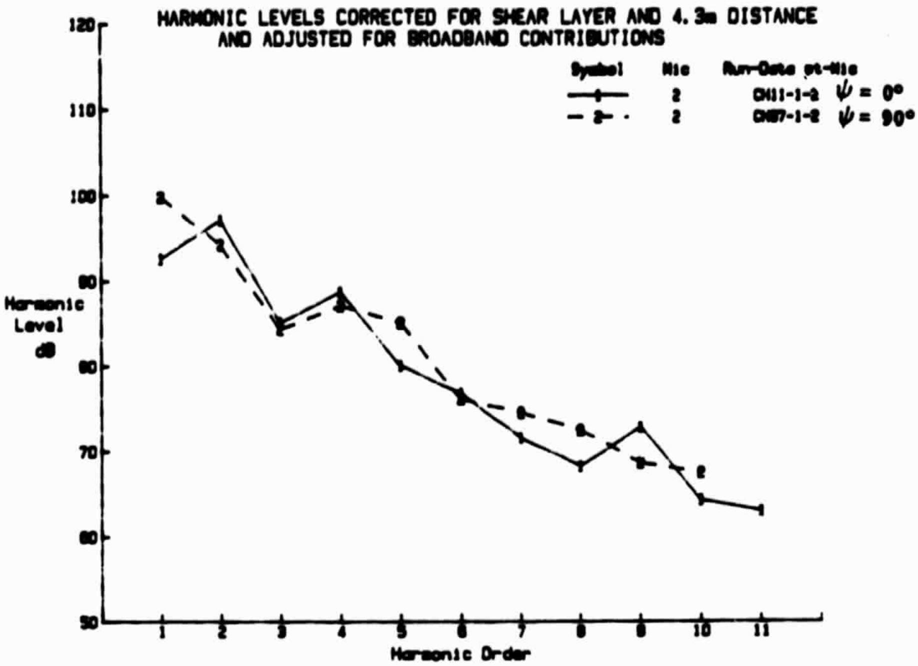

(b) Microphone 3

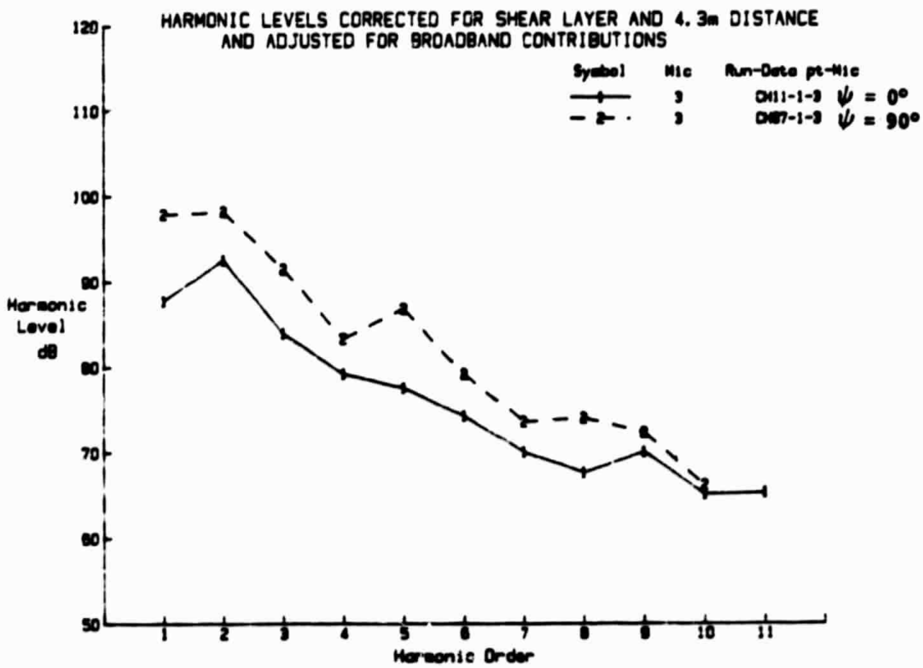

FIGURE 62. COMPARISON OF HARMONIC SOUND PRESSURE LEVELS MEASURED FOR DIFFERENT FUSELAGE ORIENTATIONS (8200 RPM, 62.4 M/S)

(c) Microphone 4

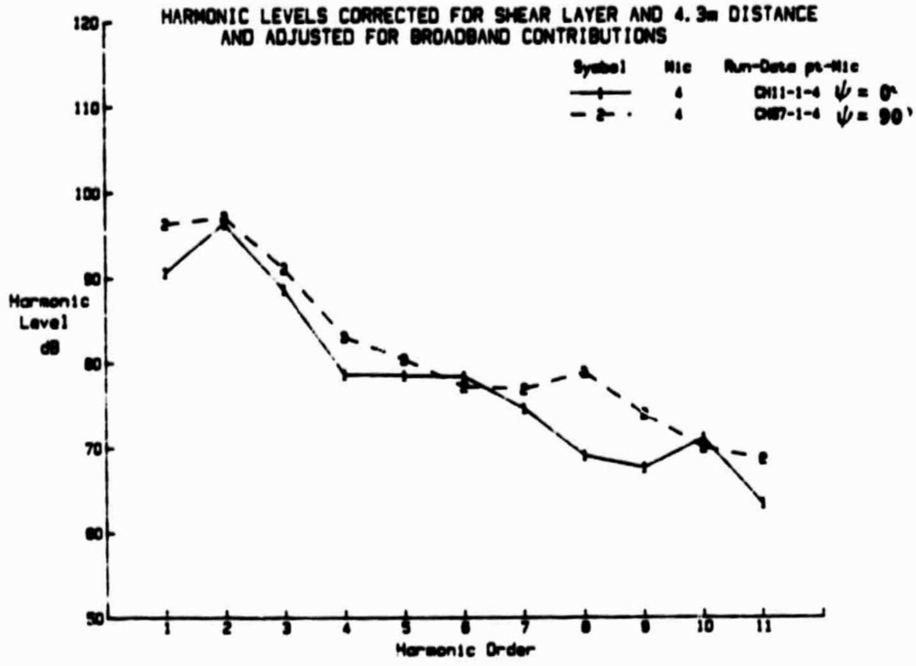

(d) Microphone 6

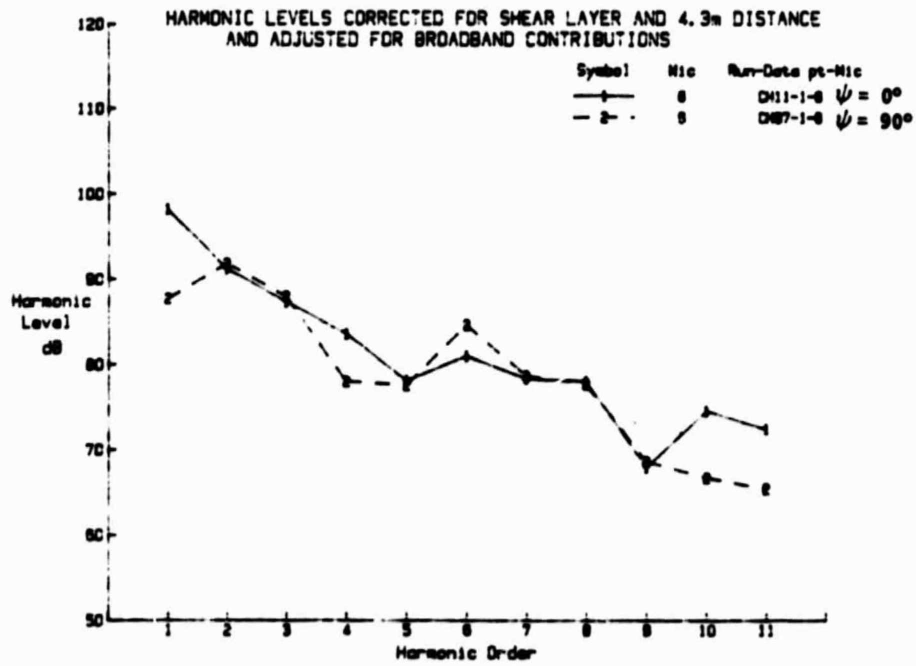

FIGURE 62. CONTINUED

(e) Microphone 11

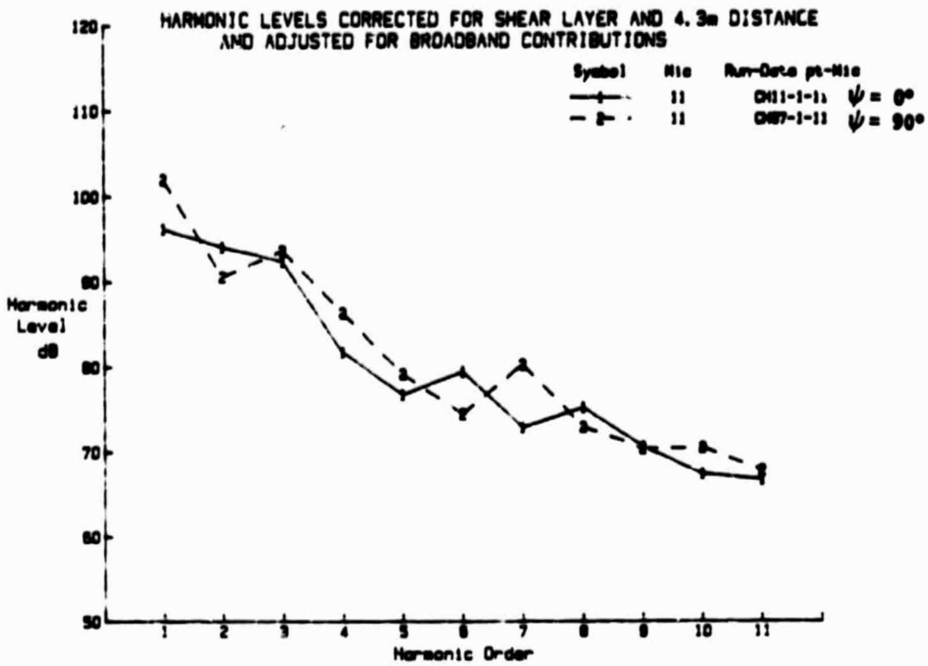

(f) Microphone 12

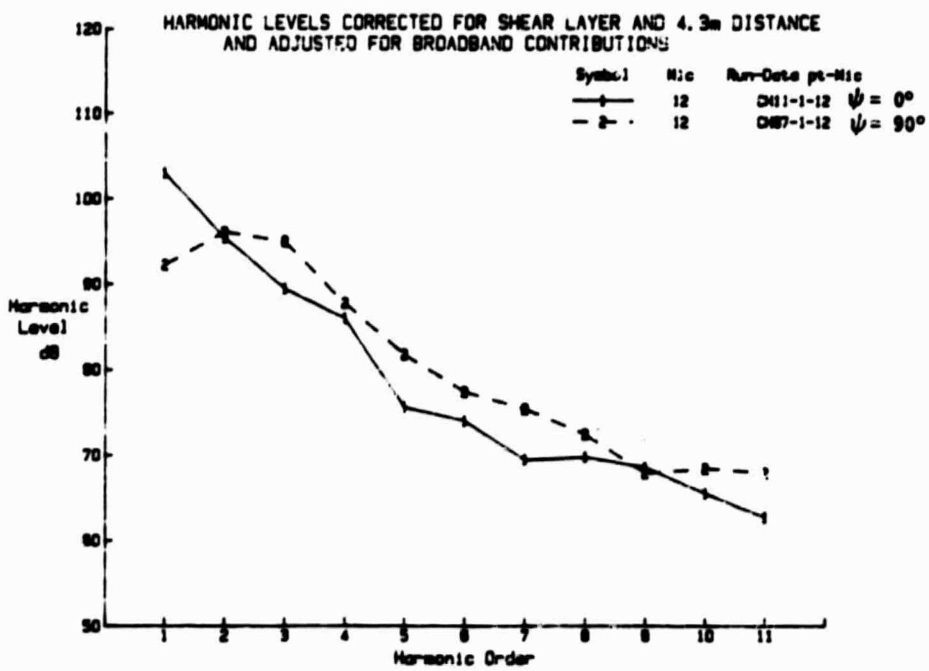

FIGURE 62. CONTINUED

given in terms of the distance x between the most rearward position on the fuselage tail cone and the plane of rotation. As discussed in Section 2.4 this distance does not give a correct indication of the distance between the trailing edge of the empennage and the propeller plane. To overcome this discrepancy mean separation distances have been estimated for several values of x referred to in Figures 63 through 68. In the case of the Y-tail separation distances have been estimated for both the V-tail and the dorsal fin.

The mean separation distances are given in Table 7 and represent the arithmetic average of the separation distances at the root of the empennage and the tip of the propeller. Also, the distances have been normalized with respect to the chord of the empennage surface, with the average value of the chord being determined in the same manner as for the separation distance. The results in Table 7 show that the separation distances for the I-tail are slightly lower than those for the Y-tail (a range of 8.5 cm to 43 cm compared to 13.5 cm to 60 cm). When normalized with respect to the appropriate chord dimension the separation distances associated with the I-tail are significantly smaller than those for the Y-tail. The range of values for s/c is 0.15 to 0.75 for the I-tail empennage and 0.47 to 2.06 for the Y-tail.

The influence of separation distance on harmonic sound pressure levels associated with the propeller operating downstream of the Y-tail is shown in Figures 63 through 65. The separation distances identified in the legend of the figures refer to the distance between tail cone and propeller. Distances between empennage and propeller are given in Table 7. As in the other comparisons, the data scatter makes interpretation difficult. However, the smallest separation distance is usually associated with the highest sound pressure level. In most cases the range of sound levels measured for a given harmonic order is not large, being less than 10 dB for a mean separation distance varying by a

(a) ψ = 0°

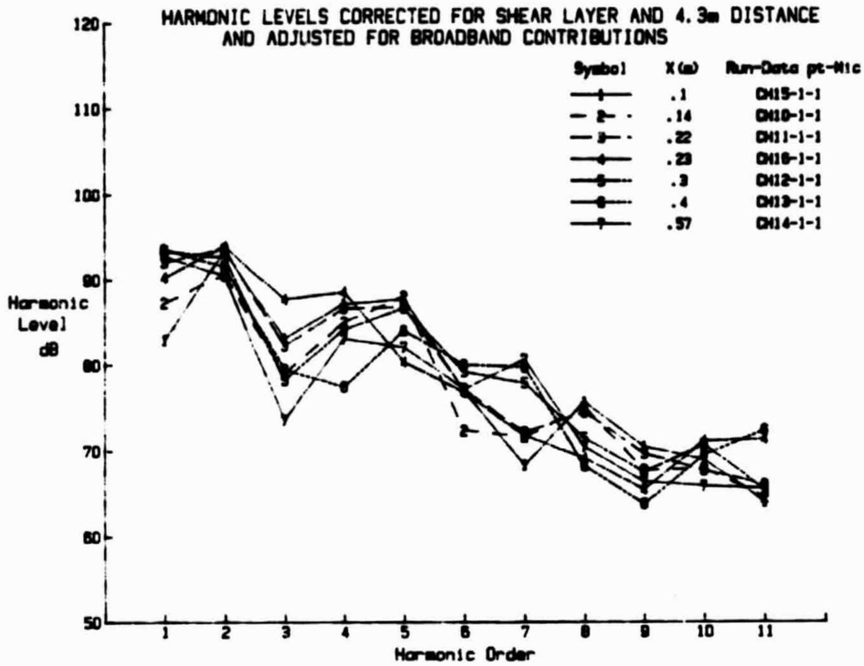

(b) ψ = 90°

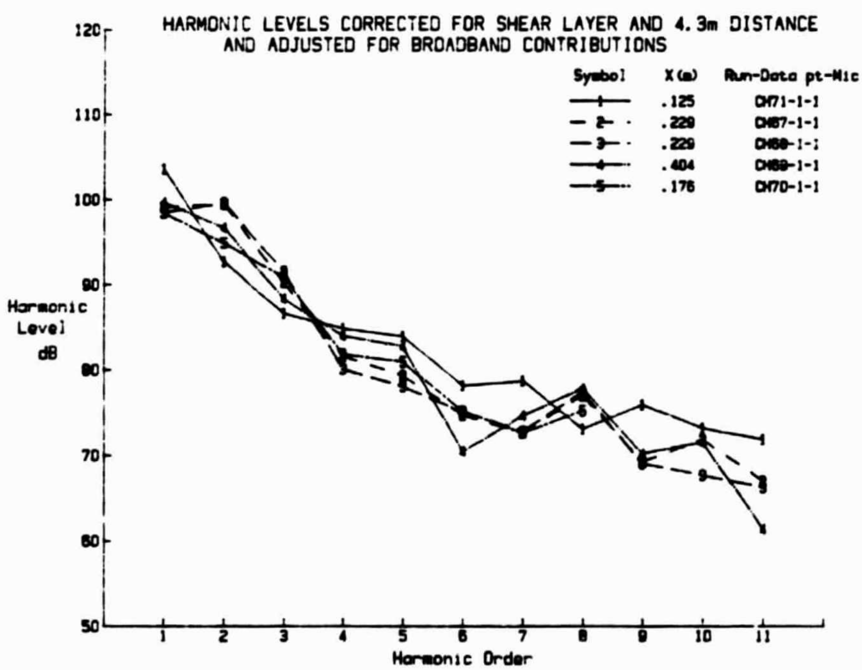

FIGURE 63. INFLUENCE OF AXIAL SEPARATION DISTANCE BETWEEN EMPENNAGE AND PROPELLER ON HARMONIC SOUND PRESSURE LEVELS (MICROPHONE 1, Y-TAIL, 8200 RPM, 62.4 M/S)

(a) ψ = 0°

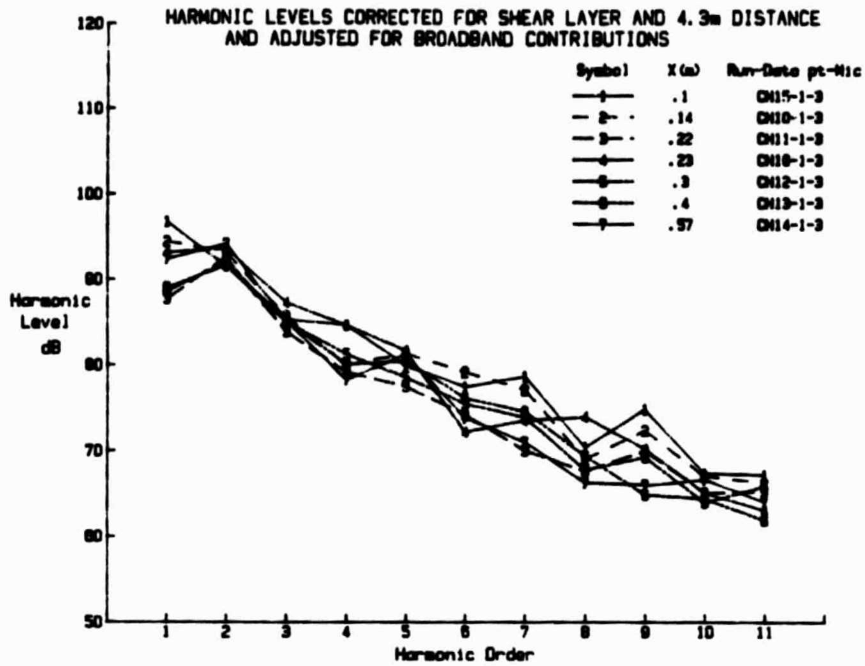

(b) ψ = 90°

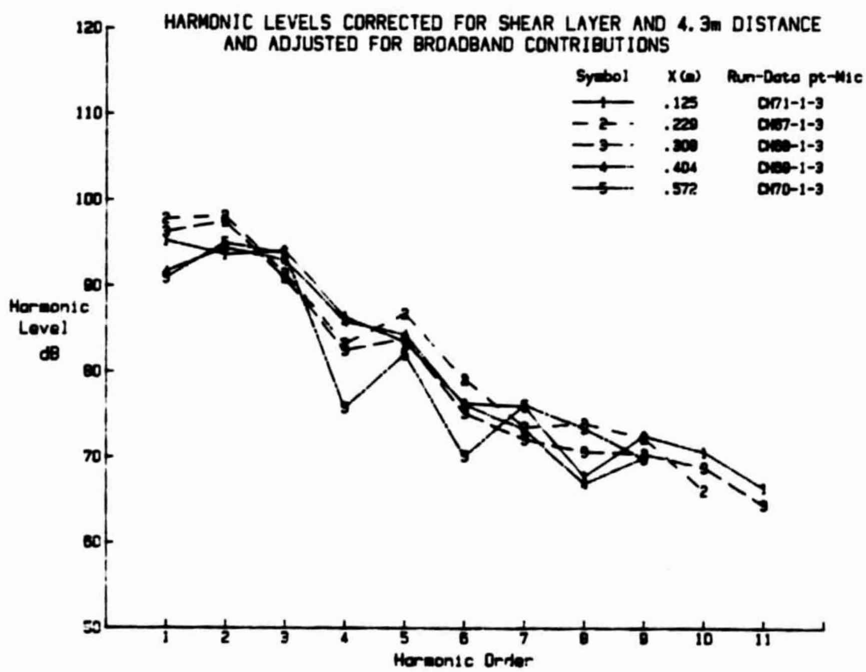

FIGURE 64. INFLUENCE OF AXIAL SEPARATION DISTANCE BETWEEN EMPENNAGE AND PROPELLER ON HARMONIC SOUND PRESSURE LEVELS (MICROPHONE 3, Y-TAIL, 8200 RPM, 62.4 M/S)

(a) $\psi = 0°$

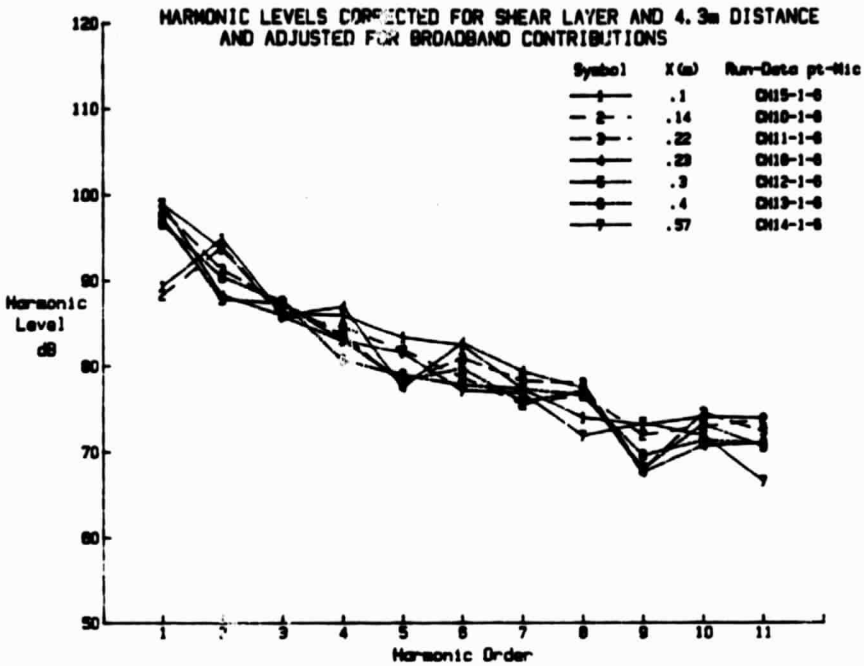

(b) $\psi = 90°$

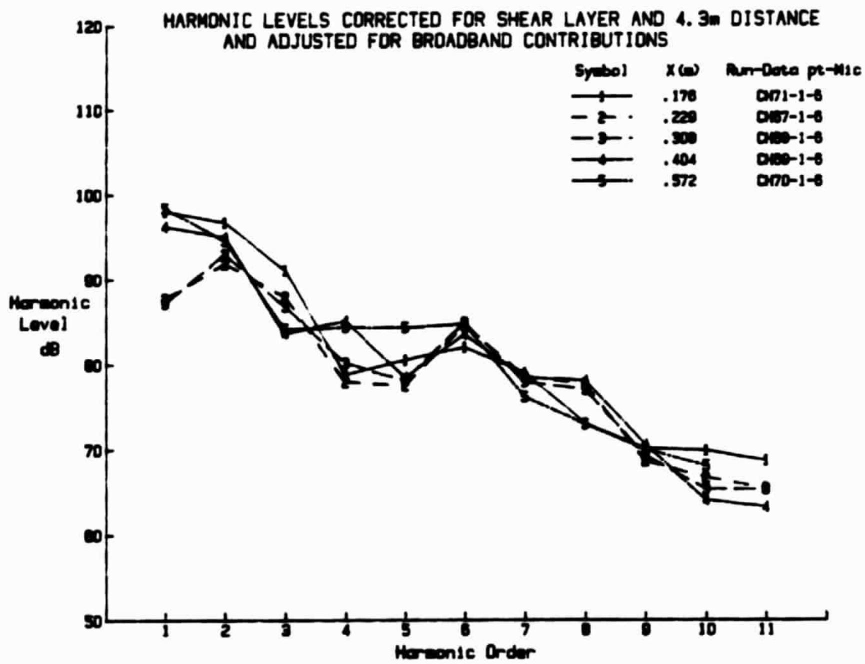

FIGURE 65. INFLUENCE OF AXIAL SEPARATION DISTANCE BETWEEN EMPENNAGE AND PROPELLER ON HARMONIC SOUND PRESSURE LEVELS (MICROPHONE 6, Y-TAIL, 8200 RPM, 62.4 M/S)

(a) ψ = 0°

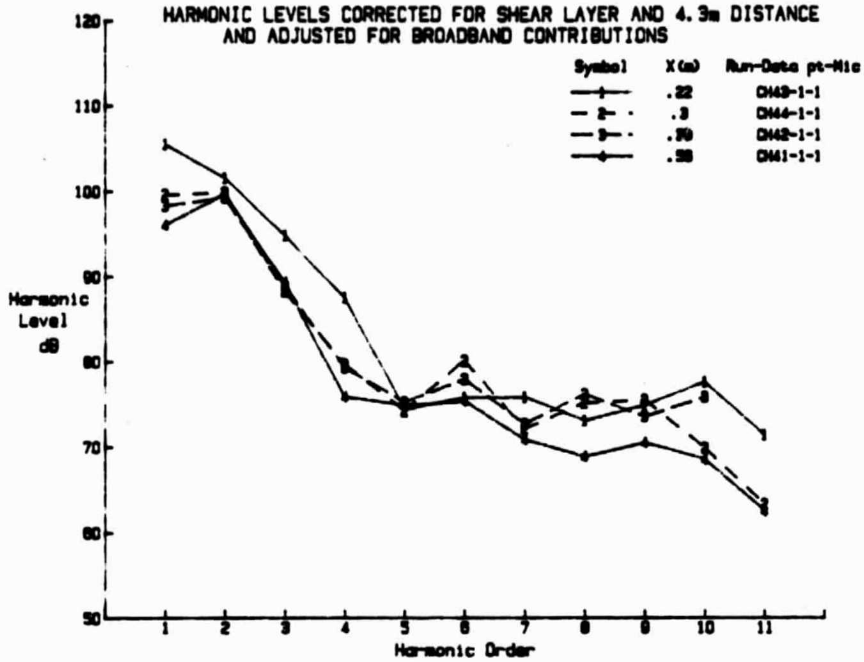

(b) ψ = 90°

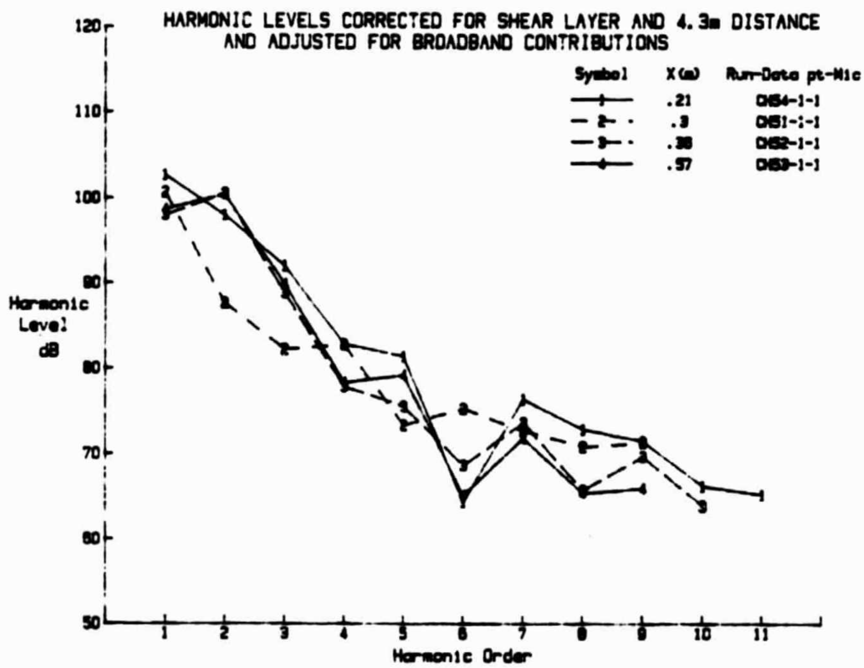

FIGURE 66. INFLUENCE OF AXIAL SEPARATION DISTANCE BETWEEN EMPENNAGE AND PROPELLER ON HARMONIC SOUND PRESSURE LEVELS (MICROPHONE 1, I-TAIL, 8200 RPM, 62.4 M/S)

(a) $\psi = 0°$

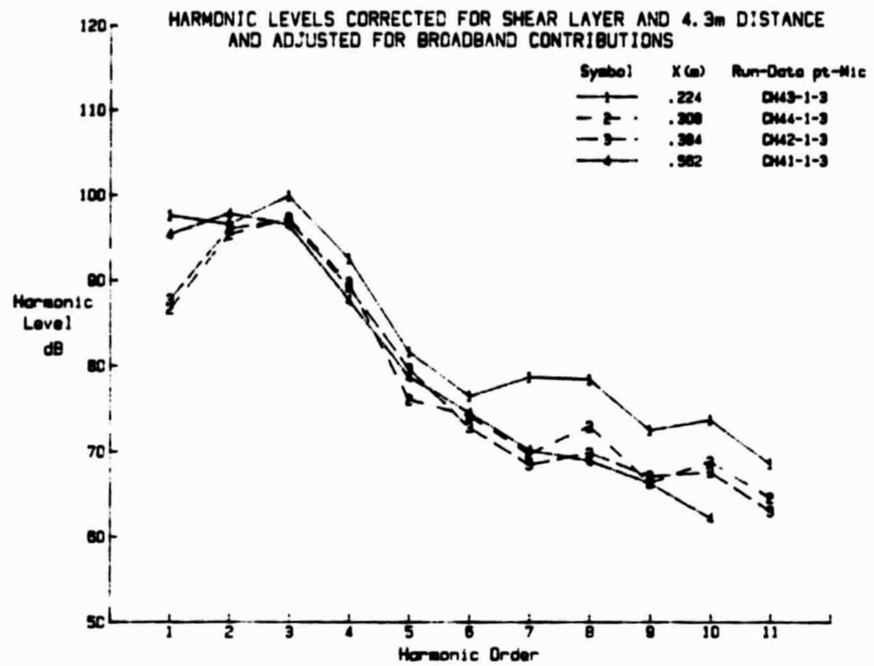

(b) $\psi = 90°$

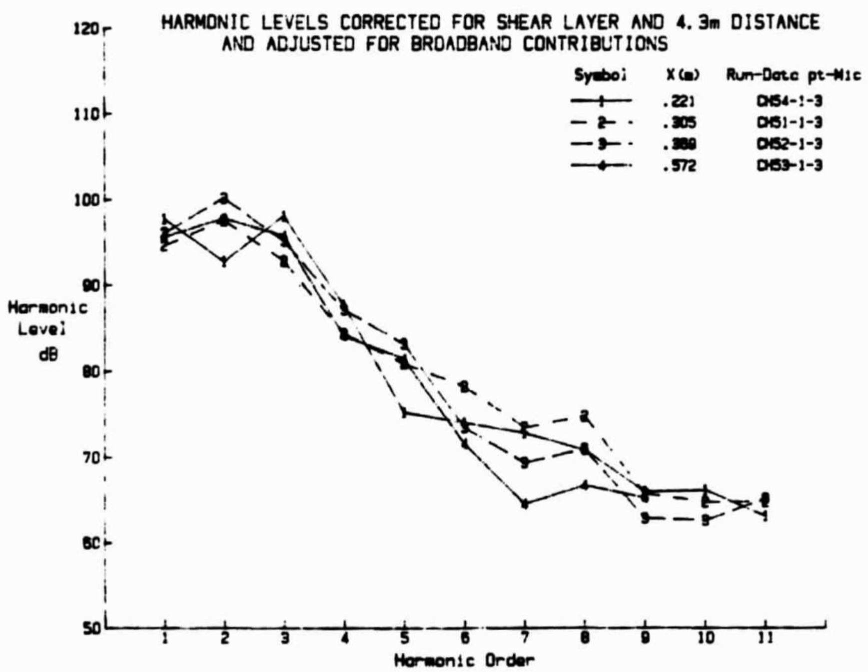

FIGURE 67. INFLUENCE OF AXIAL SEPARATION DISTANCE BETWEEN EMPENNAGE AND PROPELLER ON HARMONIC SOUND PRESSURE LEVELS (MICROPHONE 3, I-TAIL, 8200 RPM, 62.4 M/S)

(a) $\psi = 0°$

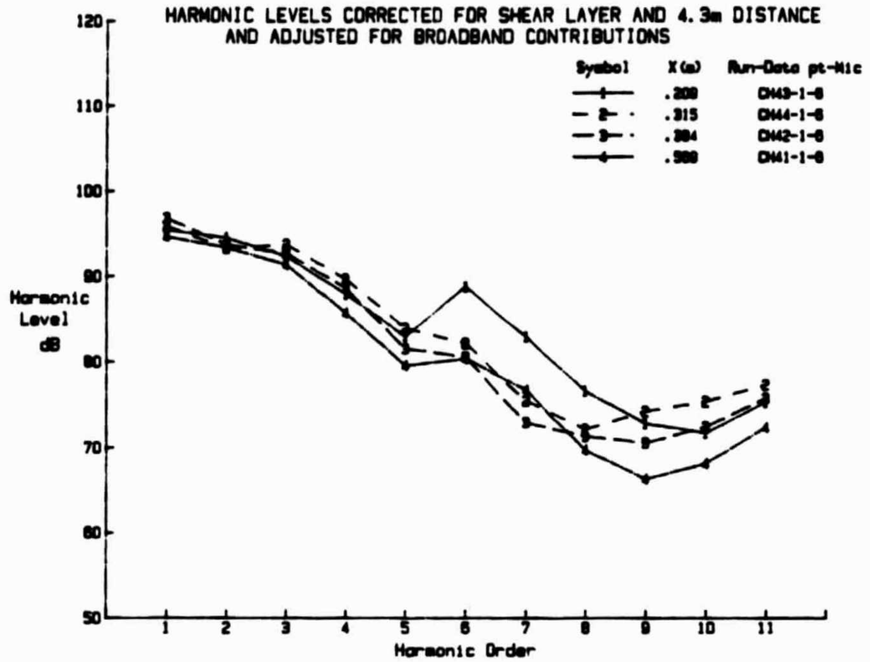

(b) $\psi = 90°$

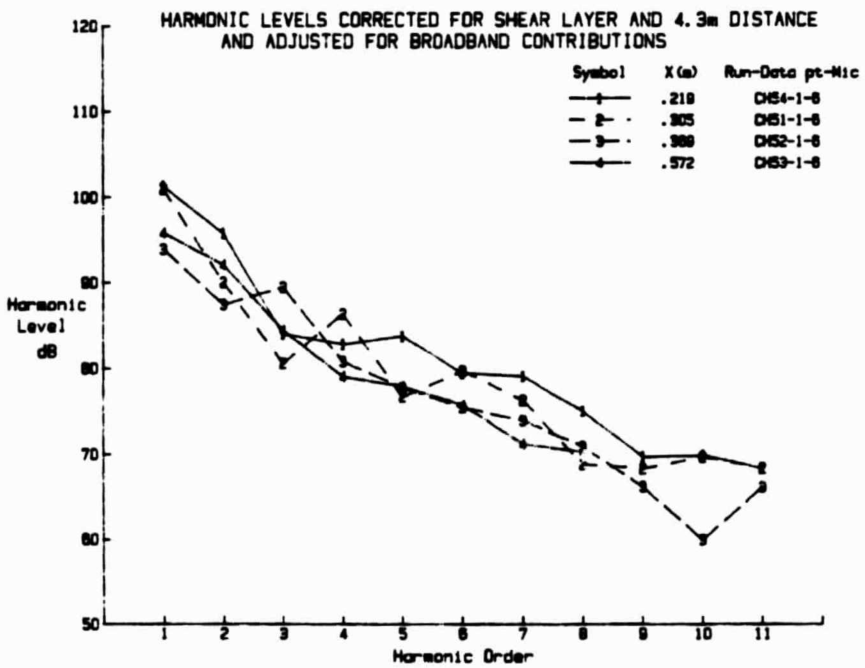

FIGURE 68. INFLUENCE OF AXIAL SEPARATION DISTANCE BETWEEN EMPENNAGE AND PROPELLER ON HARMONIC SOUND PRESSURE LEVELS (MICROPHONE 6, I-TAIL, 8200 RPM, 62.4 M/S)

TABLE 7. MEAN SEPARATION DISTANCES BETWEEN EMPENNAGE TRAILING EDGE AND PROPELLER PLANE OF ROTATION

Run No.		Separation* X	Mean Separation* S (cm)		Mean S/C	
ψ = 0°	ψ = 90°	(cm)	V-Tail	Dorsal Fin	V-Tail	Dorsal Fin
Y-Tail						
15-1	---	11	13.5	13	0.47	---
---	71-1	12.5	15	14.5	0.52	0.55
10.1	---	14.5	17.5	16.5	0.60	-.64
11-1	67-1	23	25.5	25	0.88	0.96
16-1	---	24	26.5	26	0.91	0.99
12-1	68-1	31	33.5	32.5	1.15	1.26
13-1	69-1	40.5	43	42.5	1.48	1.63
14-1	70-1	57.5	60	59.5	2.06	2.28
I-Tail						
43-1	54-1	22	8.5		0.15	
44-1	51-1	30.5	17		0.30	
42-1	52-1	37.5	24		0.42	
41-1	53-1	56.5	43		0.75	

*X is distance between fuselage tail cone and propeller plane

S is mean distance between empennage trailing edge and propeller plane

C is mean chord of empennage between hub and tip of propeller factor of almost 5. Often the sound levels change by less than 7 dB as separation distance increases.

Corresponding data for the I-tail are contained in Figures 66 through 68. The trends of the data are similar to those observed in Figures 63 through 65 for the Y-tail but the pattern is more distinct. Although the separation distance again varies by a factor of 5 the normalized distances are much smaller than in the case of the Y-tail so, presumably, the influence of the wake from the empennage is much stronger. As for the Y-tail, the range of sound pressure levels for a given harmonic order is less than 10 dB; in many cases it is less than 7 dB.

The influence of axial separation distance was measured also when the Y-tail empennage was at a 5° angle of incidence. Sample data for these configurations are presented in Figure 69. In one case, (Microphone 6, Figure 69(c)), the data are remarkably orderly considering the data scatter encountered throughout the test. The data in Figure 69(c) show a monotonic decrease in harmonic sound pressure level as separation distance increases. At other locations the pattern of the data is similar to that in Figures 63 through 68. The separation distances between empennage and propeller plane associated with the test runs for Figure 69 are not listed in Table 7, but the values from equivalent runs can be used.

5.9 Vertical Separation

Vertical separation between propeller axis and fuselage centerline was varied in only one increment (7.6 cm) upwards and downwards. The flow speed was 62.4 m/s, the propeller rotational speed was 8200 rpm, and the axial separation was either 24 cm or 57 cm. Typical harmonic spectra are shown in Figure 70 for the case of x = 24 cm.

(a) Microphone 1

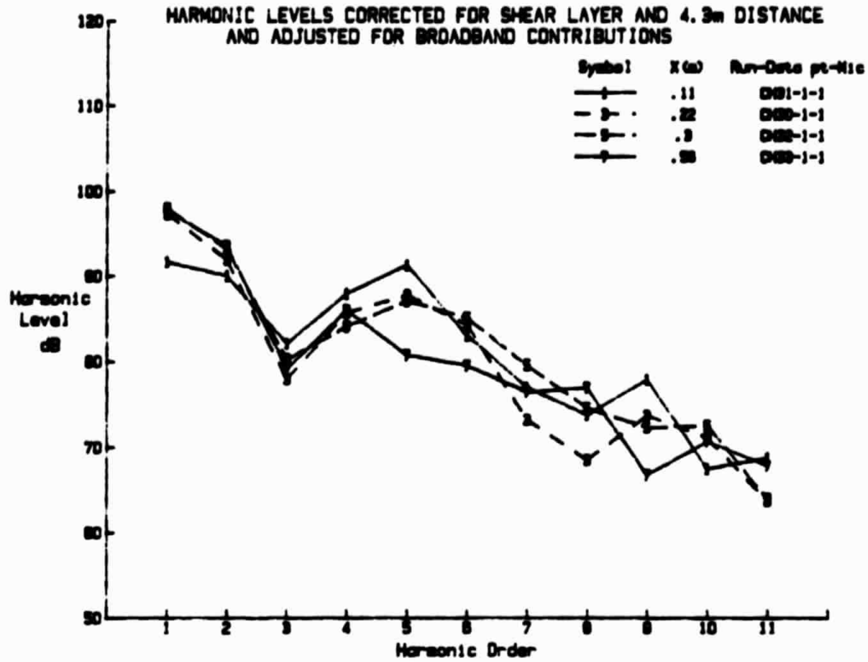

(b) Microphone 3

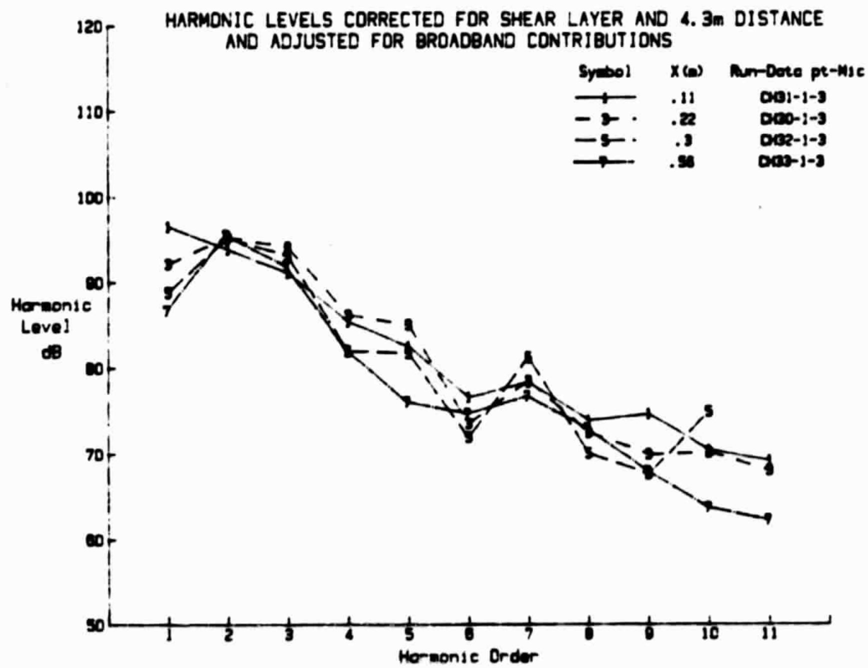

FIGURE 69. INFLUENCE OF AXIAL SEPARATION DISTANCE BETWEEN EMPENNAGE AND PROPELLER ON HARMONIC SOUND PRESSURE LEVELS; EMPENNAGE INCIDENCE 5°

(c) Microphone 6

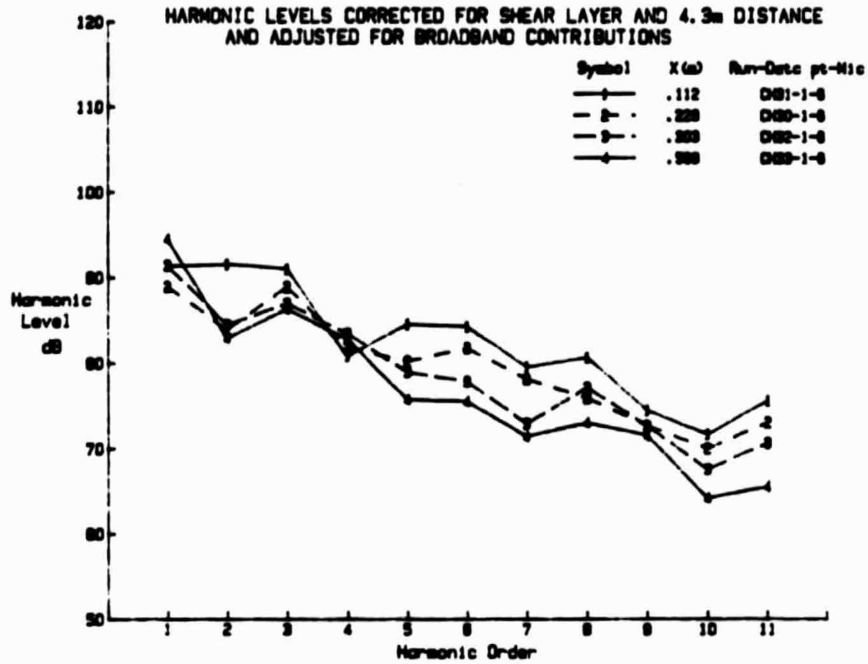

FIGURE 69. CONTINUED

(a) Microphone 2

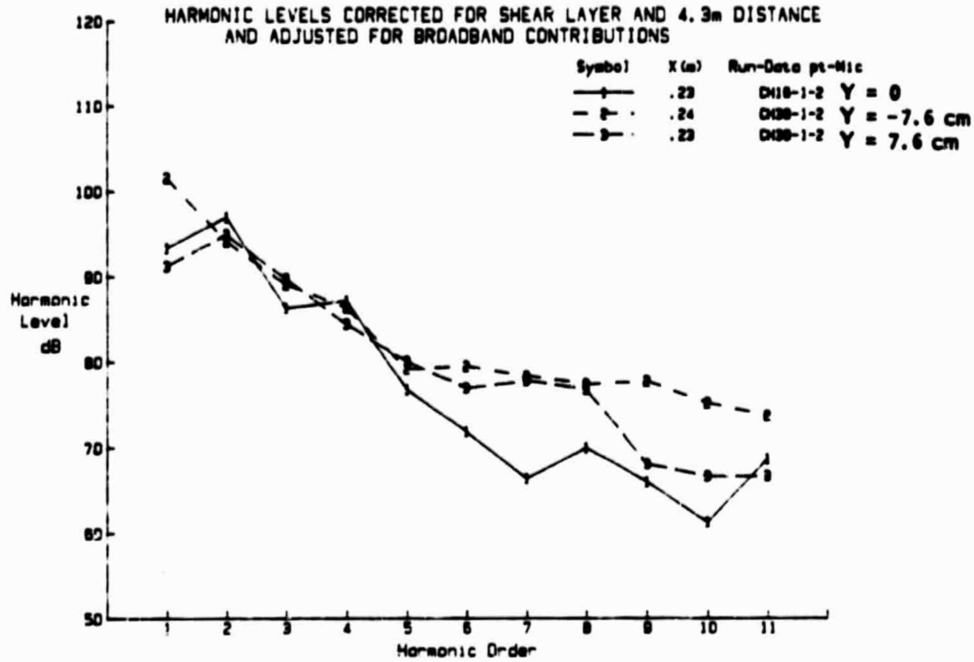

(b) Microphone 4

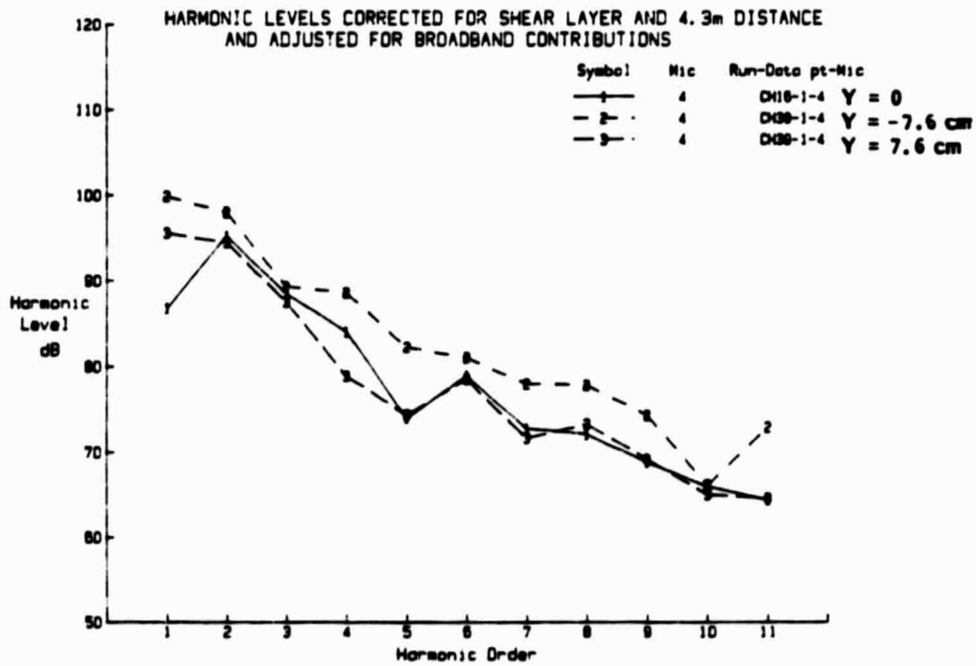

FIGURE 70. INFLUENCE OF VERTICAL SEPARATION DISTANCE BETWEEN EMPENNAGE AND PROPELLER ON HARMONIC SOUND PRESSURE LEVELS (8200 RPM, V= 62.4 M/S)

(a) Microphone 6

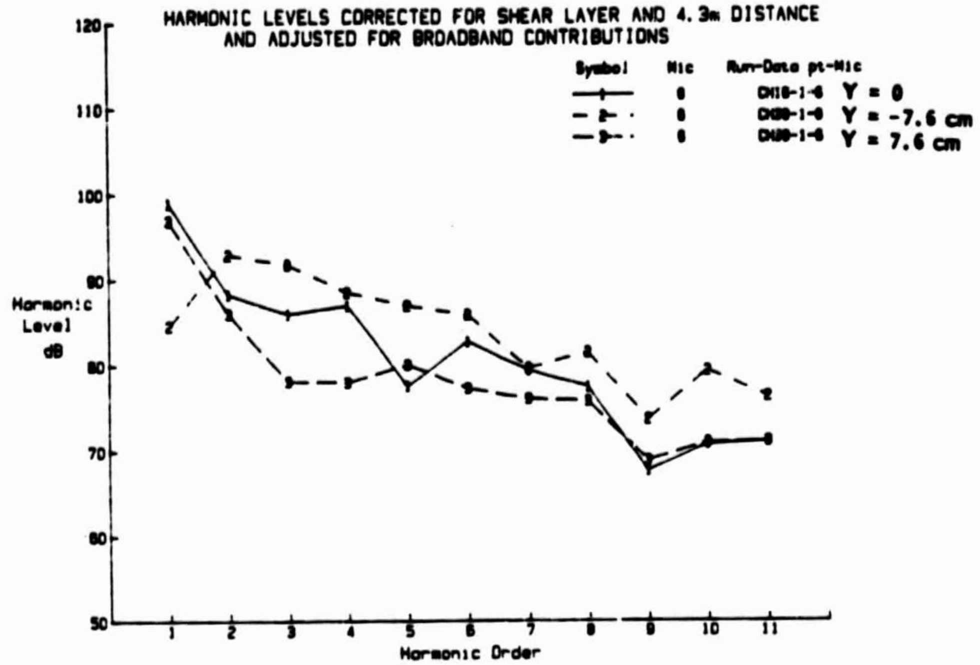

(b) Microphone 12

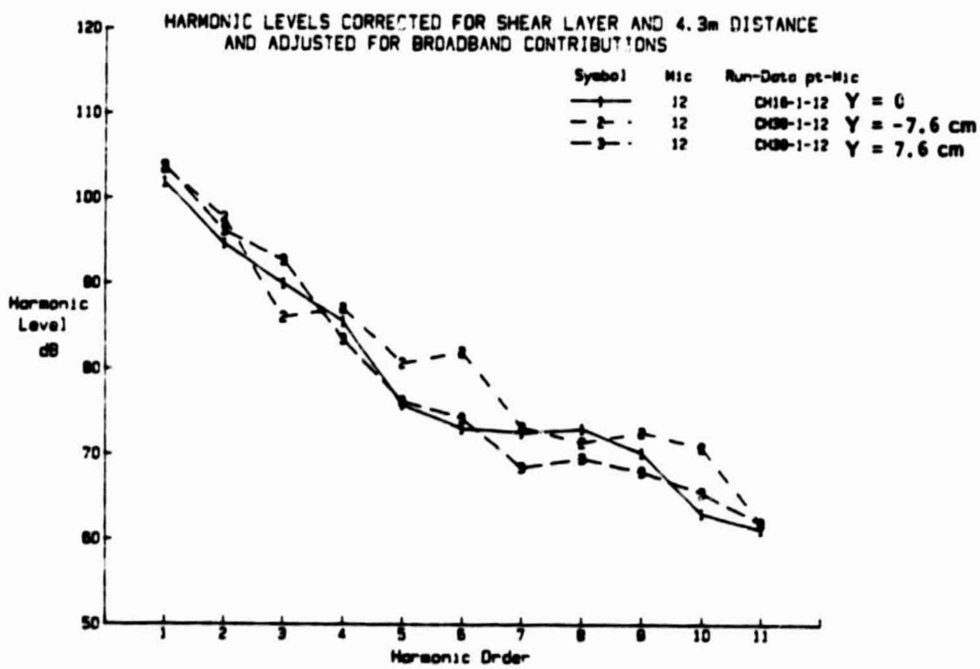

FIGURE 70. CONTINUED

It is seen that the highest sound pressure levels at all measurement locations and for all harmonic orders occurred when the propeller axis was below the fuselage ($x = -7.6$ cm). The lowest sound pressure levels often occur when there is no vertical separation between the fuselage centerline and the propeller axis, but in many cases the sound levels associated with $x = +7.6$cm are similar to those for $x = 0$.

5.10 Empennage Angle of Incidence

The next parameter considered here is the angle of incidence of the empennage. This angle was given a non-zero value (+5°) for four test runs, 30-1 through 33-1, at four different axial separation distances. Data for two of the separation distances are presented in Figures 71 through 73 for three microphone locations. Baseline sound pressure levels for zero angle of incidence (run 12-1 or 15-1) are given in each case. The data suggest that at low harmonic orders, with m less than 4, the increase in angle of incidence causes a reduction in harmonic sound pressure level. For higher order harmonics the increase in angle of incidence increases the sound pressure level.

5.11 Directivity in Vertical Plane

Directivity in the vertical plane can be measured in the plane of rotation of the propeller using data from microphones 4, 11, 12 and 13. Microphones 4, 11, and 12 are at a radius of 4.3m and microphone 13 at 2.3m; the data are adjusted to a common radius of 4.3m. Since measurements were made at two orientations of the fuselage and empennage ($\psi = 0°$ and $90°$) the data can be combined to obtain sound pressure levels for eight values of angle ϕ. The appropriate values of ϕ are given in Table 2. It is seen that most of the data points lie in the two quadrants from 180° to 360° (microphones 4, 11, and 12).

(a) x = 10.8 cm

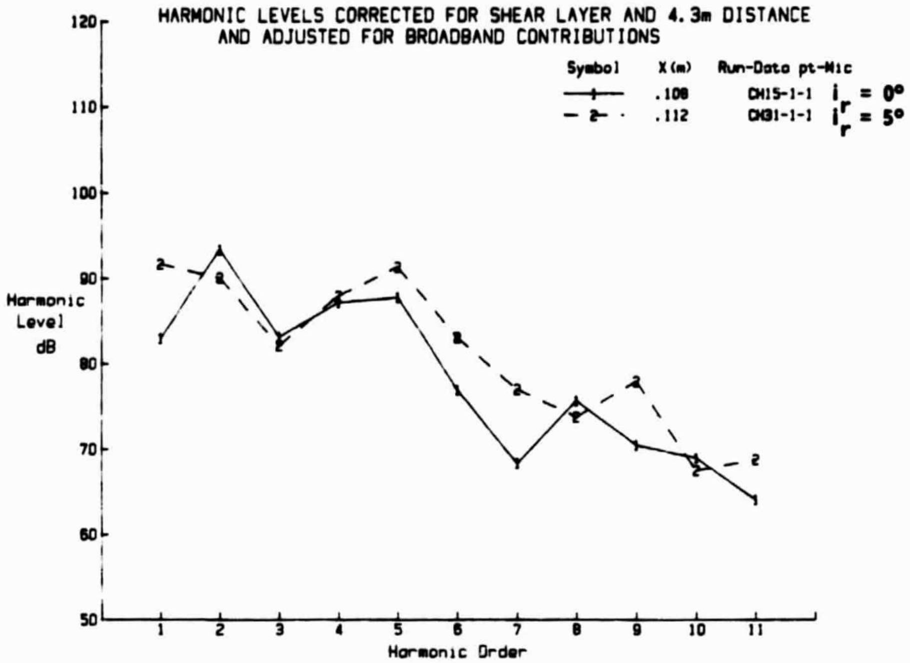

(b) x = 30.5 cm

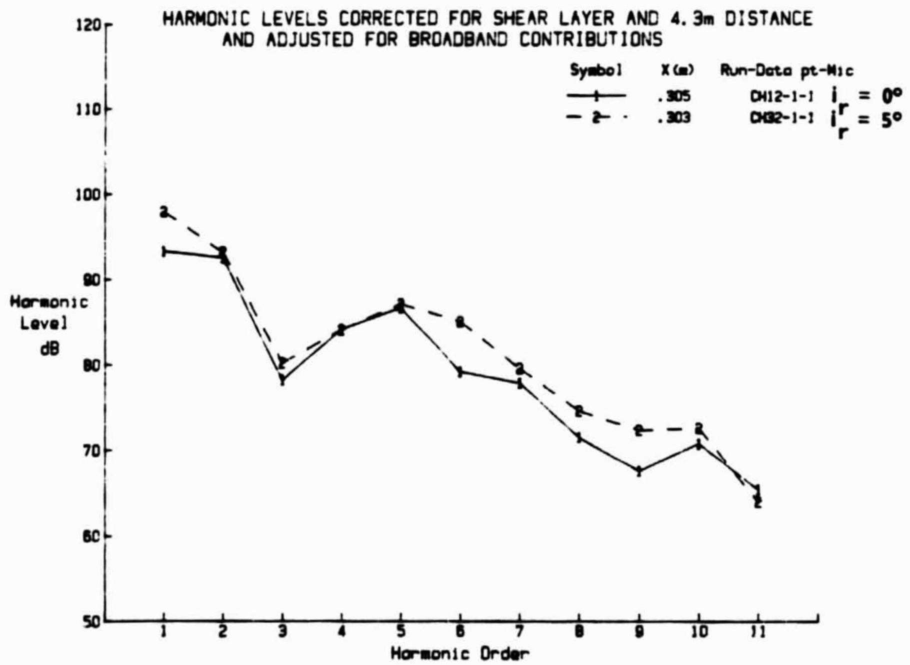

FIGURE 71. INFLUENCE OF EMPENNAGE ANGLE OF INCIDENCE ON HARMONIC SOUND PRESSURE LEVELS (MICROPHONE 1, 8200 RPM, 62.4 M/S)

(a) x = 10.8 cm

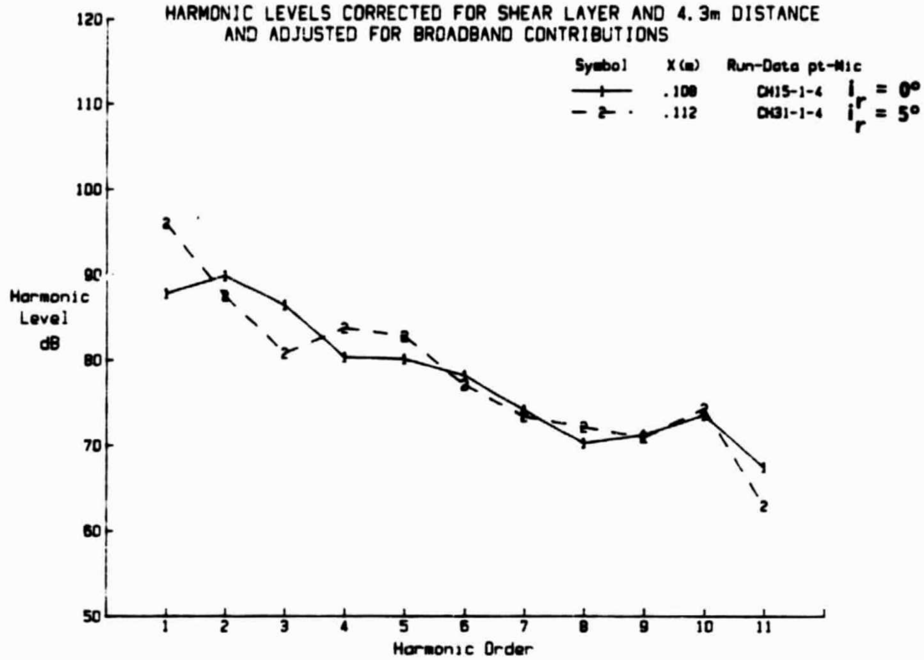

(b) x = 30.5 cm

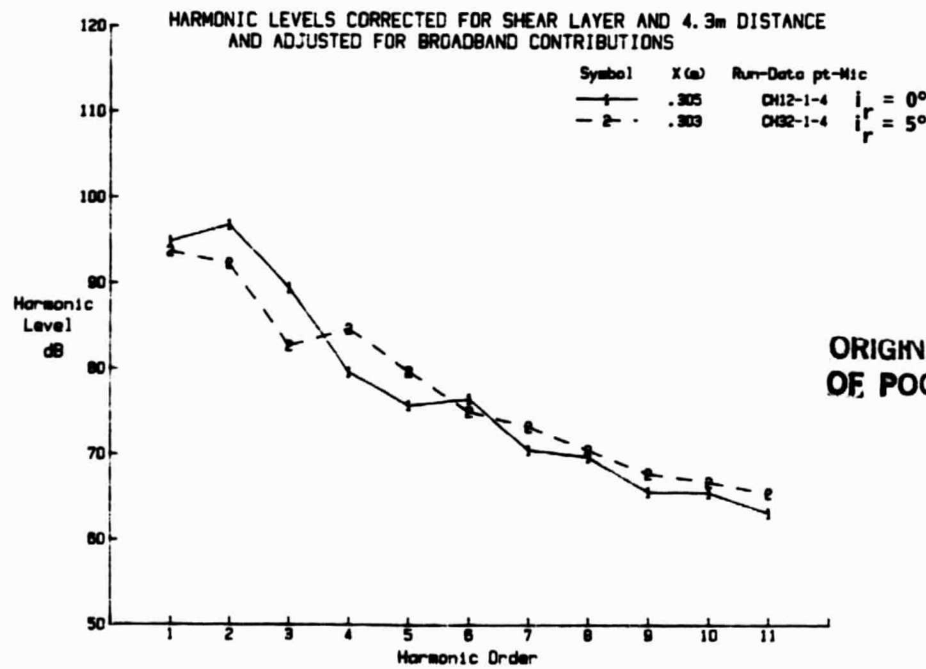

ORIGINAL PAGE IS OF POOR QUALITY

FIGURE 72. INFLUENCE OF EMPENNAGE ANGLE OF INCIDENCE ON HARMONIC SOUND PRESSURE LEVELS (MICROPHONE 4, 8200 RPM, 62.4 M/S)

(a) x = 10.8 cm

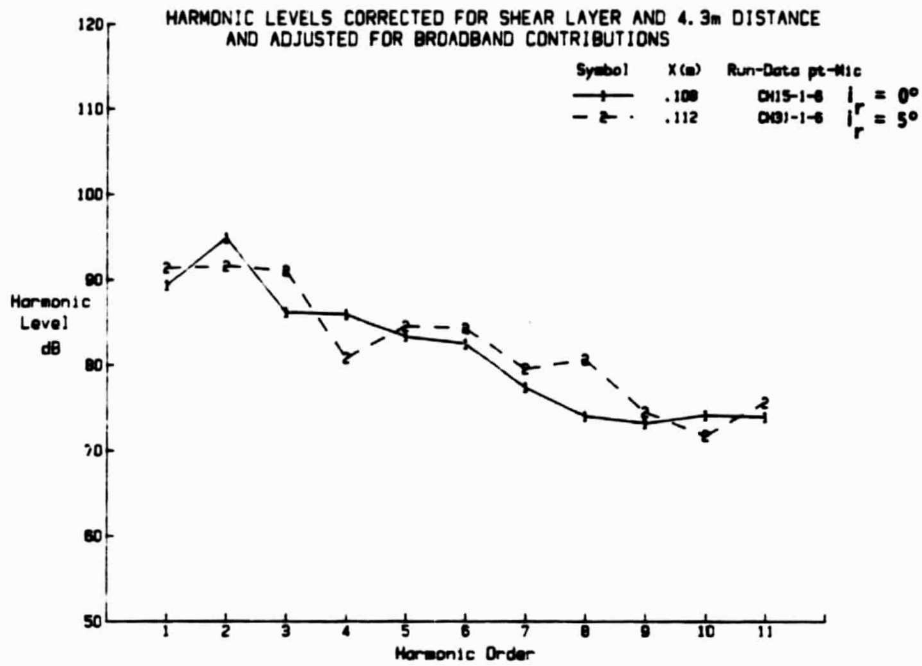

(b) x = 30.5 cm

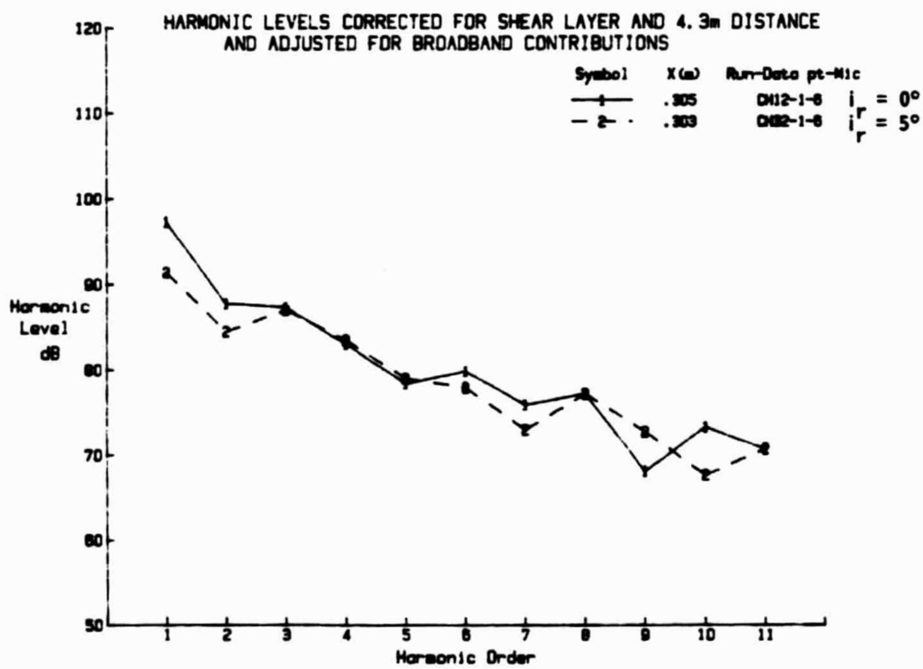

FIGURE 73. INFLUENCE OF EMPENNAGE ANGLE OF INCIDENCE ON HARMONIC SOUND PRESSURE LEVELS (MICROPHONE 6, 8200 RPM, 62.4 M/S)

Three sample directivity plots are shown in Figures 74 through 76 for test conditions associated with a flow speed of 62.4 m/s and a propeller speed of 8200 rpm. Figure 74 presents harmonic sound pressure levels measured when the propeller was operating downstream of the fuselage without an empennage. Then, Figures 75 and 76 show the directivity patterns measured when the Y and I tails, respectively, were installed. Angular locations of the empennage surfaces are identified in Figures 75 and 76.

Inspection of Figures 74 through 76 indicates that, at least for the plane of rotation of the propeller, the directivity pattern is fairly uniform. There is no indication of directivity peaks or troughs associated with the empennage surfaces. However, since such troughs may be fairly narrow in terms of angular domain it is possible that the number of measurement locations is too small to determine the detailed directivity pattern. Within the data variability the presence of the empennage appears to have little influence on the directivity pattern in the vertical plane.

5.12 Directivity in Horizontal Plane

Directivity in the horizontal plane can be measured using data from microphones 1 through 9. Six of these microphones (1-6) were located outside the tunnel shear layer and the other three microphones were in the tunnel flow (Figure 17). Microphones 1 through 6 were at a radial distance of 4.3m from the propeller; data from microphones 7 through 9 were normalized to this radius using the adjustments listed in Table 5. Since microphones 7 through 9 were in the flow, no adjustments were necessary for refraction at the shear layer. Adjustments for shear layer effects were made to data for microphones 1-6 according to Table 6 so that the directivity could be plotted in terms of radiation angle rather than receiver angle. The microphones out of the flow are restricted

(a) Harmonics 1 through 4

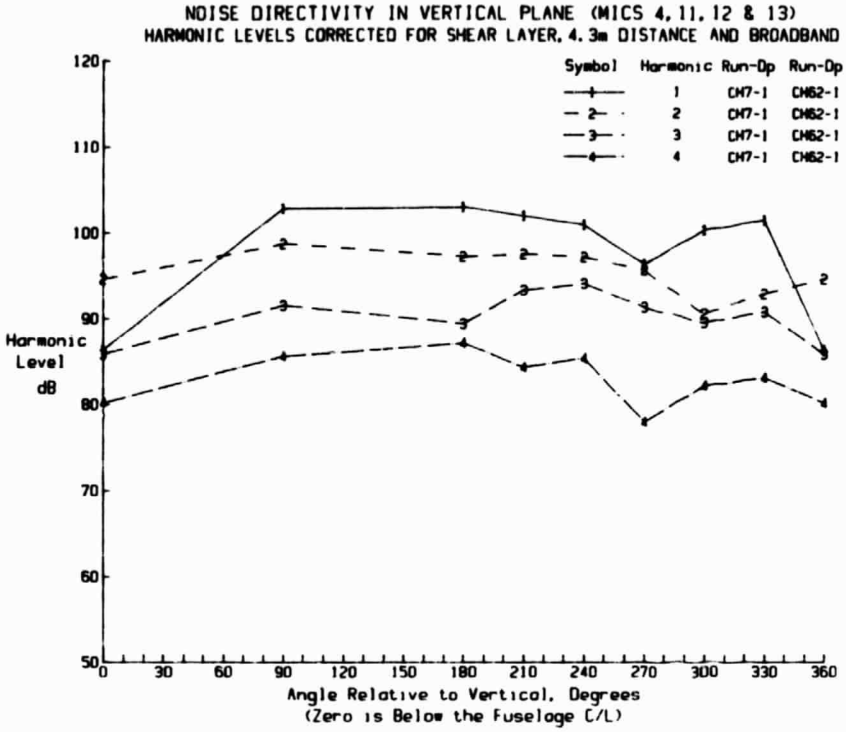

(b) Harmonics 5 through 8

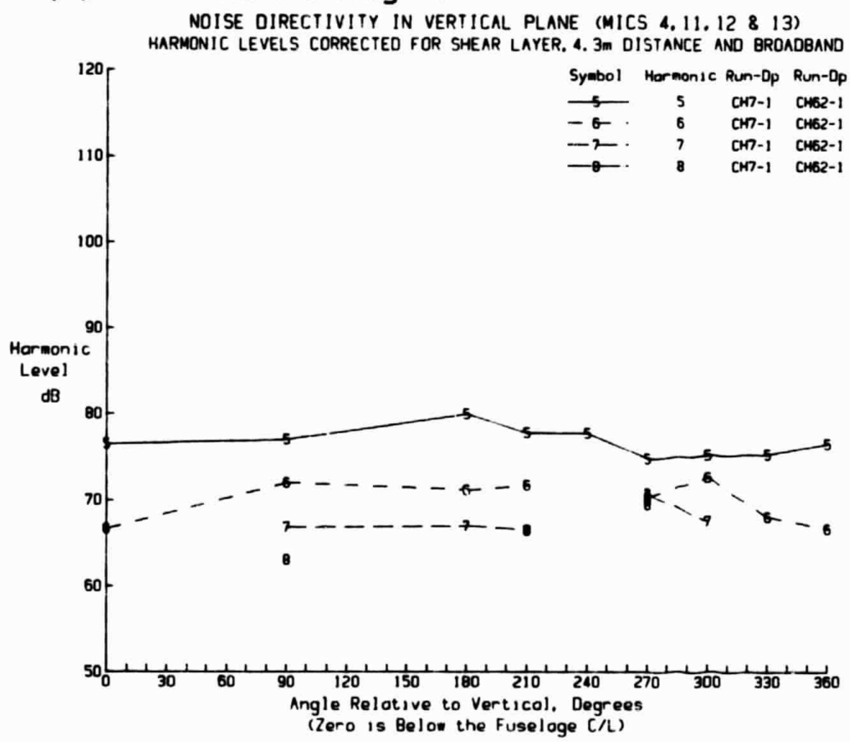

FIGURE 74. VERTICAL PLANE DIRECTIVITY OF HARMONIC SOUND PRESSURE LEVELS (FUSELAGE WITHOUT EMPENNAGE, 8200 RPM, 62.4 M/S)

(a) Harmonics 1 through 4

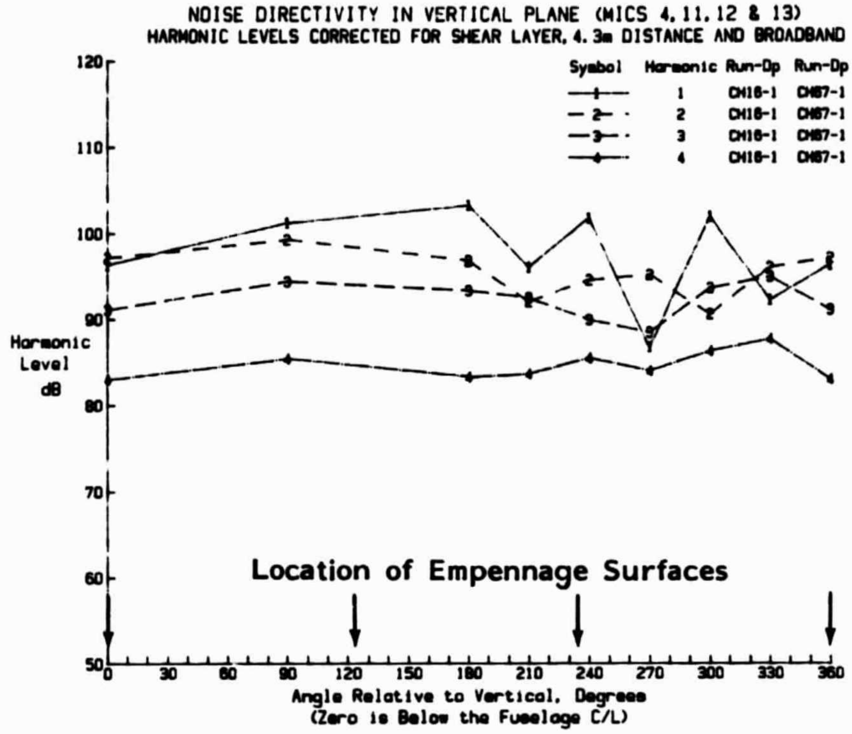

(b) Harmonics 5 through 8

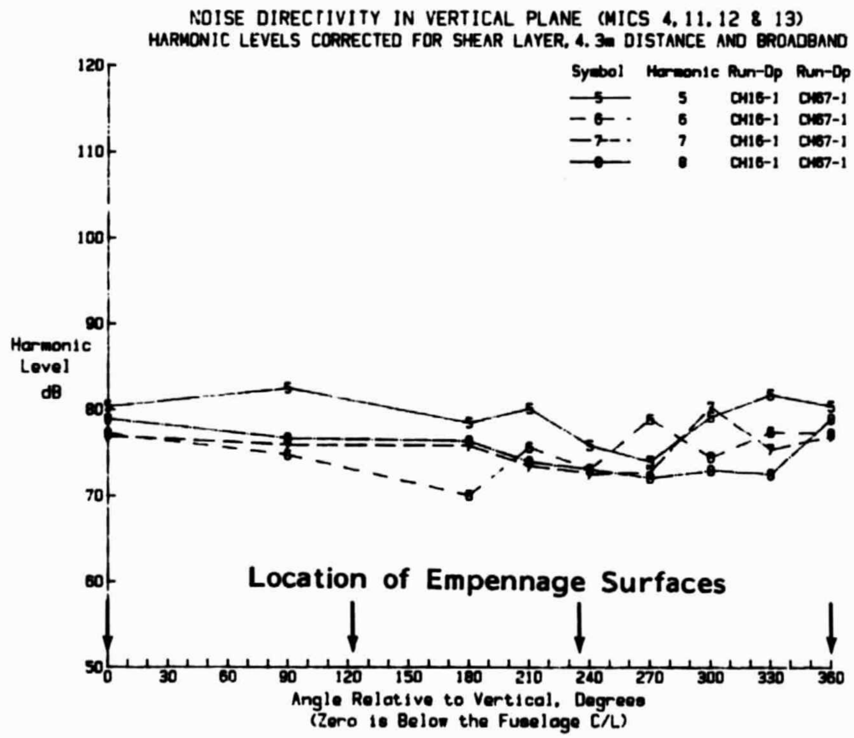

FIGURE 75. VERTICAL PLANE DIRECTIVITY OF HARMONIC SOUND PRESSURE LEVELS (Y-TAIL, X=23.8 CM, 8200 RPM, 62.4 M/S)

(a) Harmonics 1 through 4

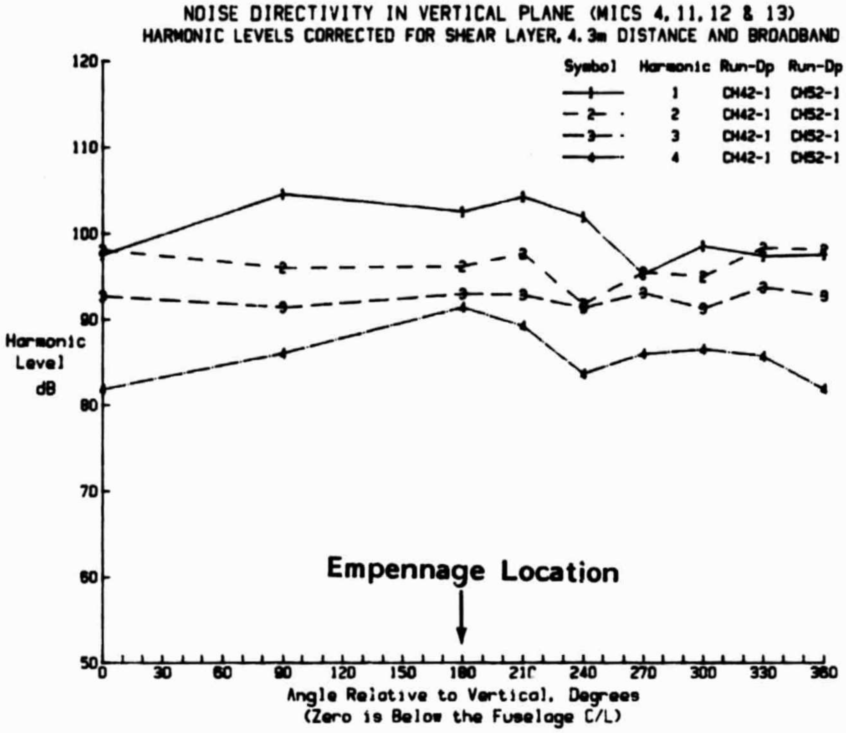

(b) Harmonics 5 through 8

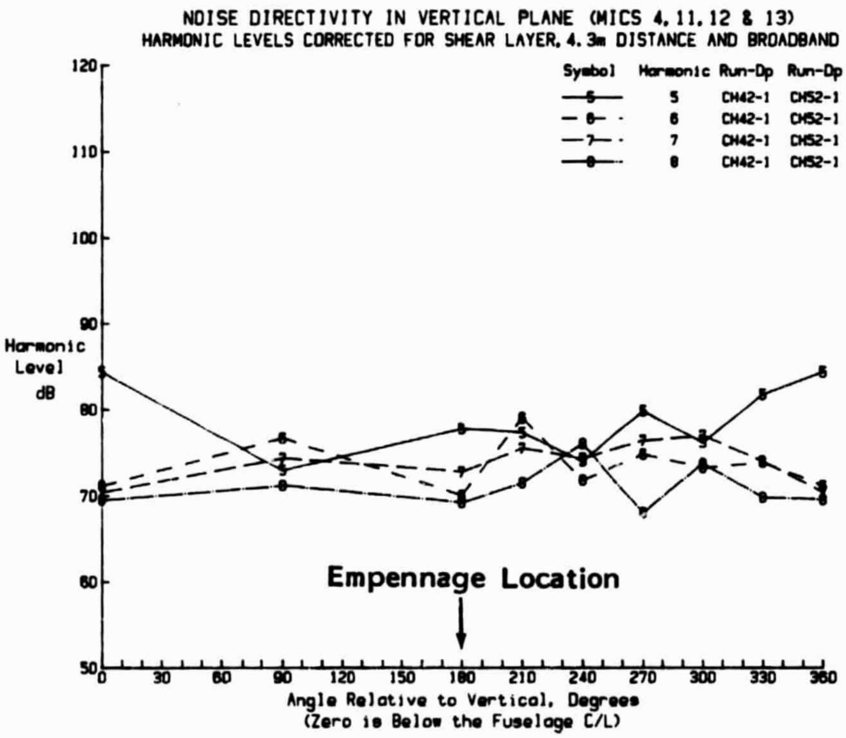

FIGURE 76. VERTICAL PLANE DIRECTIVITY OF HARMONIC SOUND PRESSURE LEVELS (I-TAIL, X=38.4 CM, 8200 RPM, 62.4 M/S)

in radiation angle to the range 68.5° to 126.1° (0° is directly upstream of the propeller). Consequently, it is of interest to include the microphones in the flow so that the range of angles can be increased to 15°-140°. Microphone 7 which is in the flow was included in some of the directivity plots but, since the associated radiation angle lies between those for microphones 4 and 5, the data are not as important to the directivity as those from microphones 8 and 9.

In preparing the directivity plots, data points were joined by straight lines without any attempt to interpolate or smooth the data. Consequently, the plotted patterns do not necessarily represent the detailed directivity characteristics of the harmonic sound pressure levels.

Directivity patterns for the propeller alone are shown in Figure 77. The plots are complete for the harmonics of order 1-3, but are incomplete or non-existent for higher order harmonics. In the latter case, the harmonic contributions could not be identified because of masking by the broadband components. The general pattern of the data indicates that the maximum sound pressure levels occur in the neighborhood of the plane of rotation of the propeller (90°) and the levels decrease as the propeller axis is approached. However, it is possible that the levels do not decrease as much as they would under free-field conditions, because of the influence of reflections from tunnel surfaces.

When the model fuselage (without empennage) is introduced, the higher order harmonics become evident at more locations. The data now suggest (Figure 78) that the region of maximum harmonic level occurs between 60° and 90°. Otherwise, the pattern is similar to that for the propeller alone in that the lowest sound pressure levels generally occur at locations near to the axis of the propeller (0° and 180°).

(a) Harmonics 1 through 4

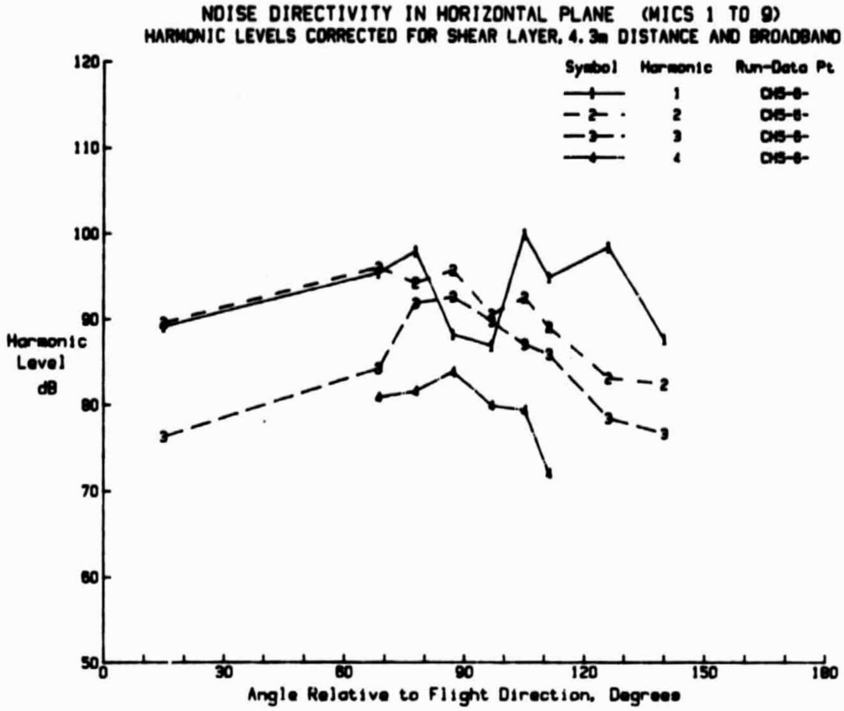

(b) Harmonics 5 through 8

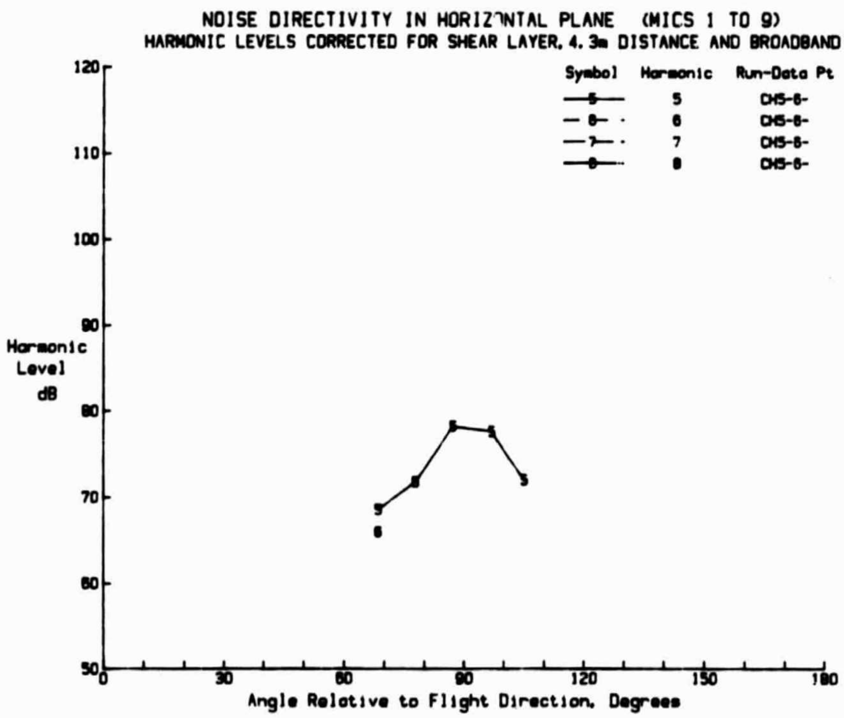

FIGURE 77. HORIZONTAL PLANE DIRECTIVITY OF HARMONIC SOUND PRESSURE LEVELS (PROPELLER ALONE, 8200 RPM, 62.4 M/S)

(a) Harmonics 1 through 4

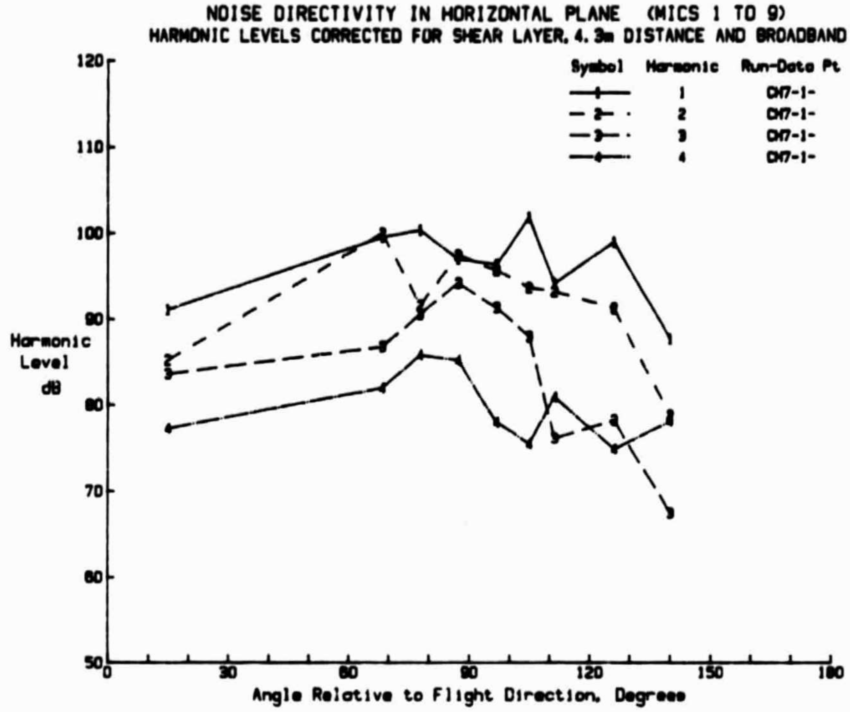

(b) Harmonics 5 through 8

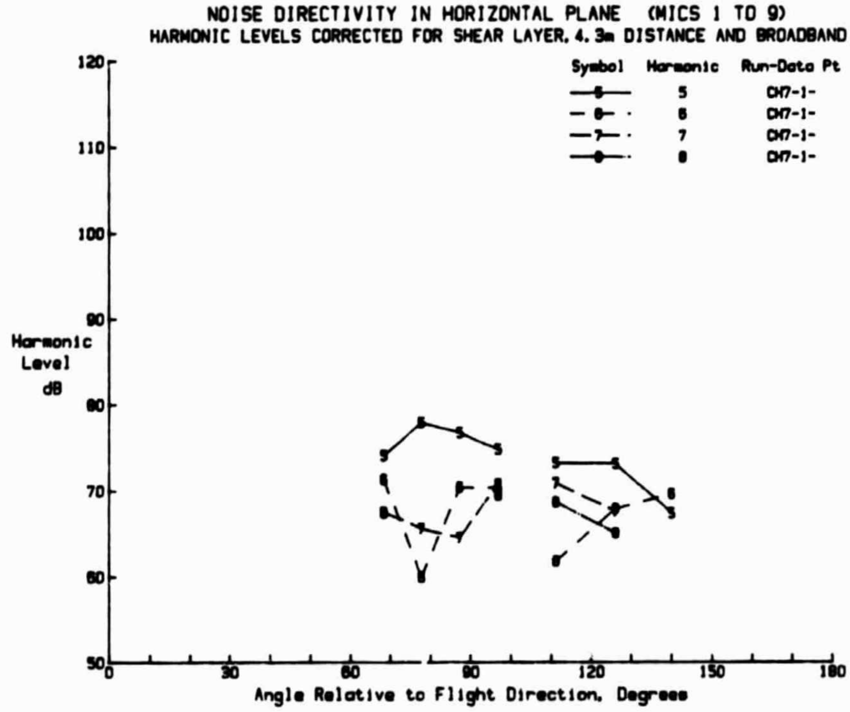

FIGURE 78. HORIZONTAL PLANE DIRECTIVITY OF HARMONIC SOUND PRESSURE LEVELS (FUSELAGE WITHOUT EMPENNAGE, 8200 RPM, 62.4 M/S)

Figures 79 through 81 contain data measured when the propeller was operating behind the Y-tail empennage in the $\psi = 0°$ configuration. Harmonic levels can now be identified at all locations. A comparison with Figure 77 shows that the presence of the empennage changes the directivity patterns of the harmonics. For harmonics of order 1 through 4 the sound pressure levels now remain fairly constant as angle is changed--the levels do not decrease as the propeller axis is approached. The change is more evident for harmonics of order 5 through 8 where now the harmonic sound pressur levels are highest at locations nearest to the propeller axis and lowest near to the propeller plane of rotation.

The data in Figures 79 through 81 show some irregularity in the variation of harmonic sound pressure levels with angle of radiation. There are several possible explanations for this irregularity and it is possible that more than one effect is playing a role. First, there is the influence of the general scatter in the data, as discussed in Section 4.4. Secondly, constructive and destructive interference effects associated with acoustic signals reflected from surfaces in the test chamber can have a strong influence on the observed sound pressure levels. These interference effects will occur at different frequencies for different locations. Thirdly, it is possible that directivity of the radiated acoustic free-field of the propeller behind an empennage has certain characteristics. It may not be possible to determine these characteristics because of the selected locations for the microphones. A larger array of more-closely spaced microphones might be required.

A comparison of Figures 79 throught 81 does not show any strong effect due to separation distance between the empennage and propeller. Even when the data for individual harmonics are compared directly, as in Figure 82, there is no readily

(a) Harmonics 1 through 4

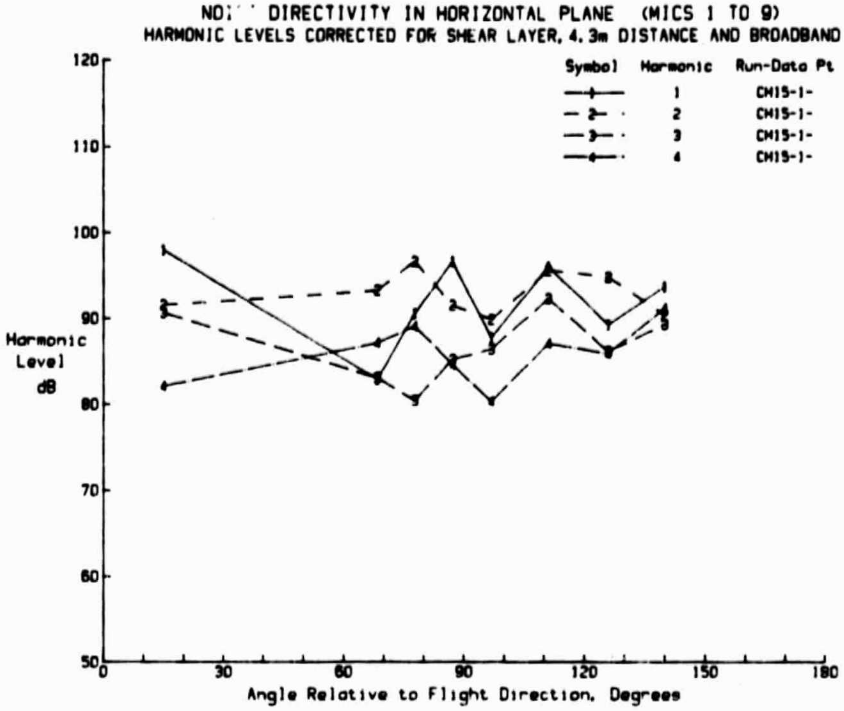

(b) Harmonics 5 through 8

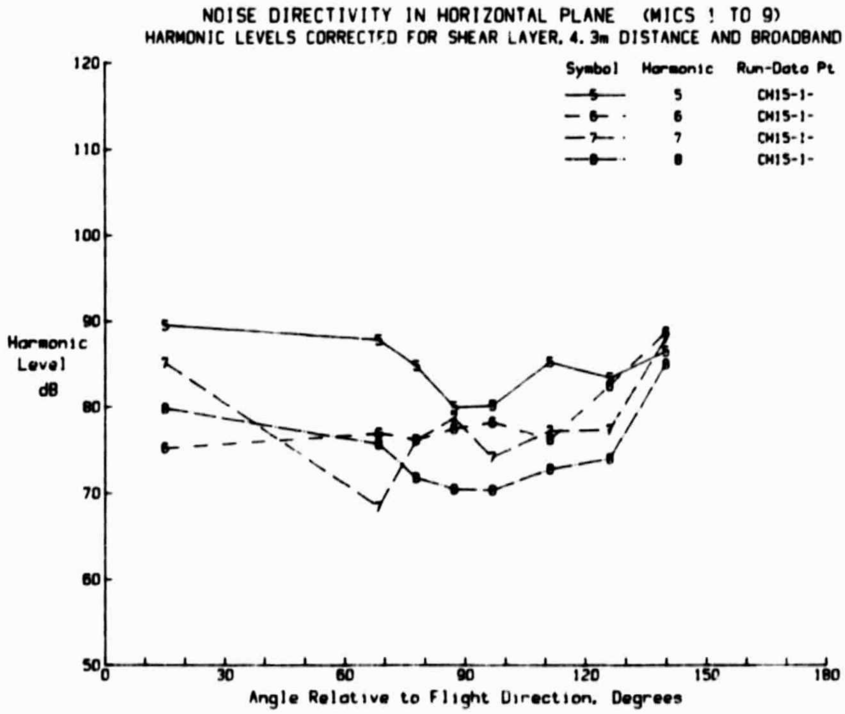

FIGURE 79. HORIZONTAL PLANE DIRECTIVITY OF HARMONIC SOUND PRESSURE LEVELS (Y-TAIL, X=10.8 CM, 8200 RPM, 62.4 M/S, ψ =0)

ORIGINAL PAGE IS
OF POOR QUALITY

(a) Harmonics 1 through 4

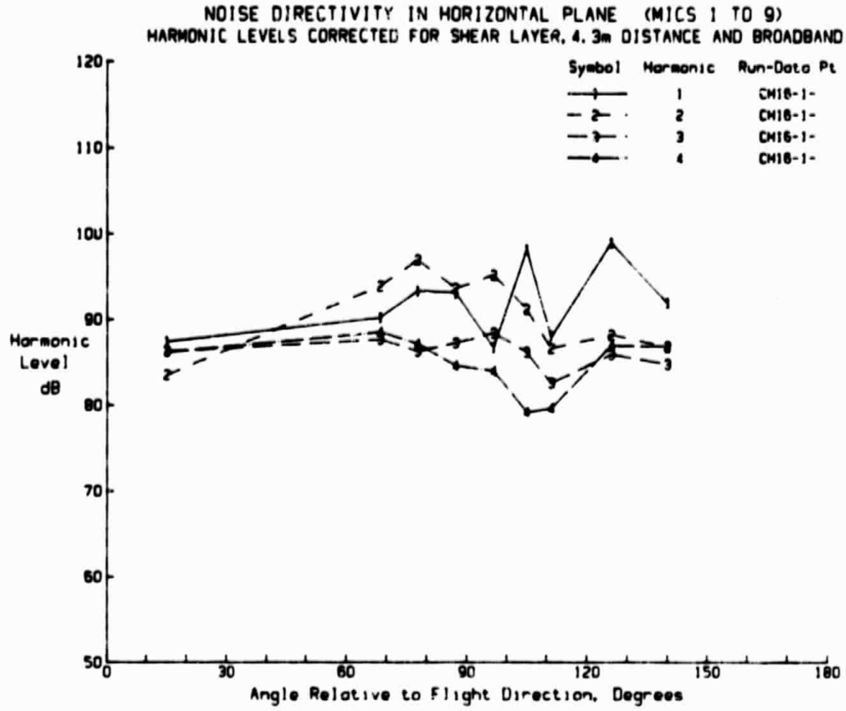

(b) Harmonics 5 through 8

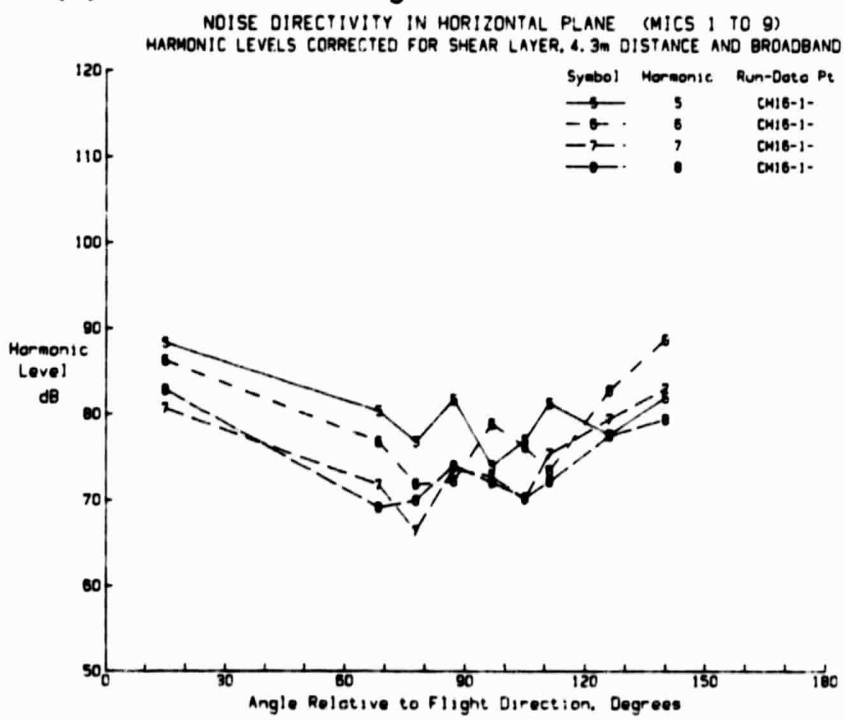

FIGURE 80. HORIZONTAL PLANE DIRECTIVITY OF HARMONIC SOUND PRESSURE LEVELS (Y-TAIL, X=23.8 CM, 8200 RPM, 62.4 M/S, ψ =0)

(a) Harmonics 1 through 4

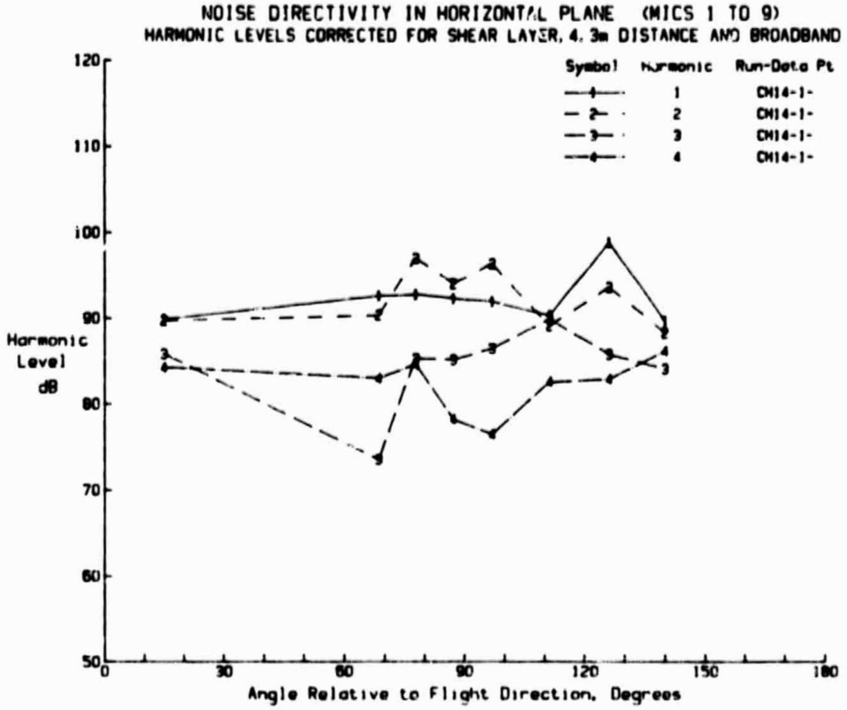

(b) Harmonics 5 through 8

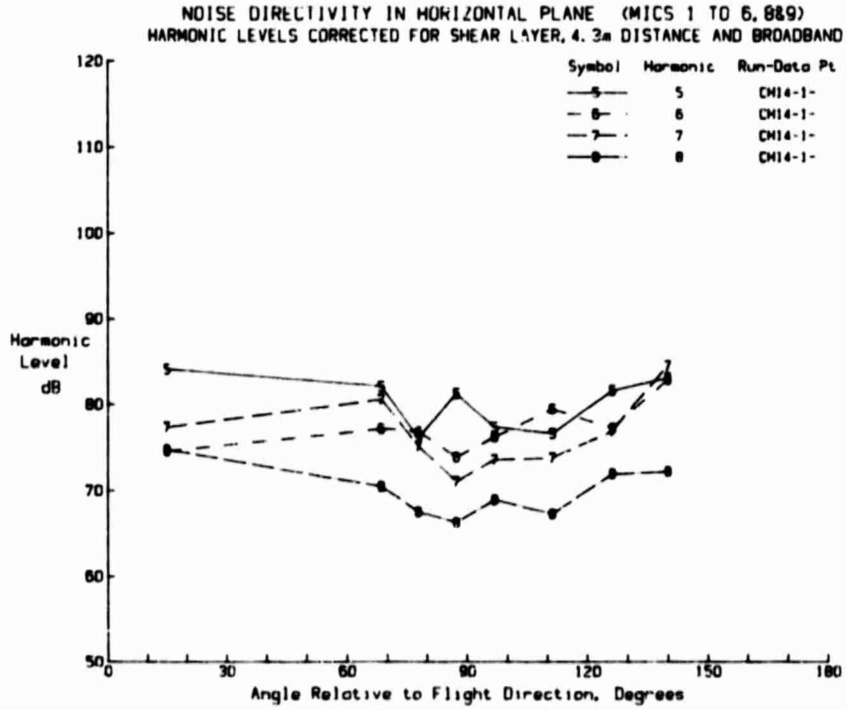

FIGURE 81. HORIZONTAL PLANE DIRECTIVITY OF HARMONIC SOUND PRESSURE LEVELS (Y-TAIL, X=57.5 CM, 8200 RPM, 62.4 M/S, ψ =0)

ORIGINAL PAGE IS
OF POOR QUALITY

(a) Harmonic 1

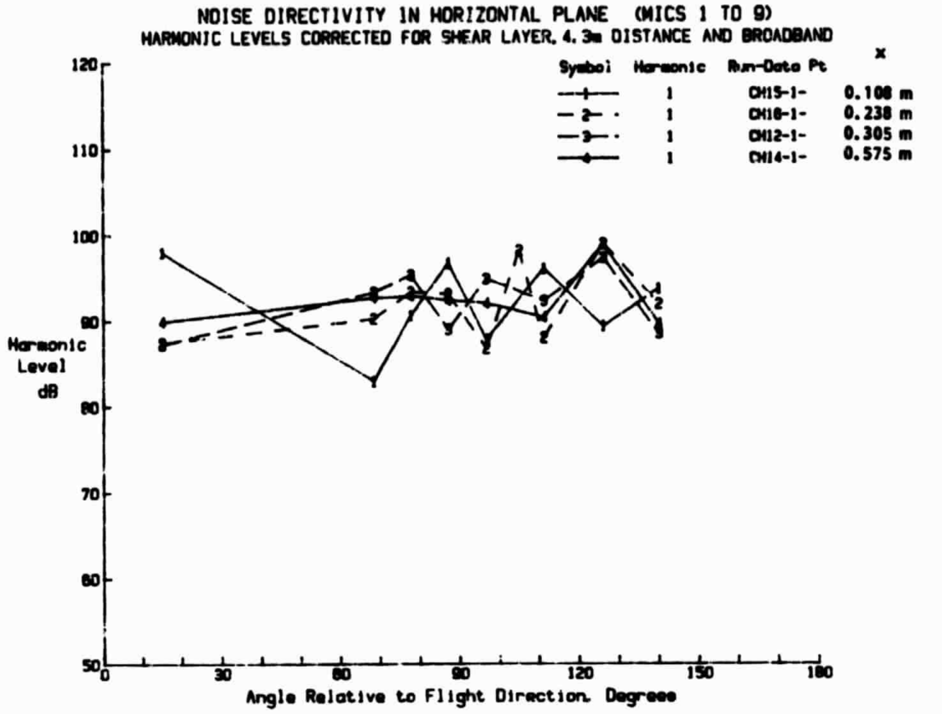

(b) Harmonic 3

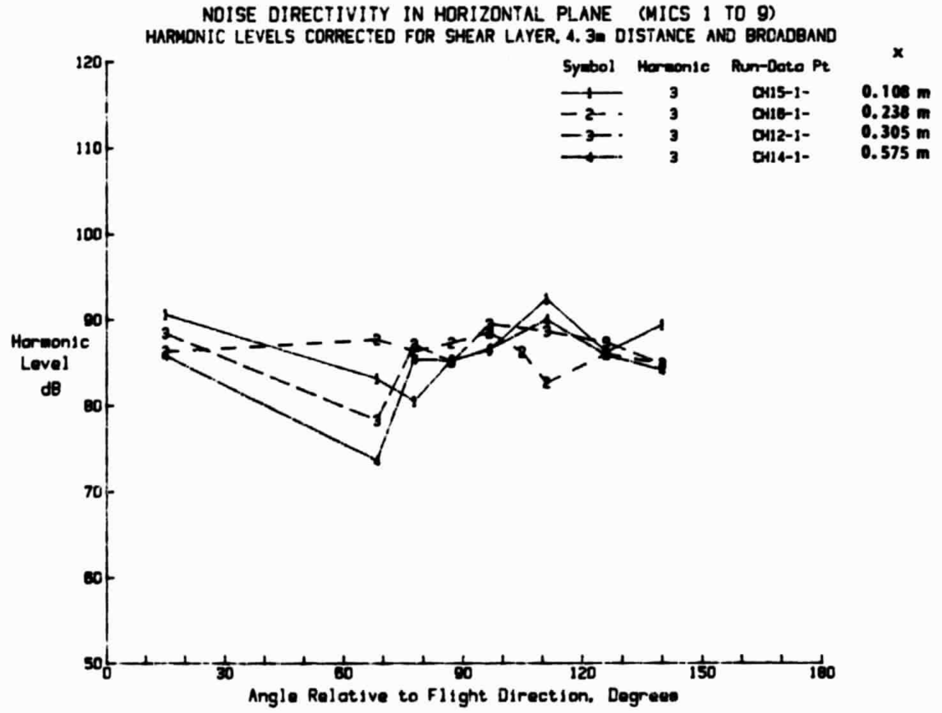

FIGURE 82. INFLUENCE OF EMPENNAGE/PROPELLER SEPARATION DISTANCE ON HORIZONTAL PLANE DIRECTIVITY OF HARMONIC SOUND PRESSURE LEVELS (Y-TAIL, 8200 RPM, 62.4 M/S)

(c) Harmonic 5

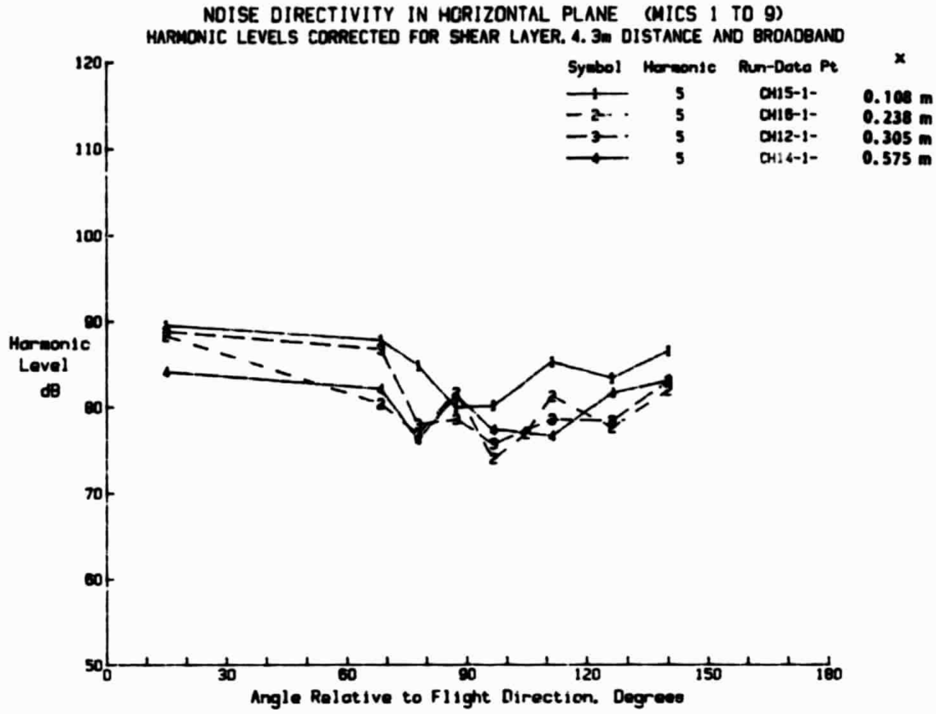

(d) Harmonic 7

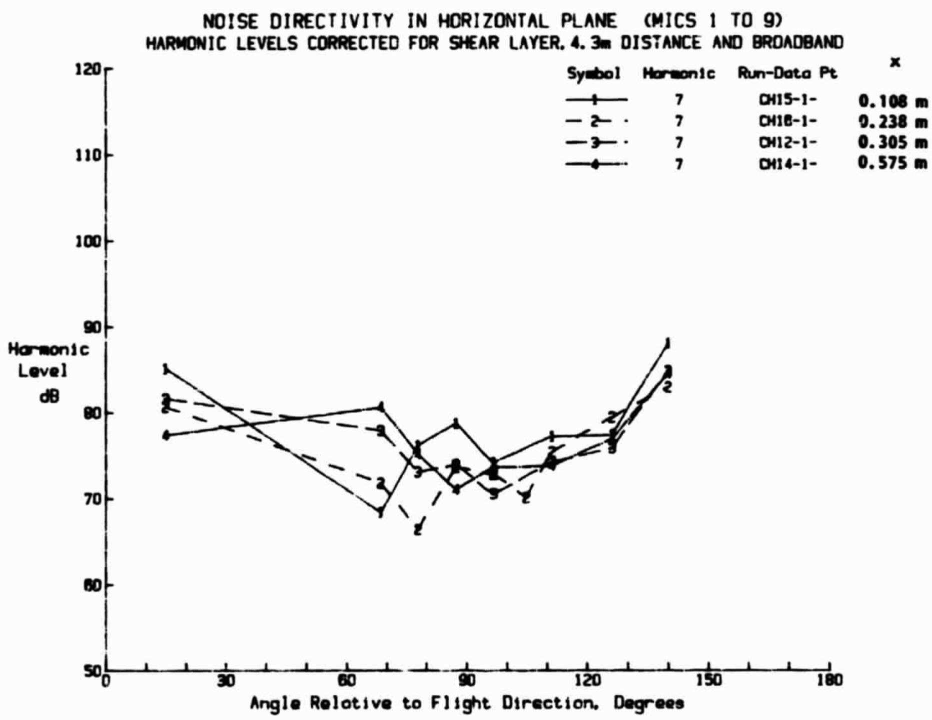

FIGURE 82. CONTINUED

discernible influence of empennage/propeller separation distance, within the range tested. This does not mean that there is no influence of separation distance. A comparison of Figures 81 and 78 shows that increasing the separation distance from 0.575 m to infinity (i.e., no empennage) has a significant effect on the radiated sound field. However, a more detailed analysis of the effect would require information regarding the strengths of the wakes behind the empennage surfaces.

When the airframe is rotated through 90° (ψ = 90°) the directivity patterns show characteristics which are similar to those for ψ = 0°. Figure 83 shows data associated with ψ = 90° and a separation distance of 0.124m between the empennage and the propeller. However, there are larger differences between sound pressure levels for different harmonics (m = 1 through 4) when ψ = 90° than when ψ = 0°.

When the propeller axis is moved vertically relative to the centerline of the empennage, the directivity for the higher order harmonics appears to be more uniform than is the case when the axis and centerline are coincident. This can be seen when comparing Figures 84 and 85 with Figure 80. When the propeller axis is below the empennage centerline (Figure 85) the measured acoustic field is almost omnidirectional in the horizontal plane.

The preceding data have been associated with test conditions for zero angle of incidence of the empennage. Data for an angle of incidence of 5° as shown in Figure 86. The general directivity characteristics are similar to those for zero angle of incidence (Figure 80) with the highest sound levels for harmonics 5 through 8 being at 15° and 160°.

Directivity patterns for the I-tail are contained in Figures 87 and 88 for ψ = 0° and 90°, respectively. The associated separation distance x between the propeller and the fuselage tail cone

(a) Harmonics 1 through 4

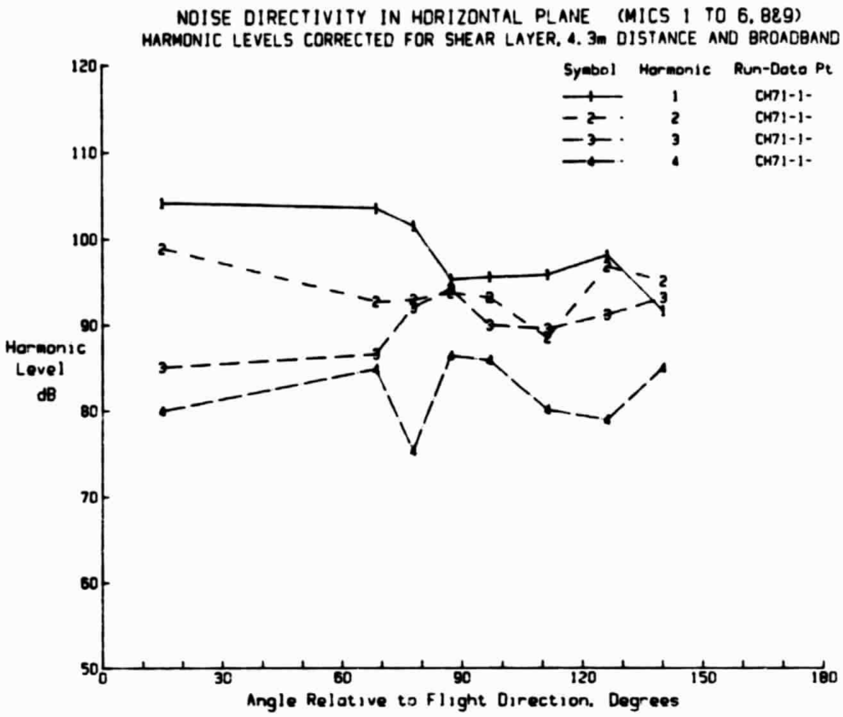

(b) Harmonics 5 through 8

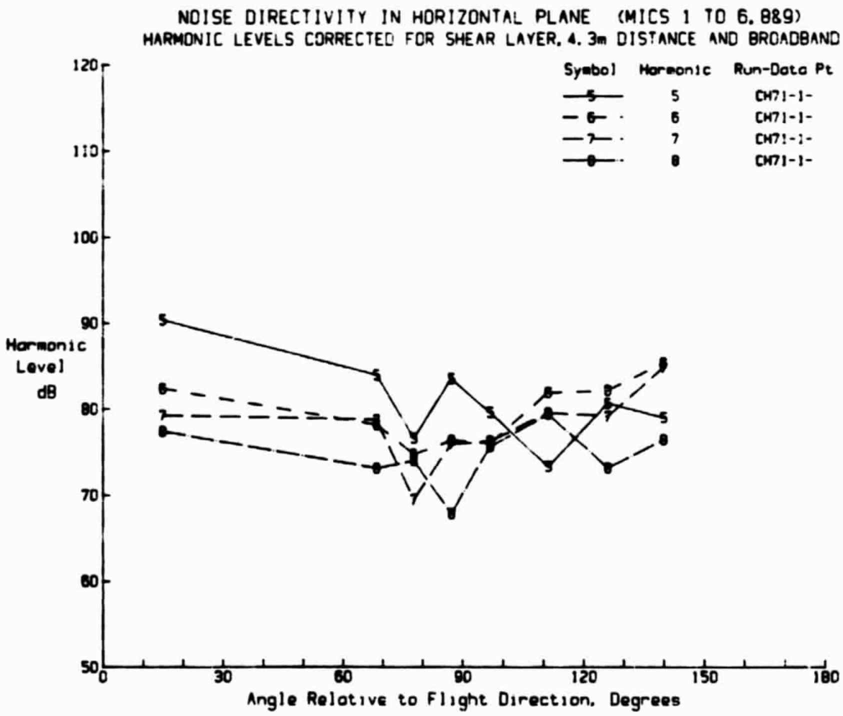

FIGURE 83. HORIZONTAL PLANE DIRECTIVITY OF HARMONIC SOUND PRESSURE LEVELS (Y-TAIL, X=12.4 CM, 8200 RPM, 62.4 M/S, ψ =90°)

(a) Harmonics 1 through 4

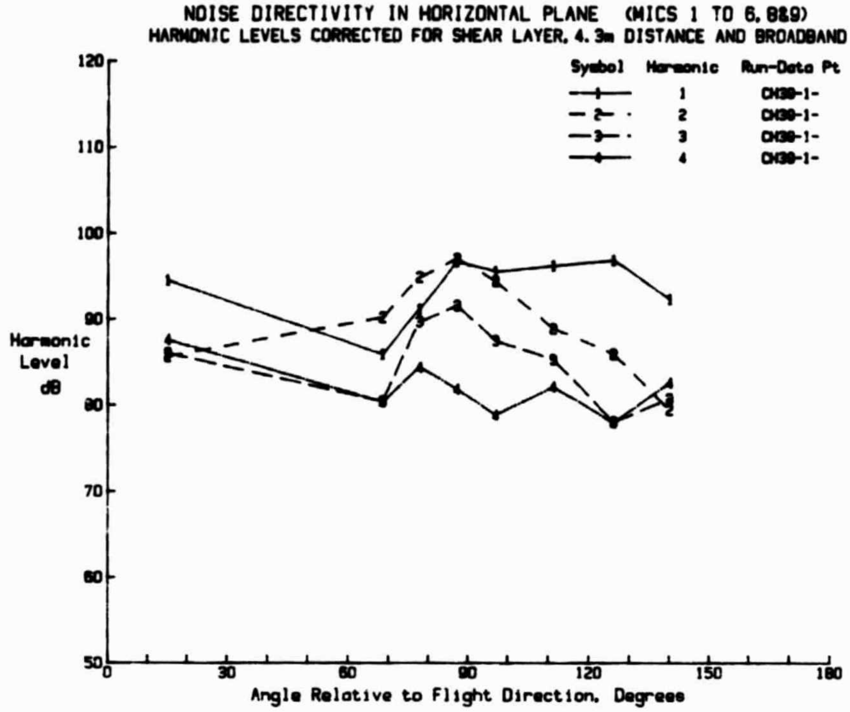

(b) Harmonics 5 through 8

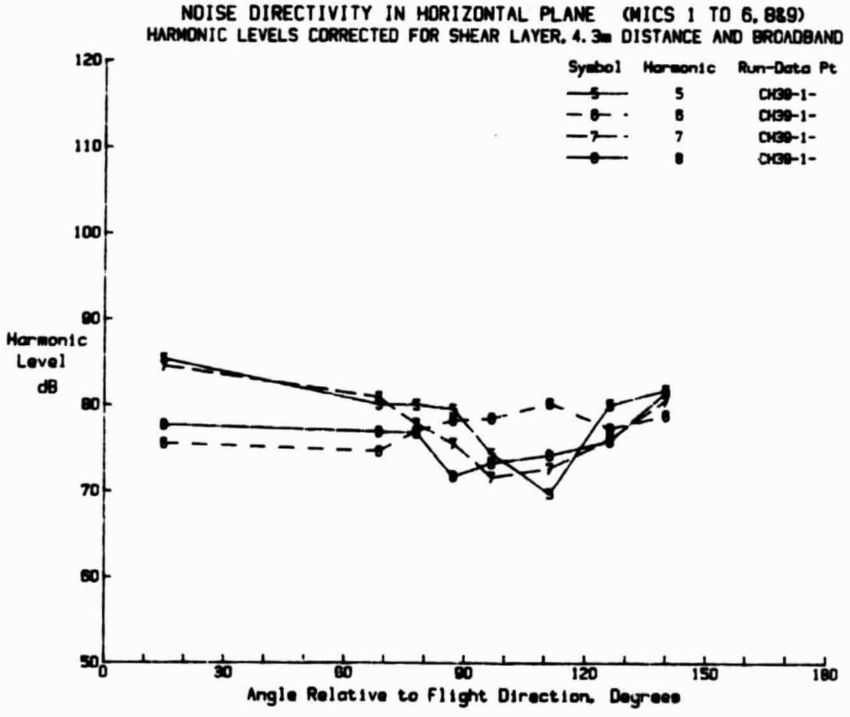

FIGURE 84. HORIZONTAL PLANE DIRECTIVITY OF HARMONIC SOUND PRESSURE LEVELS, EMPENNAGE/PROPELLER VERTICAL SEPARATION +7.6 CM (Y-TAIL, X=23.5 CM, 8200 RPM, 62.4 M/S)

(a) Harmonics 1 through 4

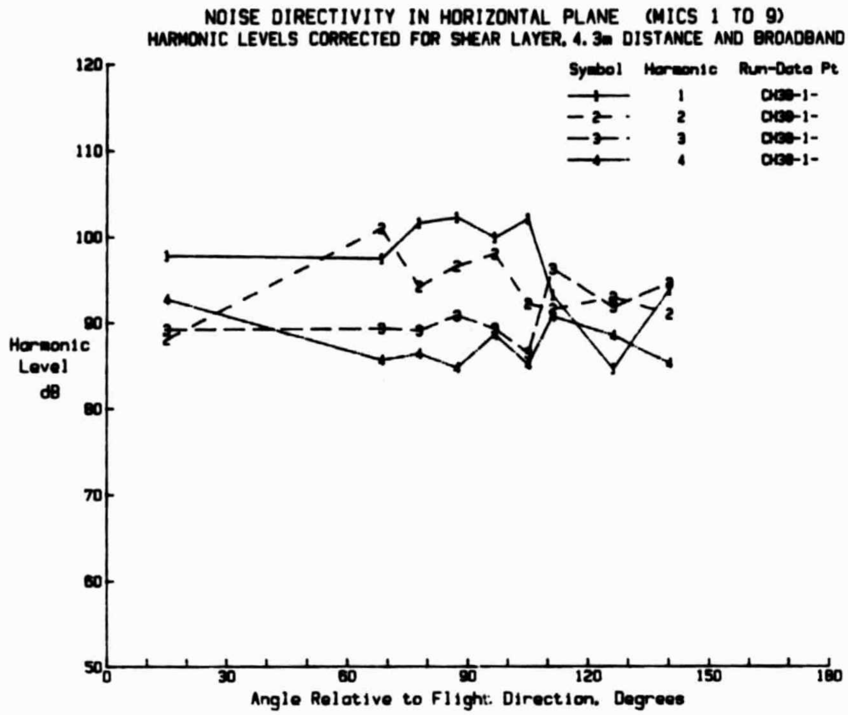

(b) Harmonics 5 through 8

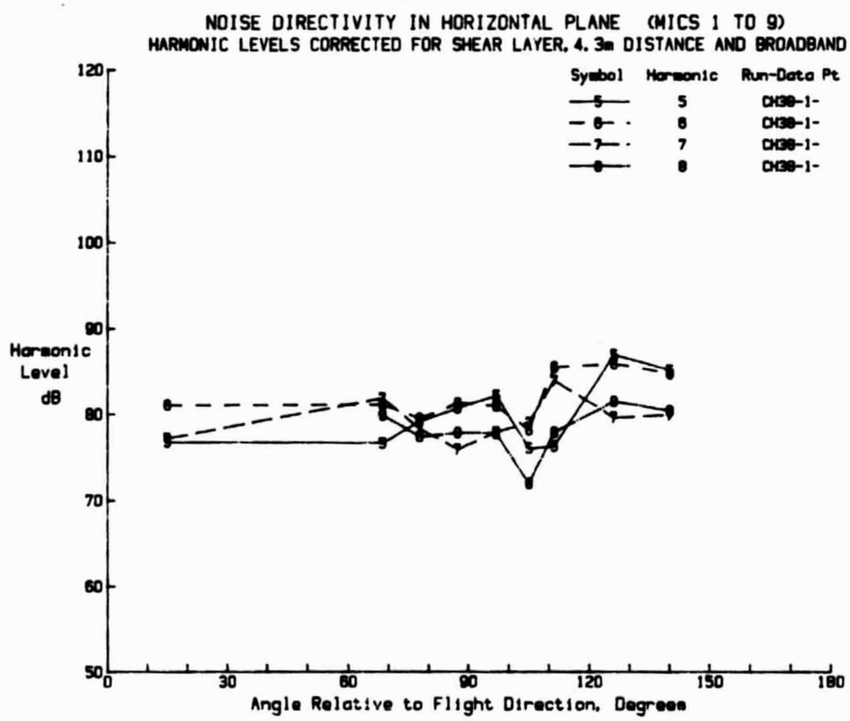

FIGURE 85. HORIZONTAL PLANE DIRECTIVITY OF HARMONIC SOUND PRESSURE LEVELS, EMPENNAGE/PROPELLER VERTICAL SEPARATION -7.6 CM (Y-TAIL, X=24.1 CM, 8200 RPM, 62.4 M/S)

(a) Harmonics 1 through 4

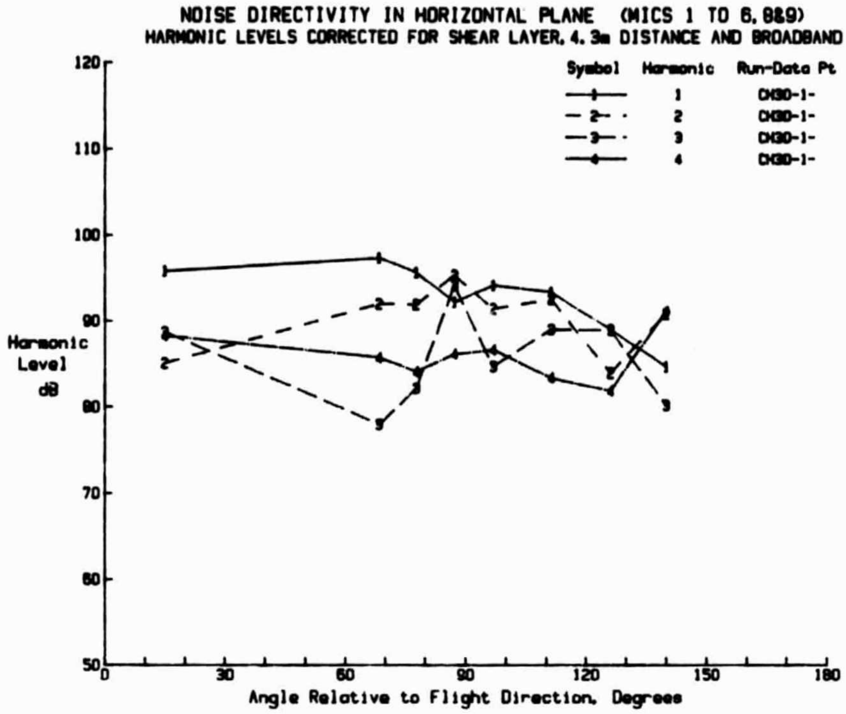

(b) Harmonics 5 through 8

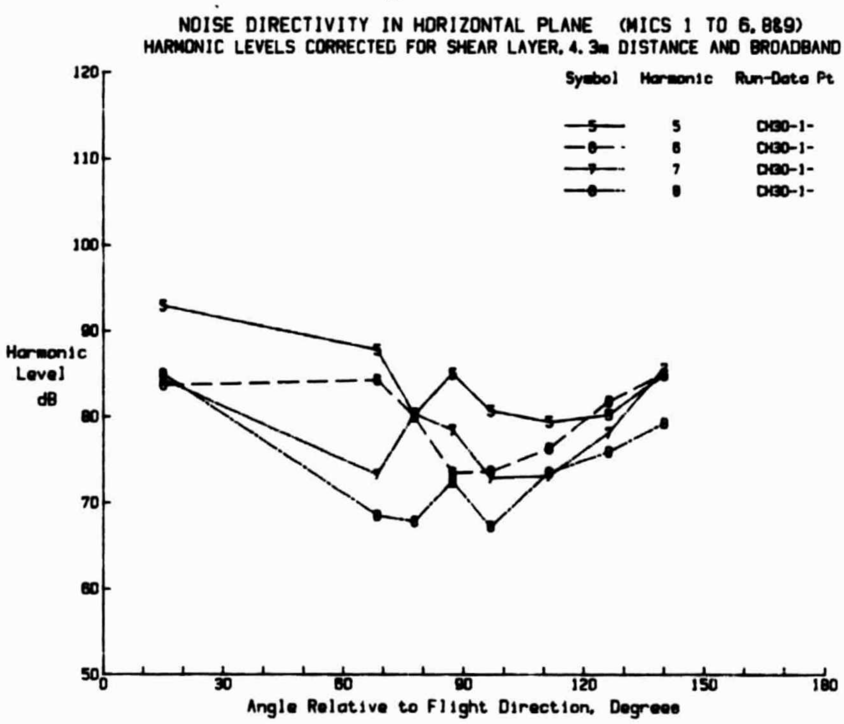

FIGURE 86. HORIZONTAL PLANE DIRECTIVITY OF HARMONIC SOUND PRESSURE LEVELS, EMPENNAGE ANGLE OF INCIDENCE 5° (Y-TAIL, X=22.9 CM, 8200 RPM, 62.4 M/S)

(a) Harmonics 1 through 4

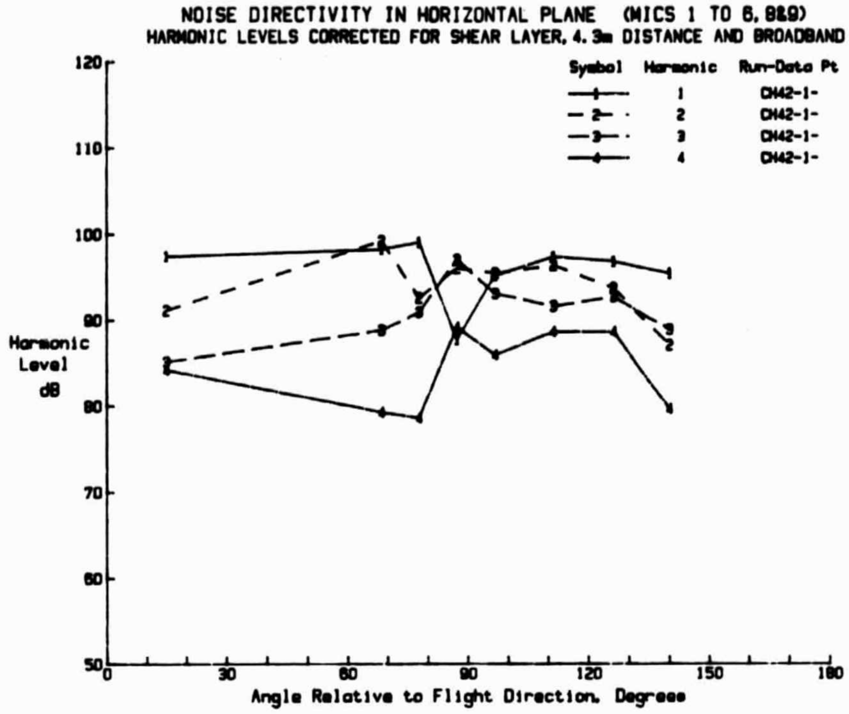

(b) Harmonics 5 through 8

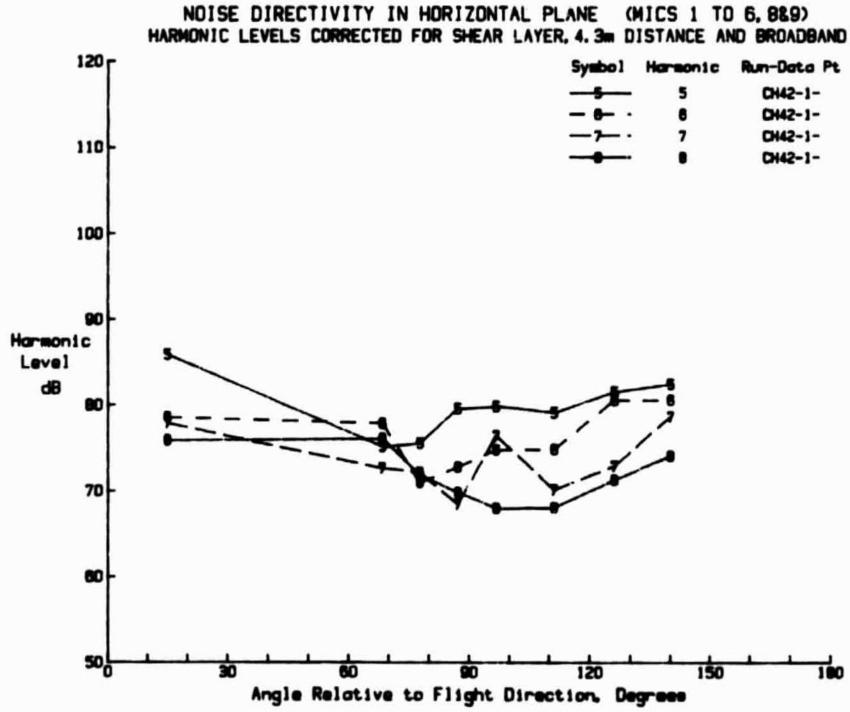

FIGURE 87. HORIZONTAL PLANE DIRECTIVITY OF HARMONIC SOUND PRESSURE LEVELS (I-TAIL, X=38.4 CM, 8200 RPM, 62.4 M/S, ψ =0°)

(a) Harmonics 1 through 4

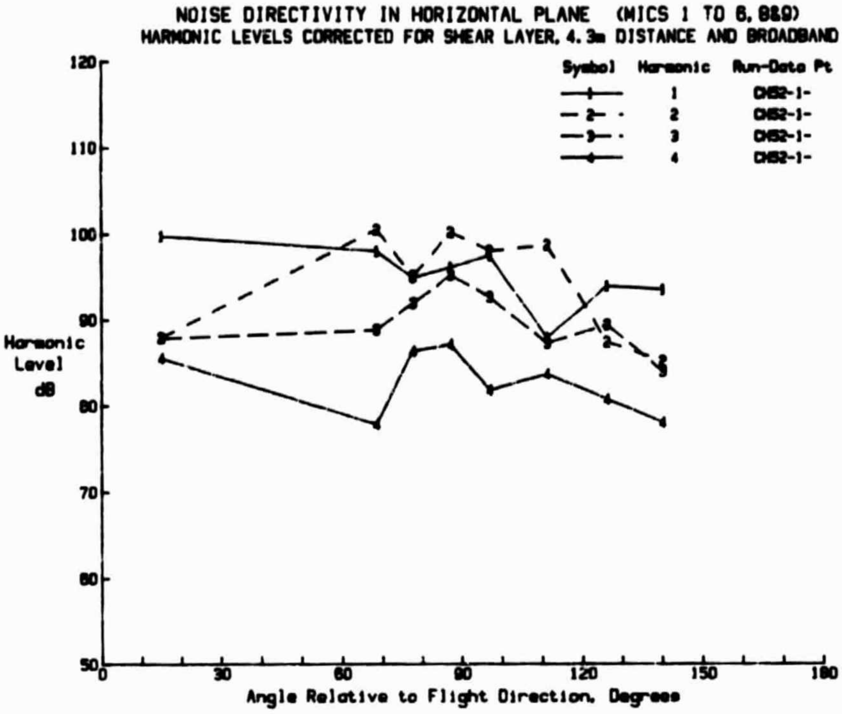

(b) Harmonics 5 through 8

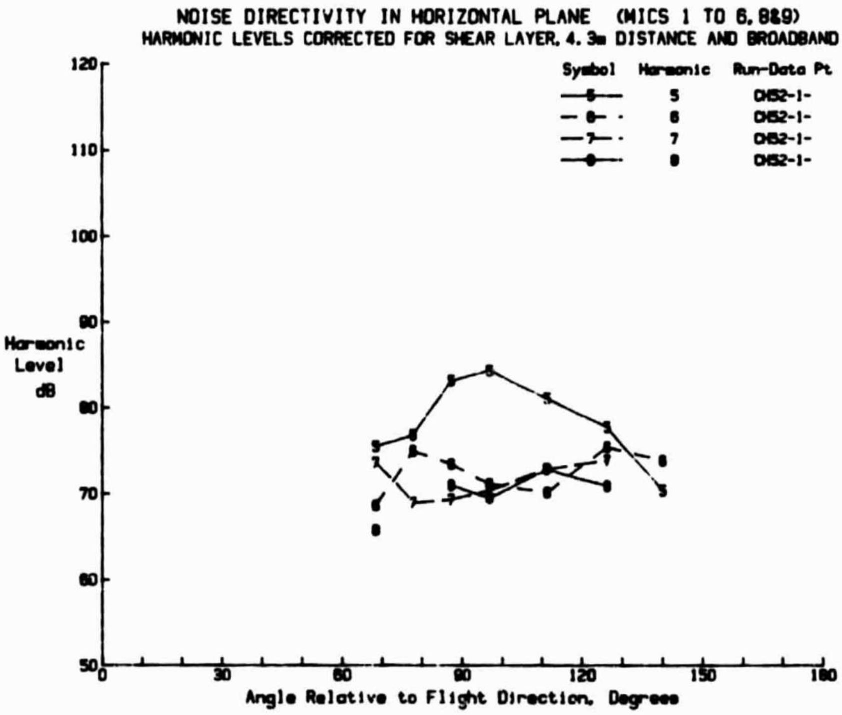

FIGURE 88. HORIZONTAL PLANE DIRECTIVITY OF HARMONIC SOUND PRESSURE LEVELS (I-TAIL, X=36.8 CM, 8200 RPM, 62.4 M/S, ψ =90°)

is about 370 mm; the corresponding mean distance between the propeller and the empennage trailing edge (see Table 7) is about 240 mm which is similar to that for the Y-tail data of Figures 80 and 83. Comparing the sound level distributions in Figure 87 with those in Figures 80 and 83 it is seen that the directivity patterns for the I-tail ($\psi = 0°$) are similar to those for the Y-tail ($\psi = 90°$). For harmonics 5 through 8 the sound pressure levels near to the axis of the propeller are slightly higher than those in the neighborhood of the plane of rotation of the propeller.

When data for the I-tail ($\psi = 90°$) are considered the directivity patterns show a similarity with those in Figure 78 for the test configuration of a fuselage without an empennage. For harmonics 5 through 8, the highest sound pressure levels appear to be in the neighborhood of the plane of rotation of the propeller--harmonics could not be identified in the data from microphone 9 at an angle of 15°.

5.13 <u>"On-Axis" Sound Pressure Levels</u>

The preceding discussion regarding the directivity of the acoustic field in the horizontal plane has emphasized the importance of noise radiated fore and aft along the axis (or near to the axis) of the propeller. Although these radiation angles may not be critical from the point of view of airplane flyover noise, they are important in understanding the physical characteristics of a propeller operating behind an empennage. Consequently, additional information is presented in this section for microphone locations 8 and 9. This information covers many of the topics which have been discussed earlier for microphones located outside the flow.

The strong influence of the empennage on the on-axis sound pressure levels is demonstrated in Figure 89. When the propeller operates alone, or behind the model fuselage without an empennage, the harmonic sound pressure levels at locations 8 and 9 are lower than those measured at larger angles to the propeller axis (Figures 89(a) and (b)). Upon introduction of the empennage, the measured sound pressure levels at locations 8 and 9 increase to be comparable to those elsewhere for harmonics of order 1 through 4, and markedly exceed those elsewhere for harmonics of order 5 through 11.

Repeatability of the harmonic sound pressure levels measured at locations 8 and 9 is demonstrated in Figure 90 where results for three repeated runs (11-1, 16-1 and 22-6) are compared. Figure 90 can be compared with Figure 42 which contains similar data for microphones outside the flow. In the case of microphones 8 and 9, the data repeatability looks quite good and is comparable with the measurements at locations 11 and 12. The average range of harmonic sound pressure levels is 2.1 dB at microphone 8 and 2.9 dB at microphone 9 (see Figure 43 for other locations).

The influence of separation distance between propeller and the Y-tail empennage can be seen in Figure 91 for $\psi = 0°$ and Figure 92 for $\psi = 90°$. These figures can be compared with Figures 63 through 65 which contain data for microphones 1, 3 and 6 outside the flow. As before, the separation distances given in Figures 91 and 92 refer to the distance between the tail cone and propeller; Table 7 gives the corresponding distances between empennage trailing edge and propeller. On the average, the data in Figures 91 and 92 show harmonic sound levels changing by about 7 dB as the separation distance varies. Although there is some scatter in the data, the general trend is that of increasing sound pressure level as separation distance decreases. The trend seems to be defined more clearly than was the case in Figures 63 through 65.

(a) Propeller Alone

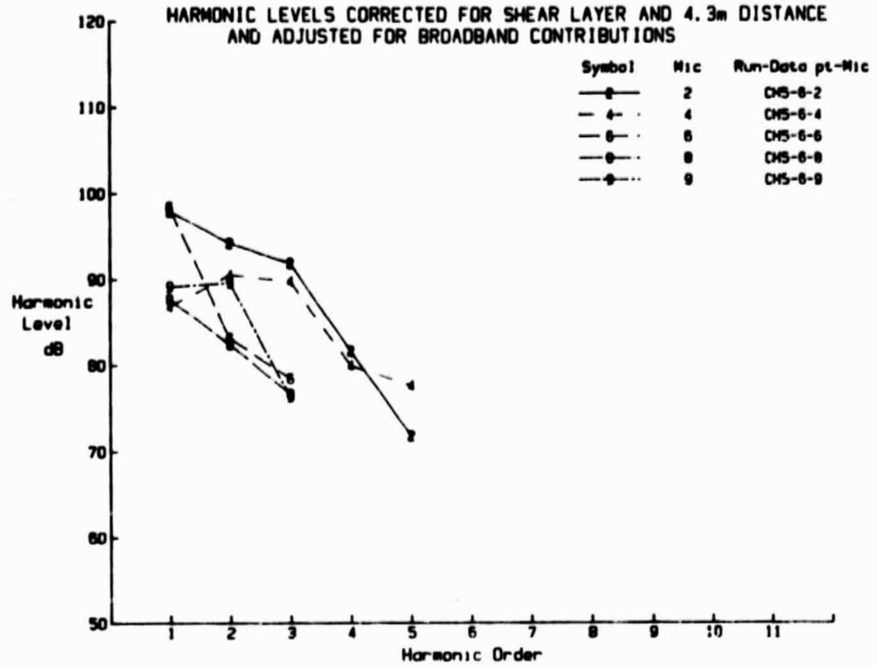

(b) Propeller behind Fuselage without Empennage

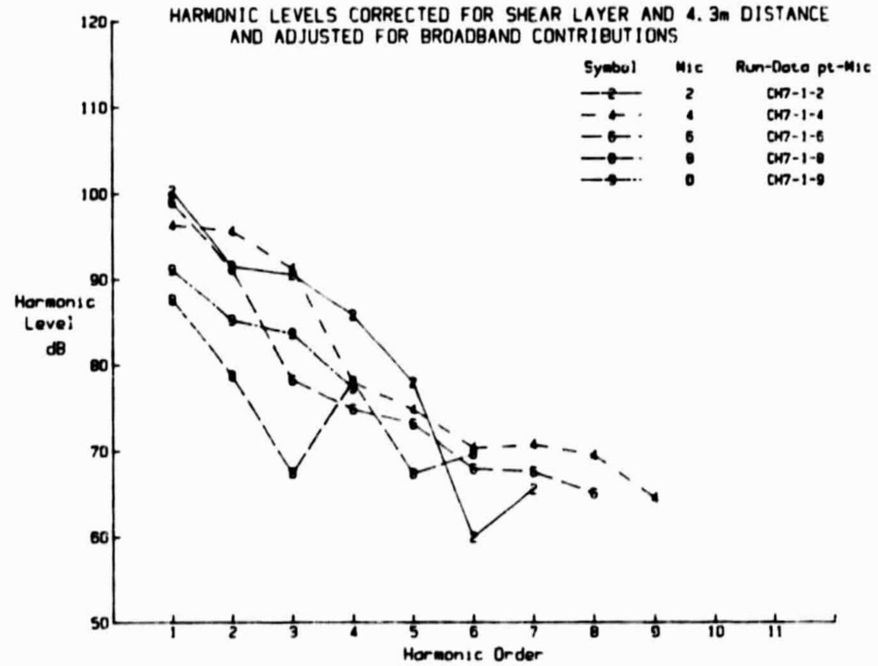

FIGURE 89. INFLUENCE OF FUSELAGE AND EMPENNAGE ON HARMONIC SOUND PRESSURE LEVELS (8200 RPM, 62.4 M/S)

(c) Propeller behind Y-Tail (ψ=0°, X=10.8 cm)

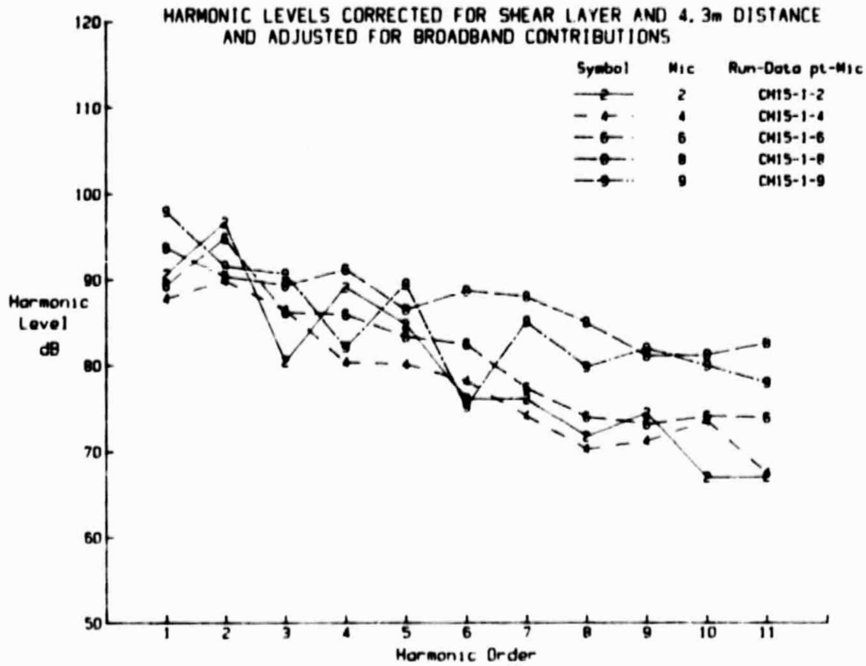

(d) Propeller behind Y-Tail (ψ=0°, X=23.8 cm)

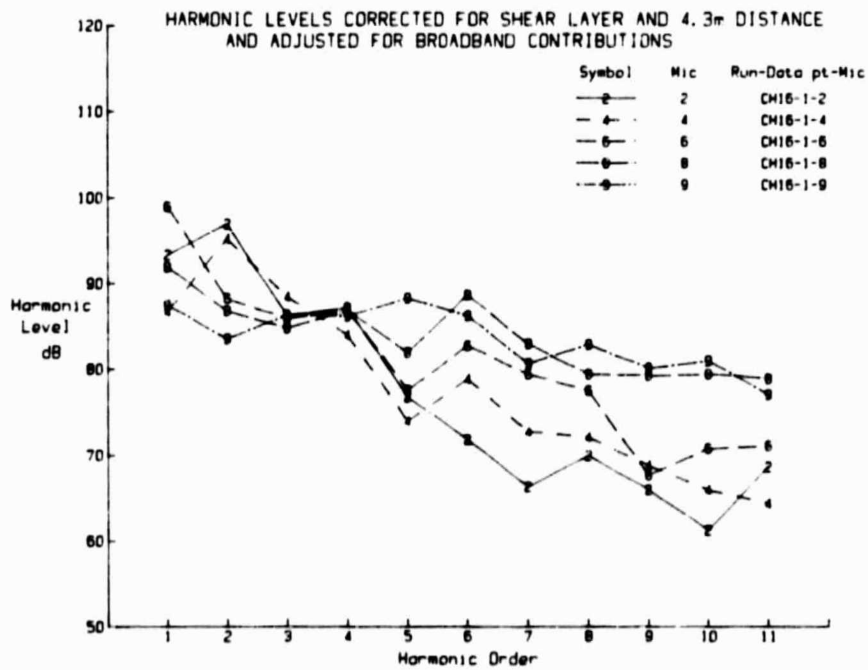

FIGURE 89. CONTINUED

(a) Microphone 8

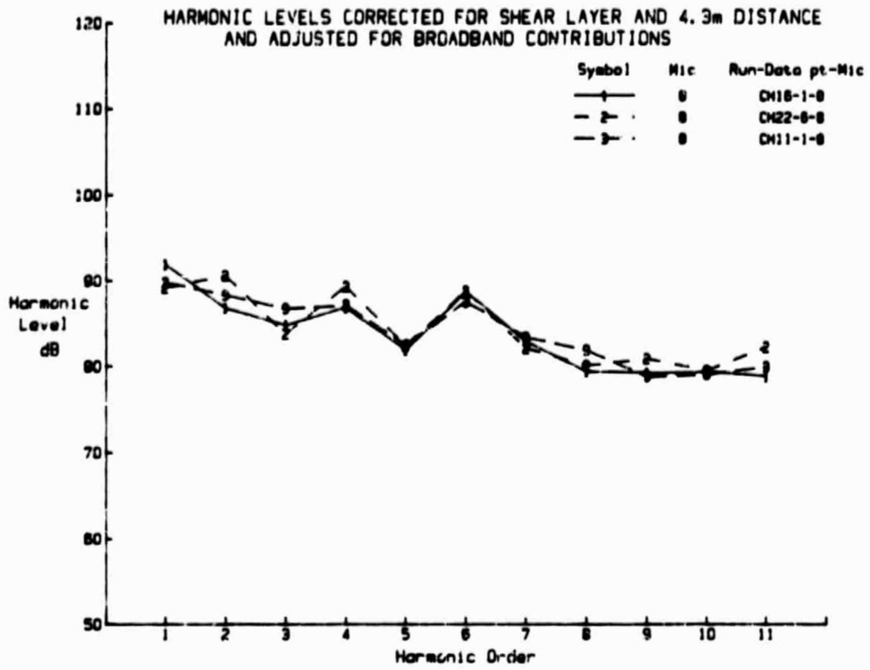

(b) Microphone 9

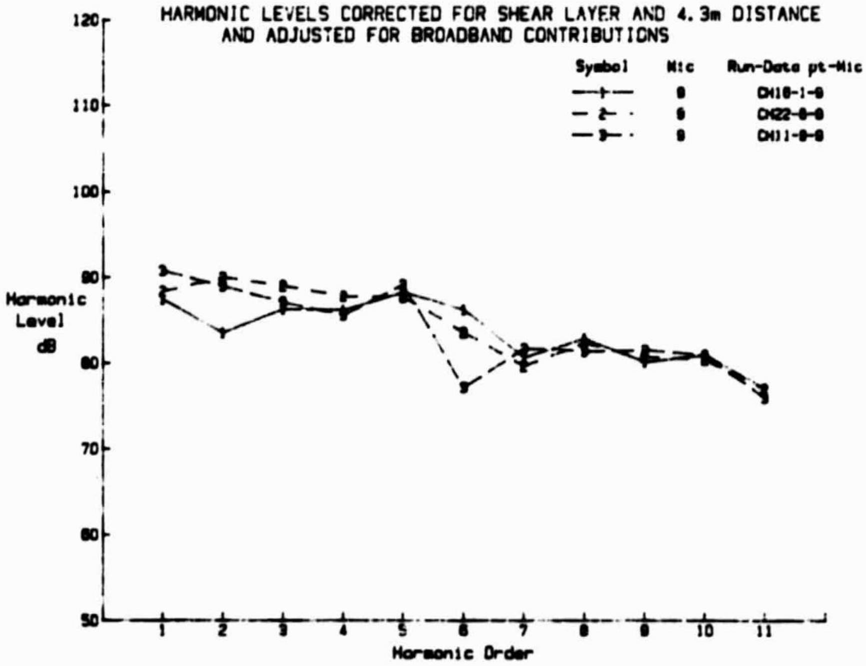

FIGURE 90. COMPARISON OF BLADE PASSAGE FREQUENCY HARMONIC LEVELS FOR REPEAT RUNS, MICROPHONES 8 AND 9 (Y-TAIL, 8200 RPM, 62.4 M/S)

(a) Microphone 8

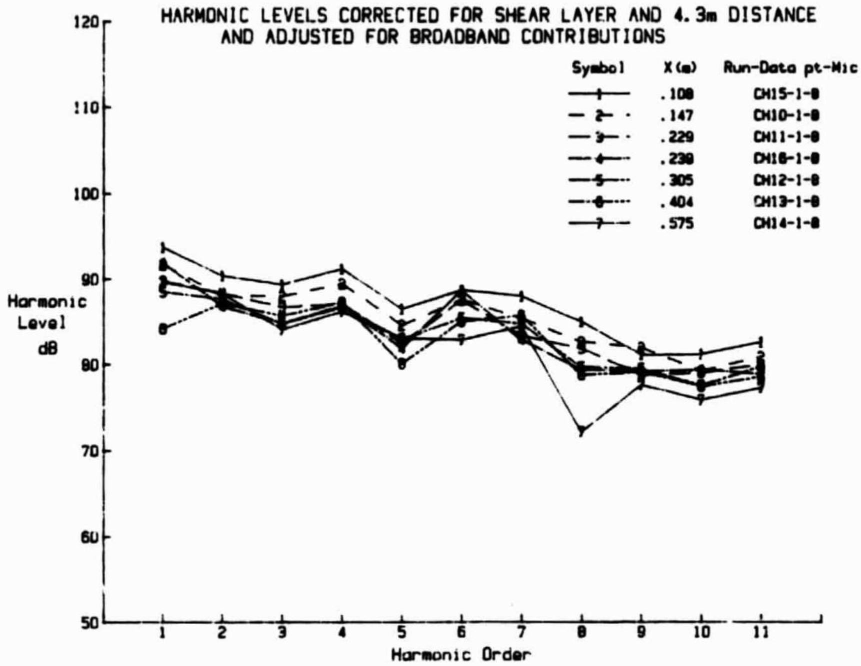

(b) Microphone 9

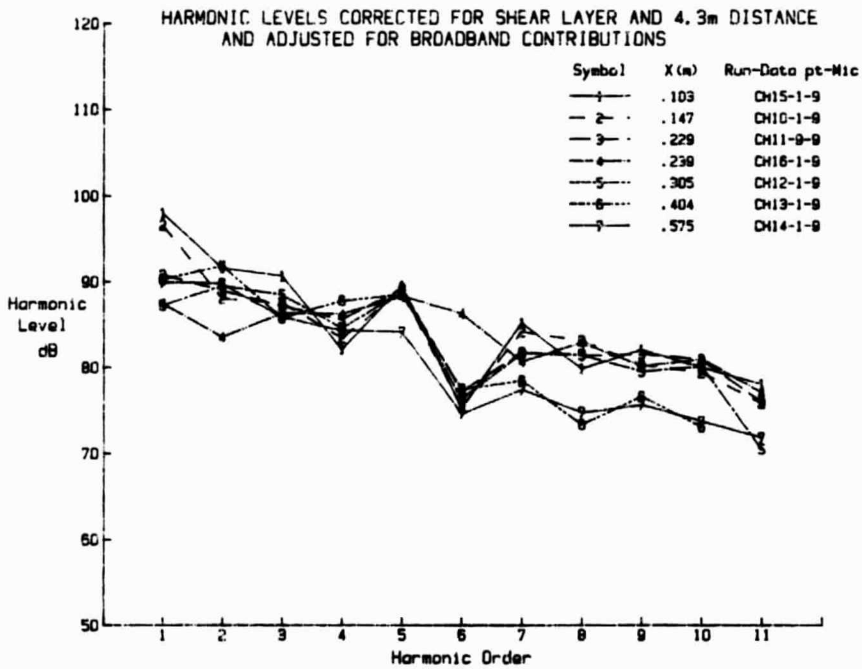

FIGURE 91. INFLUENCE OF EMPENNAGE/PROPELLER AXIAL SEPARATION DISTANCE ON HARMONIC SOUND PRESSURE LEVELS, MICROPHONES 8 AND 9 (Y-TAIL, 8200 RPM, 62.4 M/S, $\psi = 0°$)

(a) Microphone 8

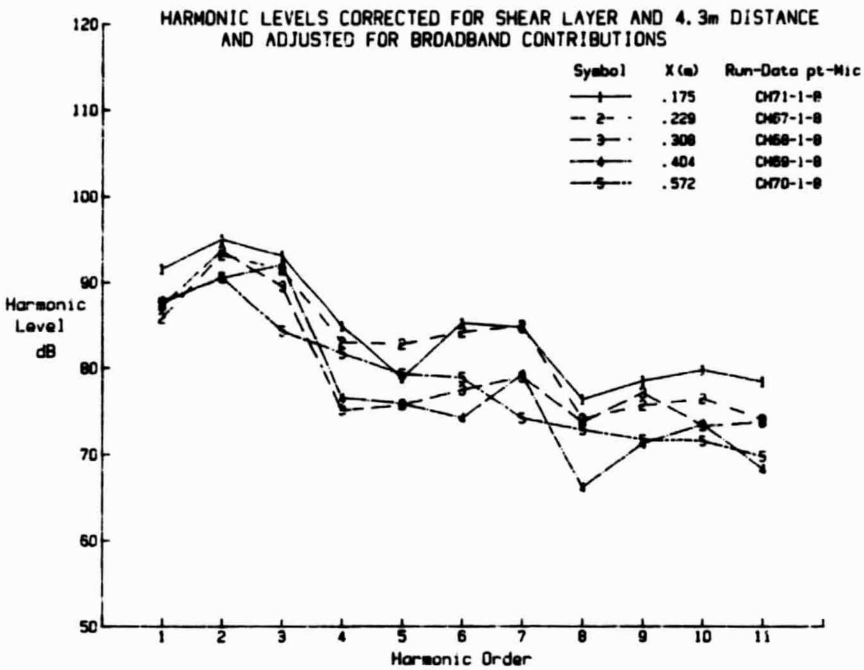

(b) Microphone 9

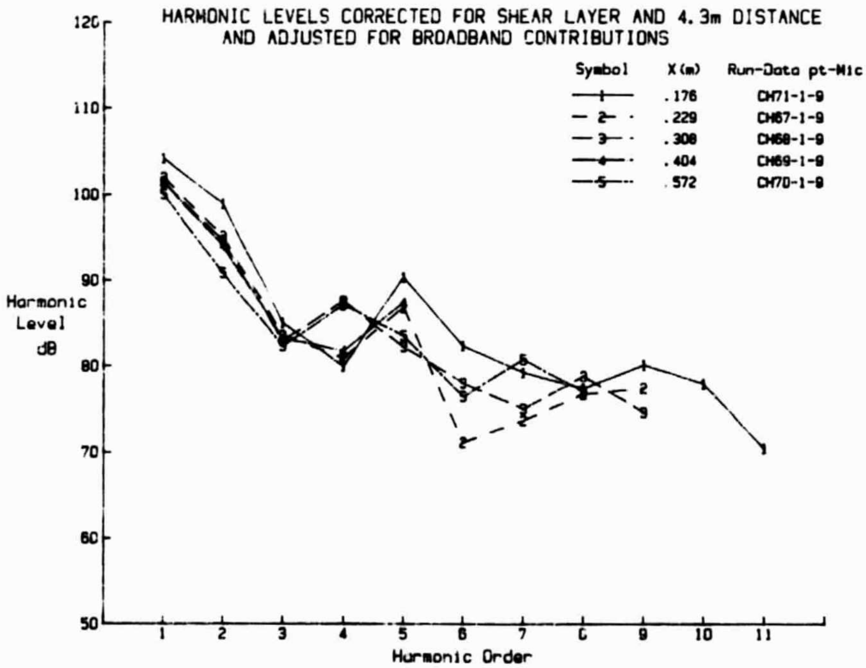

FIGURE 92. INFLUENCE OF EMPENNAGE/PROPELLER AXIAL SEPARATION DISTANCE ON HARMONIC SOUND PRESSURE LEVELS, MICROPHONES 8 AND 9 (Y-TAIL, 8200 RPM, 62.4 M/S, ψ =90°)

When the fuselage with Y-tail empennage is rotated through 90° from $\psi = 0°$ to $\psi = 90°$, the harmonic sound pressure levels decrease for most harmonics, as can be seen in Figure 93. This is in contrast to the results for microphones closer to the plane of rotation of the propeller where the sound pressure levels are higher for $\psi = 90°$ than for $\psi = 0°$ (Figure 62).

Increasing the angle of incidence of the Y-tail empennage significantly increases the harmonic sound pressure levels at microphone 9 and causes a smaller increase at microphone 8, as is shown in Figure 94. The change at microphone 9 is more distinct than at any other location (see Figures 71 through 73, for example).

The most well-defined demonstration of the effect of empennage/propeller separation on radiated sound pressure level is obtained when the separation is varied while the empennage angle of incidence is maintained at 5°. Figure 95 shows the resulting harmonic sound pressure levels measured at microphones 8 and 9. Here it is very clearly shown that the highest sound pressure levels are associated with the smallest separation distances. The average range of measured harmonic sound pressure levels is about 10 dB for microphone 8 and 8 dB for microphone 9.

(a) Microphone 8

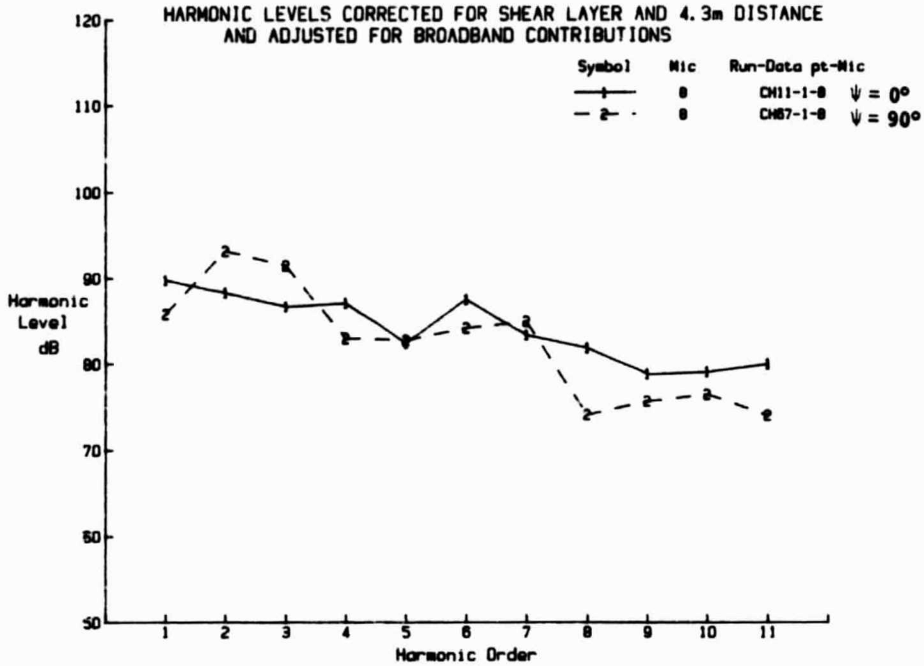

(b) Microphone 9

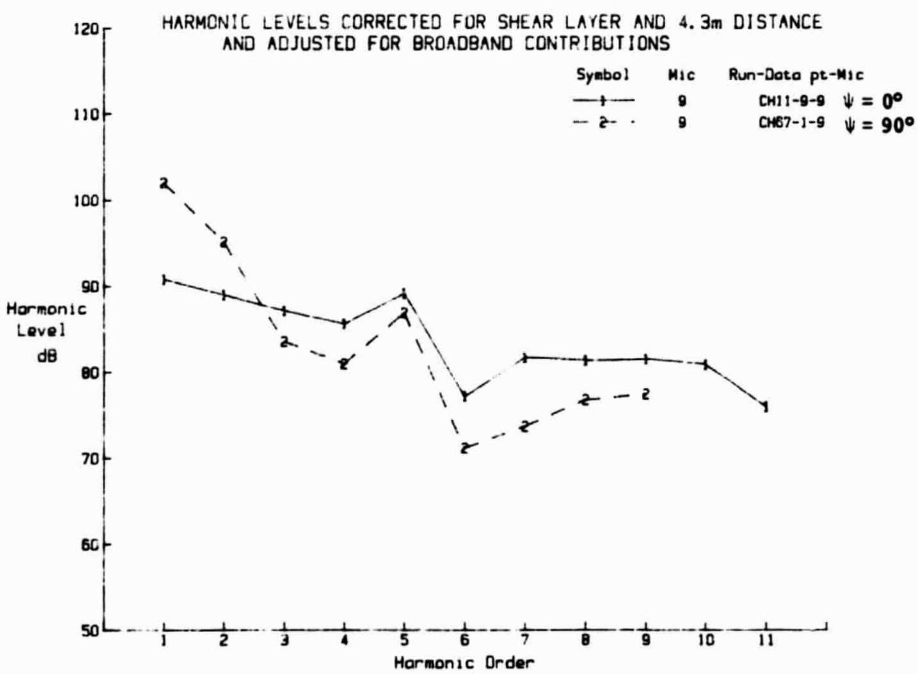

FIGURE 93. COMPARISON OF HARMONIC SOUND PRESSURE LEVELS MEASURED FOR DIFFERENT FUSELAGE ORIENTATIONS, MICROPHONES 8 AND 9 (Y-TAIL, 8200 RPM, 62.4 M/S)

(a) Microphone 8

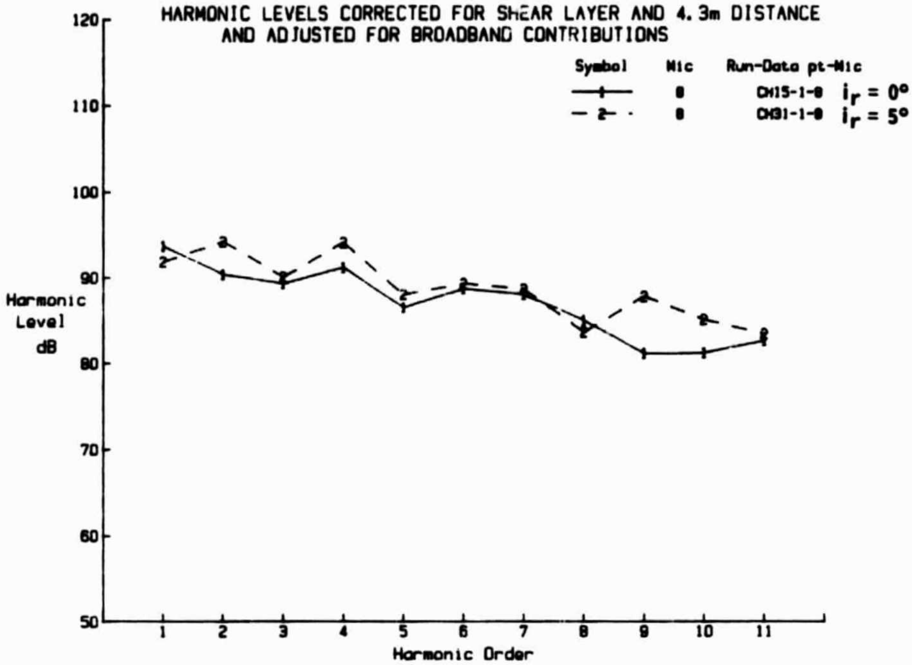

(b) Microphone 9

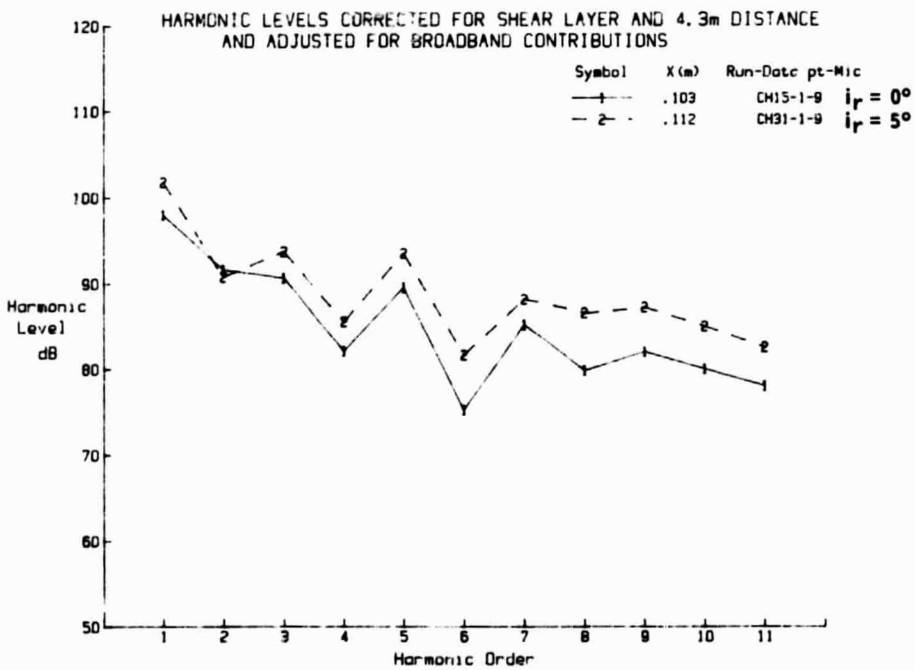

FIGURE 94. INFLUENCE OF EMPENNAGE ANGLE OF INCIDENCE ON HARMONIC SOUND PRESSURE LEVELS, MICROPHONES 8 AND 9 (Y-TAIL, 8200 RPM, 62.4 M/S)

(a) Microphone 8

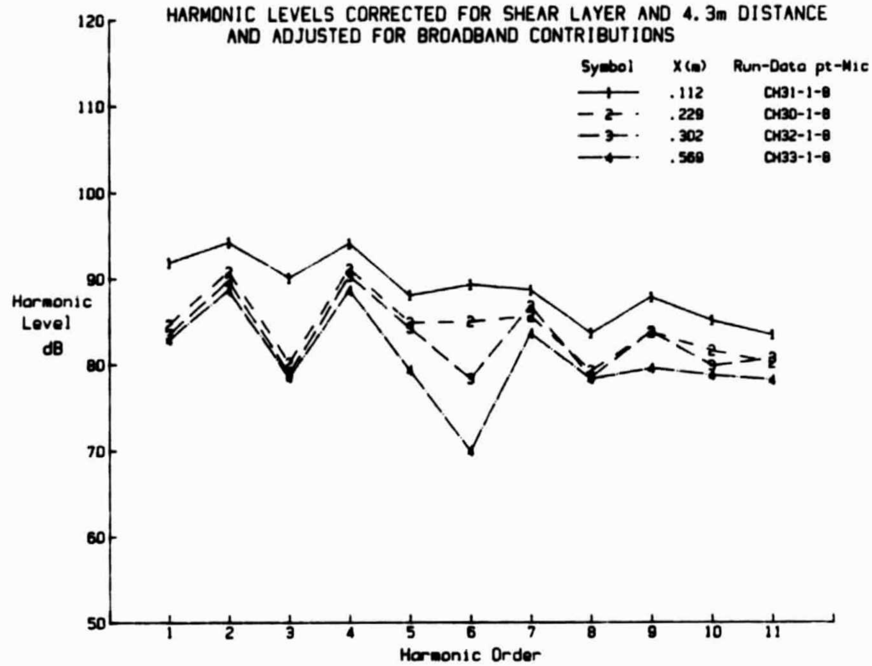

(b) Microphone 9

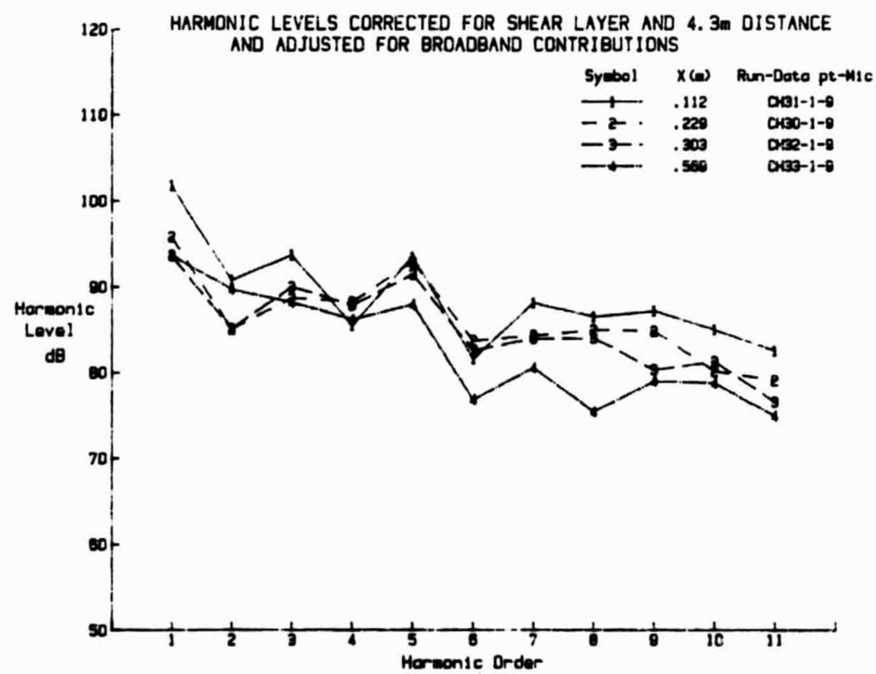

FIGURE 95. INFLUENCE OF EMPENNAGE/PROPELLER AXIAL SEPARATION DISTANCE ON HARMONIC SOUND PRESSURE LEVELS WITH EMPENNAGE INCIDENCE 5°, MICROPHONES 8 AND 9 (Y-TAIL, 8200 RPM, 62.4 M/S)

6. DISCUSSION

Section 5 has presented a large amount of acoustic data from the wind tunnel tests. These results have to be analyzed further in order to relate the radiated sound pressure levels to the characteristics of the flow field entering the propeller disc. It is not the goal of this report to conduct such an analysis since the evaluation of the aerodynamic field is performed elsewhere. However, the present section will discuss the acoustic test data in terms of results from other investigations and identify some of the problems associated with the prediction of noise from pusher propellers.

6.1 Characteristics of the Radiated Sound Field

The general results of the acoustic measurements can be summarized as follows:

(a) The test data measured at several of the microphone locations show a data variability that is higher than expected. This variability tends to mask some of the data trends, particularly when the parametric changes cause only small changes in sound pressure level at the measurement location.

(b) The presence of the empennage increases the sound pressure levels associated with the harmonics of the blade passage frequencies. The effect is small for harmonics of order 1 to 4 and increases at higher order harmonics.

(c) The influence of the empennage on radiated harmonic sound pressure levels is greatest at locations nearest to the propeller axis and least near to the plane of rotation of the propeller.

(d) The harmonic sound pressure levels generally increase as separation distance between the empennage and propeller decreases. Also, the harmonic sound pressure levels increase when the angle of incidence of the empennage is increased.

The tests reported herein are associated with the operation of a propeller behind a model empennage. A survey of published literature has not identified any other test program that is directly associated with an empennage installation, but there are other investigations which have related application [29-41]. All these investigations are associated with the generation of noise by propeller or rotor interaction with in-flows which are not axisymmetric. They include installation effects for tractor propellers [29-31], rotor-vortex interaction [32,33], response of propellers to gusts [34], propellers in a wake [35-37], effect of propeller angle of attack [38] and counter-rotating propellers [39-41].

The installation effects for tractor propellers and the effect of propeller angle of attack are similar phenomena in that there are no disturbing bodies upstream of the propeller; the general direction of the airflow is inclined to the plane of rotation of the propeller. Studies of a propeller in a wake [35-37] and rotor-vortex interaction [33] are perhaps closest to the present tests in that the flow disturbances were created by an airfoil upstream of the propeller. In the wake experiment [35-37] the airfoil was placed across the entire flow region entering the propeller, and in the rotor-vortex interaction tests the vortex was the tip vortex generated by an airfoil partially inserted into the flow. In the empennage tests reported herein, the spans of the empennage surfaces are greater than the radius of the test propeller. Consequently, any tip vortex would probably miss the propeller disc, except for runs 34-38 when the propeller axis was 76 mm below the empennage centerline. It is possible that the presence of a tip vortex from the dorsal fin of the Y-tail may account for the relatively high sound pressure levels associated with this test configuration, as shown in Figure 70. However, since the dorsal fin was nominally at zero angle of attack, the presence of a vortex will have to be verified by the aerodynamic measurements.

Qualitatively, the results from all the referenced investigations are similar to those of the present study. In terms of spectral components, the situation can be described by the schematic spectrum shown in Figure 96; this figure is based on results of Wright [32]. The low frequency noise associated with steady loading and thickness contributions consists of discrete frequency harmonic components superimposed on a broadband background. Unsteady loads generate harmonic components which are most evident in the mid-frequency range and broadband vortex noise is the contributor to the high frequency range. The magnitude of the unsteady loading noise levels depends on the characteristics of the flow entering the propeller disc and on the measurement location. Results of Trebble, et al [29], indicate that, for their particular test configuration, steady loading noise dominated at harmonic orders $m = 1$ and 2, thickness noise at $m = 3$ and 4, and unsteady loading noise at harmonics $m \geq 5$. In this particular test the inflow disturbances were not particularly large. Schlinker and Amiet [33] showed that, for their rotor-vortex interaction test, the unsteady loading noise dominated for harmonics of order $m \geq 4$.

The actual frequency range in which unsteady loading noise dominates will depend to some extent on the location of the observer. Unsteady loading noise has a dipole directivity pattern with a minimum in the plane of the propeller blade (which is different from the plane of rotation of the propeller because of the pitch of the blade). In contrast, thickness noise has a maximum in the plane of rotation of the propeller and steady loading noise has a maximum near to the plane of rotation.

These general directivity characteristics in the axial direction can be observed in the present test data plotted in Figures 77

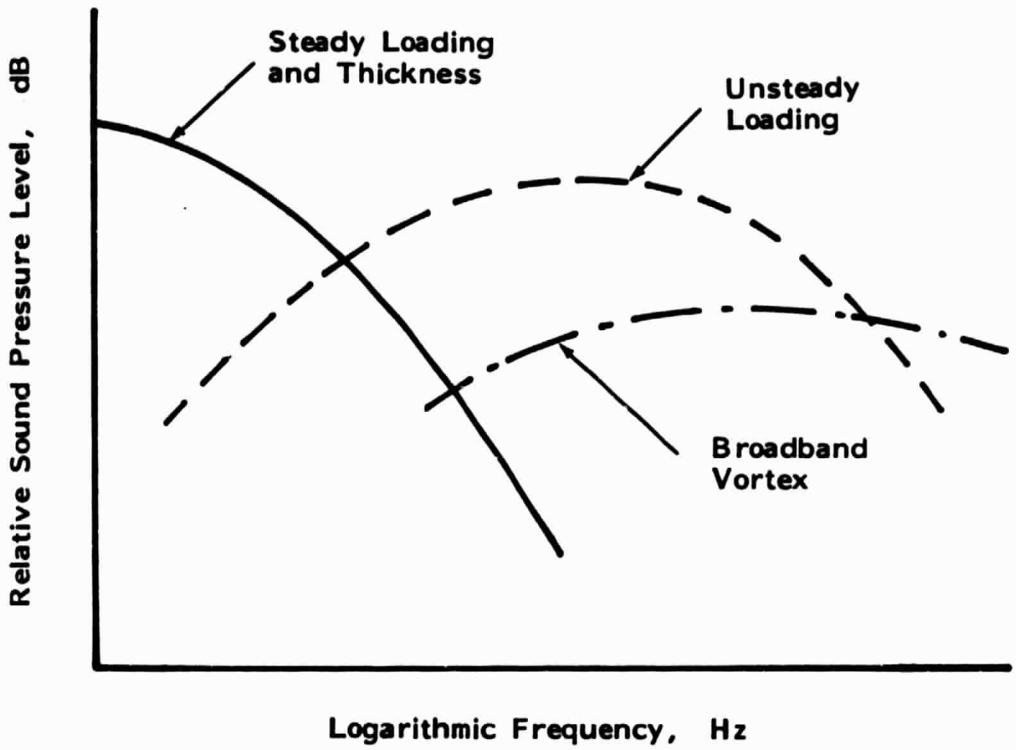

FIGURE 96. SCHEMATIC SPECTRUM SHOWING FREQUENCY REGIMES ASSOCIATED WITH DIFFERENT COMPONENTS OF PROPELLER NOISE

through 88. When there is no fuselage or empennage upstream of the propeller, the measured harmonic sound pressure levels have maximum values in the neighborhood of the propeller plane of rotation (Figure 77). In the case of higher order harmonics, the harmonic sound pressure levels are so low that they cannot be detected above the broadband noise except in the neighborhood of the plane of rotation (Figure 77(b)). When the empennage is introduced the directivity patterns for harmonics of order m = 1 through 4 show small changes due to increases in the sound pressure levels at locations near to the propeller axis. Much larger changes in the directivity patterns occur at higher order harmonics where, because of the dipole directivity with a maximum on the propeller axis, the harmonic sound pressure levels near to the propeller axis show large increases. Figure 80 is a good example of this effect.

The present test data do not show any identifiable directivity pattern in the circumferential direction. Block [37] measured sound pressure levels at three angles relative to the plane of the airfoil, but the three locations were at different angles relative to the plane of rotation of the propeller. Consequently, it is not easy to construct a circumferential directivity pattern in that case.

The magnitude of the unsteady loading noise will depend on the strength of the inflow disturbances. For example, Schlinker and Amiet [33] placed the airfoil generating the vortex at angles of incidence of 0°, 6°, and 12°. At an indicence of 0°, the airfoil caused an axial velocity defect, but there was a zero component for the vortex azimuthal velocity. The data of Schlinker and Amiet show that the sound levels increased when the vortex strength was increased, resulting in a 5 to 10 dB increase in harmonic sound level when the angle of incidence of the airfoil was

was increased from 0° to 12°. Block [32,37] also varied the strength of the inflow disturbance by varying the angle of attack of the essentialy two-dimensional airfoil upstream of the propeller. In that case, the angle of attack of the wake-producing airfoil was either 15° or 20.4° in order to generate a wake which had a thickness of either one or three propeller chords. Only small changes in harmonic sound pressure level were observed when increasing the angle of attack from 15° to 20.4°, although the thicker wake did introduce more lower frequency content into the spectrum. Since the 15° angle was larger than the maximum angle used by Schlinker and Amiet it is possible that it had reached a stage of "diminishing returns".

In the present test the empennage surfaces were at a nominal angle of incidence of zero with the exception of runs 30 through 33 when the fuselage with a Y-tail was inclined at 5° to the tunnel flow. The effect of the change in angle of attack on harmonic sound pressure levels is shown in Figures 71-73 and 94. The most distinct change in harmonic sound pressure level is observed at microphone 9 (Figure 94(b)) where the average increase is 4.8 dB for harmonics of order $m \geq 4$ when the separation distance between empennage and propeller is approximately 11 cm, and 3.2 dB when the separation distance is 30 cm. At other locations, particularly in the neighborhood of the plane of rotation of the propeller, the harmonic sound pressure levels show much smaller increases with angle of incidence. This is to be expected, because of the directivity of the radiated noise due to unsteady loads on the propeller.

6.2 Prediction Procedures--Empirical

Prediction procedures for propeller noise can be divided into near and far-field regimes and, within each regime, into empirical and analytical methods. Most of the procedures are applicable to tractor rather than pusher propellers, because most of past interest has been directed towards the design and operation of aircraft with tractor propellers. As a consequence there is little test data from pusher propellers and little experience in the validity of prediction procedures for pusher propellers.

Consider first, the empirical prediction procedures. Since these are totally dependent on test data from tractor propellers they are applicable to radiation directions close to the plane of rotation of the propellers, since it is in these directions that the maximum sound pressure levels occur. Far-field sound pressure levels are estimated in terms of unweighted or A-weighted sound levels, or Perceived Noise Level. Thus, SAE Aerospace Information Report AIR 1407 [42] calculates first the overall sound pressure level and then converts the result to Perceived Noise Level and A-weighted sound level. (This AIR is currently under revision by SAE). The procedure is in graphical form, but the equivalent equation for the overall sound pressure level is

$$\mathrm{OASPL} = 86.0 + 15.4 \log P - 10 \log \left(\frac{B^2 D^2 r^2}{N}\right) + 38.1\, M_r \qquad (9)$$

where P is the shaft power (kW), N the number of propellers, D the propeller diameter (m), B the number of blades on each propeller, M_r the propeller tip rotational Mach number and r the distance (m) of the observer from the propeller. The equation represents the maximum sideline sound level, irrespective of the angle of radiation.

Other empirical prediction procedures in terms of the A-weighted sound level or A-weighted harmonic sound levels are discussed by Galloway and Wilby [43] and Galloway [44]. For light general aviation aircraft, Galloway initially developed a simple linear regression line whose equation gave the maximum sideline A-weighted sound level L_{am}

$$L_{am} = 146 + 240 \log M_h - 20 \log r \qquad (10)$$

where M_h is the helical Mach number of the blade tip. In later work, this was revised to

$$L_{am} = 129.6 + 10 \log P + 175 \log M_h - 24 \log r \qquad (11)$$

For larger multi-engined aircraft, Galloway and Wilby [43] obtained a relationship

$$L_{am} = 103.2 + 10 \log(NP) + 66 \log M_h - 19.1 \log r \qquad (12)$$

Heller, et al, [45] derived an empirical prediction procedure for maximum unweighted sound levels for each harmonic of the blade passage frequency. The procedure can be written in the form

$$L_m(m) = C_m + 10 \log [M_h^n P^{1.5}] - 20 \log r \qquad (13)$$

where $n = 1.57mB - 1.3$ and C_m is a constant dependent on harmonic order m. Equation (13) is applicable to small, single-engined general aviation aircraft. Galloway and Wilby [43] developed a somewhat similar calculation procedure for the maximum unweighted harmonic sound pressure levels of larger aircraft

$$SPL(m) = C_m + 10 \log(NP) + 70 \log M_h - 20 \log r \qquad (14)$$

Empirical prediction procedures for near field propeller noise [42,46] calculate the unweighted overall and harmonic sound pressure levels. The overall sound pressure level is given as a function of the rotational Mach number of the propeller tip,, but the helical Mach number is used when estimating the relative values of the harmonic sound pressure levels. Comparisons of the two methods [47] suggests that the SAE method [42] is the more accurate procedure for static operation of the propeller, but the method given by Ungar, et al [46], is the more accurate when there is forward motion of the airplane. The SAE method predicts higher sound levels for the higher order harmonics than does the other method and, to that extent, estimates spectral shapes which are more similar to those measured in the empennage tests.

Although the emphasis of the present test is placed on noise radiation from the propeller operating behind an empennage, it is of interest to compared test data for the propeller alone with predicted sound levels. The prediction procedure which is most appropriate is that given in Equation (13). In order to apply this procedure it is necessary to determine values for the tip helical Mach number and power of the propeller. For a propeller rpm of 8200 and a flow speed of 62.5 m/s the tip helical Mach number is 0.77. Measurements of the propeller thrust show a fairly wide variation in values for nominally identical conditions. From the test data an average value of 84.1 N (18.9 lb) has been used for present purposes.

The relationship between thrust T and power P is given by

$$\zeta = TV/P$$

where ζ is the propeller efficiency and V the forward speed of the airplane. Thus, it is necessary to estimate the efficiency. Assuming that the efficiency lies between 0.4 and 0.8, a geometric mean value of 0.57 has been assumed. The resulting estimate for the average power of the propeller is 9.2 kW. This value of the

C-3

power is obviously much lower than the range of values associated with the development of Equation (13).

Finally, it is necessary to determine the appropriate values for C_m in Equation (13). Data of Heller, et al, show C_m varying with harmonic order m and number of blades B, with B having values of 2 or 3; in the present test B = 4. In the absence of other evidence an average value of 105 was assumed for C_m for all m.

The resulting estimated values for the harmonic sound pressure levels associated with 8200 rpm, 62.5 m/s test conditions are plotted in Figure 97 where they are compared with test data for four measurement locations. The agreement is very good considering the uncertainties in the analysis. The largest discrepancy occurs at the fundamental (m = 1) where the measured levels are lower than the predicted value. The reasons for this discrepancy have not been determined, but, since the acoustic treatment in the test chamber will be least effective at the lowest frequency, it is possible that there may be effects due to destructive interference between direct and reflected acoustic signals.

When A-weighted sound levels are computed from the model test data it is necessary to perform frequency scaling prior to the weighting so that equivalent full-scale levels can be obtained. This could be accomplished either from analysis of narrowband (harmonic sound levels) or one-third octave band spectra. In order to maintain the blade tip rotational or helical Mach number constant, frequency scaling should be performed on the basis of propeller diameter.

Use of the harmonic sound pressure levels in the calculation of A-weighted sound levels has the advantage that any concern that the broadband sound levels are not associated with the propeller

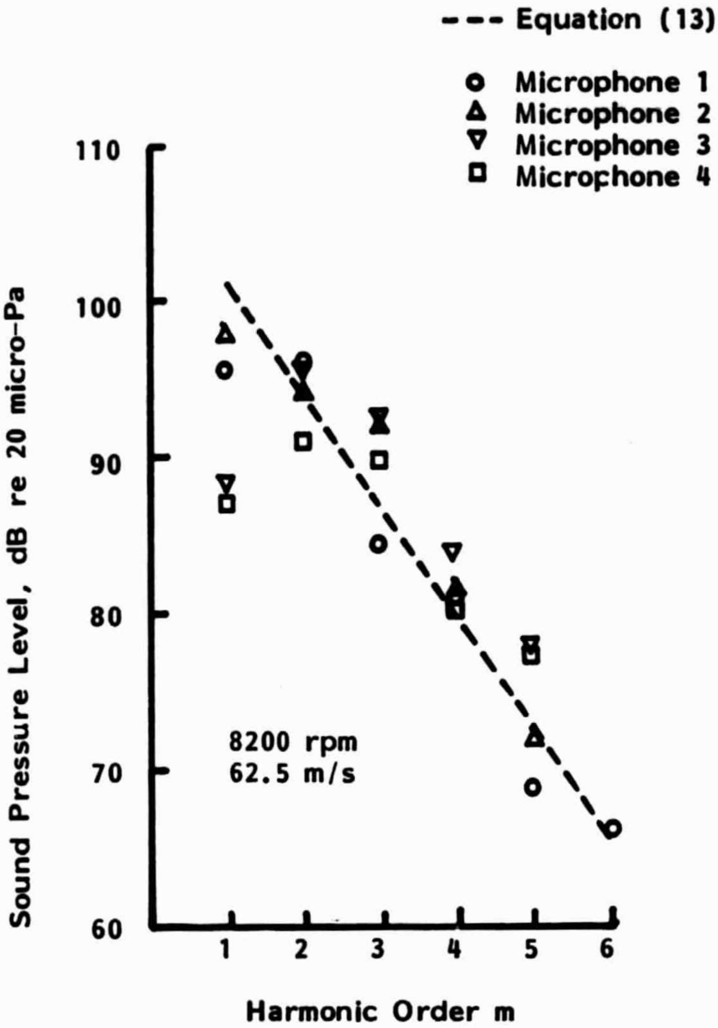

FIGURE 97. COMPARISON OF MEASURED AND PREDICTED SOUND PRESSURE LEVELS FOR PROPELLER OPERATING ALONE

can be overcome. Furthermore, it is often found that flyover noise levels of general aviation aircraft are dominated by propeller tones. Broadband noise can be included separately so that the relative contributions can be identified.

Since the empirical methods are all based on tractor propeller data they are of little use for a propeller in the wake of an empennage. It is possible that ad hoc adjustments could be incorporated, but it is not an appropriate approach for the present investigation. The alternative is to consider available analytical methods which have been developed in recent years.

6.3 Prediction Procedures--Analytical

Early analytical studies of propeller noise were restricted to uniform inflow conditions, but, more recently, attention has been directed towards effects such as inflow turbulence, wakes and counter-rotating propellers. It is this later work which is of specific interest to the present study. In this section attention will be drawn to some of the published analytical studies. However, it is not possible to use the results of the studies to predict radiated sound levels for the test propeller without having information about the wakes behind the empennage.

Current analytical models are based on the acoustic analogy developed by Lighthill and Ffowcs Williams. The models can be divided into two groups, one of which utilizes the time domain and the other the frequency domain. The time domain approach is the more common method and has the advantage that it does not involve transcendental functions, but it does require the use of high-speed computers to perform the required numerical differentiation and integration. Also it has the disadvantage that it is difficult to establish the relative importance of different parameters without performing extensive calculations involving parametric variations. Frequency domain analysis with its closed-form representations allows direct evaluation of the role played by different parameters. However, it has the disadvantage that the functions involved in the representations can become extremely complicated when the inflow is distorted. The time domain approach has been used by Farassat [48-51], Succi [50-51], and Woan and Gregorek [53]. The frequency approach used by Hanson [41,54,55] presents closed form results which demonstrate the roles of blade geometry and operating conditions. The frequency domain approach gives the harmonic sound pressure levels directly; the time domain approach gives harmonic sound levels after Fourier transformation.

The particular condition applicable to the present tests of a propeller operating in the wake of an empennage is that of a fixed distortion of the inflow (in contrast to a rotating distortion associated, for example, with counter-rotating propellers). Treatment of the fixed distortion case can be found in textbooks [56,57] as well as in published papers. A recent paper by Hanson [41] treats the fixed distortion problem as a special case of the counter-rotating propeller, but it can be addressed directly without considering counter-rotation [55,58].

Depending on the analytical model selected, calculation of the radiated sound pressure levels will require detailed inputs for the aerodynamic inflow and the blade geometry. The procedure for NASA Aircraft Noise Prediction Program (ANOPP), which is based on the work of Farassat, is described by Zorumski [59]. This procedure was used by Block [39]; a computer-generated three-dimensional display of the SR-2 blade used by Block [39] is shown in Figure 98. This is the blade used in the present study.

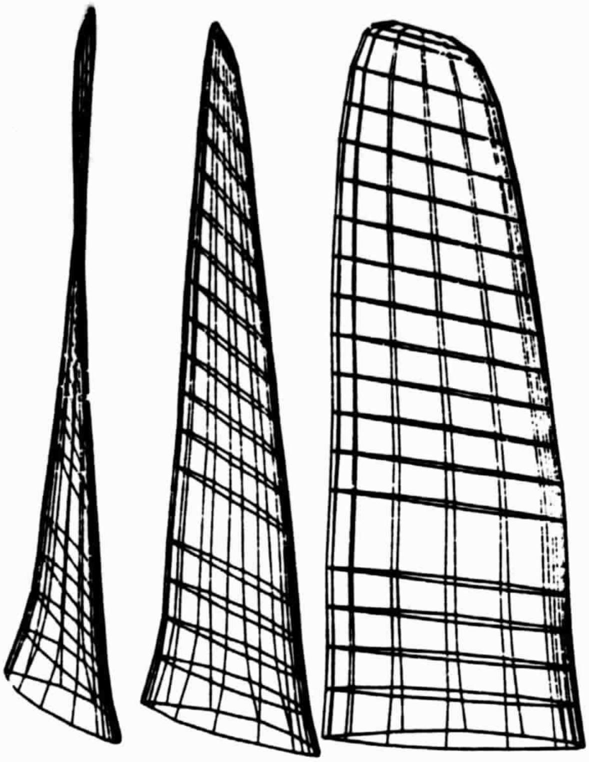

FIGURE 98. COMPUTER-GENERATED THREE-DIMENSIONAL DISPLAY OF SR-2 BLADE [39]

The model for the flow field used by Hanson [41,55] is in the form of a composite source function $g(\gamma,\xi,r)$ where, modifying Hanson's notation slightly [55],

$$g(\gamma,\xi,r) = [\rho_o U \frac{\partial^2}{\partial\gamma^2} h(\gamma,r) + \frac{\partial}{\partial\gamma} D(\gamma,r) + \frac{\partial}{\partial r} F_r(\gamma,r)]\delta(\xi+FA)$$

$$+ \Delta P(\gamma,r)\delta'(\xi+FA) + \frac{\partial^2}{\partial y_i \partial y_j} T_{ij}(\gamma,\xi,r)$$

Here U = relative velocity at source point

h = blade thickness

D = drag force per unit area

F_r = radial force per unit area

ΔP = lift force per unit area

T_{ij} = Lighthill's stress tensor

and (γ,ξ,r) are the helicoidal source point coordinates. If this model is to be used for the present test configuration the measured flow field will have to be decomposed into terms of this type. A similar approach would be required for the time domain approach.

7. CONCLUSIONS

The data presented in this report have been subjected to only a brief evaluation and analysis, but several conclusions can be drawn. Obviously a fairly extensive analysis is required if full benefit is to be obtained from results. This analysis would incorporate aerodynamic data for the flow field entering the propeller disc and would make use of available analytical prediction procedures (either time or frequency domain) in order to compare the test data with theory.

The conclusions drawn from the present evaluation and analysis can be summarized as follows:

(a) Test data measured at several of the microphone locations show a fairly high variability which masks some of the trends associated with parametric changes. The reasons for their variability have not been determined, but may be caused, in part, by propagation through the turbulent shear flow and reflections in the test chamber. It may be possible, by judicious use of averaging techniques, to overcome some of the problems created by the data variability.

(b) Measured sound pressure levels at harmonics of the blade passage frequency are consistent with values predicted on the basis of existing empirical procedures, when the propeller is operated alone in the test section.

(c) The presence of the fuselage and its supports upstream of the propeller caused an increase in the harmonic sound pressure levels generated by the propellers, but the main increase occurred when the empennage was installed.

(d) The influence of the empennage on radiated harmonic sound pressure levels is greatest at locations nearest to the propeller axis and least near to the plane of rotation of the propeller.

(e) The presence of the empennage effects the sound levels of higher order harmonics (m greater than or equal to 4, approximately) more than it does the lower order harmonics.

(f) The harmonic pressure levels generally increase as axial separation distance between the empennage and propeller decreases. Also the harmonic levels increase with angle of incidence of the empennage. An increase in harmonic sound pressure level was observed when the propeller axis was moved below the Y-tail empennage centerline. This may be associated with flow effects from the tip of the ventral fin, but this explanation is only conjectural at this stage.

(g) Increases in propeller rpm resulted in increases in harmonic sound pressure level. The effect was more pronounced when the propeller was operating alone than when it was operating downstream of an empennage.

(h) When the propeller was operated at 8200 rpm, the broadband sound pressure levels at frequencies above about 1000 Hz were generally higher than the tunnel background noise levels. However, there was little or no further increase when the fuselage, with or without an empennage, was introduced upstream of the propeller. Thus, the empennage has only a negligible effect on the measured broadband sound pressure levels.

The present study has concentrated on far-field sound pressure levels with application to airplane flyover noise. However, the data indicate that the main changes in sound pressure level occur at locations close to the propeller axis. Thus, the effect on flyover sound pressure levels should be evaluated in terms of sideline as well as constant radius locations in order to adjust for the greater propagation distances from propeller to ground associated with acoustic radiation angles closer to the propeller axis.

A second factor should also be considered. Since high sound levels radiated by a propeller behind an empennage can propagate forward along the fuselage sidewall, the influence of these sound levels on cabin interior noise should be evaluated.

REFERENCES

1. R. R. Tracy, "The Lear Fan: A Significant Step Toward Fuel Efficient Airplanes," AIAA paper 80-1860 (August 1980).

2. Anon., "Starship 1 and GP-180 Push to the Future," Flight International No. 3886, Vol.124, 1150-1151 (29 October 1983).

3. I. M. Goldsmith, "A Study to Define the Research and Technology Requirements for Advanced Turbo/Propfan Transport Aircraft," NASA CR-166138 (February 1981).

4. R. J. Pegg, B. Magliozzi, F. Farassat, "Some Measured and Calculated Effects of Forward Velocity on Propeller Noise," ASME Paper 77-GT-70 (December 1976).

5. I. J. Sharland, "Sources of Noise in Axial Fans," J. Sound and Vibration 1, 3, 302-322 (July 1964).

6. H. M. Fincher "Fan Noise--The effects of a Single Upstream Stator," J. Sound and Vibration 3, 1, 100-110 (January 1966).

7. C. L. Morfey, "A Review of the Sound Generating Mechanisms in Aircraft-Engine Fans and Compressors," Aerodynamic Noise, H. S. Ribner Editor, pp. 299-329, University of Toronto Press (1969).

8. M. J. T. Smith, M. E. House, "Internally Generated Noise from Gas Turbine Engines: Measurement and Prediction," J. Eng. Power: Trans. ASME (Series A) 89, 177-190 (April 1970).

9. M.V. Lowson, "Reduction of Compressor Noise Radiation," J. Acous. Soc. Amer. 43, 1, 37-50 (January 1968).

10. J. B. Large, J. F. Wilby, E. Grande, A. O. Andersson, "The Development of Engineering Practices in Jet, Compressor and Boundary Layer Noise," Aerodynamic Noise, H. S. Ribner, Editor, University of Toronto Press (1969).

11. R. E. Gorton, discussion following paper by M. J. T. Smith and M. E. House, Ref. 8., J. Eng. Power: Trans ASME (Series A), **89**, 185-186 (April 1970).

12. M. V. Lowson, "Theoretical Studies of Compressor Noise," NASA CR-1287 (March 1969).

13. D. A. Hilton, H. R. Henderson, B. W. Lawton, "Ground Noise Measurements during Static and Flyby Operations of the Cessna 02-T Turbine Powered Airplane," NASA Working Paper LWP-760 (June 1969).

14. D. J. Maglieri, H. H. Hubbard, "Factors Affecting the Noise from Small Propeller Driven Aircraft," SAE Paper 750516 (April 1975).

15. J. F. Wilby, T. D. Scharton, "Evaluation of the NASA Ames #1 7x10-Foot Wind Tunnel as an Acoustic Test Facility," NASA CR-137712 (June 1975).

16. J. H. Dittmar, B. J. Blaha, R. J. Jeracki, "Tone Noise of Three Supersonic Helical Tip Speed Propellers in a Wind Tunnel at 0.8 Mach Number," NASA TM-79046 (December 1978).

17. J. H. Dittmar, R. J. Jeracki, B. J. Blaha, "Tone Noise of Three Supersonic Tip Speed Propellers in a Wind Tunnel," NASA TM-79167 (June 1979).

18. J. H. Dittmar, "A Comparison between an Existing Propeller Noise Theory and Wind Tunnel Data," NASA TM-81519 (May 1980).

19. J. F. Wilby, E. G. Wilby, "A Comparison of Measured Take-Off and Flyover Sound Levels for Several General Aviation Propeller Driven Aircraft," BBN Report 5450 (November 1983).

20. R. K. Amiet, "Correction of Open Jet Wind Tunnel Measurements for Shear Layer Refraction," AIAA Paper 75-532 (March 1975).

21. R. K. Amiet, "Refraction of Sound by a Shear Layer," AIAA Paper 77-54 (January 1977).

22. R. H. Schlinker, R. K. Amiet, "Refraction of Sound by a Shear Layer--Experimental Assessment," AIAA Paper 79-0628 (March 1979).

23. J-F de Bellaval, M. Perulli, S. M. Caudel, A. Julienne, "Analysis of Problems Posed by Simulation of Flight Effects in Anechoic Open Wind Tunnels," AIAA Paper 76-533 (July 1976).

24. C. L. Morfey, B. J. Tester, "Noise Measurement in a Free-Jet, Flight Simulation Facility: Shear Layer Refraction and Facility-to-Flight Corrections," AIAA Paper 76-531 (July 1976).

25. W. M. Herkes, F. G. Strout, R. Ross, "Acoustic Evaluation of DNW Free Jet Shear Layer Correction using a Model Jet," AIAA Paper 83-0757 (April 1983).

26. R. Ross, "Spectral Broadening Effects in Open Wind Tunnels in Relation to Noise Assessment," AIAA Journal 19, 5, 567-572 (May 1981).

27. R. Ross, K. J. Young, R. M. Allen, J. C. A. van Ditshuizen, "Acoustic Wave Propagation through the Shear Layer of the DNW Large Open Jet Wind Tunnel," AIAA Paper 83-0699 (April 1983).

28. A. Guedel, "Scattering of an Acoustic Field by a Free-Jet Shear Layer," AIAA Paper 83-0698 (April 1983).

29. W. J. G. Trebble, J. Williams, R. P. Donnelly, "Comparative Acoustic Wind-Tunnel Measurements and Theoretical Correlations on Subsonic Aircraft Propellers at Full-Scale and Model Scale," Royal Aircraft Establishment (UK) Tech. Memo. Aero 1909 (July 1981). Also AIAA Paper 81-200 (October 1981).

30. H. K. Tanna, R. H. Burrin, H. E. Plumblee, Jr., "Installation Effects on Propeller Noise," J. Aircraft 18, 4, 305 (April 1981).

31. R. H. Burrin, M. Salikuddin, "Sources of Installed Turboprop Noise," AIAA Paper 83-0744 (April 1983).

32. S. E. Wright, "Spectral Trends in Rotor Noise Generation," AIAA Paper 73-1033 (October 1973).

33. R. H. Schlinker, R. K. Amiet, "Rotor-Vortex Interaction Noise," AIAA Paper 83-0720 (April 1983).

34. G. J. Jonkouski, W. C. Horne, P. T. Soderman, "The Acoustic Response of a Propeller Subjected to Gusts Incident from Various Inflow Angles," AIAA Paper 83-0692 (April 1983).

35. P. J. W. Block, R. M. Martin, "Results from Performance and Noise Tests of Model Scale Propellers," SAE Paper 830730 (April 1983).

36. P. J. W. Block, "Noise Generated by a Propeller in a Wake," NASA Technical Memorandum 85794 (May 1984).

37. P. J. W. Block, "Analysis of Noise Measured from a Propeller in a Wake," NASA Technical Paper 2358 (November 1984).

38. S. L. Padula, P. J. W. Block, "Predicted Changes in Advance of Turboprop Noise with Shaft Angle of Attack," AIAA Paper 84-2347 (October 1984).

39. P. J. W. Block, "The Effects of Installation on Single- and Counter-Rotation Propeller Noise," AIAA Paper 84-2263 (October 1984).

40. K. D. Korkan, C. C. Cornell, J. Camba III, "Experimental Study of Noise Generated by Counter-Rotating Propeller Systems," AIAA Paper 84-2264 (October 1985).

41. D. B. Hanson, "Noise of Counter Rotation Propellers," AIAA Paper 84-2305 (October 1985).

42. Anon., "Prediction Procedure for Near Field and Far Field Propeller Noise," SAE Aerospace Information Report AIR 1407 (May 1977, currently under revision).

43. W. J. Galloway, J. F. Wilby, "Noise Abatement Technology Options for Conventional Turboprop Airplanes," FAA-EE-80-19 (1980).

44. W. J. Galloway, "Review of Empirical Procedures for Predicting Sound Levels Produced on the Ground by Propeller-Driven Small Airplanes in Flight," BBN Report 5055 (August 1982).

45. H. H. Heller, M. Kallergis, M. Alswede, W. M. Dobrzynski, "Rotational- and Vortex-Noise of Propellers in the 100-150 kW Class," AIAA Paper 79-0611 (March 1979).

46. E. E. Ungar, J. F. Wilby, D. B. Bliss, "A Guide for Estimation of Aeroacoustic Loads on Flight Vehicle Structures," AFFDL-TR-76-91 Vol 1. (Feburary 1977).

47. C. K. Barton, J. S. Mixson, "Characteristics of Propeller Noise on an Aircraft Fuselage," J. Aircraft 18, 3, 200-205 (March 1981).

48. F. Farassat, T. J. Brown, "A New Capability for Predicting Helicopter Rotor and Propeller Noise including the Effect of Forward Motion," NASA TM X-74037 (June 1977).

49. F. Farassat, "Advanced Theoretical Treatment of Propeller Noise," Von Karman Institute for Fluid Dynamics Lecture Series 1982-08, Propeller Performance and Noise, Belgium (May 1982).

50. F. Farassat, G. P. Succi, "A Review of Propeller Noise Prediction Technology with Emphasis on Two Current Methods for Time Domain Calculations," Journal Sound and Vibration, 71, 3, 399-419 (August 1980).

51. F. Farassat, "Linear Acoustic Formulas for Calculation of Rotating Blade Noise," AIAA Journal, 19, 9, 1122-1130 (September 1981).

52. G. P. Succi, "Design of Quiet Efficient Propellers," SAE Paper 790584 (April 1979).

53. C. J. Woan, G. M. Gregorek, "The Exact Numerical Calculation of Propeller Noise," AIAA Paper 78-1122 (July 1978).

54. D. B. Hanson, "Influence of Propeller Design Parameters on Far-Field Harmonic Noise in Forward Flight," AIAA Journal, 18, 11, 1313-1319 (November 1980). See also AIAA Paper 79-0609 (March 1979).

55. D. B. Hanson, "Compressible Helicoidal Surface Theory for Propeller Aerodynamics and Noise," AIAA Journal 21, 6, 881-889 (June 1983).

56. P. M. Morse, K. U. Ingard, Theoretical Acoustics, McGraw-Hill, New York (1968).

57. M. E. Goldstein, Aeroacoustics, McGraw-Hill, New York (1976). See also NASA SP-346 (1974).

58. J. B. H. M. Schulten, "Aeroacoustics of Wide-Chord Propellers in Non-Axisymmetric Flow," AIAA Paper 84-2304 (October 1984).

59. W. E. Zorumski, "Propeller Noise Prediction," NASA Technical Memorandum 85636 (May 1983).

APPENDIX A

HP87 Computer Programs

This appendix presents listings, sample outputs and brief discussion of computer programs used during reduction of the test data.

A.1 Program SHEARSCALE

The corrected pressures and angles due to the presence of a shear layer are calculated using Amiet's method [20]. These corrections are independent of frequency.

Input required:

Microphone Number
Angle (degrees)
Radial distance (feet) from source to microphone
Distance (Feet) from source to shear layer

The convention for microphone angles is

0° = upstream
90° = port side

Output:

Corrected angle (in degrees)
Shear Layer Correction (dB), to be <u>added</u> to measured pressure spectrum levels

The corrected pressures and angles are entered and stored in the programs GENRAD3 and CEDAR2, for the two Mach numbers used in the current test.

```
10    REM-----------------------------------------------------------------
20    REM PROGRAM "SHEARSCALE" CALCULATES AMIET'S SHEAR LAYER CORRECTIONS
30    REM                          BASED ON AIAA PAPER 75-532
40    REM-----------------------------------------------------------------
50    REM
60    REM  ORIGINALLY WRITTEN BY P.SODERMAN MARCH 1984 FOR HP87
70    REM  CONVERTED TO APPLE III
80    REM
100    OPEN#2 AS OUTPUT,".PRINTER"
110    LF$=CHR$(10):REM LINEFEED
120    FF$=CHR$(12):REM FORMFEED
121    PI=3.14159265
122    DEG=PI/180
123    DX=0.2*DEG
125    B$="4X.2#.6X, 2#.2#.5X, 2#.2#,7X,+3#.2#,6X,+3#.2#,8X,+2#.2#"
130    REM
140    HOME
150    PRINT"START OF PROGRAM"
160    PRINT"UNITS ARE FEET AND DEGREES"
190    PRINT"SHEAR LAYER CORRECTIONS WILL BE CALCULATED FOR POINTS AT GIVEN"
200    PRINT"INPUT RADIAL DISTANCES"
220    PRINT" "
230    INPUT"MACH NUMBER = ";M
240    PRINT" "
242    PRINT" ANGLE CONVENTIONS - UPSTREAM = 0 , PORT SIDE = 90"
244    BETA=(1-M^2)^0.5
250    PRINT#2;FF$
260    PRINT#2;LF$
270    PRINT#2;LF$
280    PRINT#2;"  SHEAR LAYER CORRECTIONS USING AMIET'S METHOD"
310    PRINT#2;" "
320    PRINT#2;"  MACH NUMBER = ";M
330    PRINT#2;" "
340    PRINT#2;"  MIC No   RADIAL   SHEAR LAYER  UNCORRECTED  CORRECTED    SHEA
       R LAYER"
350    PRINT#2;"            DISTANCE   DISTANCE        ANGLE        ANGLE     CORRE
       CTION (dB)"
360    PRINT#2;" "
370    REM INPUT MIC No and ANGLE
380    INPUT"MICROPHONE NUMBER = ";MC
390    INPUT"MICROPHONE ANGLE (in Degrees) = ";THETA
392    INPUT"RADIAL DISTANCE (in feet) = ";R
394    INPUT"SHEAR LAYER DISTANCE (feet) = ";H
400    IF THETA<180 THEN THETAM=180-THETA
410    IF THETA>180 THEN THETAM=THETA-180
420    REM AMIETS CONVENTION FOR ANGLES
425    Y1=R*SIN(THETAM*DEG)
430    REM STARTING POINT IN ITERATION
440    TH=THETAM*DEG
450    IF THETAM<90 THEN TH=(THETAM+20)*DEG
460    PRINT"THETA";TH
470    ZETA=((1-M*COS(TH))^2-(COS(TH))^2)^0.5
480    PRINT"ZETA";ZETA
490    PRIME=ZETA/(BETA^2*COS(TH)+M)
500    THETAP=ATN(PRIME)
510    IF PRIME<0 THEN THETAP=THETAP+PI
520    COAT=(Y1/TAN(THETAM*DEG)-H/TAN(THETAP))/(Y1-H)
530    THETA2=ATN(1/COAT)
540    IF(1/COAT)<0 THEN THETA2=THETA2+PI
550    DIFF=TH-THETA2
560    PRINT"DIFF ";DIFF;"  THETAP ";THETAP;"  COAT ";COAT;"  THETA2 ";THETA2
570    PRINT" "
580    IF DIFF<-DX OR DIFF>DX THEN TH=TH-DIFF/2
590    IF DIFF<-DX OR DIFF>DX THEN GOTO 460
```

```
600   P1=(SIN(TH)+ZETA*(Y1/H-1))^0.5*H/(R*ZETA^2*SIN(TH))
610   P2=(SIN(TH)^3+(Y1/H-1)*ZETA^3)^0.5
620   P3=(M^2*(1-M*COS(TH))^2+(1-M^2*(COS(TH))^2))^.5/(2.0*SIN(TH))
630   P4=ZETA+SIN(TH)*(1-M*COS(TH))^2
640   PBPM=P1*P2*P3*P4
650   DELDB=20*LOG(PBPM)/LOG(10)
660   IF THETA<180 THEN THETAP=180-THETAP/DEG
670   IF THETA>180 THEN THETAP=180+THETAP/DEG
680   REM
690   PRINT#2 USING B$;MC,R,H,THETA,THETAP,DELDB
700   INPUT" ANY MORE MICS? (Y/N) ";A$
710   IF A$="Y" THEN GOTO 370
712   INPUT" ANY MORE MACH NUMBERS ? (Y/N)";C$
714   IF C$="Y" THEN GOTO 230
720   PRINT" END OF PROGRAM"
730   STOP
```


SHEAR LAYER CORRECTIONS USING AMIET'S METHOD

MACH NUMBER = .134

MIC No	RADIAL DISTANCE	SHEAR LAYER DISTANCE	UNCORRECTED ANGLE	CORRECTED ANGLE	SHEAR LAYER CORRECTION (dB)
1	14.00	5.00	+ 60.00	+ 65.93	+ 0.81
2	14.00	5.00	+ 70.00	+ 75.53	+ 0.59
3	14.00	5.00	+ 80.00	+ 85.21	+ 0.37
4	14.00	5.00	+ 90.00	+ 94.97	+ 0.13
5	14.00	5.00	+105.00	+109.70	- 0.22
6	14.00	5.00	+120.00	+124.61	- 0.52
10	7.92	5.00	+290.00	+286.91	+ 0.46
11	14.00	4.04	+ 90.00	+ 95.52	+ 0.12
12	14.00	5.77	+ 90.00	+ 94.60	+ 0.13
13	7.58	5.00	+270.00	+267.33	+ 0.13

SHEAR LAYER CORRECTIONS USING AMIET'S METHOD

MACH NUMBER = .183

MIC No	RADIAL DISTANCE	SHEAR LAYER DISTANCE	UNCORRECTED ANGLE	CORRECTED ANGLE	SHEAR LAYER CORRECTION (dB)
1	14.00	5.00	+ 60.00	+ 68.48	+ 1.19
2	14.00	5.00	+ 70.00	+ 77.79	+ 0.89
3	14.00	5.00	+ 80.00	+ 87.23	+ 0.57
4	14.00	5.00	+ 90.00	+ 96.80	+ 0.25
5	14.00	5.00	+105.00	+111.21	- 0.24
6	14.00	5.00	+120.00	+126.06	- 0.64
10	7.92	5.00	+290.00	+285.62	+ 0.71
11	14.00	4.04	+ 90.00	+ 97.53	+ 0.23
12	14.00	5.77	+ 90.00	+ 96.30	+ 0.25
13	7.58	5.00	+270.00	+266.33	+ 0.25

A.2 Program GENRAD3

A flow chart for program GENRAD3 is given in Figure A.1. The one-third octave band average pressure spectrum is formed on the GR1995 and transferred to the HP87 by the program. There is an option for the spectrum levels to be corrected for shear layer and normalized to a distance of 4.3m (14 feet). The correction data is stored for Mach numbers 0, 0.13 and 0.18 only. The spectra may be stored on disc, either in uncorrected or corrected form, for future retrieval.

Since the model is not full scale, an A-weighted spectrum level calculated directly from the model measurements will have no meaning full scale. Thus, a scale factor is input, representing the fullscale/model size ratio, which must be in the range 1 to 10. This is used to shift the spectrum <u>down</u> in frequency for the calculation of the scaled A-level. For example, a scale factor of 2 shifts the spectrum down by 3 one-third octave bands.

Input required:

- Scale factor (in the range 1 to 10)
- Run Number
- Data Point
- Microphone Number
- Microphone Gain, relative to calibration signal
- Wind speed (ft/sec)

Outputs (as selected):

- Plot of spectrum
- Listing of spectrum, overall SPL, A-level and scaled A-level
- Spectra stored on disk using the file names
  - Uncorrected: RT Run No - Data Pt - Mic. No.
  - Corrected: CT Run No - Data Pt - Mic No.

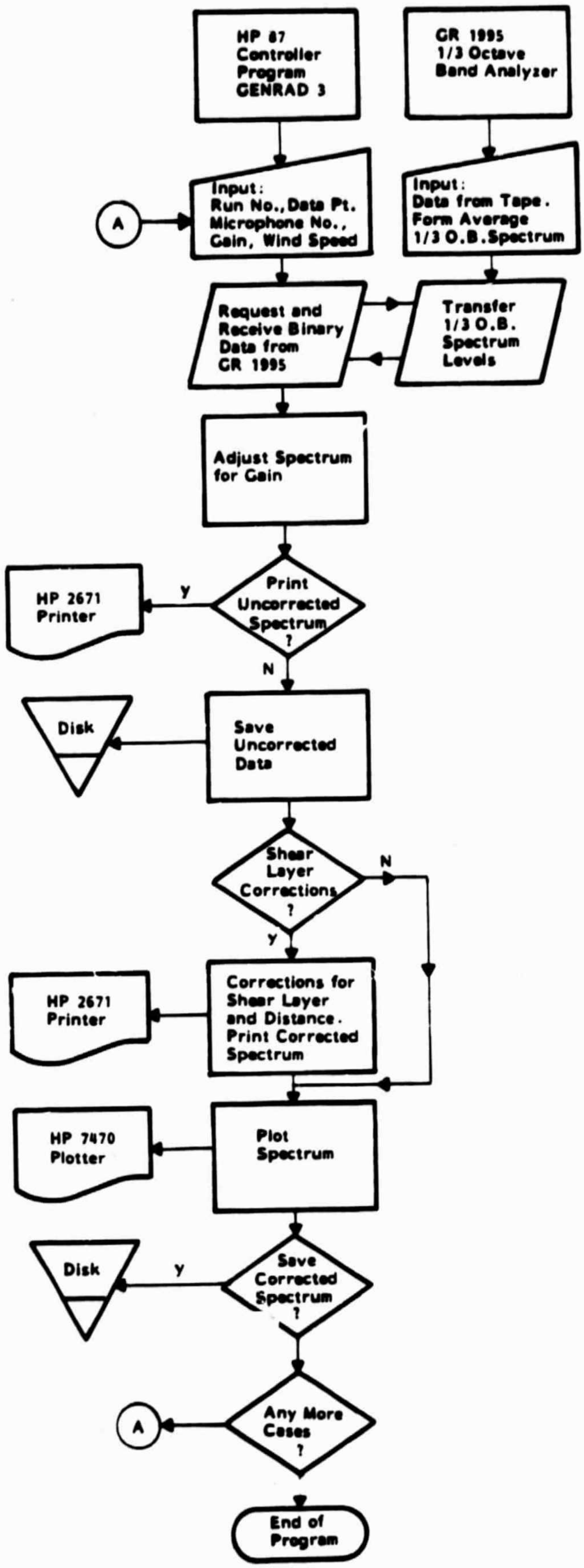

FIGURE A.1 FLOW CHART FOR PROGRAM GENDRAD 3

```
10      !    "GENRAD3" TAKES DATA FROM THE GR 1995 1/3-OCTAVE BAND ANALYZER
20      !    AND TABULATES, GRAPHS AND STORES IT ON DISC DRIVE D701.
30      !    THIS VERSION IS TO BE USED FOR THE PUSHER-PROP TEST IN 7X10.
40      !    DATA CAN BE CORRECTED DIRECTLY.
50      !
60      !    HP87 VERSION
70      !
80      !    PAUL SODERMAN -LISA LEE 6/8/84
90      !
100      PRINTER IS 1
110      OPTION BASE 1
120      DIM T(670),Band(33),Level(33),Freq(30),C(30)
130      DIM Micno(13),Q(4),Speed(4),Refdist(4),Cangle(13,4),Corr(13,4)
140      DIM Dist(13),Shift(11),Factor(11),Aweight(33)
150      DIM A$[668]
160     DATA 1,2,3,4,5,6,7,8,9,10,11,12,13
170     ! AT MICROPHONE RADIAL DISTANCES
180     DATA 14,14,14,14,14,14,4.5,4.5,8,7.92,14,14,7.58
190     ! CORRECTIONS FOR Q=0,U=0,NO DISTANCE CORRECTION
200     !  UNCORRECTED ANGLES AND ZERO CORRECTIONS
210     DATA 0,0,0
220     DATA 60,70,80,90,105,120,105,140,15,290,90,90,270
230     DATA 0,0,0,0,0,0,0,0,0,0,0,0,0
240     ! CORRECTIONS FOR Q=0,U=0,REF DISTANCE=14 feet
250     !  UNCORRECTED ANGLES AND DISTANCE CORRECTIONS ONLY
260     DATA 0,0,14
270     DATA 60,70,80,90,105,120,105,140,15,290,90,90,270
280     DATA 0,0,0,0,0,0,-9.9,-9.9,-4.9,-4.9,0,0,-5.3
290     ! CORRECTIONS FOR Q=27,U=150,REF DISTANCE=14 feet
300     !  CORRECTED ANGLES AND SHEAR/DISTANCE CORRECTIONS
310     DATA 27,150,14
320     DATA 65.9,75.5,85.2,95,109.7,124.6,105,140,15,286.9,95.5,94.6,267.3
330     DATA .8,.6,.4,.1,-.2,-.5,-9.9,-9.9,-4.9,-4.4,.1,.1,-5.2
340     ! CORRECTIONS FOR Q=50,U=205,REF DISTANCE=14 feet
350     !  CORRECTED ANGLES AND SHEAR/DISTANCE CORRECTIONS
360     DATA 50,205,14
370     DATA 68.5,77.8,87.2,96.8,111.2,126.1,105,140,15,285.6,97.5,96.3,266.3
380     DATA 1.2,.9,.6,.2,-.2,-.6,-9.9,-9.9,-4.9,-4.2,.2,.2,-5.1
390     ! THESE CORRECTIONS MUST BE ADDED TO THE SPECTRUM LEVELS
400     !
410     !   FREQUENCY DATA FOR BANDS
420     !
430     DATA 25,31.5,40,50,63,80,100,125,160,200,250,315,400,500,630,800,1000
440     DATA 1250,1600,2000,2500,3150,4000,5000,6300,8000,1000,12500,16000,20000
441     !
442     ! DATA FOR SCALE FACTOR SHIFT IN A-WEIGHTING
443     DATA 0,1,2,3,4,5,6,7,8,9,10
444     DATA 1,1118,1.4086,1.7819,2.2361,2.8169,3.5638,4.4723,5.5897,7.0721,8.9445,
11.186
445     ! A-Weightings for 16 Hz to 20 Hz (33 Values)
446     DATA -64,-56.7,-50.5,-44.7,-39.4,-34.6,-30.2,-26.2,-22.5,-19.1,-16.1
447     DATA -13.4,-10.9,-8.6,-6.6,-4.8,-3.2,-1.9,-.8,0,.6,1,1.2,1.3,1.2
448     DATA 1,.5,-.1,-1.1,-2.5,-4.3,-6.6,-9.3
450     !
460     FOR I=1 TO 13
470     READ Micno(I)
480     NEXT I
490     FOR I=1 TO 13
500     READ Dist(I)
510     NEXT I
520     FOR J=1 TO 4
530     READ Q(J),Speed(J),Redist(J)
540     FOR I=1 TO 13
550     READ Cangle(I,J)
560     NEXT I
```

```
570    FOR I=1 TO 13
580    READ Corr(I,J)
590    NEXT I
600    NEXT J
610    FOR I=1 TO 30
620    READ Freq(I)
630    NEXT I
631 FOR I=1 TO 11
632 READ Shift(I)
633 NEXT I
634 FOR I=1 TO 11
635 READ Factor(I)
636 NEXT I
637 FOR I=1 TO 23
638 READ Aweight(I)
639 NEXT I
640    RESTORE
650    !
660    !   USER INPUTS
670    !
680    CLEAR
689 DISP " "
690    LINPUT "INPUT DATE",Jour$
691    DISP " "
692 DISP " INPUT SCALE FACTOR TO BE USED FOR SCALED A-LEVEL"
693 DISP " Factor should be in the Range 1 to 10"
694 INPUT ScaleF
695 Tobshift=0
696 FOR I=1 TO 11
697 IF ScaleF>Factor(I) THEN GOTO 700
698 Tobshift=Shift(I)
699 GOTO 710
700 NEXT I
701 IF ScaleF>Factor(11) THEN Tobshift=10
710    PRINT "SET UP AND INTEGRATE SIGNAL INTO THE GENRAD"
720    DISP " "
730    DISP " "
740    DISP "INPUT RUN NUMBER"
750    INPUT Rn
760    DISP " "
770    DISP "INPUT DATA POINT"
780    INPUT Dp
790    DISP " "
800    DISP "INPUT MIC NUMBER"
810    INPUT Mic
820    DISP " "
830    DISP "INPUT MIC GAIN RELATIVE TO CALIBRATION"
840    INPUT Gain
850    DISP " "
860    DISP "INPUT WIND SPEED (f/s)"
870    INPUT U
880    DISP " "
890    Flog=0
900    DISP "TRANSFERE IS STARTING"
980    RESET 7
990    !
1000    !   THIS COMMAND TELLS THE GR TO SEND THE BINARY DATA
1010    !
1020    OUTPUT 720 USING "#,K" : "L5"
1030    SEND 7 : MTA MLA UNT TALK 20
1040    !
1050    !   THIS COMMAND ENTERS THE DATA INTO THE T ARRAY AS DECIMAL NUMBERS
1060    !
1070    FOR I=1 TO 33
1080    ENTER 7 USING "#,#B" : T(I)
1090    NEXT I
```

```
1100    RESET 7
1110    DISP "TRANSFER IS FINISHED"
1120    !
1130    !   COMPUTE AND LIST THE dB LEVELS
1140    !
1150    FOR I=1 TO 33
1160     Level(I)=T(I)/4+T(1)/2-Gain ! FOR L5 BINARY TRANSFER
1170     Band(I)=I+10
1180     NEXT I
1190     Overalla$="A"
1200     Overallf$="F"
1210     Oa=T(2)/4+T(1)/2-Gain
1220     Of=T(3)/4+T(1)/2-Gain
1230     Bottom=T(1)/2+3.5-Gain
1231 Temp=0
1232 FOR I=4 TO 33
1233 K=I-Topshift
1234 IF K<1 THEN GOTO 1237
1235 Ax=10^((Level(I)+Aweight(K))/10)
1236 Temp=Temp+Ax
1237 NEXT I
1238 Ascaled=10*LGT (Temp)
1240     DISP " "
1249     GOTO 1595
1250     LINPUT "DO YOU WISH TO PRINT THE RAW DATA ON THE PRINTER ?",Qp$
1260     IF Qp$="N" THEN GOTO 1600
1270     PRINTER IS 708
1280     PRINT " "
1290     IF Flog=1 THEN GOTO 1340
1300     PRINT "             1/3-OCTAVE BAND RAW DATA       TEST 706"
1310     PRINT " "
1320     PRINT "             RUN":Rn:"   DATA POINT ":Dp:"    MIC":Mic
1330     GOTO 1370
1340     PRINT "             1/3 OCTAVE BAND CORRECTED DATA         TEST 706"
1350     PRINT " "
1360     PRINT "             RUN":Rn:"   DATA POINT ":Dp:"    MIC":Mic:
1370     PRINT "                                      GAIN":Gain
1380     PRINT " "
1390     PRINT "             ",Jour$,"           GENRAD PROGRAM"
1400     PRINT " "
1410     PRINT "             BAND NUMBER      FREQUENCY, Hz           Lp, dB  "
1420     PRINT "             ------------------------------------------------------"

1430     IMAGE 14X,AA,34X,DDD.D
1440     PRINT USING 1430 : Overalla$,Oa
1450     PRINT USING 1430 : Overallf$,Of
1460     IMAGE 14X,DD,12X,DDDDD,17X,DDD.D
1470     FOR I=1 TO 30
1480          PRINT USING 1460 : Band(I+3),Freq(I),Level(I+3)
1490    NEXT I
1500    PRINT " "
1501 Ascaled=IP (Ascaled*10)
1502 Ascaled=Ascaled/10
1510    PRINT "            MINIMUM LEVEL ON GP SCREEN WAS ":Bottom:" dB"
1511 PRINT " "
1512 PRINT "           SCALE FACTOR =":ScaleF:" SHIFTS THE SPECTRUM DOWN"
1513 PRINT "           BY":Topshift:" 1/3 OCTAVE BANDS FOR THE SCALED A-LEVEL ONLY
"
1514 PRINT " "
1515 PRINT "           SCALED A-LEVEL = ":Ascaled:" dBA"
1520    PRINT CHR$ (12)
1530    PRINTER IS 1
1540    DISP " "
1550    DISP " "
1560    DISP " ADVANCE FORM FEED ON PRINTER WHEN FINISHED PRINTING"
1570    DISP " "
1580    DISP " "
```

```
1590   IF Flog=1 THEN GOTO 1920
1595   GOTO 1670
1600   PRINT "RAW DATA ARE BEING SAVED IN FILE RT-RUN-POINT-MIC"
1610   DISP " "
1612  File$="RT"&VAL$ (Rn)&"-"&VAL$ (Dp)&"-"&VAL$ (Mic)
1614 MASS STORAGE IS ":D701"
1616 CREATE File$,3
1618 ASSIGN# 1 TO  File$
1620   PRINT# 1 : Overalla$,Oa,Overallf$,Of,0
1621 Level(1)=Ascaled
1630   FOR I=1 TO 33
1640   PRINT# 1 : Band(I),Level(I)
1650   NEXT I
1660   ASSIGN# 1 TO  *
1670 !
1671   LINPUT "DO YOU WANT TO CORRECT THE DATA FOR SHEAR LAYER EFFECTS ?",A1$
1680   IF A1$="N" THEN GOTO 1920
1690  IM=0
1700  FOR I=1 TO 13
1710  IF Mic<> Micno(I) THEN GOTO 1740
1720  IM=I
1730  GOTO 1750
1740 NEXT I
1750  Theta=Cangle(IM,1)
1760  Thetac=Theta
1770   Flog=1
1780 IU=0
1790 FOR I=2 TO 4
1800 IF U<> Speed(I) THEN GOTO 1820
1810 IU=I
1820 NEXT I
1830 Thetac=Cangle(IM,IU)
1840 FOR I=1 TO 33
1850  C(1)=Corr(IM,IU)
1860  Level(I)=Level(I)+C(1)
1870  NEXT I
1871 Ascaled=Ascaled+C(1)
1881  Oa=Oa+C(1)
1882  Of=Of+C(1)
1883   GOTO 1270
1890  !
1900  ! PLOTTER
1910  !
1920  !
1921  PLOTTER IS 705
1930  GRAPHICS
1940  LIMIT 20,200,20,185
1950  LOCATE 20,100,20,87
1960  !
1970  ! LABEL THE PLOT
1980  !
1990  CSIZE 3.7
2000  LORG 5
2010  MOVE 70,99
2020  LABEL USING "K" : "PUSHER PROP DATA        TEST 706    ",Jour$
2030  MOVE 64,94
2040  IF Flog=1 THEN GOTO 2080
2050  LABEL USING "K" : "RAW 1/3-OCTAVE BAND SPECTRUM FROM 'GENRAD'"
2060  MOVE 64,94
2070  GOTO 2090
2080  LABEL USING "K" : "CORRECTED 1/3-OCTAVE BAND SPECTRUM FROM 'GENRAD' "
2090  MOVE 68,89
2100  LABEL USING "K,X,K,X" : "RUN ":Rn:"   DATA POINT ":Dp:"     MIC":Mic:"
GAIN ":Gain
2110  LORG 1
2120  CSIZE 3.4
2130  SCALE 0,30,60,120
2140  AXES 0,10,0,60,0,1
```

```
2150  !
2160  ! LABEL THE AXES OF THE PLOT
2170  !
2180  ! Y AXIS
2190  !
2200  FOR I=60 TO 120 STEP 10
2210      MOVE -2.I-1
2220      LABEL USING "K.X" : I
2230  NEXT I
2240  MOVE -5.8.85
2250  LABEL USING "K" : "Lp. dB"
2260  !
2270  !  X AXIS
2280  !
2290  CSIZE 3.2
2300  MOVE 4.57
2310  FOR I=3 TO 30 STEP 3
2320       MOVE I-1.57
2330       LABEL USING "K.X" : Freq(I)
2340  NEXT I
2350  CSIZE 3.4
2360  MOVE 10.51
2370  LABEL USING "K" : "1/3 O.B. FREQUENCY. HZ"
2380  !
2390  ! GRAPH THE SPL'S
2400  !
2410   FOR I=1 TO 30
2420      IF Level(I+3)<60 THEN GOTO 2450
2430      CLIP I-1.I.60.Level(I+3)
2440      FRAME
2450   NEXT I
2460  UNCLIP
2470  MOVE 2.5.60
2480  DRAW 2.5.60.5
2490  FOR I=1 TO 9 ! PUT TICKS ON X AXIS
2500  MOVE 2.5+I*3.60
2510  DRAW 2.5+I*3.60.5
2520  NEXT I
2530  PEN UP
2540  ALPHA
2550  PRINTER IS 1
2560  DISP " "
2570  IF Flag=0 THEN GOTO 2700
2580  LINPUT "DO YOU WANT TO SAVE THE CORRECTED DATA IN A FILE ?(Y/N)".A2$
2590  IF A2$="N" THEN GOTO 2700
2600  MASS STORAGE IS ":D701"
2602  Qfile$="CT"&VAL$ (Rn)&"-"&VAL$ (Dp)&"-"&VAL$ (Mic)
2604  CREATE Qfile$.3
2605  ASSIGN# 3 TO  Qfile$
2610  DISP " "
2620  PRINT "CORRECTED FILE IS BEING SAVED ON D701 AS":Qfile$
2630  PRINT "(A-WEIGHT AND OVERALL LEVELS ARE CORRECTED)"
2640  PRINT " "
2650  PRINT# 3 : Overalla$.Oa.Overallf$.Of.U
2651 Level(1)=Ascaled
2660  FOR I=1 TO 33
2670  PRINT# 3 : Band(I).Level(I)
2680  NEXT I
2690  ASSIGN# 3 TO  *
2700  LINPUT "ANY MORE MICS ?".Q1$
2710  DISP " "
2720  IF Q1$="Y" THEN GOTO 710
2730  MASS STORAGE IS ":D700"
2740  REMOTE 720
2750  RESET 7
2760  PRINT "PROGRAM END"
2770   END
```

PUSHER PROP DATA TEST 706 3/26/84

CORRECTED 1/3-OCTAVE BAND SPECTRUM FROM 'GENRAD' T2052

RUN 7 DATA POINT 1 MIC 2 GAIN 20

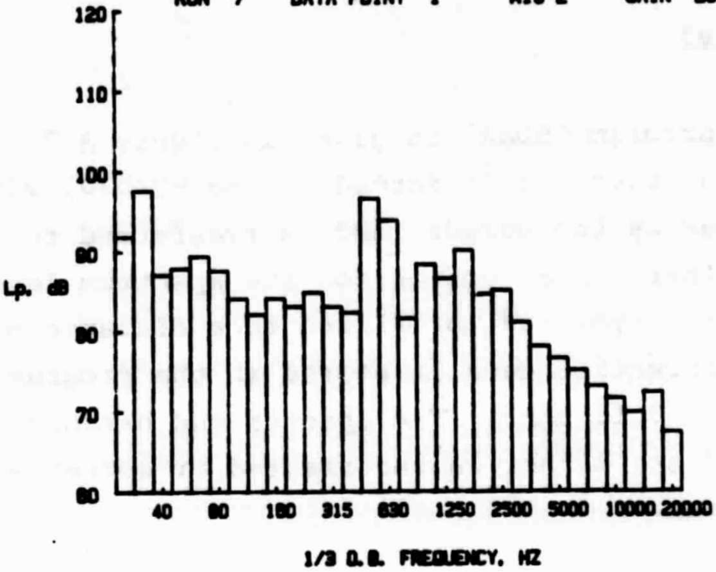

1/3 OCTAVE BAND CORRECTED DATA TEST 706

RUN 7 DATA POINT 1 MIC 2
GAIN 20

4/17/84 GENRAD PROGRAM

BAND NUMBER	FREQUENCY, Hz	Lp, dB
A		101.7
F		107.7
14	25	93.7
15	32	99.4
16	40	88.9
17	50	89.7
18	63	91.2
19	80	89.4
20	100	85.9
21	125	83.9
22	160	85.9
23	200	84.5
24	250	86.7
25	315	84.5
26	400	84.2
27	500	98.4
28	630	95.7
29	800	83.4
30	1000	90.2
31	1250	88.4
32	1600	91.9
33	2000	86.4
34	2500	86.9
35	3150	82.5
36	4000	79.9
37	5000	78.4
38	6300	76.9
39	8000	74.9
40	1000	73.4
41	12500	71.7
42	16000	74.2
43	20000	69.2

MINIMUM LEVEL ON GR SCREEN WAS 70 dB

SCALE FACTOR = 2 SHIFTS THE SPECTRUM DOWN
BY 3 1/3 OCTAVE BANDS FOR THE SCALED A-LEVEL ONLY

SCALED A-LEVEL = 97.6 dBA

A.3 Program CEDAR2

A flow chart for program CEDAR2 is given in Figure A.2. The averaged narrowband spectrum is formed on the HP4520, with the harmonics indicated by the cursor, and is tranferred to the HP87 by the program. There is an option for the spectrum levels to be corrected for shear layer and normalized to a distance of 4.3 m (14 feet). The correction data is stored in the program for Mach numbers 0, 0.13 and 0.18 only. The spectra and harmonic levels may be stored on disk, either in uncorrected or corrected form, for future retrieval.

Input required:

Run Number
Data Point
Microphone Number
Microphone Gain, relative to calibration signal
Wind Speed (ft/sec)
Propeller rpm
Propeller angle, β (degrees)
Separation distance, X(inches), between propeller and empennage

Output (as selected):

Plot of spectrum
Listing of harmonic frequencies and levels
Spectra and harmonics stored on disk using the file names
Uncorrected: RH Run No - Data Pt - Mic No
Corrected: CH Run No - Data Pt - Mic No

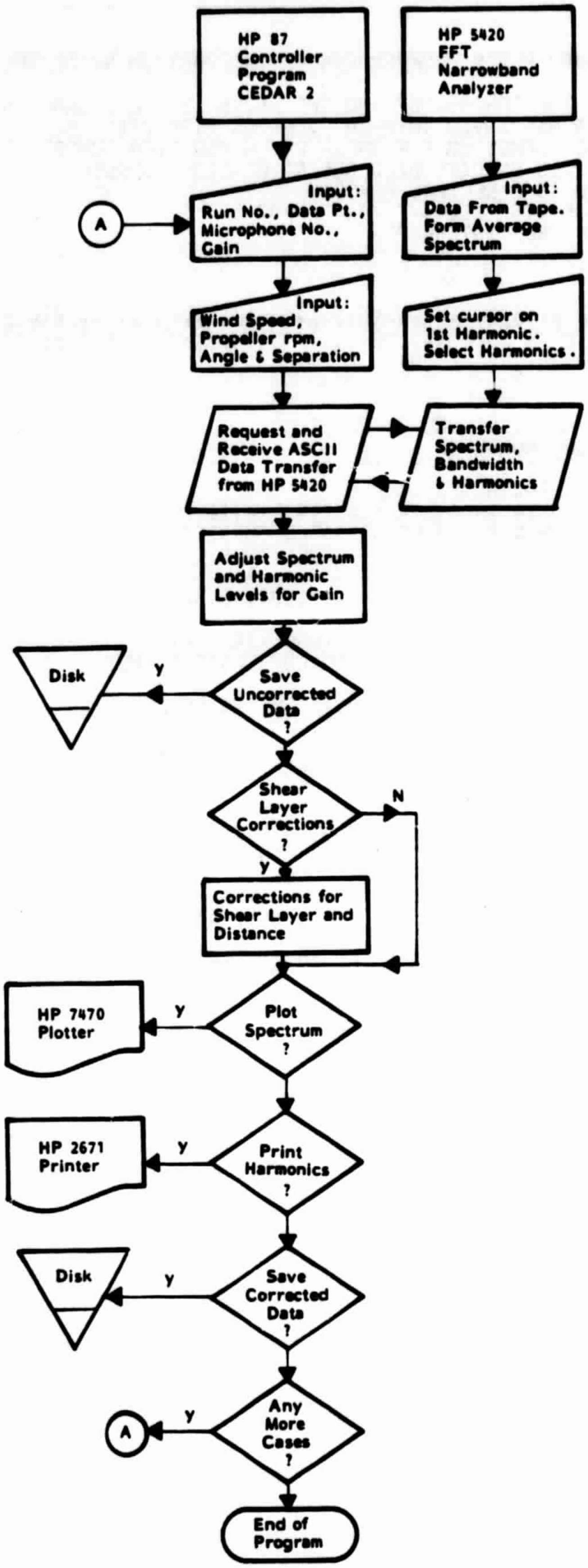

FIGURE A.2 FLOW CHART FOR PROGRAM CEDAR 2

```
10   ! PROGRAM CEDAR2 PLOTS PROP/EMPENNAGE INTERACTION NOISE SPECTRA
20   !
30   ! THE HP87 IS THE CONTROLLER AND THE 5420B IS THE SIGNAL ANALYZER
40   ! THE RAW DATA ARE SAVED IN DATA FILES ON DISC D701
50   ! THE DATA ARE CORRECTED FOR SHEAR LAYER MODIFICATION OF LEVEL AND ANGLE
60   ! FROM DATA FILES ON DISC D700 GENERATED FROM 'SPRUCE'
70   ! ROUNDS OFF U TO 2 DECIMAL PLACES
80   ! PAUL SODERMAN-LISA LEE 4/17/84   HP87
90   ! THIS PROGRAM USES INTERRUPTS
100   !
110  OPTION BASE 1
120  CLEAR
130  DIM C(30),H(9),D(1024),Hfreq(50),Harm(50),Arr(5,2),Brr(16,2),Crr(32)
140  DIM Micno(13),Q(4),Speed(4),Refdist(4),Cangle(13,4),Corr(13,4),Dist(13)
150  COM A(1050),B(530),Freq(530)
160  IMAGE D.8DE
170  !
180  ! SHEAR LAYER AND DISTANCE CORRECTIONS
190  ! FOR MICROPHONE NUMBERS
200  DATA 1,2,3,4,5,6,7,8,9,10,11,12,13
210  ! AT MICROPHONE RADIAL DISTANCES
220  DATA 14,14,14,14,14,14,4.5,4.5,8,7.92,14,14,7.58
230  ! CORRECTIONS FOR Q=0,U=0,NO DISTANCE CORRECTION
240  !  UNCORRECTED ANGLES AND ZERO CORRECTIONS
250  DATA 0,0,0
260  DATA 60,70,80,90,105,120,105,140,15,290,90,90,270
270  DATA 0,0,0,0,0,0,0,0,0,0,0,0,0
280  ! CORRECTIONS FOR Q=0,U=0,REF DISTANCE=14 feet
290  !  UNCORRECTED ANGLES AND DISTANCE CORRECTIONS ONLY
300  DATA 0,0,14
310  DATA 60,70,80,90,105,120,105,140,15,290,90,90,270
320  DATA 0,0,0,0,0,0,-9.9,-9.9,-4.9,-4.9,0,0,-5.3
330  ! CORRECTIONS FOR Q=27,U=150,REF DISTANCE=14 feet
340  !  CORRECTED ANGLES AND SHEAR/DISTANCE CORRECTIONS
350  DATA 27,150,14
360  DATA 65.9,75.5,85.2,95,109.7,124.6,105,140,15,286.9,95.5,94.6,267.3
370  DATA .8,.6,.4,.1,-.2,-.5,-9.9,-9.9,-4.9,-4.4,.1,.1,-5.2
380  ! CORRECTIONS FOR Q=50,U=205,REF DISTANCE=14 feet
390  !  CORRECTED ANGLES AND SHEAR/DISTANCE CORRECTIONS
400  DATA 50,205,14
410  DATA 68.5,77.8,87.2,96.8,111.2,126.1,105,140,15,285.6,97.5,96.3,266.3
420  DATA 1.2,.9,.6,.2,-.2,-.6,-9.9,-9.9,-4.9,-4.2,.2,.2,-5.1
430  ! THESE CORRECTIONS MUST BE ADDED TO THE SPECTRUM LEVELS
440  !
450  DISP " SETTING UP CORRECTION MATRICES  "
460  FOR I=1 TO 13
470  READ Micno(I)
480  NEXT I
490  FOR I=1 TO 13
500  READ Dist(I)
510  NEXT I
520  FOR J=1 TO 4
530  READ Q(J),Speed(J),Refdist(J)
540  FOR I=1 TO 13
550  READ Cangle(I,J)
560  NEXT I
570  FOR I=1 TO 13
580  READ Corr(I,J)
590  NEXT I
600  NEXT J
610  RESTORE
620  FOR I=1 TO 2
630  FOR J=1 TO 5
640  Arr(J,I)=0
650  NEXT J
660  FOR J=1 TO 16
```

```
670    Brr(J,I)=0
680    NEXT J
690    NEXT I
700    FOR I=1 TO 32
710    Crr(I)=0
720    NEXT I
730    FOR I=1 TO 21
740    Hfreq(I)=0
750    Harm(I)=0
760    NEXT I
770    DISP " "
780    PRINT "THIS PROGRAM  DESIGNED FOR HIGH RESOLUTION AUTO-SPECTRUM ANALYSIS O
N 5420 USING LOG MAG FORMAT, WITH SINUSOIDAL WINDOW"
790    DISP " "
800    !
810    Maxs=120
820    PRINT " MAXIMUM SPECTRUM LEVEL PLOTTED IS ";Maxs;"dB"
830    LINPUT "DO YOU WISH TO CHANGE THIS?",A9$
840    IF A9$="N" THEN GOTO 870
850    DISP "INPUT MAXIMUM SPECTRUM LEVEL FOR PLOT IN dB"
860    INPUT Maxs
870    Mins=Maxs-70
880    DISP " "
890    PRINT "THIS PROGRAM WILL SAVE RAW AND/OR CORRECTED DATA ON DISC"
900    LINPUT "DO YOU WANT TO SAVE AND PLOT ONLY CORRECTED DATA ?",P2$
910    IF P2$="Y" THEN A1$="N"
920    IF P2$="Y" THEN A2$="Y"
930    DISP " "
940    RESET 7
950    REMOTE 704
960    OUTPUT 704 ;"1FM" ! SINGLE SCREEN FORMAT FOR 5420
970    OUTPUT 704 ;"1TC" ! TRACE A IS ACTIVE
980    !
990    DISP " "
1000    DISP "INPUT RUN NUMBER" ! USER INPUTS
1010    INPUT Rn
1020    DISP "INPUT DATA POINT"
1030    INPUT Dp
1040    DISP "INPUT MIC NUMBER"
1050    INPUT Mc
1060    DISP "INPUT MIC GAIN RELATIVE TO CALIBRATION"
1070    INPUT Gain
1080    DISP "INPUT WIND SPEED (f/s)"
1090    INPUT U
1100    !
1110    PRINT "THE FOLLOWING PARAMETERS ARE ONLY REQUIRED FOR TITLES"
1120    DISP "INPUT PROP RPM"
1130    INPUT Rpm
1140    DISP "INPUT BETA IN Degrees"
1150    INPUT Beta
1160    DISP "INPUT SEPARATION X IN Inches"
1170    INPUT Sepx
1180    !
1190    DISP " "
1200    PRINT "  CAPTURE PROPER DATA RECORD ON 5420" ! SET UP 5420 CH 1
1210    PRINT "  AFTER CAPTURE HIT `CONTINUE' ON HP87 (Ch 1 IS ACTIVE)"
1220    DISP " "
1230    PAUSE
1240    !
1250    REMOTE 704
1260    ON INTR 7 GOSUB Srq  ! INTERRUPT FROM 5420
1270    ENABLE INTR 7:8
1280    S=0
1290    OUTPUT 704 ;"401SA" ! REQUEST ASCII SAVE OF Ch 1 DATA TRACE TO HP87
1300    IF S<> 96 THEN 1300 ! WAIT FOR SAVE TO START AND COMPLETE
1310                                ! OUTPUT 704 CAUSES INTERRUPT #7
```

```
1320  !
1330  ! CONVERT FROM WATTS TO DB. AND ADJUST FOR GAIN
1340  PRINT " TRANSFER COMPLETE. ADJUSTING FOR GAIN"
1350  PRINT " SET UP CURSOR AND HARMONICS ON 5420"
1360  K=0
1370  FOR I=17 TO Fin
1380  K=K+1
1390  B(K)=10*LGT (A(I))-Gain
1400  NEXT I
1410  Nlines=K
1420  !
1430  ! SETTING UP FREQUENCY INFORMATION
1440  Delf=A(13)
1450  Range=Delf*(Nlines-1)
1460  PRINT " AFTER HARMONICS ARE SET UP. HIT 'CONTINUE' ON HP87"
1470  DISP " "
1480  PAUSE
1490  ENABLE INTR 7;8
1500  S=0
1510  OUTPUT 704 ;",0.1PRPR" ! REQUEST ASCII DATA TRANSFER
1520  IF S<> 100 THEN 1520
1530  PRINT "SETTING UP HARMONIC MATRICES"
1540  Nharm=T/2
1550  IF Nharm>25 THEN Nharm=25
1560  PRINT "NUMBER OF HARMONICS =";Nharm
1570  FOR I=1 TO Nharm
1580  Hfreq(I)=D(2*I-1)
1590  Harm(I)=D(2*I)-Gain
1600  NEXT I
1610  IM=0
1620  FOR I=1 TO 13
1630  IF Mc<> Micno(I) THEN GOTO 1660
1640  IM=I
1650  GOTO 1670
1660  NEXT I
1670  Theta=Cangle(IM,1)
1680  Thetac=Theta
1690  !
1700  DISP " "
1710  C$="N"
1720  Nharmc=0
1730  Flog=1
1740  IF P2$="Y" THEN GOTO 1840
1750  LINPUT "DO YOU WANT TO SAVE THE RAW DATA IN A DATA FILE ?",A1$
1760  IF A1$="N" THEN GOTO 1860
1765  A4$="N"
1770  DISP " "
1780  PRINT "SPECTRUM IS BEING SAVED ON D701 AS RAW$='RH'-RUN-POINT-MIC"
1790  DISP " "
1800  !
1810  GOSUB Spectra  ! SAVE RAW DATA ON DISC D701
1820  ! CAT ":D701" !LISTS FILES WITH NEW ONE ADDED
1830  DISP " "
1840  !
1850  IF P2$="Y" THEN GOTO 1980
1860  LINPUT "DO YOU WANT TO CORRECT THE DATA FOR SHEAR LAYER EFFECTS & DISTANC
E ?",A2$
1870  IF A2$="N" THEN GOTO 2200
1880  GOTO 1980
1890  !
1900  ! OUTPUT 704 ;"2FM" ! SPLIT SCREEN
1910  ! OUTPUT 704 ;"2TCLM" ! MAKE LOWER TRACE ACTIVE
1920  !
1930  DISP "CORRECTION FACTORS ARE STORED FOR WIND SPEEDS 0,150 AND 205 ONLY"
1940  DISP "AND FOR A DISTANCE OF 14 FEET"
1950  DISP " "
```

```
1960   DISP "INPUT WIND SPEED (f/s)"
1970   INPUT U
1980   DISP "CORRECTION FOR SHEAR LAYER AND DISTANCE IS SELECTED"
1990   IU=0
2000   FOR I=2 TO 4
2010   IF U<> Speed(I) THEN GOTO 2040
2020   IU=I
2030   GOTO 2050
2040   NEXT I
2050   PRINT "CORRECTION FILE PARAMETERS ARE: MIC =":Micno(IM);" U=";Speed(IU)
2060   LINPUT "IS THIS CORRECT?",A7$
2070   IF A7$="N" THEN GOTO 1930
2080   Thetac=Cangle(IM,IU)
2090   Dbcorr=Corr(IM,IU)
2100   FOR I=1 TO Nlines
2110   B(I)=B(I)+Dbcorr
2120   NEXT I
2130   FOR I=1 TO Nharm
2140   Harm(I)=Harm(I)+Dbcorr
2150   NEXT I
2160   !
2170   ! OUTPUT 704 ;"401RA" ! SEND CORRECTED DATA BACK TO THE 5420 LOWER TRACE
2180   ! IF S<> 112 THEN 1340
2190   DISP " "
2200   LINPUT "DO YOU WANT TO PLOT THE RESULTS?",A3$
2210   IF A3$="N" THEN GOTO 2250
2220   !
2230   GOSUB Plotting  ! PLOT RESULTS
2240   !
2250   LINPUT " DO YOU WANT TO LIST THE HARMONICS ON THE PRINTER?",A8$
2260   IF A8$="N" THEN GOTO 2300
2270   !
2280   GOSUB Printing  ! PRINT HARMONICS
2290   !
2300   LINPUT " DO YOU WANT TO SAVE THE CORRECTED DATA  IN A FILE ? (Y/N)",A4$
2310   IF A4$="N" THEN GOTO 2390
2320   PRINT " CORRECTED FILE IS BEING SAVED ON D701 AS `CH'-RUN-POINT-MIC"
2330   Flog=2
2340   !
2350  GOSUB Spectra
2360   ! CAT ":D701" ! LISTS FILES WITH NEW ONE ADDED
2370   !
2380    DISP " "
2390   LINPUT "MEASUREMENT COMPLETED. DO YOU HAVE ANOTHER?",A5$
2400   IF A5$="Y" THEN GOTO 950
2410   PRINT "PROGRAM END"
2420    DISP " "
2430   MASS STORAGE IS ":D700"
2440   STOP ! END PROGRAM
2450   !
2460   ! ******************************************************************

2470   !
2480  Srq: S=SPOLL (704)
2490   STATUS 7,1 ; B ! DETERMINES STATUS OF 5420
2500   PRINT "SRQ =";S
2510   IF S=96 THEN GOSUB Asave_trace  ! ON INTERUPT #7
2520   IF S=100 THEN GOSUB Aprint  ! ON INTERRUPT #7
2530   IF S=102 THEN GOSUB Aprint  ! ON INTERRUPT #7
2540   IF S=104 THEN SEND 7 ; CMD "?D%"
2550   IF S=112 THEN GOSUB Arecall_trace
2560   IF S=120 THEN SEND 7 ; CMD "?E$"
2570   IF S=98 THEN PRINT "END OF PLOT"
2580   PRINT "SRQ=";S
2590   RESUME 7
2600   ENABLE INTR 7;8
2610   RETURN
```

```
2620    !
2630    ! THIS ROUTINE IS NOT BEING USED
2640 Freqplot: PRINT "PLOTTING SPECTRUM" ! PLOTS ON 7470A USING HP5420A
2650    S=0
2660   IF A2$="N" THEN GOTO 2700
2670    OUTPUT 704 ;"-1 TX  RAW AND CORRECTED DATA (TOP/BOTTOM);" ! TEXT EDIT
2680    WAIT 1000
2690   GOTO 2720
2700   OUTPUT 704 ;"-1 TX RAW DATA:" ! TEXT EDIT
2710   WAIT 1000
2720    PRINT "AT LINE 963"
2730    OUTPUT 704 ;"0,523,656PL1.7206,6300PL.1PLPL"
2740   ! PLOT FORMAT: ORIGIN.X.Y PL UPPER RIGHT X,Y PL  GO PLOT
2750    IF S<> 98 THEN 2750
2760    RETURN
2770   !
2780   !
2790 Asave_trace: PRINT "ASCII SAVE TRACE FROM 5420"
2800   FOR I=1 TO 16 ! READ HEADER VARIABLES FROM 5420
2810   ENTER 704 : A(I)
2820   NEXT I
2830   T=A(3)/2
2840   Fin=16+T
2850   PRINT "READING DATA   STAND BY"
2860   FOR I=17 TO Fin ! READ DATA FROM 5420
2870   ENTER 704 : A(I)
2880   NEXT I
2890   RETURN
2900   !
2910   ! THIS ROUTINE IS NOT BEING USED
2920 Arecall_trace: PRINT "ASCII RECALL TRACE FROM 9845"
2930   FOR I=1 TO 16 ! WRITE HEADER VARIABLES TO 5420
2940   OUTPUT 704 ;A(I)
2950   NEXT I
2960   T=A(3)/2
2970   Fin=16+T
2980   PRINT "SENDING DATA        STAND BY"
2990   FOR I=17 TO Fin ! WRITE DATA TO 5420
3000   OUTPUT 704 ;A(I)
3010   NEXT I
3020   RETURN
3030    !
3040 Aprint: PRINT "ASCII DATA TRANSFER"
3050    IF S=100 THEN GOTO 3090
3060    FOR I=1 TO 9
3070    ENTER 704 ; H(I) ! READS 9 HEADERS
3080    NEXT I
3090    ENTER 704 ; T ! READS NO OF VARIABLES
3100    FOR I=1 TO T
3110    ENTER 704 : D(I) ! READS DATA VARIABLES
3120    NEXT I
3130    PRINT " DATA TRANSFER ENDED"
3140    RETURN
3150    !
3160    ! ****************************************************************

3170    !
3180 Spectra: ! CREATE DATA FILE ON DISC D701
3190    ! RAW DATA FILE NAME IS RHRn-Dp-Mc (RH RUN-POINT-MIC)
3200    ! CORRECTED DATA FILE NAME IS CHRn-Dp-Mc (CH RUN-POINT-MIC)
3210    MASS STORAGE IS ":D701"
3230    IF A1$="Y" THEN Raw$="RH"&VAL$ (Rn)&"-"&VAL$ (Dp)&"-"&VAL$ (Mc)
3250    IF A4$="Y" THEN Raw$="CH"&VAL$ (Rn)&"-"&VAL$ (Dp)&"-"&VAL$ (Mc)
```

```
3260  CREATE Raw$,18,256 ! (18*256)= 576 NUMBERS X 8 BYTES/NUMBER
3270  ASSIGN# 2 TO  Raw$
3280  FOR I=1 TO 5
3290  Arr(I,1)=Hfreq(I)
3300  Arr(I,2)=Harm(I)
3310  NEXT I
3320  PRINT# 2,1 ; Nlines,Delf,Nharm,Rpm,U,Beta,Sepx,Thetac,Nharmc,C$,Arr(,)
3330  IF Nharm<= 5 THEN GOTO 3390
3340  FOR K=6 TO Nharm
3350  Brr(K-5,1)=Hfreq(K)
3360  Brr(K-5,2)=Harm(K)
3370  NEXT K
3380  PRINT# 2,2 ; Brr(,)
3390  Number=INT ((Nlines-4)/32)+1
3400  IF Number>16 THEN Number=16
3410  FOR I=3 TO Number+2
3420  FOR J=1 TO 32
3430  Crr(J)=B((I-3)*32+J)
3440  NEXT J
3450  PRINT# 2,I ; Crr()
3460  NEXT I
3470  ASSIGN# 2 TO  *
3480  RETURN
3490  END
3500  !
3510 Plotting: ! PLOTS ON 7470A DIRECTLY
3520  PRINT "START PLOT"
3530  !
3540  Npoints=26
3550  Spacing=Range/Npoints
3560  IF Spacing>250 THEN Value=50
3570  IF Spacing<= 250 THEN Value=25
3580  IF Spacing<= 125 THEN Value=12.5
3590  IF Spacing<= 100 THEN Value=10
3600  !
3610  PLOTTER IS 1
3620  PLOTTER IS 705
3630  GRAPHICS
3640  LIMIT 10,200,15,170
3650  LOCATE 20,120,16,98 ! SCALE AREA
3660  SCALE 0,256,Mins,Maxs
3670  AXES 10,10,0,Mins
3680  !
3690  ! PLOT SPECTRUM LEVEL VS FREQUENCY
3700  MOVE 0,Mins
3710  FOR I=1 TO Nlines
3720  Freq(I)=Delf*(I-1)
3730  Xcoord=Freq(I)/Value
3740  PLOT Xcoord,B(I),1
3750  NEXT I
3760  !
3770  ! LABEL PLOTS
3780  CSIZE 3.2
3790  LORG 1
3800  MOVE 21,Maxs
3810  IF A2$="N" THEN GOTO 3840
3820  LABEL USING "K" : "NARROW BAND SPECTRUM CORRECTED FOR SHEAR LAYER AND 4.3
m DISTANCE"
3830  GOTO 3850
3840  LABEL USING "K" : "RAW NARROW BAND SPECTRUM"
3850  CSIZE 3.2
3860  LORG 1
3870  MOVE 50,Maxs-2.5
3880  LABEL USING "K" : "TEST 706     RUN ";Rn;"     DATA POINT ";Dp
3890  MOVE 21,Maxs-5
3900  V=U*.3048
3910 V=V+.005
```

```
3920  V=V*10
3930  V=IP (V)
3940  V=V/10
3950  IF A2$="N" THEN GOTO 3980
3960  LABEL USING "K" ; "MIC ";Mc;"   THETA = ";Thetac;" deg (corrected) ";"U ="
;V;" m/sec";"  GAIN=";Gain
3970  GOTO 3990
3980  LABEL USING "K" ; "MIC ";Mc;"   THETA = ";Theta;" deg (uncorrected)  U =";
V;" m/sec ";"  GAIN=";Gain
3990  !
4000  ! LABEL Y-AXIS
4010  CSIZE 2.8
4020  LORG 8
4030  FOR Y=Mins TO Maxs STEP 10
4040  MOVE -.1,Y
4050  LABEL USING "K,X" : Y
4060  NEXT Y
4070  CSIZE 3.4
4080  MOVE -11,Maxs-34
4090  LABEL USING "K" : "Lp(f)"
4100  MOVE -17,Maxs-37
4110  LABEL USING "K" ; "dB"
4120  !
4130  ! LABEL X-AXIS
4140  LORG 6
4150  MOVE 120,Mins-7
4160  LABEL USING "K" ; "FREQUENCY, Hz"
4170  LORG 5
4180  CSIZE 2.4
4190  FOR J=1 TO 26 STEP 2
4200  JJ=10*(J-1)
4210  Freq(J)=Value*JJ
4220  MOVE JJ,Mins-1
4230  LABEL USING "K" ; Freq(J)
4240  JK=10*J
4250  Freq(J)=Value*JK
4260  MOVE JK,Mins-2.7
4270  LABEL USING "K" ; Freq(J)
4280  NEXT J
4290  !
4300  ALPHA
4310  DISP " "
4320  DISP " "
4330  ALPHA
4340  PRINTER IS 1
4350  RETURN
4360  !
4370 Printing: ! PRINTS ON 708
4380  PRINTER IS 708
4390  PRINT " "
4400  PRINT " "
4410  PRINT " "
4420  PRINT " "
4430  PRINT " "
4440  PRINT " "
4450  PRINT " "
4455  V=(U*.3048+.005)*10
4456  V=.1*IP (V)
4460  IF A2$="N" THEN GOTO 4540
4470  PRINT "                         NARROWBAND SPECTRUM"
4480  PRINT "           CORRECTED FOR SHEAR LAYER AND 4.3 m DISTANCE"
4490  PRINT "               TEST 706     RUN";Rn;"     DATA POINT";Dp;"  GAIN=";
Gain
4500  PRINT "              MIC";Mc;"  THETA=";Thetac;"deg (corrected)  U=";V;"m/s
ec"
4510  PRINT " "
```

ORIGINAL PAGE IS
OF POOR QUALITY

```
4520  PRINT "        THESE LEVELS ARE NOT ADJUSTED FOR BROADBAND CONTRIBUTIONS"
4530  GOTO 4570
4540  PRINT "                          RAW NARROWBAND SPECTRUM"
4550  PRINT "                 TEST 706      RUN":Rn:"      DATA POINT":Dp:"  GAIN=":
Gain
4560  PRINT "               MIC":Mc:"  THETA=":Thetac:"deg (corrected)  U=":V:"m/s
ec"
4570  PRINT " "
4580  PRINT " "
4590  PRINT "                   HARMONIC    FREQUENCY,Hz    LEVEL,dB"
4600  PRINT "                   ------------------------------------"
4610  IMAGE 19X,DD,9X,DDDDD.D,9X,DDD.D
4620  FOR I=1 TO Nharm
4630  PRINT USING 4610 : I,Hfreq(I),Harm(I)
4640  NEXT I
4650  PRINT CHR$ (12)
4660  PRINTER IS 1
4670  RETURN
4680  END
```

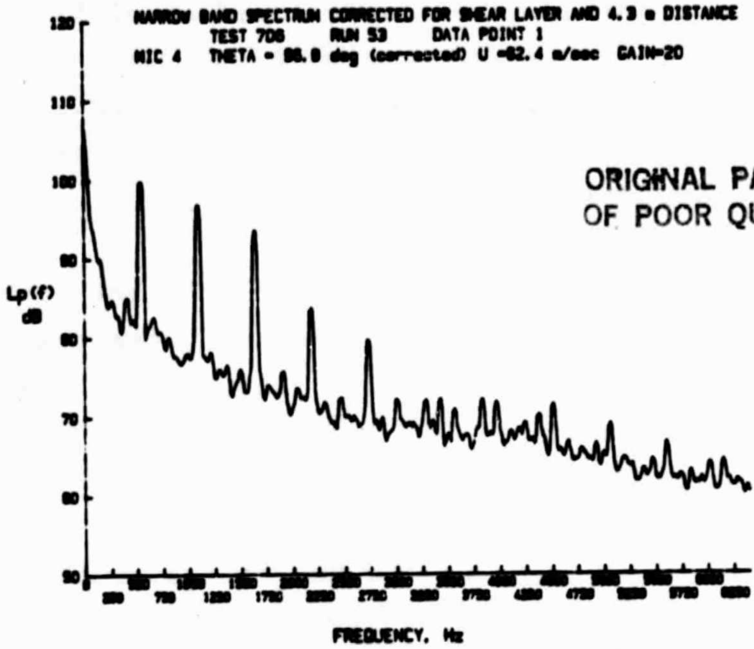

NARROWBAND SPECTRUM
CORRECTED FOR SHEAR LAYER AND 4.3 m DISTANCE
TEST 706 RUN 53 DATA POINT 1 GAIN= 20
MIC 4 THETA= 96.8 deg (corrected) U= 62.4 m/sec

THESE LEVELS ARE NOT ADJUSTED FOR BROADBAND CONTRIBUTIONS

HARMONIC	FREQUENCY,Hz	LEVEL,dB
1	550.0	99.8
2	1087.5	96.7
3	1637.5	93.5
4	2187.5	83.7
5	2737.5	79.5
6	3275.0	71.8
7	3825.0	72.1
8	4375.0	70.2
9	4912.5	66.1
10	5462.5	64.5
11	6012.5	64.1

A.4 Program HARMPLOT2

The program plots harmonic level versus harmonic order for up to 7 cases on each graph. The harmonic levels, stored on disk by program CEDAR2, must be adjusted to allow for broadband contributions before plotting. These adjustments (always negative) to the harmonic levels must be estimated manually from the narrowband plots output by CEDAR2, and entered as input to program HARMPLOT2 for each harmonic in turn. The adjusted harmonic levels are plotted for the cases selected, and stored on disk.

The program checks whether the harmonic levels have already been adjusted when reading from disk, so that the adjustments are performed only once for each case.

It is necessary to select the appropriate storage disk for each case to be plotted. If the file associated with that case cannot be found on the disk currently being read, the program will expect another disk to be input.

Input required:

Parameter to be used for the key to the graph
(Mic No, Mic Angle θ, Wind Speed U, RPM, Propeller Angle β or Separation X)

For each plot:

Run Number
Data Point
Microphone Number

For adjustments to harmonic levels:

Number of valid harmonics
Harmonic number
Correction (dB) to be added to the harmonic level
These are entered for each harmonic to be adjusted.

Disks containing files, either with or without shear layer and distance corrections created by CEDAR2

Uncorrected: RH Run No - Data Pt - Mic No

Corrected: CH Run No - Data Pt - Mic No

Output:

Listing of adjusted harmonic levels

Graph of harmonic level vs order for 7 cases maximum

Adjusted harmonic levels, stored on disk, overwriting the unadjusted levels, with an indicator to show that adjustments have been made to that file.

```
100 ! PROGRAM HARMPLOT2.  5/11/84   E.WILBY
110 !
120 ! CORRECTED NARROWBAND HARMONIC DATA ARE SELECTED FROM DATA FILES
130 ! ON DISC 701 (GENERATED BY CEDAR2, RH OR CH), AND UP TO 7 CASES
140 ! MAY BE PLOTTED ON ONE GRAPH
150 !
160 OPTION BASE 1
170 CLEAR
180 MASS STORAGE IS ":D701"
190 DIM Title$(6),Key(7),Nharm(7),Rpm(7),U(7),Beta(7),Sepx(7),File1$(7)
200 DIM Thetac(7),Nharmc(7),Code$(7),Harm(7,21),Arr(5,2),Brr(16,2)
210 DIM Change(21),Harmx(7,21),Hfreq(7,21),Symbol(7)
220 !
230 DATA " Mic ","Theta","U(m/s)"," Rpm "," Beta"," X(m)"
240 FOR I=1 TO 6
250 READ Title$(I)
260 NEXT I
270 RESTORE
280 PRINT "SETTING UP MATRICES"
290 FOR I=1 TO 2
300 FOR J=1 TO 5
310 Arr(J,I)=0
320 NEXT J
330 FOR J=1 TO 16
340 Brr(J,I)=0
350 NEXT J
360 FOR I=1 TO 21
370 Change(I)=0
380 NEXT I
390 !
400 PRINT "CASES WILL BE SELECTED FROM THE CORRECTED FILES ONLY, WHICH"
410 PRINT "ARE STORED AS CH Run-Point-Mic . UNLESS THE OPTION FOR "
420 PRINT "RAW DATA IS SPECIFIED"
430 LINPUT "WILL ANY RAW DATA BE PLOTTED? (Y/N) ",A1$
440 ! A1$="N" ONLY CORRECTED MAY BE SELECTED
450 ! A1$="Y" RAW OR CORRECTED DATA MAY BE SELECTED
460 IF A1$="N" THEN A5$="N"
470 !
480 ! SET UP SCALE
490 Maxs=120
500 PRINT "MAXIMUM SPECTRUM LEVEL PLOTTED IS ";Maxs;" dB"
510 LINPUT "DO YOU WISH TO CHANGE THIS?",P1$
520 IF P1$="N" THEN GOTO 550
530 DISP "INPUT MAXIMUM SPECTRUM LEVEL FOR PLOT IN DB"
540 INPUT Maxs
550 Mins=Maxs-70
560 !
570 PRINT " "
580 Nplot=0
590 PRINT "Maximum Number of Plots on this Graph = 6"
600 Nplot=Nplot+1
610 PRINT "Plot Number ";Nplot;" on Graph"
620 Y$="Y"
630 DISP " "
640 DISP "INPUT RUN NUMBER"
650 INPUT Rn
660 DISP "INPUT DATA POINT"
670 INPUT Dp
680 DISP "INPUT MIC NUMBER"
690 INPUT Mc
700 Symbol(Nplot)=Nplot
710 ! PRINT "INPUT SYMBOL FOR PLOT";Nplot;" (NUMBERS 0 TO 9)"
720 ! INPUT Symbol(Nplot)
730 IF A1$="N" THEN GOTO 750
740 LINPUT "DO YOU WANT THE RAW DATA FILE?",A5$
750 DISP " "
760 IF Nplot<> 1 THEN GOTO 850
```

ORIGINAL PAGE IS
OF POOR QUALITY

```
770 DISP "THE KEY FOR THE GRAPH WILL DISPLAY Run-Point-Mic FOR EACH CURVE"
780 DISP "WHAT ADDITIONAL PARAMETER DO YOU WANT ON THE KEY?"
790 DISP "POSSIBLE PARAMETERS ARE :"
800 DISP "Mic=1, Theta=2, U=3, Rpm=4, Beta=5, X=6 "
810 DISP "INPUT THE PARAMETER NUMBER YOU REQUIRE "
820 INPUT KK
830 IF KK<1 THEN KK=1
840 IF KK>6 THEN KK=1
850 K=Nplot
860 Ntimes=0
870 Y$="Y"
880 IF A5$="Y" THEN File1$(K)="RH"&VAL$ (Rn)&"-"&VAL$ (Dp)&"-"&VAL$ (Mc)
890 IF A5$="N" THEN File1$(K)="CH"&VAL$ (Rn)&"-"&VAL$ (Dp)&"-"&VAL$ (Mc)
900 ON ERROR GOTO 3220
910 ASSIGN# K TO  File1$(K)
920 OFF ERROR
930 PRINT "File Requested from D701 is ";File1$(K)
940 PRINT "READING DATA"
950 READ# K,1 ; Nlines,Delf,Nharm(K),Rpm(K),U(K),Beta(K),Sepx(K),Thetac(K),Nharm
c(K),Code$(K),Arr(,)
960 V=(U(K)*.3048+.005)*10
970 V=IP (V)/10
980 X=(Sepx(K)/12*.3048+.001)*1000
990 X=IP (X)/1000
1000 FOR I=1 TO 5
1010 Harm(K,I)=Arr(I,2)
1020 Hfreq(K,I)=Arr(I,1)
1030 NEXT I
1040 IF Nharm(K)<= 5 THEN GOTO 1110
1050 READ# K,2 ; Brr(,)
1060 FOR I=6 TO Nharm(K)
1070 Harm(K,I)=Brr(I-5,2)
1080 Hfreq(K,I)=Brr(I-5,1)
1090 NEXT I
1100 OFF ERROR
1110 PRINT "DATA TRANSFER ENDED"
1120 IF KK=1 THEN Key(K)=Mc
1130 IF KK=2 THEN Key(K)=Thetac(K)
1140 IF KK=3 THEN Key(K)=V
1150 IF KK=4 THEN Key(K)=Rpm(K)
1160 IF KK=5 THEN Key(K)=Beta(K)
1170 IF KK=6 THEN Key(K)=X
1180 DISP " "
1190 IF Code$(K) <> "Y" THEN GOTO 1230
1200 PRINT "THIS FILE HAS ALREADY BEEN ADJUSTED FOR BROADBAND CONTRIBUTIONS"
1210 PRINT "THE MAXIMUM NO OF HARMONICS TO BE USED IS ",Nharmc(K)
1220 GOTO 1700
1230 PRINT "THIS FILE HAS NOT BEEN ADJUSTED FOR BROADBAND CONTRIBUTIONS"
1240 DISP " "
1250 PRINT "NO OF HARMONICS STORED = ";Nharm(K)
1260 PRINT "INPUT NO OF VALID HARMONICS "
1270 INPUT Nharmc(K)
1280 Nharm(K)=Nharmc(K)
1290 FOR I=1 TO Nharmc(K)
1300 Harmx(K,I)=Harm(K,I)
1310 NEXT I
1320 LINPUT "ARE THERE ANY CORRECTIONS TO BE MADE TO THE HARMONIC LEVELS?",A2$
1330 IF A2$="N" THEN GOTO 1530
1340 FOR I=1 TO 21
1350 Change(I)=0
1360 NEXT I
1370 DISP " "
1380 PRINT " INPUT THE HARMONIC ORDER TO BE CORRECTED (Max=21)"
1390 INPUT J
1400 IF Change(J)=0 THEN GOTO 1460
1410 PRINT "THIS HARMONIC HAS ALREADY BEEN CHANGED BY ";Change(J);" dB"
1420 LINPUT "DO YOU WISH TO MAKE ADDITIONAL CHANGES TO THIS HARMONIC ? ",A3$
1430 IF A3$="N" THEN GOTO 1500
1440 PRINT "INPUT THE ADDITIONAL CHANGE IN dB FOR HARMONIC ";J
```

```
1450 GOTO 1470
1460 PRINT "INPUT THE CHANGE IN dB FOR  HARMONIC":J
1470 INPUT Ch
1480 Change(J)=Change(J)+Ch
1490 Harm(K,J)=Harm(K,J)+Ch
1500 LINPUT "ANY MORE CORRECTIONS ?",A4$
1510 IF A4$ <> "N" THEN GOTO 1380
1520 PRINT "THE FILE HAS BEEN ADJUSTED FOR BROADBAND CONTRIBUTIONS"
1530 PRINT "PRINT ADJUSTED HARMONIC LEVELS"
1540 GOSUB Printing
1550 !
1560 LINPUT "ARE THE ADJUSTED HARMONICS OK TO STORE ON DISC701 ?",A9$
1570 IF A9$="N" THEN GOTO 1700
1580 Code$(K)="Y"
1590 DISP " "
1600 FOR I=1 TO 5
1610 Arr(I,2)=Harm(K,I)
1620 NEXT I
1630 PRINT# K,1 ; Nlines,Delf,Nharm(K),Rpm(K),U(K),Beta(K),Sepx(K),Thetac(K),Nha
rmc(K),Code$(K),Arr(,)
1640 IF Nharm(K)<= 5 THEN GOTO 1690
1650 FOR I=6 TO Nharm(K)
1660 Brr(I-5,2)=Harm(K,I)
1670 NEXT I
1680 PRINT# K,2 ; Brr(,)
1690 PRINT "DATA TRANSFER ENDED"
1700 ASSIGN# K TO  *
1710 !
1720 GOSUB Plotting
1730 !
1740 PRINT "YOU HAVE JUST FINISHED PLOT ":Nplot
1750 PRINT "THIS GRAPH IS FINISHED"
1760 DISP " "
1770 IF Nplot=7 THEN GOTO 1800
1780 LINPUT "ANY MORE PLOTS ON THIS GRAPH ?",A7$
1790 IF A7$ <> "N" THEN GOTO 600
1800 LINPUT "ANY MORE GRAPHS ? ",A8$
1810 IF A8$ <> "N" THEN GOTO 1850
1820 MASS STORAGE IS ":D700"
1830 DISP "PROGRAM END"
1840 STOP
1850 PRINT "STARTING A NEW GRAPH, WITH MAX LEVEL = ":Maxs:" dB"
1860 IF A1$="N" THEN PRINT "ONLY CORRECTED DATA WILL BE PLOTTED"
1870 IF A1$ <> "N" THEN PRINT "RAW OR CORRECTED DATA MAY BE PLOTTED"
1880 LINPUT "ANY CHANGES ? (Y/N) ",A6$
1890 IF A6$="N" THEN GOTO 570
1900 IF A6$ <> "N" THEN GOTO 400
1910 !
1920 ! ****************************************************************
1930 !
1940 Plotting: ! Plots Harmonic Level versus Order
1950           ! For a Maximum of 7 Plots on 1 Graph
1960           ! Maximum No of Harmonics = 11
1970 !
1980 PRINT "START PLOT"
1990 PLOTTER IS 1 ! Sets Default Size
2000 PLOTTER IS 705
2010 GRAPHICS
2020 LIMIT 10,210,15,170
2030 LOCATE 20,120,16,98
2040 SCALE 0,12,Mins,Maxs
2050 IF Nplot<> 1 THEN GOTO 2530
2060 AXES 1,10,0,Mins
2070 !
2080 ! LABEL Y-AXIS
2090 CSIZE 2.8
2100 LORG 8
2110 FOR Y=Mins TO Maxs STEP 10
```

```
2120 MOVE -.1,Y
2130 LABEL USING "K" : Y
2140 NEXT Y
2150 CSIZE 3.2
2160 MOVE -.3,Maxs-32.5
2170 LABEL USING "K" : "Harmonic"
2180 MOVE -.3,Maxs-35
2190 LABEL USING "K,2X" : "Level"
2200 MOVE -.3,Maxs-38
2210 LABEL USING "K,3X" ; "dB"
2220 !
2230 ! LABEL X-AXIS
2240 LORG 6
2250 MOVE 6,Mins-3
2260 LABEL USING "K" ; "Harmonic Order"
2270 CSIZE 2.8
2280 FOR I=1 TO 11
2290 MOVE I,Mins-.5
2300 LABEL USING "K" : I
2310 NEXT I
2320 !
2330 ! LABEL PLOTS
2340 CSIZE 3.5
2350 LORG 1
2360 MOVE 1,Maxs
2370 IF A5$="Y" THEN LABEL USING "K" : "HARMONIC LEVELS ADJUSTED FOR BROADBAND C
ONTRIBUTIONS"
2380 IF A5$="N" THEN LABEL USING "K" : "HARMONIC LEVELS CORRECTED FOR SHEAR LAYE
R AND 4.3m DISTANCE"
2390 MOVE 2,Maxs-2.5
2400 IF A5$="N" THEN LABEL USING "K" : "AND ADJUSTED FOR BROADBAND CONTRIBUTIONS
"
2410 !
2420 ! LABEL Key
2430 ! KK is the Key Number
2440 LORG 4
2450 Y=Maxs-6
2460 MOVE 8.3,Y
2470 CSIZE 2.8
2480 LABEL USING "K" : "Symbol"
2490 MOVE 9.6,Y
2500 LABEL USING "K" : Title$(KK)
2510 MOVE 11.5,Y
2520 LABEL USING "K" : "Run-Data pt-Mic"
2530 !
2540 ! Plot Spectrunm Level versus Order
2550 YK=Maxs-6
2560 J=Nplot
2570 IF Y$="N" THEN GOTO 2770
2580 KT=Nplot+2
2590 IF Nplot=1 THEN KT=1
2600 LINE TYPE KT
2610 MOVE 7.8,YK-2.5*J
2620 DRAW 8.8,YK-2.5*J
2630 PEN UP
2640 MOVE 0,Mins
2650 LORG 5
2660 CSIZE 2.6
2670 Nh=Nharm(J)
2680 IF Nharm(J)>11 THEN Nh=11
2690 FOR I=1 TO Nh
2700 IF Harm(J,I)=0 THEN GOTO 2750
2710 PLOT I,Harm(J,I),2
2720 LABEL Symbol(J)
2730 PLOT I,Harm(J,I),1
2740 GOTO 2760
2750 MOVE I,Mins
2760 NEXT I
2770 LINE TYPE 1
```

```
2780 !
2790 ! Key
2800 LORG 5
2810 Y=Maxs-6
2820 YJ=Y-2.5*Nplot
2830 MOVE 8.3,YJ
2840 CSIZE 2.6
2850 IF Y$ <> "N" THEN LABEL Symbol(Nplot)
2860 CSIZE 2.6
2870 MOVE 9.6,YJ
2880 IF Y$ <> "N" THEN LABEL Key(Nplot)
2890 MOVE 10.9,YJ
2900 LORG 2
2910 LABEL USING "K" : File1$(J)
2920 PLOTTER IS 1
2930 RETURN
2940 !
2950 ! *****************************************************************
2960 !
2970 Printing: ! Prints Adjusted and Unadjusted Harmonic Levels
2980 !
2990 PRINTER IS 708
3000 FOR I=1 TO 6
3010 PRINT " "
3020 NEXT I
3030 PRINT "                        NARROWBAND HARMONIC LEVELS"
3040 IF A5$="N" THEN PRINT "          CORRECTED FOR SHEAR LAYER AND 4.3m DISTANC
E"
3050 PRINT " "
3060 PRINT "                  TEST 706     RUN";Rn;"     DATA POINT";Dp
3070 PRINT "                MIC";Mc;"  THETA=";Thetac(K);"deg (corrected)  U =";V;"
m/sec"
3080 PRINT " "
3090 PRINT " "
3100 PRINT "                                                  ADJ  ADJUSTED"
3110 PRINT "            HARMONIC  FREQUENCY,Hz  LEVEL,dB   dB  LEVEL,dB"
3120 PRINT "            ---------------------------------------------------"
3130 PRINT " "
3140 IMAGE 12X,DD,7X,DDDDD.D,7X,DDD.D,2X,DDD.D,3X,DDD.D
3150 FOR I=1 TO Nharm(K)
3160 PRINT USING 3140 : I,Hfreq(K,I),Harmx(K,I),Change(I),Harm(K,I)
3170 NEXT I
3180 PRINT CHR$ (12)
3190 PRINTER IS 1
3200 RETURN
3210 !
3220 ! ERROR RECOVERY
3230 Ntimes=Ntimes+1
3240 IF Ntimes=1 THEN GOTO 3400
3250 PRINT "DOES THE FILE ";File1$(K);" EXIST ?"
3260 DISP "IF THE FILE DOES EXIST, TRY ANOTHER DISC AND TYPE 'Y'"
3270 DISP "IF THE FILE DOES NOT EXIST, TYPE 'N'"
3280 LINPUT "IF THE FILE NUMBER IS IN ERROR, TYPE 'E'",Y$
3290 IF Y$="Y" THEN GOTO 900
3300 OFF ERROR
3310 IF Y$="E" THEN GOTO 610
3320 PRINT "THE PROGRAM WILL ASSUME THE FILE ";File1$(K);" DOES NOT EXIST"
3330 Key(K)=0
3340 Nharm(K)=1
3350 Code$(K)="Y"
3360 FOR I=1 TO 21
3370 Harm(K,I)=0
3380 NEXT I
3390 GOTO 1710
3400 DISP " TRY ANOTHER DISC "
3410 DISP " WHEN READY, PRESS ANY LETTER, THEN 'END LINE'"
3420 INPUT X$
3430 GOTO 900
3440 ! END OF PROGRAM
```

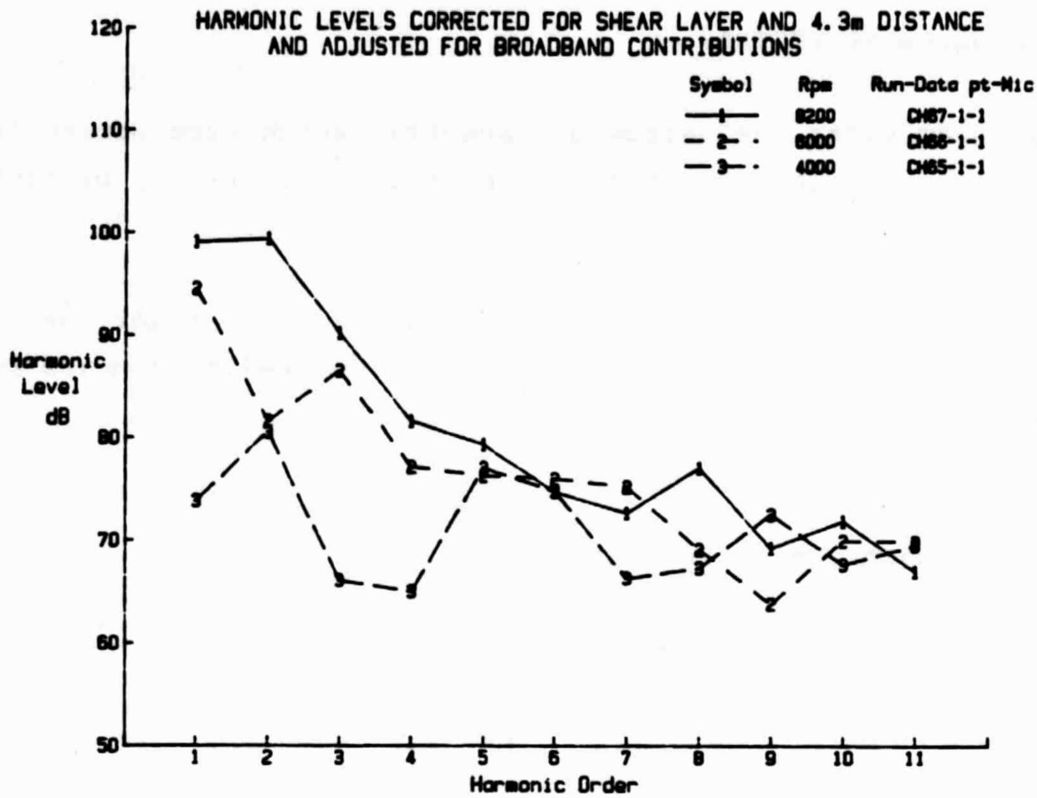

NARROWBAND HARMONIC LEVELS
CORRECTED FOR SHEAR LAYER AND 4.3m DISTANCE

TEST 706 RUN 67 DATA POINT 1
MIC 1 THETA= 68.5 deg (corrected) U = 62.4 m/sec

HARMONIC	FREQUENCY.Hz	LEVEL.dB	ADJ dB	ADJUSTED LEVEL.dB
1	550.0	99.1	0.0	99.1
2	1087.5	99.4	0.0	99.4
3	1637.5	90.2	0.0	90.2
4	2187.5	82.2	-.6	81.6
5	2737.5	80.0	-.7	79.3
6	3275.0	76.2	-1.5	74.7
7	3825.0	73.9	-1.2	72.7
8	4375.0	77.5	-.5	77.0
9	4912.5	71.3	-2.0	69.3
10	5462.5	73.0	-1.1	71.9
11	6012.5	69.5	-2.5	67.0

ORIGINAL PAGE IS
OF POOR QUALITY

A.5 Program NBSPECTRA2

The program plots the narrowband spectra, which were stored on disk by program CEDAR2. Either one or two spectra may be plotted on each graph.

The program is useful if the plots obtained from CEDAR2 need to be replotted on a different scale. It is also used to compare two narrowband spectra.

Input required:

For each plot:- Run Number
Data Point
Microphone Number

Disks containing files, with shear layer and distance corrections, created by CEDAR2

CH Run No - Data Pt - Mic No

Output:

Plot of narrowband spectra

```
10    ! PROGRAM NBSPECTRA2 PLOTS PROP/EMPENNAGE INTERACTION NOISE SPECTRA
20    ! FROM FILES OF DATA CREATED BY CEDAR AND STORED ON D701
30    ! TWO CURVES CAN BE PLOTTED ON ONE GRAPH
40    ! TYPICAL FILE NAMES ARE C-RUN-POINT-MIC
50    !
60    ! PAUL SODERMAN-LISA LEE 4/4/84  HP87
70    !
80    OPTION BASE 1
90    PRINTER IS 1
100   DIM A(540),Lp1(540),Lp2(540),Domain(540),C(540)
110   DIM Theta(2),Crr(32)
120   DISP " "
130   PRINT "THIS IS DISC D701"
140    MASS STORAGE IS ":D701"
150   CAT ":D701"
160   DISP " "
170   PRINT "CORRECTED FILES ARE LISTED CH RUN-POINT-MIC"
180   DISP " "
190   DISP " INPUT TODAYS DATE"
200   INPUT Jour$
210   DISP " "
220   Maxs=120
230   PRINT "MAXIMUM SPECTRUM LEVEL PLOTTED IS ";Maxs;" dB"
240   LINPUT "DO YOU WISH TO CHANGE THIS?",P1$
250   IF P1$="N" THEN GOTO 280
260   DISP "INPUT MAXIMUM SPECTRUM LEVEL FOR PLOT IN dB"
270   INPUT Maxs
280   Mins=Maxs-70
290   Flog=1
300   K=0
310   Fin=274
320   !
330   !         INPUTS FOR ONE SPECTRA
340   !
350   DISP " "
360   DISP " WHAT RUN DO YOU WANT ?"
370   INPUT Rn
380   DISP " WHAT DATA POINT ?"
390   INPUT Dp
400   DISP " WHAT MICROPHONE ?"
410   INPUT Mc
420   IF Flog=2 THEN GOTO 470
430   DISP " "
440   IF Flog=1 THEN Rn1=Rn
450   IF Flog=1 THEN Dp1=Dp
460   IF Flog=1 THEN Mc1=Mc
470   K=K+1
480   !
490   !                    READ THE DATA FILE ON DISC 701
500   !
510   File1$="CH"&VAL$ (Rn)&"-"&VAL$ (Dp)&"-"&VAL$ (Mc)
520   PRINT "FILE NAME CALLED IS",File1$
530   ASSIGN# K TO  File1$
540   READ# K,1 ; Nlines,Delf,Nharm,Rpm,U,Beta,Sepx,Theta(Flog)
550   IF Flog=1 THEN Delf1=Delf
560   IF Flog=1 THEN GOTO 600
570   IF Delf1=Delf THEN GOTO 600
580   PRINT "BANDWIDTHS DIFFER. RETURN TO INPUT FIRST SPECTRUM AGAIN"
590   GOTO 290
600   Number=INT ((Nlines-4)/32)+1
610   IF Number>16 THEN Number=16
620   FOR I=3 TO Number+2
630   READ# K,I ; Crr()
640   FOR J=1 TO 32
650   IF Flog=1 THEN Lp1((I-3)*32+J)=Crr(J)
660   IF Flog=2 THEN Lp2((I-3)*32+J)=Crr(J)
670   NEXT J
680   NEXT I
690    IF Nlines>512 THEN Nlines=512
700    IF Flog=1 THEN Theta1=Theta(Flog)
730     DISP " "
740   !        SECOND CURVE OPTIONAL
```

```
760   IF Flog=2 THEN GOTO 830
770   Flog=2
780    DISP " "
790   LINPUT "DO YOU WANT A SECOND CURVE ON THE SAME GRAPH ?",Q2$
800   DISP " "
810   IF Q2$="Y" THEN DISP "MUST USE THE SAME Bw"
820   IF Q2$="Y" THEN GOTO 300
830   Fin=260
840   Steps=13
850   Nstep=Nlines/13
860   IF Nstep>21 THEN Nstep=40
870   IF Nstep<21 THEN Nstep=20
880   NL=Nstep/20
890  DISP " "
900  DISP " COMPUTING FREQUENCIES TO BE PLOTTED      STAND BY"
910  DISP " "
920  FOR I=1 TO Fin STEP 20
930  Domain(I)=Delf*(I-1)*NL
940  IF Domain(I)<50 THEN Domain(I)=50
950  NEXT I
960   !
970   ! ******************************************************************
980   !    PLOT RESULTS
990   !
1000   PLOTTER IS 705
1010   GRAPHICS
1020   LIMIT 10,200,15,170
1030   LOCATE 20,120,16,98
1040   SCALE 0,256,Mins,Maxs
1050   AXES 0,10,0,Mins
1060   !
1070   !                    TITLE
1080   !
1090   CSIZE 3.6
1100   LORG 2
1110   MOVE 31,Maxs
1120   LABEL USING "K" : "POWER SPECTRAL DENSITY   ":Jour$:" (NBSPECTRA2)"
1130   MOVE 68,Maxs-3
1140   LABEL USING "K" : "RUN ":Rn1:" PT ":Dp1:"   MIC ":Mc1:"  Theta= ":Theta1
1150   PEN 1
1160   MOVE 208,Maxs-3
1170   DRAW 228,Maxs-3
1180   PEN UP
1190   IF Q2$="N" THEN GOTO 1320
1200   PEN 1
1210   LINE TYPE 1
1220   MOVE 68,Maxs-6
1230   LABEL USING "K" : "RUN ":Rn:" PT ":Dp:"   MIC ":Mc:"  Theta= ":Theta(Flog
)
1240   PEN 2
1250   LINE TYPE 6
1260   MOVE 208,Maxs-6
1270   DRAW 228,Maxs-6
1280   PEN UP
1290   PEN 1
1300   !             LABEL Y-AXIS
1310   !
1320   LORG 8
1330   FOR Y=Mins TO Maxs STEP 10
1340   MOVE -.1,Y
1350   LINE TYPE 1
1360   LABEL USING "K.X" : Y
1370   NEXT Y
1380   MOVE -11,Maxs-34
1390  LABEL USING "K" : "Lp(f)"
1400  MOVE -17,Maxs-37
1410  LABEL USING "K" : "dB"
1420  !
1430  !              LABEL X-AXIS
1440  !
1450  LORG 5
1460  MOVE 120,Mins-7
```

ORIGINAL PAGE IS
OF POOR QUALITY

```
1470  LABEL USING "K" : "FREQUENCY. Hz "
1480  CSIZE 3
1490  FOR J=1 TO Fin STEP 20
1500  MOVE J,Mins-2
1510  LABEL USING "K" : Domain(J)
1520  NEXT J
1530  !
1540  FOR I=1 TO Fin STEP 20 ! PUT TICKS ON X-AXIS
1550  MOVE I,Mins
1560  DRAW I,Mins+.6
1570  NEXT I
1580  MOVE 256,Mins
1590  DRAW 256,Mins+.6
1600  PEN UP
1610  !
1620  !       PLOTTING FIRST DIRECTIVITY PLOT
1630  !
1640  FOR I=1 TO Nlines
1650  K=I/NL
1660  PLOT K,Lp1(I),1 ! PLOTS WITH LEFT PEN 1
1670  NEXT I
1680  !
1690  !
1700  !       PLOTTING SECOND DIRECTIVITY PLOT
1710  !
1720  IF Q2$="N" THEN GOTO 1830
1730  PEN 2 ! PLOT WITH RIGHT PEN 2
1740  LINE TYPE 6
1750  MOVE 1,Lp2(1)
1760  FOR K=1 TO Nlines
1770  J=K/NL
1780  PLOT J,Lp2(K),1
1790  NEXT K
1800  LINE TYPE 1
1810  PEN 1
1820  !
1830  ALPHA
1840  ! ********************************************************************
1850  PRINT " "
1860  DISP "DO YOU HAVE ANOTHER GRAPH TO MAKE ?"
1870  INPUT Q3$
1880  IF Q3$="Y" THEN GOTO 150
1890  DISP " "
1900  MASS STORAGE IS ":D700"
1910  PRINT "PROGRAM END"
1920  END
```

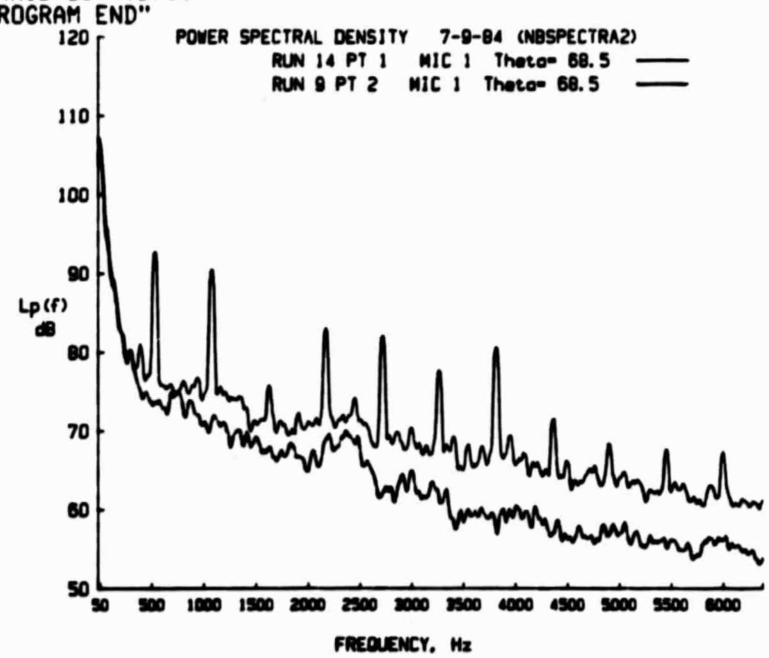

A.6 Program PINEVERT

The program plots the noise directivity in the vertical plane, only for test conditions with runs made with both fuselage test orientations (ψ = 0 and 90°). The adjusted harmonic levels are plotted versus angle relative to the vertical. The angles and associated microphones are:

Vertical Angle (degrees)	Mic. No.	ψ
0	4	90
90	13	0
180	13	90
210	11	0
240	12	0
270	4	0
300	11	90
330	12	90
360	4	90

A maximum of 6 plots can appear on each graph and two options are available.

(1) The SAME harmonic order will be used for all curves on the graph.
(2) Each curve will refer to a DIFFERENT harmonic order of the same data set.

Input required:

For ψ = 0, Run Number
Data point

For ψ = 90, Run Number
Data point

Disks containing files for Microphones 4, 11, 12 and 13, with shear layer and distance corrections, created by CEDAR2 and adjusted by HARMPLOT2.

Output:

Listing of harmonic levels plotted

Plot of noise directivity in vertical plane.

```
10     ! PROGRAM 'PINEVERT' PLOTS PROP/EMPENNAGE INTERACTION NOISE DIRECTIVITY
20     !                IN THE VERTICAL PLANE
30     ! AT SELECTED HARMONIC FREQUENCIES (NARROW BAND)
40     ! A MAXIMUM OF 6 CURVES CAN BE PLOTTED ON ONE GRAPH
50     ! THE DATA ARE TAKEN FROM CORRECTED SPECTRA CREATED BY 'CEDAR2' AND      1
35     ! ADJUSTED BY 'HARMPLOT',FOR MICROPHONES 4,11,12,13 FOR PSI=0 AND 90
60     ! STORED ON DISC 1
70     ! THE FILE NAMES ARE CH-RUN-POINT-MIC
80     ! PAUL SODERMAN -  LISA LEE    5/10/84     HP87
90     !
100     OPTION BASE 1
110    PRINTER IS 1
120    DIM Nharm(20),Code$(20),File1$(20)
130    DIM File$(20),Arr(5,2),Brr(16,2)
140    DIM Level(21,9),Mic(4),Order(8),Angle(9)
150    DATA 4,11,12,13,6,4,5,2,1,7,8,3,0,90,180,210,240,270,300,330,360
160    FOR I=1 TO 4
170    READ Mic(I)
180    NEXT I
190    FOR I=1 TO 8
200    READ Order(I)
210    NEXT I
220    FOR I=1 TO 9
230    READ Angle(I)
240    NEXT I
250    RESTORE
260    FOR I=1 TO 21
270    Level(I,2)=0
280    Level(I,3)=0
290    NEXT I
300    FOR I=1 TO 9
310    Nharm(I)=1
320    File$(I)="CH  - "
330    File1$(I)="CH  - -13"
340    NEXT I
350    MASS STORAGE IS ":D701"
360    DISP " "
370    PRINT "A DATA SET COMPRISED OF DIFFERENT DIRECTIVITY ANGLES"
380    PRINT "FOR THE SAME OPERATING CONDITIONS WILL BE COMPILED AND PLOTTED "
390    DISP " "
400    PRINT "CASES WILL BE SELECTED FROM CORRECTED FILES OF HARMONIC LEVELS "
410    PRINT "WHICH ARE STORED AS FILES CH Run-Data Pt-Mic"
420    PRINT "FILES FOR MICROPHONES 4,11,12,AND (EVENTUALLY) 13 ARE REQUIRED IN T
URN"
430    DISP " "
440    ! SET UP SCALE
450    Maxs=120
460    PRINT "MAXIMUM SPECTRUM LEVEL PLOTTED IS";Maxs;"dB"
470    LINPUT "DO YOU WISH TO CHANGE THIS ?",P1$
480    IF P1$="N" THEN GOTO 510
490    DISP "INPUT MAXIMUM SPECTRUM LEVEL FOR PLOT IN dB"
500    INPUT Maxs
510    Mins=Maxs-70
520    Nmics=9
530    Nmicin=4
540    Nplot=0
550    DISP " "
560    DISP "A MAXIMUM OF 6 CURVES CAN APPEAR ON THIS GRAPH"
570    DISP "THERE ARE 2 OPTIONS FOR PLOTTING"
580    DISP " Option 1 :"
590    DISP "            The SAME Harmonic Order will be used for all Curves on thi
s Graph"
600    DISP " Option 2 :"
610    DISP "            DIFFERENT Harmonics of the same Data set will be used for
each Curve"
620    DISP " "
```

```
630   DISP " Which Option do you wish ?  1 or 2 ?"
640   INPUT Option
650   DISP " "
660   PRINT "CURVE NUMBER";Nplot+1;"ON GRAPH"
670   DISP " "
680   DISP "THE FIRST DATA SET IS FOR VERTICAL TAIL. PSI=0"
690   DISP " "
700   Nset=1
710   DISP " WHAT RUN DO YOU WANT ?"
720   INPUT Rn
730   DISP " WHAT DATA POINT ?"
740   INPUT Dp
750   Nplot=Nplot+1
760   IF Option=1 THEN GOTO 810
770   PRINT "INPUT HARMONIC ORDER FOR PLOT";Nplot
780   INPUT Harm
790   IF Nplot=1 THEN GOTO 840
800   IF Nplot<> 1 THEN GOTO 1320
810   IF Nplot<> 1 THEN GOTO 840
820   IF Option=1 THEN PRINT "INPUT HARMONIC ORDER. TO BE USED FOR ALL CURVES ON
 THIS GRAPH"
830   INPUT Harm
840   Symbol=Nplot
850   !
860   ON ERROR GOTO 2670
870   FOR JK=1 TO Nmicin
880   K=Order(JK+(Nset-1)*4)
890   !                    READ THE DATA FILE ON DISC 1. FOR MICS 1 TO 6
900   Mc=Mic(JK)
910   Ntimes=0
920   File1$(K)="CH"&VAL$ (Rn)&"-"&VAL$ (Dp)&"-"&VAL$ (Mc)
930   File$(K)="CH"&VAL$ (Rn)&"-"&VAL$ (Dp)
940   ON ERROR GOTO 2670
950   ASSIGN# K TO  File1$(K)
960   OFF ERROR
970   IMAGE AAAAAAAAAA," HARM = ".DD."
980   PRINT USING 970 : File1$(K).Harm
990   READ# K,1 : Nlines,Delf,Nharm(K),Rpm,U,Beta,Sepx,Thetac,Nharmc,Code$(K),Ar
r(,)
1000   READ# K,2 : Brr(,)
1010   IF Code$(K)="Y" THEN Nharm(K)=Nharmc
1020   IF Code$(K)="Y" THEN GOTO 1060
1030   IF Code$(K) <> "Y" THEN LINPUT "UNADJUSTED DATA. DO YOU WISH TO PLOT IT ?
",X1$
1040   IF X1$="N" THEN PRINT " START A NEW GRAPH"
1050   IF X1$="N" THEN GOTO 540
1060   FOR J=1 TO 5
1070   Level(J,K)=Arr(J,2)
1080   NEXT J
1090   IF Nharm(K)<6 THEN GOTO 1140
1100   FOR J=6 TO Nharm(K)
1110   Level(J,K)=Brr(J-5,2)
1120   NEXT J
1130   ASSIGN# K TO  *
1140   NEXT JK
1150   Nset=Nset+1
1160   IF Nset<> 2 THEN GOTO 1240
1170   DISP " "
1180   DISP "THE SECOND DATA SET IS FOR HORIZONTAL TAIL. PSI=90"
1190   DISP "WHAT RUN DO YOU WANT ?"
1200   INPUT Rn
1210   DISP "WHAT DATA POINT ?"
1220   INPUT Dp
1230   GOTO 870
1240   FOR J=1 TO Nharm(1)
1250   Level(J,9)=Level(J,1)
1260   NEXT J
```

```
1270    Nharm(9)=Nharm(1)
1280    File$(9)=File$(1)
1290    File1$(9)=File1$(1)
1300    !
1310    ! ***********************************************************************
1320    !     PLOT RESULTS
1330    !
1340    PLOTTER IS 705
1350    GRAPHICS
1360    ! FRAME
1370    LIMIT 10,210,15,170
1380    LOCATE 20,120,10,92
1390    SCALE 0,18,Mins,Maxs
1400    IF Nplot<> 1 THEN GOTO 1980
1410    AXES .5,10,0,Mins
1420    !
1430    !                        TITLE
1440    Mixs=Maxs+4.8
1450    CSIZE 3.5
1460    LORG 4
1470    MOVE 9.7,Mixs
1480    LABEL USING "K" : "NOISE DIRECTIVITY IN VERTICAL PLANE (MICS 4,11,12 & 13
)"
1490    CSIZE 3.2
1500    MOVE 9.7,Mixs-2.5
1510    LABEL USING "K" : "HARMONIC LEVELS CORRECTED FOR SHEAR LAYER,4.3m DISTANC
E AND BROADBAND"
1520    !
1530    ! LABEL KEY
1540    !
1550    LORG 4
1560    Y=Mixs-6
1570    MOVE 12.2,Y
1580    CSIZE 2.8
1590    LABEL USING "K" : "Symbol"
1600    MOVE 14.3,Y
1610    LABEL USING "K" : "Harmonic"
1620    MOVE 16.1,Y
1630    LABEL USING "K" : "Run-Dp"
1640    MOVE 17.8,Y
1650    LABEL USING "K" : "Run-Dp"
1660    !
1670    !
1680    !                   LABEL Y-AXIS
1690    !
1700    CSIZE 2.8
1710    LORG 8
1720    FOR Y=Mins TO Maxs STEP 10
1730    MOVE -.15,Y
1740    LABEL USING "K" : Y
1750    NEXT Y
1760    CSIZE 3.2
1770    MOVE -.45,Maxs-32.5
1780    LABEL USING "K" : "Harmonic"
1790    MOVE -.45,Maxs-35
1800    LABEL USING "K,2X" : "Level"
1810    MOVE -.45,Maxs-38
1820    LABEL USING "K,3X" : "dB"
1830    !
1840    !                   LABEL X-AXIS
1850    !
1860    CSIZE 3.2
1870    LORG 6
1880    MOVE 9,Mins-3
1890    LABEL USING "K" : "Angle Relative to Vertical, Degrees"
```

```
1900 MOVE 9,Mins-5.5
1910 LABEL USING "K" : "(Zero is Below the Fuselage C/L)"
1920 CSIZE 2.8
1930 FOR J=0 TO 36 STEP 3
1940 MOVE J/2,Mins-.5
1950 LABEL USING "K" : 10*J
1960 NEXT J
1970 !
1980 !         PLOT HARMONIC LEVEL VERSUS ANGLE
1990 !
2000 YK=Mixs-6
2010 KT=Nplot+2
2020 IF Nplot=1 THEN KT=1
2030 LINE TYPE KT
2040 MOVE 11.5,YK-2.5*Nplot
2050 DRAW 13,YK-2.5*Nplot
2060 PEN UP
2070 MOVE 0,Mins
2080 LORG 5
2090 CSIZE 2.6
2100 FOR I=1 TO Nmics
2110 IF Harm>Nharm(I) THEN Level(Harm,I)=0
2120 IF Level(Harm,I)=0 THEN GOTO 2180
2130 PLOT Angle(I)/20,Level(Harm,I),2
2140 IF Option=1 THEN LABEL Symbol
2150 IF Option=2 THEN LABEL Harm
2160 PLOT Angle(I)/20,Level(Harm,I),1
2170 GOTO 2190
2180 MOVE Angle(I)/20,Mins
2190 NEXT I
2200 LINE TYPE 1
2210 LORG 5
2220 Y=Mixs-6
2230 YJ=Y-2.5*Nplot
2240 MOVE 12.2,YJ
2250 CSIZE 2.6
2260 IF Option=1 THEN LABEL Symbol
2270 IF Option=2 THEN LABEL Harm
2280 MOVE 14.3,YJ
2290 LABEL Harm
2300 MOVE 16.1,YJ
2310 LABEL USING "K" ; File$(6)
2320 MOVE 17.8,YJ
2330 LABEL USING "K" ; File$(1)
2340 ALPHA
2350 ! ****************************************************************
2360 PRINTER IS 708
2370 PRINT " "
2380 IMAGE "  TABULATED OUPUT. ","Harmonic",DDD
2390 PRINT USING 2380 ; Harm
2400 PRINT " "
2410 PRINT "            FILE      ANGLE    LEVEL,dB "
2420 PRINT " "
2430 FOR I=1 TO Nmics
2440 PRINT USING "10X,AAAAAAAAAA,2X,DDD.D,2X,DDD.D" ; File1$(I),Angle(I),Level(
Harm,I)
2450 NEXT I "
2460 DISP " "
2470 IF Option=1 THEN DISP "YOU HAVE JUST FINISHED CURVE":Nplot
2480 IF Option=2 THEN DISP "YOU HAVE JUST FINISHED THE CURVE FOR HARMONIC":Harm

2490 DISP " "
2500 IF Nplot=8 THEN GOTO 2560
2510 LINPUT "ANY MORE CURVES ON THIS GRAPH?",A7$
2520 IF A7$="N" THEN GOTO 2560
```

```
2530  PRINTER IS 1
2540  IF Option=1 THEN GOTO 650
2550  IF Option=2 THEN GOTO 750
2560  DISP "THIS GRAPH IS FINISHED"
2570  PRINT CHR$ (12)
2580  PRINTER IS 1
2590  LINPUT "ANY MORE GRAPHS?",A8$
2600  IF A8$="N" THEN GOTO 2880
2610  PRINT "STARTING A NEW GRAPH WITH MAX LEVEL =";Maxs;"dB"
2620  LINPUT "ANY CHANGES?",A6$
2630  IF A6$="N" THEN GOTO 540
2640  IF A6$ <> "N" THEN GOTO 450
2650  !
2660 ! ERROR RECOVERY
2670  Ntimes=Ntimes+1
2680  IF Ntimes=1 THEN GOTO 2810
2690  PRINT "DOES THE FILE ";File1$(K);" EXIST ?"
2700  DISP "IF THE FILE DOES EXIST, TRY ANOTHER DISC AND TYPE 'Y'"
2710  LINPUT "IF THE FILE DOES NOT EXIST, TYPE'N'",Y$
2720  IF Y$ <> "N" THEN GOTO 940
2730  DISP "THE PROGRAM WILL ASSUME THE FILE DOES NOT EXIST"
2740  OFF ERROR
2750  Code$(K)="Y"
2760  Nharm(K)=1
2770  FOR I=1 TO 21
2780  Level(I,K)=0
2790  NEXT I
2800  GOTO 1140
2810  DISP " "
2820  PRINT "LOOKING FOR FILE ";File1$(K)
2830  DISP " "
2840 PRINT "REMAINING FILES ARE ON A DIFFERENT DISC."
2850 PRINT "LOAD THE CORRECT DISC AND PRESS ANY LETTER AND (END LINE)"
2860 INPUT GO$
2870 GOTO 940
2880  MASS STORAGE IS ":D700"
2890  DISP "PROGRAM END"
2900  STOP
```

NOISE DIRECTIVITY IN VERTICAL PLANE (MICS 4, 11, 12 & 13)
HARMONIC LEVELS CORRECTED FOR SHEAR LAYER, 4.3m DISTANCE AND BROADBAND

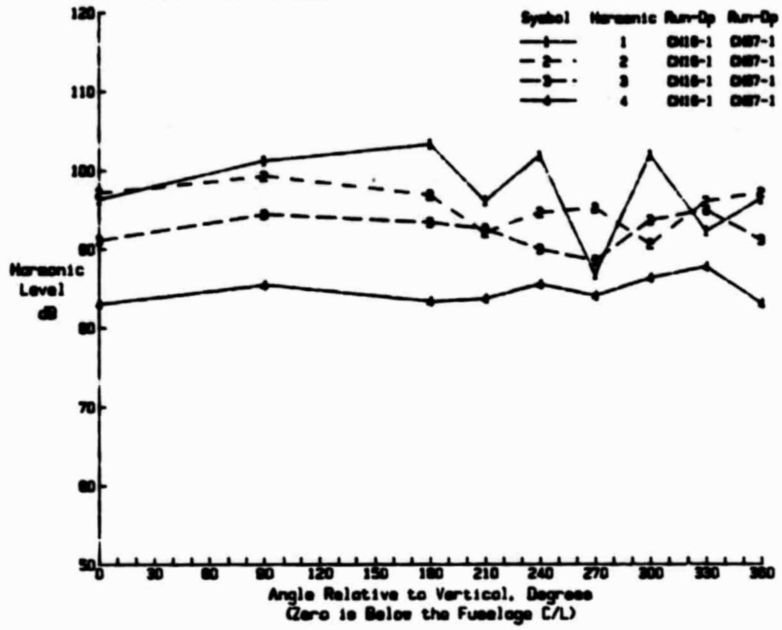

TABULATED OUPUT. Harmonic 1

FILE	ANGLE	LEVEL.dB
CH67-1-4	0.0	96.3
CH16-1-13	90.0	[illegible]
CH67-1-13	180.0	103.3
CH16-1-11	210.0	96.1
CH16-1-12	240.0	10[illegible].8
CH16-1-4	270.0	86.7
CH67-1-11	300.0	102.0
CH67-1-12	330.0	92.2
CH67-1-4	360.0	96.3

TABULATED OUPUT. Harmonic 2

FILE	ANGLE	LEVEL.dB
CH67-1-4	0.0	97.2
CH16-1-13	90.0	99.3
CH67-1-13	180.0	96.9
CH16-1-11	210.0	92.1
CH16-1-12	240.0	94.5
CH16-1-4	270.0	95.2
CH67-1-11	300.0	90.6
CH67-1-12	330.0	96.1
CH67-1-4	360.0	97.2

TABULATED OUPUT. Harmonic 3

FILE	ANGLE	LEVEL.dB
CH67-1-4	0.0	91.1
CH16-1-13	90.0	94.4
CH67-1-13	180.0	93.3
CH16-1-11	210.0	92.5
CH16-1-12	240.0	89.9
CH16-1-4	270.0	88.5
CH67-1-11	300.0	93.6
CH67-1-12	330.0	95.0
CH67-1-4	360.0	91.1

A.7 Program PINEHOR

The program plots the noise directivity in the horizontal plane, for microphones 1 through 9. The adjusted harmonic levels are plotted versus angle relative to the flight direction, using the angles corrected for shear layer effects.

A maximum of 6 curves may appear on each graph and two options are available.

(1) The SAME harmonic order will be used for all curves on this graph.
(2) Each curve will refer to a DIFFERENT harmonic order of the same data set.

Input required:

Run Number
Data Point

Disks containing files for Microphones 1 - 9, with shear layer and distance corrections, created by CEDAR2 and adjusted by HARMPLOT2. If Microphone 7 data is not available, the directivity plot will be made without it.

Output:

Listing of harmonic levels plotted
Plot of noise directivity in horizontal plane.

```
10    ! PINEHOR
20    ! PLOTS RPOP/EMPENNAGE INTERACTION NOISE DIRECTIVITY
30    ! IN THE HORIZONTAL PLANE
40    ! AT SELECTED HARMONIC FREQUENCIES (NARROW BAND)
50    ! A MAXIMUM OF 6 CURVES CAN BE PLOTTED ON ONE GRAPH
60    ! THE DATA ARE TAKEN FROM CORRECTED SPECTRA CREATED BY `CEDAR2' AND      1
65    ! ADJUSTED BY 'HARMPLOT'.FOR MICROPHONES 1 TO 9
70    ! STORED ON DISC !
80    ! THE FILE NAMES ARE CH-RUN-POINT-MIC
90    !
100    ! PAUL SODERMAN -  LISA LEE    5/10/84     HP87    DISC 2.5
110    !
120    OPTION BASE 1
130   PRINTER IS 1
140   DIM Code$(20),File1$(20)
150   DIM Arr(5,2),Brr(16,2),Thetac(20),Nharm(20)
160   DIM Level(21,9),Order(9)
170   DATA 9,1,2,3,4,7,5,6,8
180   FOR I=1 TO 9
190   READ Order(I)
200   NEXT I
210   DISP " "
220   MASS STORAGE IS ":D701"
230   DISP " "
240   PRINT "A DATA SET COMPRISED OF DIFFERENT DIRECTIVITY ANGLES"
250   PRINT "FOR THE SAME OPERATING CONDITIONS WILL BE COMPILED AND PLOTTED "
260   DISP " "
270   PRINT "CASES WILL BE SELECTED FROM CORRECTED FILES OF HARMONIC LEVELS "
280   PRINT "WHICH ARE STORED AS FILES CH Run-Data Pt-Mic"
290   PRINT "FILES FOR MICROPHONES 1 TO 9 ARE REQUIRED IN TURN"
300   DISP " "
310   ! SET UP SCALE
320   Maxs=120
330   PRINT "MAXIMUM SPECTRUM LEVEL PLOTTED IS";Maxs;"dB"
340   LINPUT "DO YOU WISH TO CHANGE THIS ?",P1$
350   IF P1$="N" THEN GOTO 380
360   DISP "INPUT MAXIMUM SPECTRUM LEVEL FOR PLOT IN dB"
370   INPUT Maxs
380   Mins=Maxs-70
390   Nmics=9
400   Nplot=0
410   DISP " "
420   DISP "A MAXIMUM OF 6 CURVES CAN APPEAR ON THIS GRAPH"
430   DISP "THERE ARE 2 OPTIONS FOR PLOTTING"
440   DISP " Option 1 :"
450   DISP "          The SAME Harmonic Order will be used for all Curves on thi
s Graph"
460   DISP " Option 2 :"
470   DISP "          Each Curve will refer to a DIFFERENT Harmonic Order of SAM
E Data Set"
480   DISP " "
490   DISP " Which Option do you wish ?  1 or 2 ?"
500   INPUT Option
510   DISP " "
520   Y$="Y"
530   IF Y$="E" THEN Nplot=Nplot-1
540   PRINT "CURVE NUMBER";Nplot+1;"ON GRAPH"
550   DISP " "
560   DISP " WHAT RUN DO YOU WANT ?"
570   INPUT Rn
580   DISP " WHAT DATA POINT ?"
590   INPUT Dp
600   LINPUT " IS THERE DATA FOR MIC 7 (Y/N) ?",P7$
610   Nplot=Nplot+1
620   PRINTER IS 1
630   IF Option=1 THEN GOTO 680
```

```
640    PRINT "INPUT HARMONIC ORDER FOR PLOT";Nplot
650    INPUT Harm
660    IF Nplot=1 THEN GOTO 710
670    IF Nplot<> 1 THEN GOTO 1040
680    IF Nplot<> 1 THEN GOTO 710
690    IF Option=1 THEN PRINT "INPUT HARMONIC ORDER, TO BE USED FOR ALL CURVES ON
 THIS GRAPH"
700    INPUT Harm
710    Symbol=Nplot
720    !
730    FOR K=1 TO Nmics
740    !                     READ THE DATA FILE ON DISC 1, FOR MICS 1 TO 6
750    IF K=7 AND P7$="N" THEN GOTO 1000
760    Mc=K
770    Ntimes=0
780    File1$(K)="CH"&VAL$ (Rn)&"-"&VAL$ (Dp)&"-"&VAL$ (Mc)
790    File$="CH"&VAL$ (Rn)&"-"&VAL$ (Dp)&"-"
800    ON ERROR GOTO 2380
810    ASSIGN# K TO  File1$(K)
820    OFF ERROR
830    IMAGE AAAAAAAAAA," HARM = ",DD,"
840    PRINT USING 830 ; File1$(K),Harm
850    READ# K,1 ; Nlines,Delf,Nharm(K),Rpm,U,Beta,Sepx,Thetac(K),Nharmc,Code$(K)
,Arr(,)
860    READ# K,2 : Brr(,)
870    IF Code$(K)="Y" THEN Nharm(K)=Nharmc
880    IF Code$(K)="Y" THEN GOTO 920
890    IF Code$(K) <> "Y" THEN LINPUT "UNADJUSTED DATA. DO YOU WISH TO PLOT IT ?"
,X1$
900    IF X1$="N" THEN PRINT " START A NEW GRAPH"
910    IF X1$="N" THEN GOTO 400
920    FOR J=1 TO 5
930    Level(J,K)=Arr(J,2)
940    NEXT J
950    IF Nharm(K)<6 THEN GOTO 990
960    FOR J=6 TO Nharm(K)
970    Level(J,K)=Brr(J-5,2)
980    NEXT J
990    ASSIGN# K TO  *
1000    NEXT K
1010    OFF ERROR
1020    !
1030    ! ******************************************************************

1040    !     PLOT RESULTS
1050    !
1060    PLOTTER IS 705
1070    GRAPHICS
1080    ! FRAME
1090    LIMIT 10,210,15,170
1100    LOCATE 20,120,10,92
1110    SCALE 0,18,Mins,Maxs
1120    IF Nplot<> 1 THEN GOTO 1680
1130    AXES 1,10,0,Mins
1140    !
1150    !                          TITLE
1160    Mixs=Maxs+4.8
1170    CSIZE 3.5
1180    LORG 4
1190    MOVE 9.7,Mixs
1200    LABEL USING "K" ; "NOISE DIRECTIVITY IN HORIZONTAL PLANE  (MICS 1 TO 9)"
1210    CSIZE 3.2
1220    MOVE 9.7,Mixs-2.5
1230    LABEL USING "K" ; "HARMONIC LEVELS CORRECTED FOR SHEAR LAYER,4.3m DISTANC
E AND BROADBAND"
```

```
1240    !
1250    ! LABEL KEY
1260    !
1270    LORG 4
1280    Y=Mixs-6
1290    MOVE 12.2,Y
1300    CSIZE 2.8
1310    LABEL USING "K" : "Symbol"
1320    MOVE 14.3,Y
1330    LABEL USING "K" : "Harmonic"
1340    MOVE 17,Y
1350    LABEL USING "K" : "Run-Data Pt"
1360    !
1370    !
1380    !                   LABEL Y-AXIS
1390    !
1400    CSIZE 2.8
1410    LORG 8
1420    FOR Y=Mins TO Maxs STEP 10
1430    MOVE -.15,Y
1440    LABEL USING "K" : Y
1450    NEXT Y
1460    CSIZE 3.2
1470    MOVE -.45,Maxs-32.5
1480    LABEL USING "K" : "Harmonic"
1490    MOVE -.45,Maxs-35
1500   LABEL USING "K,2X" : "Level"
1510   MOVE -.45,Maxs-38
1520   LABEL USING "K,3X" : "dB"
1530   !
1540   !                   LABEL X-AXIS
1550   !
1560   CSIZE 3.2
1570   LORG 6
1580   MOVE 9,Mins-3
1590   LABEL USING "K" : "Angle Relative to Flight Direction, Degrees"
1600   ! MOVE 9,Mins-5.5
1610   ! LABEL USING "K" : "(90 is Starboard Side)"
1620   CSIZE 2.8
1630   FOR J=0 TO 18 STEP 3
1640   MOVE J,Mins-.5
1650   LABEL USING "K" : 10*J
1660   NEXT J
1670   !
1680   !          PLOT HARMONIC LEVEL VERSUS ANGLE
1690   !
1700   YK=Mixs-6
1710   KT=Nplot+2
1720   IF Nplot=1 THEN KT=1
1730   LINE TYPE KT
1740   MOVE 11.5,YK-2.5*Nplot
1750   DRAW 13,YK-2.5*Nplot
1760   PEN UP
1770   MOVE 0,Mins
1780   LORG 5
1790   CSIZE 2.6
1800   FOR J=1 TO Nmics
1810   IF J=6 AND P7$="N" THEN GOTO 1910
1820   I=Order(J)
1830   IF Harm>Nharm(I) THEN Level(Harm,I)=0
1840   IF Level(Harm,I)=0 THEN GOTO 1900
1850   PLOT Thetac(I)/10,Level(Harm,I),2
1860   IF Option=1 THEN LABEL Symbol
1870   IF Option=2 THEN LABEL Harm
1880   PLOT Thetac(I)/10,Level(Harm,I),1
1890   GOTO 1910
1900   MOVE Thetac(I)/10,Mins
1910   NEXT J
1920   LINE TYPE 1
1930   LORG 5
```

```
1940  Y=Mixs-6
1950  YJ=Y-2.5*Nplot
1960  MOVE 12.2,YJ
1970  CSIZE 2.6
1980  IF Option=1 THEN LABEL Symbol
1990  IF Option=2 THEN LABEL Harm
2000  MOVE 14.3,YJ
2010  LABEL Harm
2020  MOVE 17,YJ
2030  LABEL USING "K" ; File$
2040  ALPHA
2050  ! ****************************************************************
2060  PRINTER IS 708
2070  PRINT " "
2080  IMAGE "  TABULATED OUPUT.    Run",DDD,3X,"Data Point",DD,3X,"Harmonic",DDD
2090  PRINT USING 2080 : Rn,Dp,Harm
2100  PRINT " "
2110  PRINT "          FILE      THETA   Lp(f)    "
2120  PRINT " "
2130  FOR J=1 TO Nmics
2140  IF J=6 AND P7$="N" THEN GOTO 2170
2150  I=Order(J)
2160  PRINT USING "10X,AAAAAAAAAA,2X,DDD.D,2X,DDD.D" : File1$(I),Thetac(I),Level
(Harm,I)
2170  NEXT J
2180  DISP " "
2190  IF Option=1 THEN DISP "YOU HAVE JUST FINISHED CURVE":Nplot
2200  IF Option=2 THEN DISP "YOU HAVE JUST FINISHED THE CURVE FOR HARMONIC":Harm
2210  DISP " "
2220  IF Nplot=8 THEN GOTO 2280
2230  LINPUT "ANY MORE CURVES ON THIS GRAPH?",A7$
2240  IF A7$="N" THEN GOTO 2280
2250  PRINTER IS 1
2260  IF Option=1 THEN GOTO 510
2270  IF Option=2 THEN GOTO 610
2280  DISP "THIS GRAPH IS FINISHED"
2290  PRINT CHR$ (12)
2300  PRINTER IS 1
2310  LINPUT "ANY MORE GRAPHS?",A8$
2320  IF A8$="N" THEN GOTO 2600
2330  PRINT "STARTING A NEW GRAPH WITH MAX LEVEL =":Maxs:"dB"
2340  LINPUT "ANY CHANGES?",A6$
2350  IF A6$="N" THEN GOTO 400
2360  IF A6$ <> "N" THEN GOTO 320
2370  !
2380  Ntimes=Ntimes+1
2390  IF Ntimes=1 THEN GOTO 2540
2400  PRINT "DOES THE FILE ":File1$(K):" EXIST ?"
2410  DISP "IF THE FILE DOES EXIST,TRY ANOTHER DISC AND TYPE 'Y'"
2420  DISP "IF THE FILE DOES NOT EXIST, TYPE 'N' "
2430  LINPUT "IF THE FILE NUMBER IS IN ERROR, TYPE 'E' ",Y$
2440  IF Y$="E" THEN GOTO 530
2450  IF Y$ <> "N" THEN GOTO 500
2460  DISP "THE PROGRAM WILL ASSUME THE FILE DOES NOT EXIST"
2470  OFF ERROR
2480  Code$(K)="Y"
2490  Nharm(K)=1
2500  FOR I=1 TO 21
2510  Level(I,K)=0
2520  NEXT I
2530  GOTO 1000
2540 PRINT "LOOKING FOR FILE ":File1$(K)
2550 DISP " "
2560 PRINT "REMAINING FILES ARE ON A DIFFERENT DISC."
2570 PRINT "LOAD THE CORRECT DISC AND PRESS ANY LETTER AND (END LINE)"
2580 INPUT G0$
2590  GOTO 800
2600  MASS STORAGE IS ":D700"
2610  DISP "PROGRAM END"
2620  STOP
```

NOISE DIRECTIVITY IN HORIZONTAL PLANE (MICS 1 TO 9)
HARMONIC LEVELS CORRECTED FOR SHEAR LAYER, 4.3m DISTANCE AND BROADBAND

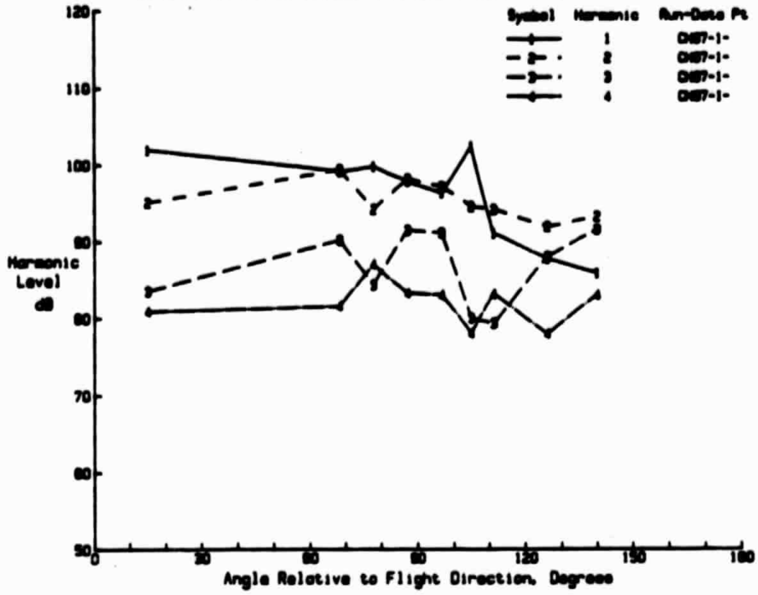

ORIGINAL PAGE IS
OF POOR QUALITY

TABULATED OUPUT. Run 67 Data Point 1 Harmonic 1

FILE	THETA	Lp(f)
CH67-1-9	15.0	102.0
CH67-1-1	68.5	99.1
CH67-1-2	77.8	99.8
CH67-1-3	87.2	97.8
CH67-1-4	96.8	96.3
CH67-1-7	105.0	102.4
CH67-1-5	111.2	91.0
CH67-1-6	126.1	87.7
CH67-1-8	140.0	85.8

TABULATED OUPUT. Run 67 Data Point 1 Harmonic 2

FILE	THETA	Lp(f)
CH67-1-9	15.0	95.1
CH67-1-1	68.5	99.4
CH67-1-2	77.8	94.2
CH67-1-3	87.2	98.2
CH67-1-4	96.8	97.2
CH67-1-7	105.0	94.5
CH67-1-5	111.2	94.1
CH67-1-6	126.1	91.9
CH67-1-8	140.0	93.2

TABULATED OUPUT. Run 67 Data Point 1 Harmonic 3

FILE	THETA	Lp(f)
CH67-1-9	15.0	83.6
CH67-1-1	68.5	90.2
CH67-1-2	77.8	84.3
CH67-1-3	87.2	91.5
CH67-1-4	96.8	91.1
CH67-1-7	105.0	80.0
CH67-1-5	111.2	79.3
CH67-1-6	126.1	88.0
CH67-1-8	140.0	91.5

TABULATED OUPUT. Run 67 Data Point 1 Harmonic 4

FILE	THETA	Lp(f)
CH67-1-9	15.0	80.9
CH67-1-1	68.5	81.6
CH67-1-2	77.8	87.0
CH67-1-3	87.2	83.2
CH67-1-4	96.8	83.0
CH67-1-7	105.0	78.0
CH67-1-5	111.2	83.1
CH67-1-6	126.1	78.0
CH67-1-8	140.0	83.0

APPENDIX B

ADDITIONAL COMMENTS ON SPECTRAL BROADENING

The influence of turbulence scattering on the acoustic signal propagating through the shear layer is discussed in Section 3.5 and example spectra are presented in Figures 23 and 24 to demonstrate the resulting spectral broadening. The spectra were obtained using the sinusoidal, high resolution spectrum mode of the HP 5420B analyzer (see Section 2.3.2). The effective filter bandwidth was approximately 42Hz. An alternative data reduction procedure available in the analyzer is the random, high resolution spectrum mode, in which case the effective filter bandwidth is about 18.75 Hz for the frequency range of interest. In the random mode the spectra are presented in terms of power spectral density instead of power-in-the-band (as is the case for the sinusoidal mode), but the difference is of no consequence when interest is directed to the spectral broadening phenomenon.

Data reduction of the acoustic signals analyzed in Figures 23 and 24 was repeated using the random, high resolution spectrum mode; the resulting spectra are plotted in Figures B.1 and B.2. Because of the smaller bandwidth, the effect of spectral broadening can be seen more clearly in Figures B.1 and B.2 than in Figures 23 and 24.

Figures B.1 compares spectra measured at locations 5 and 7, which are on either side of the shear layer and at approximately the same angle of radiation. Spectral broadening can be observed at the higher frequencies.

Figure B.2 compares spectra measured outside the shear layer at locations 2 and 6. Following the simple empirical analysis developed in Section 3.5 it is predicted that spectral broadening

(a) Microphone 7 (In Flow)

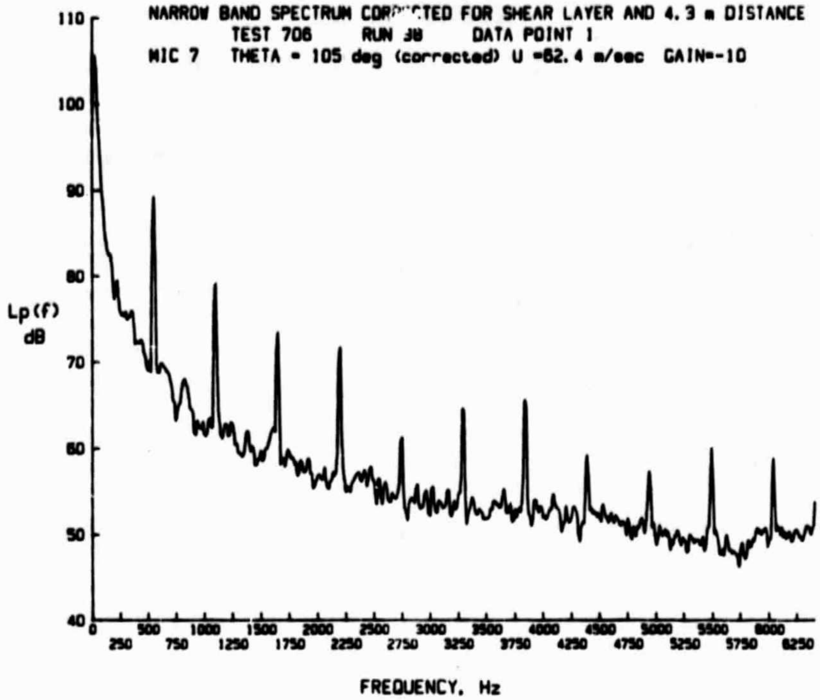

(b) Microphone 5 (Out of Flow)

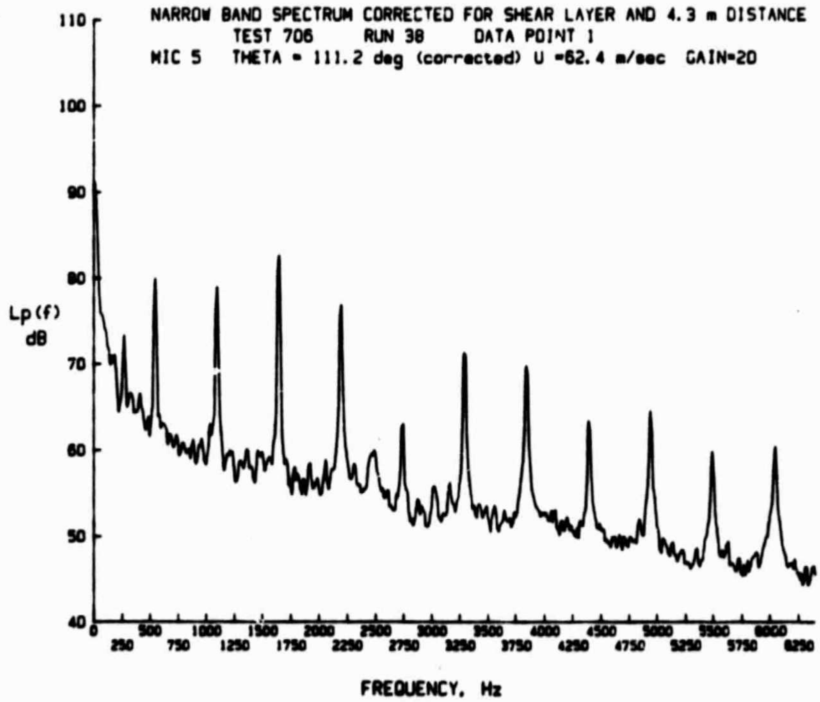

FIGURE B-1. COMPARISON OF NARROWBAND PROPELLER NOISE SPECTRA MEASURED IN AND OUT OF FLOW, RANDOM SIGNAL ANALYSIS MODE

(a) Microphone 2 (Forward of Plane of Rotation)

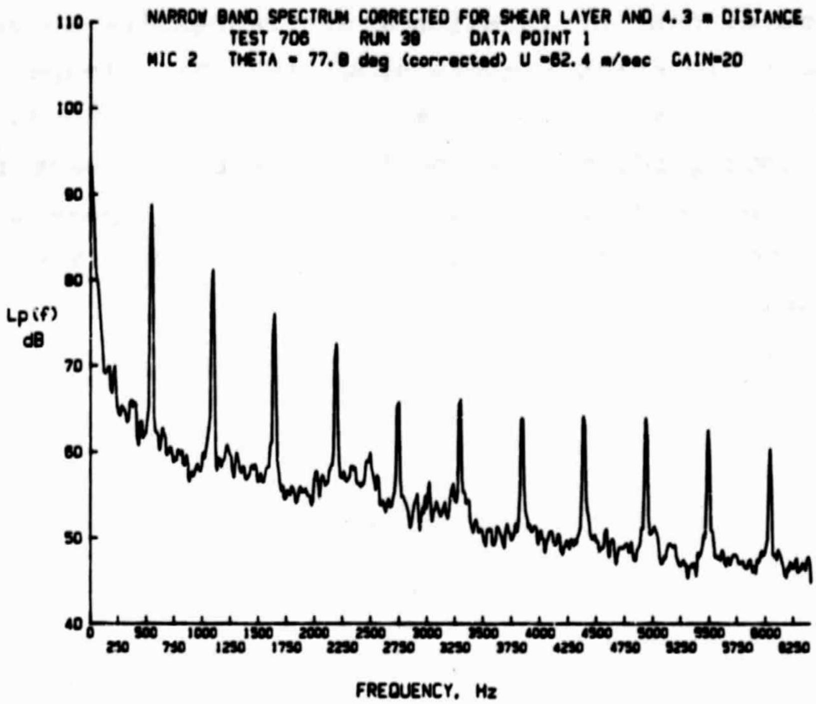

(b) Microphone 6 (Aft of Plane of Rotation)

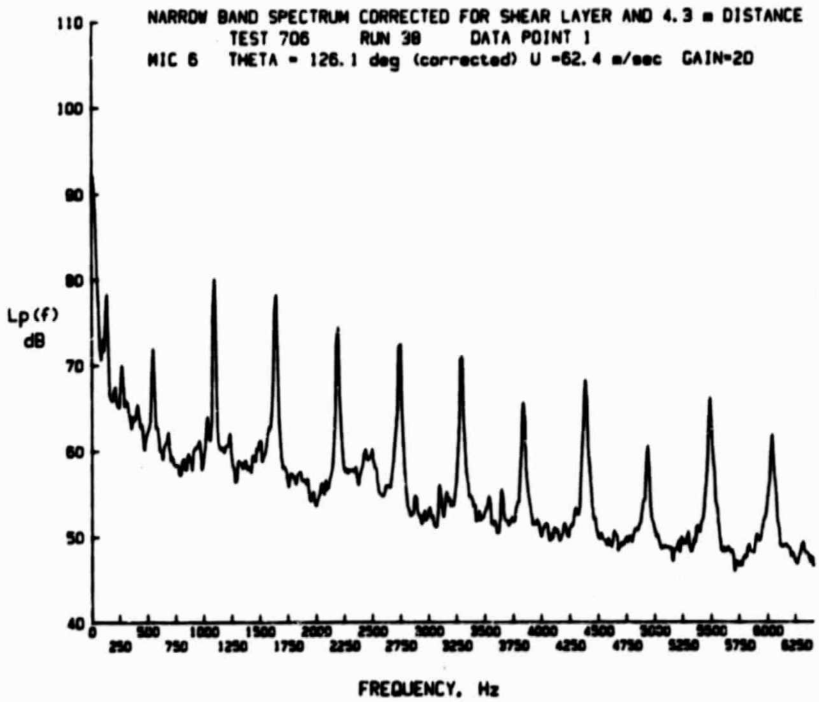

FIGURE B-2. COMPARISON OF NARROWBAND PROPELLER NOISE SPECTRA MEASURED FORWARD AND AFT OF PLANE OF ROTATION, RANDOM SIGNAL ANALYSIS MODE would become evident at location 2 at frequencies above about 2700 Hz and at location 6 above about 1450 Hz. Inspection of Figure B.2 suggests that the simple prediction procedure is a reasonably good guide to the onset of spectral broadening. In the case of microphone 6, the width of the spectral peak at 5500 Hz, measured at the 10dB-down point, is about three times larger than the width at 1000 Hz.